TABLE OF CONTENTS

Bestpfe.com

LIST OF FIGURES

BEST PFE.COM
List of research project topics and materials

LIST OF TABLES

Bestpte.com

LIST OF ABBREVIATIONS

ACM	Astrocyte-conditioned medium
ACN	Acetonitrile
ANOVA	Analysis of variance
AP	Apical side
AR	Analytical reagent
ATCC	American type culture collection
ATP	Adenosine 5’-triphosphate
AUC	Area under the curve
BCA	Bicinchoninic acid
BL	Basolateral
°C	Degree Celsius
Caco-2	Colon adenocarcinoma cells
CCD	Central composite design
CLSM	Confocal laser scanning microscopy
C_{max}	Peak at maximum drug concentration
CMC	Critical micelle concentration
Da	Dalton
DAPI	4’6-diamidino-2-phenylindole
DCM	Dichloromethane
DDS	Drug delivery system
DLS	Dynamic light scattering
DMEM	Dulbecco’s modified Eagle’s medium

DSC	Differential scanning calorimetry
DMSO	Dimethyl sulfoxide
DSC	Differential scanning calorimetry
EDTA	Ethylenediamine tetra-acetic acid (disodium salt)
EC	Endothelial cell
EE	Entrapment efficiency
FACS	Fluorescence activated flow cytometry
FBS	Foetal bovine serum
FDA	Food and drug administration
FITC	Fluorescein isothiocyanate
FTIR	Fourier transform infrared
g/mol	Grams per mole
GI	Gastrointestinal
hr	Hour (s)
H_2O_2	Hydrogen peroxide
HBSS	Hank's balanced salt solution
HCl	Hydrochloric acid
HEPES	*N*-2-hydroxyethylpiperazine-*N*'-2-ethanesulphonic acid
HPLC	High performance liquid chromatography
IC_{50}	Concentration inhibiting 50% cell growth
ICH	International conference on harmonization
KCl	Potassium chloride
l	Litre
LC	Loading capacity

BESTPFE.COM
List of research project topics and materials

LOD	Limit of detection
LOQ	Limit of quantitation
M	Molar (mole per litre)
mg	Milligram
mg/ml	Milligram per millilitre
min	Minute(s)
ml	Millilitre
µg	Micrograms
µM	Micromolar
MW	Molecular weight
NaH_2PO_4	Sodium phosphate monobasic
Na_2HPO_4	Sodium phosphate dibasic
NaOH	Sodium hydroxide
NEAA	Non-essential amino acid
nm	Nanometre
NPs	Nanoparticles
O/W	Oil in water
P_{app}	Apparent permeability coefficient
PACA	Poly(alkyl cyanoacrylate)
PBCA	Poly(butyl cyanoacrylate)
PBS	Phosphate buffered saline
PCR	Polymerase chain reaction
PCS	Photon correlation spectroscopy
PD	Pharmacodynamic

P-gp	P-glycoprotein
PI	Polydispersity index
PK	Pharmacokinetic
PK_a	Dissociation constant
PLA	Poly(D,L-lactide)
PLGA	Poly(D,L-lactide-co-glycolide)
PVA	Poly(vinyl alcohol)
RH	Relative humidity
RI	Reflective index
rpm	Revolutions per minute
RSM	Response surface methodology
SD	Standard deviation
SE	Standard error
SEM	Scanning electron microscopy
SRB	Sulforhodamine B
TCA	Trichloroacetic acid
TEER	Transendothelial electrical resistance
TEM	Transmission electron microscopy
TFA	Trifluoroactic acid
TJ	Tight junction
Tris	Tris(hydroxymethyl)aminomethane
UV	Ultraviolet
v/v	Volume per volume
W/O	Water in oil

w/v	Weight per volume
w/w	Weight per weight

Chapter 1

General Introduction

Chapter 1 . GENERAL INTRODUCTION

1.1 Breast cancer

1.1.1 Background

Breast cancer affects one in nine women over their lifetime in New Zealand. The risk of being diagnosed with breast cancer increases with age. Over 70% of women are diagnosed of breast cancer at the age of 50 years or older. Most will survive 5 years or longer if the cancer is found early enough but tragically, it accounts for over 600 deaths every year (Ferlay, Soerjomataram et al. 2015, Torre, Bray et al. 2015). In addition to age, several other risk factors, such as a history of breast cancer in the contralateral breast; a history of bilateral premenopausal breast cancer in a first degree relative; a history of fibrocystic disease; whether or not an oophorectomy has been performed; obesity; previous exposure to high levels of radiation in the chest, socioeconomic status, and a previous cancer in the ovary or endometrium are associated with relative risks to trigger breast cancer (Romieu, Berlin et al. 1990, Coates, Gebski et al. 1992).

Normal cells have their own life cycle, they are created, grow and die in a controlled way. But when abnormal changes occur in the gene of the cells, the cell life cycle will be affected, the growing process will be regulated, and the normal function can be turned on or off. If the abnormal cells continue to grow and divide, eventually a tumour is formed. Breast cancer is caused by genetic abnormalities which trigger breast cells to grow in an uncontrollable manner. These abnormal gene mutations are usually acquired with increasing age, and 85 – 90% of breast cancers are caused by this process, and the other 5 - 10% breast cancer patients are due to inherited gene mutations (Bansil and Turner 2006, Al-Qadi, Grenha et al. 2012). A tumour may be benign or malignant. A benign tumour is not considered as ‘cancer’, and not generally life-threatening, it will not spread to other part of the human body, but it may still causes other health problems as it grows. A malignant tumour, such a breast cancer, has the potential to grow sufficiently in size. At the later stage, the breast cancer cells can spread beyond its original site and gain access to lymphatic and blood vessels, which allows the cancer cells to spread around the body and invading other healthy tissue (Al-Qadi, Grenha et al. 2012).

There are few immediate prospects in identifying the main causes of breast cancer, despite an accumulation of experimental and clinical information. Scientists have identified several etiologic factors. Genes, hormones, different chemical agents, and even viruses have influence in triggering breast cancer. Epidemiologic data indicated a great difference in risk of getting breast cancer between populations in different countries. It has been reported, for instant, that Western women have general high rate in obtaining breast cancer than Japanese women. Clinically, to control the disease by earlier detection and more effective therapies have not reflected in decreased mortality rates. In fact, younger generation has substantial increased in both incidences of breast cancer and mortality rates (Tiyaboonchai 2003, Ferlay, Soerjomataram et al. 2015).

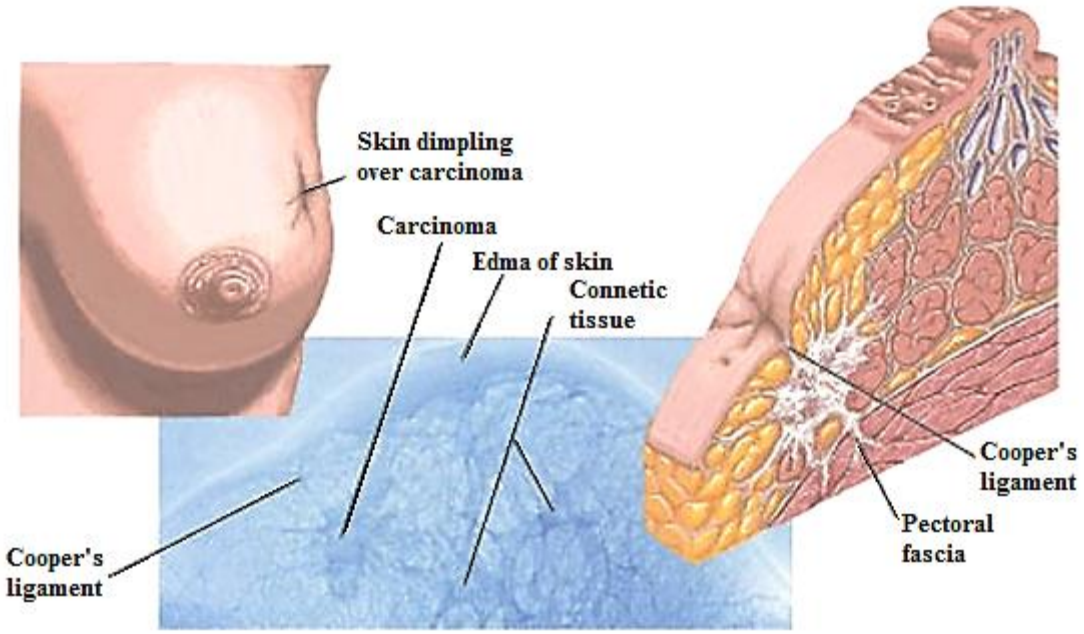

Figure 1-1. Clinical signs of breast cancer (Tiyaboonchai 2003).

Early stage breast cancer usually causes no symptoms. Therefore, routine screening tests are important, as they can detect the early stage breast cancer. As the breast cancer grows, it will result in various symptoms (Bansil and Turner 2006, Katas and Alpar 2006) including:

- A change in the breast skin appearance, nipple, or areola, such as becoming dimpled or puckered or turning purple or red.
- A lump, swelling or thickening at the breast site or under your arm.
- Breast or nipple aching and tenderness.

- Nipple discharge, especially if it is bloody.
- Nipple inversion, meaning the nipple pulls back into the breast.
- A change in the shape or size of the breast.
- A change in the skin condition of the breast, such as turning scaly or itchy.

1.1.2 Treatment of the breast cancer

There are various methods for the breast cancer treatment based on whether it is at early or later stage of the cancer. Surgery remains the primary methods for cancer treatment. Radiation therapy and chemotherapy are also used as adjunctive therapies before and after the surgery, based on individual patient's condition and other associate medical factors (Smart 2005, Carvalho, Bruschi et al. 2010).

Surgery can catch localised cancer cells, problems in picking up all metastasis. It has been reported that a great percentage of breast cancer cells have spread to lymph node or nearby organs at the later stage of breast cancer (Devine and McKenzie 1992). Therefore, the efficient treat of breast cancer, the use of combination treatments is necessary.

Radiation therapy is only suitable for several particular tumours, and it makes use of radio isotope to impose action on the cancer. While chemotherapy can be applied for many types of tumours, generally involves use of a certain anticancer drug or combination of anticancer drugs (Smart 2005, Carvalho, Bruschi et al. 2010).

Radiation therapy is a popular method to treat cancer and is generally used for reducing the size of the tumour. As the tumours grow larger, they can trigger compression to the nearby organs and nerves, causing pain for the patients. Thus radiation therapy is capable to shrink down the tumours and alleviates the pains. Sometimes it might be a concern that radiation therapy can cause skin redness for patients, thus the appropriate operating process is crucial (Carvalho, Bruschi et al. 2010).

There are several popular administration routes of chemotherapy. Intravenous chemotherapy is the most common one, which deliver anticancer drugs directly into the systemic circulation

to kill the tumours (Smart 2005). It is generally applied to treat cancers patients. In some cases, in order to shrink a large tumour, intravenous injection of anticancer drug is proceeded before surgery, this is also termed 'neoadjuvant therapy' (Velmurugan, Ali et al. 2014). If the intravenous chemotherapy is proceeded after the surgery, it is called 'adjuvant therapy'. The purpose of the adjuvant therapy is to kill any remnant tumour cells as well as to avoid cancers from returning to the breast site (Kumar, Dhawan et al. 2014).

However, the intravenous chemotherapy often leads to a high peak of drug above the maximum tolerable concentration (MTC) in systemic circulation, followed by a fast elimination of drug from the plasma, resulting in a limited area-under-the-curve (AUC) (Mei, Zhang et al. 2013). Instead, oral chemotherapy could maintain a sustained moderate concentration of the drug in the circulation to achieve a prolonged exposure of cancerous cells to the drug as well as to avoid high peak above MTC. This will increase the therapeutic efficacy and decrease the side effects (Feng 2011). In addition, oral administration is the most preferred due to good patient adherence, promising therapeutic efficacy, low production costs, etc (Venturoli and Rippe 2005), and it is a main step towards 'Chemotherapy at Home', which is especially important for the patients who are very weak to withstand harsh cancer treatment. Thus it at least provides a palliative treatment to bring them hope for survival prolongation (Feng, Mei et al. 2009).

The biological and physical barriers in gastrointestinal (GI) tract offer various obstacles to oral delivery of active potential ingredient (API), resulting in short half-life and low oral bioavailability (Lee, MacKay et al. 2005). In general, a lot of APIs have low oral bioavailabilities of lower than 20% in animals, compared to intravenous injection, regardless of their molecular weight (MW) (Olsson and Reese 1971, Azzi, Bernaudin et al. 1990), such low bioavailabilities imply that even if drug delivery is targeted to a specific part of the GI tract it will still experience huge obstacles to its stability and absorption (Olsson and Reese 1971, Takahashi, Sugimoto et al. 1994). Although the results were gathered from previous studies that may have used various parameters making comparison difficult, it may present the challenges incurred in the oral delivery of APIs (Schneeberger 1974).

Thus there is a need to design a suitable delivery system which not only protects the APIs from various enzymatic degradations but also aids in enhancing its oral absorption and penetration across the intestinal epithelial membrane without altering its biological activity,

especially for the hydrophilic compounds in nature (Lutty, Hasegawa et al. 2010). Lipid based carriers are promising carrier systems for delivery of APIs. They exhibit high permeability characteristic over the intestinal wall because of their size range and high surface to volume ratio (Clough and Smaje 1984, Sottani, Zucchetti et al. 2004). These delivery systems enhance the stability of APIs *in vivo* leading to increased circulation time in the body as well (Deen, Ueki et al. 1976, Sottani, Zucchetti et al. 2004).

1.2 Introduction to gemcitabine

Gemcitabine [2'-deoxy-2',2'difluorocytidine monohydrochloride (β isomer), dFdC] is an antineoplastic drug effective in treating a variety of malignancies, including breast, pancreatic, non-small cell lung cancers (Snoeys, Lievens et al. 2007, Wisse, Jacobs et al. 2008). Gemcitabine, depicted in Figure 1-1, was first synthesized in Larry Hertel's lab at Eli Lilly during the early 1980s (Avasthi and Koshy 1988). It was intended as an antiviral drug, but preclinical testing showed that it killed leukemia cells *in vitro*. It was first licensed in the UK in 1995 (Avasthi and Koshy 1988, Daldrup-Link, Link et al. 2000).

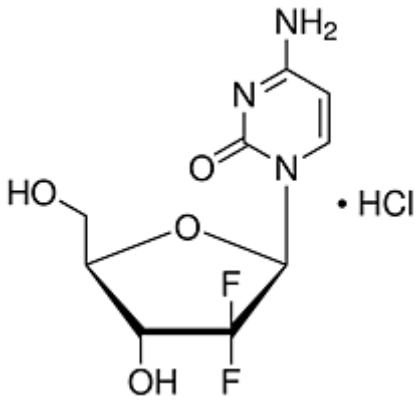

Figure 1-2. The chemical structure of gemcitabine.

Table 1-1. The physicochemical properties of gemcitabine.

Physicochemical properties	
Chemical formula	$C_9H_{11}F_2N_3O_4$
IUPAC name	1-[(2R,4R,5R)-3,3-difluoro-4-hydroxy-5-hydroxymethyl)oxolan-2-yl]-4-imino-1,4-dihydropyrimidin-2-ol hydrochloride
Molecular weight	299.66 g/mol
Water solubility	25 mg/mL
Solubility in others	Methanol and acetone (slightly), DMSO (50 mM), Insoluble in ethanol.
Melting point	292°C
Boiling point	482.7°C at 760 mmHg
LogP	-1.4
pKa	3.5
Storage	Store at 4° C
Oral bioavailability	< 10%
Plasma half-life	short infusions ranged from 32 to 94 min

Gemcitabine is a prodrug which is activated via intracellular phosphorylation to gemcitabine monophosphate (dFdCMP) by deoxycytidine kinase (dCK). This monophosphate is then converted further to active diphosphate and triphosphate metabolites (Chen 1978). Gemcitabine triphosphate inhibits DNA synthesis by two different mechanisms (Norris, Puri et al. 1998). The first mechanism of inhibition occurs after the triphosphate moiety is incorporated into the DNA chain. Adjacent to this, a single additional nucleotide is allowed to be incorporated before the chain extension process is completed. This step is of particular importance as the non-terminal position of gemcitabine triphosphate prevents detection and repair by DNA repair enzymes. The second mechanism is by direct inhibition of DNA polymerase. Both mechanism have the effect of retarding DNA synthesis and these processes ultimately result in cytotoxic cell death (Chen 1978, Norris, Puri et al. 1998).

BEST PFE.COM
List of research project topics and materials

1.3 Overview of oral drug delivery of gemcitabine

1.3.1 Barriers limiting the oral delivery

The absorption of orally administered gemcitabine from the GIT into the systemic circulation may be limited by various factors. These include the release of the gemcitabine from the drug delivery system and the changing conditions that gemcitabine has to pass on its way to the target receptors. The primary difficulty encountered with orally delivered pharmaceuticals include the poor intrinsic permeability across the intestinal epithelium which is considered as physical barrier, and susceptibility to enzymatic degradations in the gastrointestinal tract (GIT) which represent the enzymatic barrier (Baldeschwieler 1983). Furthermore, the post-absorptive clearance is also another barrier for oral drug delivery (Beaumier and Hwang 1983). All present limitations also associated with gemcitabine among variable barriers, physical and enzymatic barriers play major roles to obstacle the absorption of gemcitabine *via* oral administration.

1.3.1.1 Enzymatic barriers

This first enzymatic barrier for orally delivered gemcitabine is the stomach. The stomach contains two major threats to stability: intensive acidic environment and the presence of pepsin. Pepsin is the major digestive enzyme in our stomach which degrades many orally administered drugs (Kraft, Freeling et al. 2014). Gastric pH might alter the ionisation of the drug candidate causing a loss of specific structure and function (Pecora 2013). The small intestine is the major site of drug digestion and represents the second enzymatic barrier to oral drug delivery. The drug candidates after reaching the intestine are further degraded by various digestive enzymes such as trypsin and α-chymotrypsin (Ingebrigtsen and Brandl 2002).

1.3.1.2 Physical barriers

The absorption of any gemcitabine surviving enzymatic attack in the GIT into systemic circulation is further reduced by the physical barriers. The mucus layer covering GIT epithelial membrane is considered as the first barrier for the permeation of the drug candidate.

Second, the layer of intestinal mucosa, consist layers of epithelial cells connecting with tight junctions, which forming a seal wall for the drug permeation.

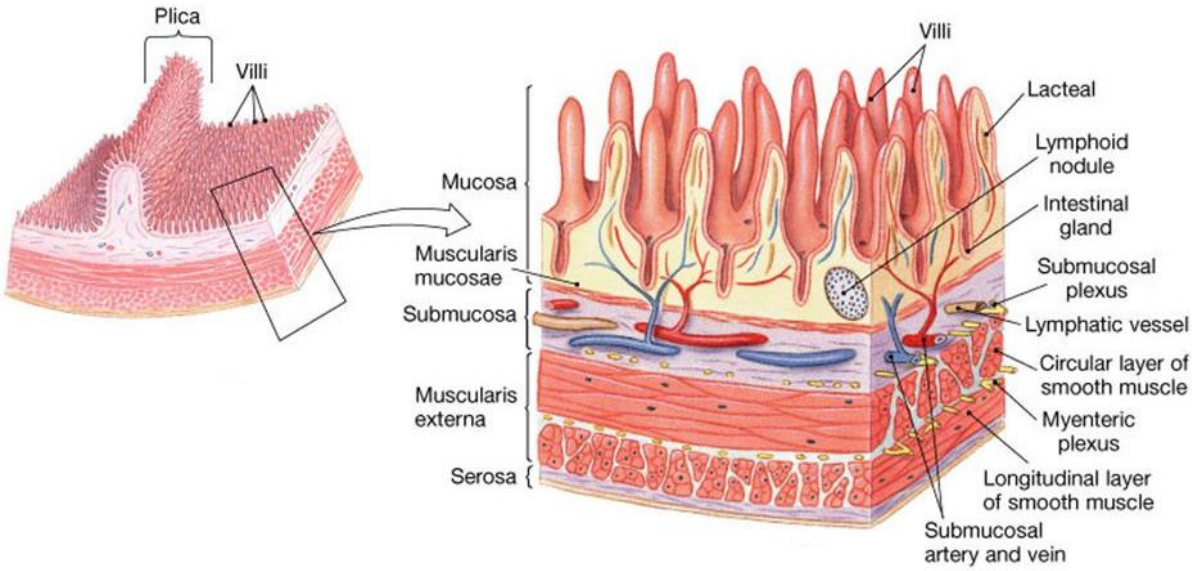

Figure 1-3. The structure of intestinal mucosa (Wang, Byrne et al. 2011).

Permeability has been found to be size dependent and decrease rapidly when MW is greater than 700 Da (Hunter 2013). Lipophilic drug candidates are primarily absorbed by epithelial cells *via* the transcellular pathway, whereas more hydrophilic drug, such as gemcitabine is able to enter the systemic circulation to a limited extent *via* the paracellular pathway through tight junctions (Jacobs and Müller 2002). Both of the enzymatic and the physical barriers contribute to the overall poor oral bioavailability of gemcitabine across intestinal epithelium. As a result, the absolute oral bioavailability of gemcitabine is less than 10% (Venturoli and Rippe 2005).

1.3.2 Mechanism of drug permeation through intestinal mucosa

Figure 1-4 shows two possible mechanisms of permeation of drugs through the oral intestinal mucosa: passive diffusion (via the transcellular or paracellular pathway) or carrier-mediated transport (e.g., active transport and facilitated diffusion) (Harush-Frenkel, Debotton et al. 2007, Liu, Xu et al. 2012). The permeation mechanism for a particular compound depends on its physical and chemical properties such as molar mass, hydrophilicity, lipophilicity and polarity (Harush-Frenkel, Debotton et al. 2007).

1.3.2.1 Passive diffusion

Passive diffusion is the major mechanism for delivering most drug candidates. Generally, drug candidates that can be readily dissolved in various types of solvent would move well through the intestinal mucosa, and those with slight preferential lipid solubility would demonstrate even higher permeability (Plank, Mechtler et al. 1996). In general, non-ionized forms of the weak acid and base, drugs are observed to have higher permeability across intestinal epithelial membrane (Zhang, Tan et al. 2006). This could be explained by considering that non-ionized form of the compound possesses a much higher degree of lipophilicity and thus an affinity for the mucosal membrane, while the ionized form tends to remain in the aqueous intestinal environment, and penetrate across the intestinal epithelial membrane via paracellular pathway (Panyam, Williams et al. 2004, Zhang, Tan et al. 2006). The driving force for passive diffusion of a drug molecule to cross the epithelial membrane is mainly dependant on the concentration gradient of drug candidates (Zhang, Tan et al. 2006).

Two pathways are available for drug transport through the intestinal epithelial membranes by passive diffusion: (1) the transcellular way, where the compounds move across the epithelial cells and (2) paracellular way, where the compounds diffuse through the tight junctions between the epithelial cells (Figure 1-4) (Govender, Stolnik et al. 1999, Agnihotri, Jawalkar et al. 2006). A permeant that can move through the intestinal mucosa will predominantly take the pathway with the lease resistance (Govender, Stolnik et al. 1999).

1.3.2.2 Transcellular pathway

Drug permeation via the transcellular pathway involves movement across the cell membrane and traversing the transcellular spaces. Lipophilic compounds are more likely to cross this way since the cell membrane is lipophilic itself. It is difficult for hydrophilic compounds to cross the cell membrane due to a low partition coefficient (Jiang, Gan et al. 2012), but the passive diffusion of small hydrophilic compound may take place through the aqueous pores in the cell membrane (Snehalatha, Venugopal et al. 2008).

1.3.2.3 Paracellular pathway

The paracellular route involves the passage through the cell-cell junctions and the intercellular spaces between the epithelial cells (Fredenberg, Wahlgren et al. 2011). Compared to the transcellular pathway, tight junction in paracellular pathway generates the main obstacles for drug permeation (Möckel and Lippold 1993). Lipophilic drugs are absorbed via diffusion through the lipids in the paracellular spaces, and hydrophilic compounds are absorbed via aqueous channels in the transcellular spaces (Fredenberg, Wahlgren et al. 2011).

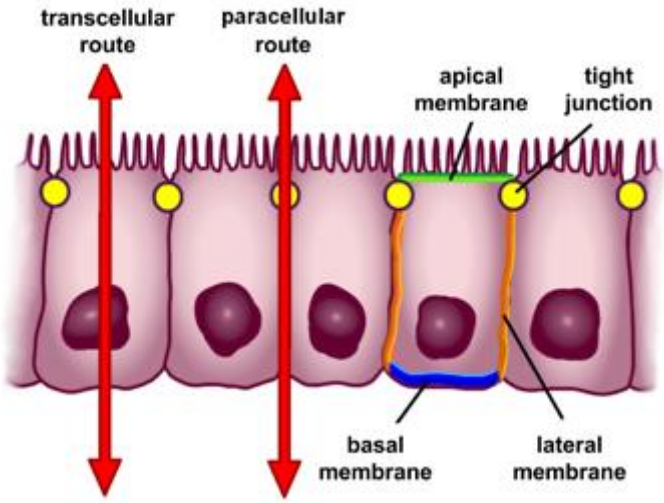

Figure 1-4. Mechanism of drug permeation through intestinal epithelial membrane (Luan and Bodmeier 2006).

1.3.2.4 Carrier-mediated transport

The most notable features of carrier-mediated transport are its substrate specificity, saturability and regional. In general, carrier mediate transport is an energy dependence transport, which is considered as active transport. Passive diffusion is generally considered to be the predominant transport mechanism for drug absorption through the intestinal mucosa, however, specialized transport systems that facilitate carrier-mediated transport and facilitated diffusion have also been reported for a small number of compounds (Jiang, Gan et al. 2012). Sugar transporter systems have been reported to be involved in the transport of D-

glucose (Qi, Xu et al. 2005). Additionally, a specific transport mechanism has also been identified in the transport of vitamin C (Makhlof, Werle et al. 2011), nicotinic acid and nicotinamide (Kulkarni and Feng 2013) and thiamine (Unger, Wittmar et al. 2007).

1.4 Strategies to enhance bioavailability of gemcitabine

In order to enhance oral bioavailability of drug candidates, many approaches have been carried out in the past. Including chemical modification, absorption enhancer, enzymatic inhibitor, and advanced drug carrier systems.

1.4.1 Chemical modification

Chemical modification of the drug candidate is a direct way to change the chemical structure and function of the drug, and improving its physicochemical characteristics. For instant, lipidization of the drug; cationization of the drug; and PEGylation of the drug are the common chemical modifications to enhance oral bioavailability of drug candidates (Habgood, Begley et al. 2000).

1.4.1.1 Lipidization

Lipophilicity is a main parameter in determining the rate at which drugs passively cross the intestinal mucosa. Rapidly and completely transported drugs are generally lipophilic and distribute readily into the epithelial cell membranes of GIT. In a drug molecule, the polar side groups impart a degree of dipolarity and hydrogen bonding. In general, the hydrophilicity decreases as the increase in hydrogen bonds. More polar groups within a molecule lead to more hydrogen bonds, thus, lower lipophilicity. The overall polarity of a drug molecule can be reduced either by adding a non-polar or removal a polar group (Habgood, Begley et al. 2000). Once the modified drug molecule has entered into the systemic circulation, it should be converted to its active form for utilisation in the body system.

One example is the formation of heroine. Morphine has two hydroxyl groups and does not enter to systemic circulation readily. Morphine can be acetylated by substituting two hydroxyl groups, thus forming heroine. The substitution of two hydroxyl groups results in the removal of two pairs of hydrogen bonds (Pardridge and Mietus 1979). Therefore, the heroine

is highly lipid-soluble and readily enters to blood circulation. Once within the systemic circulation, the diaceyl morphine is rapidly metabolized to morphine, and it is in this form that it interacts with opoid receptors within the brain (Hansen, Stapelfeld et al. 1992).

1.4.1.2 Cationization

Molecular charge plays a significant role in the oral drug delivery across the intestinal barriers. Cationic compounds are more permeable while anionic compounds do not readily penetrate through the intestinal mucosa. This is due to the overall anionic nature of the intestinal wall (Witt, Gillespie et al. 2001). Hence, formulating a cationic drug is postulated to increase uptake of the drug into the systemic circulation by increase membrane permeability. However, potential toxicity of this strategy limits its therapeutic clinical use. Cationization has been shown to form immune complex with membranous neuropathy (Witt and Davis 2006). This strategy also has non-specific targeting in terms of tissue uptake. Furthermore, cationization may cause potential toxicity in the kidney and liver due to increase plasma protein binding as well as rapid and significant changes to drug clearance.

1.4.1.3 Prodrug formation

Acetylation of hydrophilic compounds is known as prodrug formation. Prodrug approach involves the conjugation of active moieties to either molecules with known transporters or to lipophilicity enhancers, which are cleaved at or near the site of action, allowing drugs to induce their effects (Witt, Gillespie et al. 2001, Lao, Venkatraman et al. 2008). Ester is a good compound to be designed as prodrug for oral drug delivery, due to the numerous endogenous esterases in body system. Esterification of hydroxyl, amino acid, or carboxylic acid containing drugs may significantly increase lipophilicity, thus, increase permeation of drug over intestinal mucosa. Hydrolysis of the esterfied groups will eventually releases the active compound (Wang, Wang et al. 2002, Loo, Tan et al. 2010).

However, the highly lipid-soluble drugs may be extensively bound by plasma protein, this may lead to a significant reduction of free drugs in the plasma. As a result, the amount of drug that available at site of action is reduced. Especially for a peptide drug, modification of a peptide drug maybe diminishes the specificity to the receptor and reduces the specific receptor binding. In addition, considerations need to be made for unhindered conversion into

the active component once the drug has crossed the intestinal mucosa (Janoria and Mitra 2007).

1.4.1.4 PEGylation

The covalent attachment of polyethylene glycol (PEG) to therapeutic polypeptides is termed PEGylation and has been shown to elongate a biological half-life due to steric hindrance against proteolytic enzyme, increase in the molecular mass and improve both pharmacokinetic and pharmacodynamic properties (63). These features of PEGylation hold true for most of the oral administered drugs (Sansdrap and Moës 1997, Berchane, Carson et al. 2007).

Many PEG derivatives have been developed as bioconjugation reagents. Liu, *et al* have used a novel graphitic material called nanographene oxide (NGO) with branched PEG forming NGO-PEG conjugate, and using this conjugate to PEGylated a drug carrier system loading water-insoluble cancer drugs SN38. This NGO-PEG-SN38 exhibited great water solubility while maintaining its promising anticancer potency (Manjunath and Venkateswarlu 2005). Dembereldorj, *et al* developed a promising PEGylated graphene oxide (PEG-GO) platform for delivery of anticancer drugs doxorubicin (DOX). This PEG-GO-DOX showed greater *in-vitro* drug release and higher bioavailability in mice compared to the unmodified drug solution without PEGylation (Peltonen and Hirvonen 2008). Oishi, *et al* developed a pH-sensitive PEGylated nanogel for delivery of anticancer drug DOX, showing a great drug loading, and great drug uptake on the human hepatoma cell line HuH-7, which is a natural drug-resistant tumor line, as well as a promising anticancer effect in *in-vivo* pharmacodynamic studies (Chattopadhyay, Huff et al. 2006).

1.4.2 Absorption enhancers

The absorption enhancers are a varied class of chemical moieties that enhance the permeability or transport of molecules across intestinal epithelial membrane (Vihola, Laukkanen et al. 2002). They may alter the structural integrity of the epithelium or by simply improving drug diffusion across the intestinal epithelial membrane (Vihola, Laukkanen et al. 2002, Kafka, Rades et al. 2010). Absorption enhancers have different mechanisms of action

which include: a change in membrane fluidity, a decrease in mucus viscosity, leakage of proteins through membranes, and opening tight junctions (Kafka, Rades et al. 2010).

It is known that permeation through the intestinal epithelium occurs either by the transcellular or by the paracellular route, but in general, the overall process can be considered to be governed by passive diffusion (Pappenheimer 1987) and modeled by Fick's first law of diffusion, as shown in the following equation:

$$\mathrm{Jss} = \frac{\mathrm{D} \times \mathrm{A} \times \mathrm{CD}}{\mathrm{h}}$$

Where the steady state flux (Jss) is what we are measuring when studying diffusion. D is diffusion coefficient which is the constant that describes how fast or slow drug diffuses, (A) is the area of the membrane, the concentration of drug in the donor compartment (C_D) is that concentration difference across the membrane, and (h) the thickness of the membrane. Most of the permeation enhancers will alter the mucosa or the permeating molecule in such a way that D or K or both can be enhanced (King and Johnson 1985, Pappenheimer 1987).

Current absorption enhancers in oral drug delivery include various classes such as surfactants, fatty acids, chelators, detergents, and chitosan, which are usually applied in formulations in various capacities and concentrations, and often promote the drug absorption over intestinal mucosa. Among all of these, chitosan is more commonly used, it has been studies for its enhanced permeation effect for many oral administered drugs (Lu, Kopečková et al. 1999, Shire, Shahrokh et al. 2004, Houchin and Topp 2008). Chitosan is a biodegradable, nontoxic polymer obtained by deacetylation of the N-acetyl glucosamine units of chitin, generally by hydrolysis under alkali conditions at high temperature (Shire, Shahrokh et al. 2004). Chitosan also constitute semi-natural bioadhesive polymer. The phenomenon of bioadhesion allows a greater amount of drug to be retained at the target absorption site resulting in increased systemic delivery (Tomita, Hayashi et al. 1988). The ability of the mucoadhesive polymers to adhere to mucin layer on the mucosal epithelium can improve oral bioavailability of drug candidates. Therefore, chitosan owing to its multifunctional effects have generated significant interest. In the review article of Park, *et al*. They reported the chitosan and its derivatives have significant improvement in oral delivery of anticancer drug to treat various cancers (Rubas, Cromwell et al. 1996).

Currently, other new chitosan derivatives have been developed to improve permeation enhancement, such as chitosan-thiobutylamidine (Giannasca, Giannasca et al. 1999), methyl-pyrolidinone chitosan (Clark, Hirst et al. 2000), and N-trimethy chitosan (TMC) (Frey and Neutra 1997). TMC is a partially quaternized chitosan derivative which, unlike chitosan, is soluble at neutral and basic environments, thus it is characterized by good solubility in neutral physical pH, and permeation enhancing effect as well (Sandri, Bonferoni et al. 2010, Jin, Song et al. 2012). The drug carrier system prepared by TMC have demonstrated superior absorption relative to chitosan carrier systems through increased contact with intestinal epithelium and mucoadhesion with the ability to promote both transcellular and paracellular absorption. Therefore, TMC has been studied in this project. Furthermore, it is widely recognised that chitosan and its derivatives should have no toxic adverse effects (Porter and Charman 1997, Li, Zhao et al. 2009). However, several reports indicated absorption enhancers can cause damage, or can even enter the systemic circulation due to their low molecular mass leading to systemic toxic effect (Yuan, Chen et al. 2007)

1.4.3 Microparticulate carrier systems

Microparticles are generally defined as a solid porous spherical particle with the size varying 1-100 micrometer (μm) containing a core substance (Lin, Zeng et al. 2004, Veltkamp, Jansen et al. 2008, Shrivastava and Gupta 2011). The word microparticle means particles with micrometric dimensions classifiable in microcapsules and microspheres, according to their structure, illustrated in Figure 1-4.

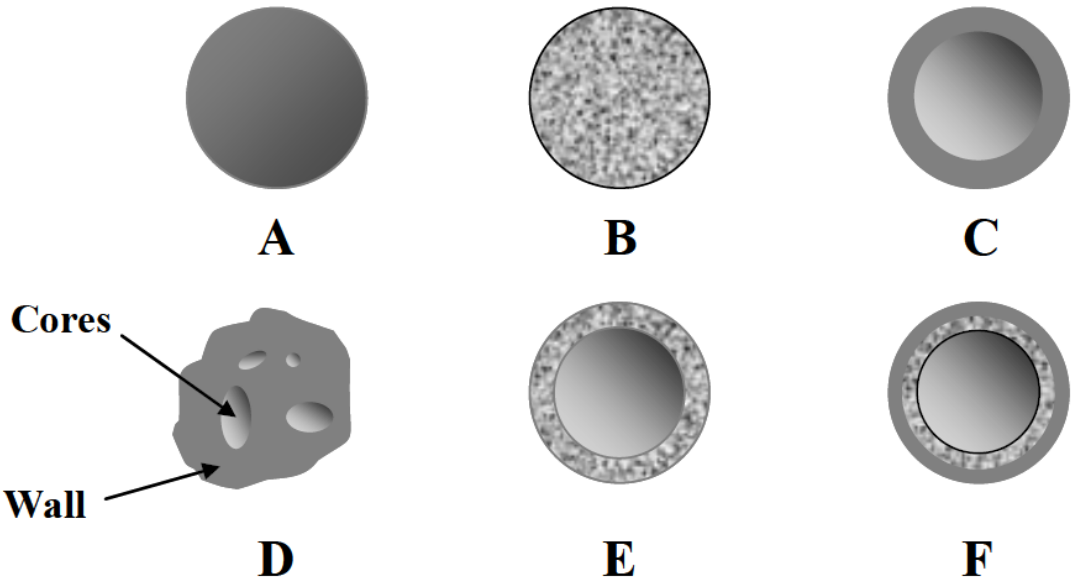

Figure 1-4. Structure of microparticles: A) Homogeneous microsphere or gel type; B) Monolithic microcapsule (matrix type); C) Mono-nucleated microcapsule; D) Poly-nucleated microcapsule; E) Type double core microcapsule; F) Microcapsule with double wall (Lauren, J.R *et al*., 2003).

Microparticles are popular to be used is due to the major advantage of absorption enhancement and thus elevation in bioavailability of the drugs, since the high surface to volume ratio and more intimate contact of the drugs with the intestinal epithelial layer. The presence of bioadhesive polymers, results in easier to uptake by epithelial cells, thus improve the permeation through the cell membrane (Faisant, Siepmann et al. 2002, Lin, Zeng et al. 2004). It can be formed from a number of different polymers such as chitosan (Guideline 2005, Chen, Svirskis et al. 2015), methyl cellulose (Chen, Li et al. 2014) or polylactide-co-glycolide acid (PLGA) (Chen, Li et al. 2014). Microparticles have been investigated for drug delivery and it has been shown that encapsulation of various hormones (e.g. leuprorelin and androgens) in PLGA microparticles achieved a sustained biological activity both in animal models and human (Kirkland, Yau et al. 1977, Hayakawa, Kondo et al. 1980). Other components such as polyvinyl acetate (PVA) and tocopheryl polyethylene glycol succinate (TPGS) can be applied as particle stabilizer and drug loading enhancer when fabricating PLGA microparticles (Mathialagan and Hansen 1996, Li, Martini et al. 2012). Surface modification of microparticles by conjugation, crosslinking or coating, for example, collagen microparticles modified by photochemical crosslinking (Armbruster, Tillman et al. 1994,

BESTPPE.COM
List of research project topics and materials

Dongre, Shah et al. 2008). gelatine microparticles crosslinked with genipin (Sistla, Tata et al. 2005) and silk coated PLGA and alginate microparticles (Blessy, Patel et al. 2014) has been used to further prolong the release of drugs. Moreover, Boisdron-celle, *et al*. developed a biodegradable microparticle as an anticancer drug carrier for delivery of 5-fluorourcil. The microparticle showed a great drug loading capacity and drug entrapment efficiency, as well as a sustained drug release manner, indicating its suitability for anticancer drug delivery (Borisagar, Patel et al. 2012). Yu, *et al.* synthesized an insulin-loaded composite alginate/PLGA microparticulate system which exhibited improved encapsulation efficiency (EE) and prolonged drug release compared to conventional microparticles (Naga Malleswararao, Suryanaryana et al. 2012). Several new microparticulate systems such as temperature-responsive microspheres (Jansen, Akers et al. 2000), dynamic hydrogel microspheres (Magenheim, Levy et al. 1993) and glucose-responsive microspheres (Saab, Magda et al.) have been designed to release drug candidate following stimulation by various triggers.

Although various microparticles mentioned above could be prepared for encapsulation of anticancer drugs, their particle characteristics, such as size, physical stability and release rate, are important for enhancing anticancer drug activity. It is important to optimize the conditions of microparticles so that they can deliver the drug candidate efficiently to the target. Kumar, *et al.* showed the β-glucan microparticles might protect the loaded drug against gastric conditions (Marschütz and Bernkop-Schnürch 2000). However, chitosan will swell and dissolve at gastric pH. To address this short coming of chitosan derivatives such as chitosan-succinate, chitosan-phthalate and trimethyl chitosan have been proposed due to their low solubility under acidic condition and higher solubility under alkaline condition (Marschütz and Bernkop-Schnürch 2000).

1.4.4 Nanoparticulate carrier systems

Nano-particulate carrier systems, usually with particle size of less than 1000 nm, such as polymeric or lipid nanoparticles, microemulsions, niosomes and liposomes for oral drug delivery are of interest mainly owing to the possibility of absorption by transcellular endocytic pathways. During the process of endocytosis, the plasma membrane invaginates and pinches off to form enclosed vesicles. Thus, upon uptake by cells through receptor-mediated endocytosis, particles would deliver encapsulated drug from the intestine to the

systemic circulation (Jung, Kamm et al. 2000). Particle size has a significant impact on the pathways of intestinal drug absorption. Particles smaller than 500 nanometer (nm) are usually internalized by endocytosis (Zhang, Li et al. 2009). Literature evidence also indicates that particles of less than 500 nm showed significantly higher absorption than larger particles (1 μm to 10 μm) (Petros and DeSimone 2010). Furthermore nano-particulate delivery systems are of interest for the orally delivery gemcitabine because they may provide protection of gemcitabine from enzymatic degradation, provide a controlled release rate, and targeting gemcitabine to specific intestinal sites, sustained releasing the drug in the systemic circulation, thus to enhance the therapeutic effect. However, limitations of nano-particulate carrier systems are usually associated with low loading efficiency and particle aggregates due to thermodynamic instability (Weiss, Decker et al. 2008). The major challenge facing such delivery systems for oral delivery of gemcitabine includes ensuring sufficient gemcitabine with uniform nano-scale dimension is delivered to the site of absorption and its release profile in the body.

1.4.4.1 Microemulsion

Definitions of what constitutes a microemulsion have been proposed since at least as early as 1981. Microemulsion is an isotropic, thermodynamically stable transparent system which consists of oil, water, and surfactant, frequently in combination with a co-surfactant (Artursson, Palm et al. 1996). Droplet size is typically less than 200 nm (Wilson, Hassan et al. 1990, Walter, Janich et al. 1996). Structurally, they are divided into oil-in-water (O/W), water-in-oil (W/O) and bicontinuous microemulsion (the amounts of water and oil are similar) (Agullo, Gamet et al. 1994). The type of microemulsion formed is influenced by the surfactant type. Surfactants with a hydrophilic lipophilic balance (HLB) value > 12 are predominantly hydrophilic and favour the formation of O/W emulsions, while surfactants with HLB values < 12 are hydrophobic and form W/O emulsion (Yang, Lu et al. 1999). Surfactants having HLB greater than 20 often require the presence of co-surfactants to modify the overall HLB of the system. In addition, the surfactant and co-surfactant ratio was a key factor influencing the phase properties of microemulsions. Thus a mixture of oil, water, and surfactants/or co-surfactants are able to form a wide variety of structures and phases depending on the proportions of these components (Yang, Geng et al. 2009).

The use of microemulsion as carriers for orally administrated drugs has been investigated for the improved drug solubilisation and protection against enzymatic degradation as well as the potential for enhanced absorption due to the inclusion of absorption afforded by surfactant/or co-surfactant induced membrane fluidity and thus permeability changes (Grit and Crommelin 1993, Grit, Underberg et al. 1993). It has been reported that microemulsions have successfully enhanced the oral bioavailability of various drugs. For example, Naicker *et al.* described cyclosporin A in an O/W microemulsion system which provided superior drug bioavailability and reduced adverse effects associated with oral administration (Wulff-Pérez, Barrajón-Catalán et al. 2014). Kraeling and Ritschel found that the oral bioavailability of insulin dissolved in W/O microemulsions showed an increase (~2.1%) compared to intravenous insulin (Chiou 1978). The improved oral delivery of insulin from microemulsion systems has been reported by others (Lipinski 2000, Han and Wang 2005, Davis, Little et al. 2006). There are limited numbers of investigations into microemulsion based formulations of gemcitabine, focused mostly on the ability of gemcitabine to influence emulsion stability (Brechue and Maren 1993, Prausnitz and Noonan 1998, Davis, Little et al. 2006). Additionally, gemcitabine has also been shown to be able to improve the physical stability of microemulsion in response to pH changes, high salt concentration and temperature (Amidon, Lennernäs et al. 1995, Hubatsch, Ragnarsson et al. 2007, Williams and Barry 2012). Furthermore, microemulsion systems have also been claimed to improve storage stability of drug candidates. For example, improved chemical stability of horse radish peroxidase after storage in W/O microemulsion compared to aqueous solution has been reported (Zhang and Benet 2001). In recent years, self-microemulsifying drug delivery systems (SMEDDS), which emulsify spontaneously when exposed to fluids of the GI tract to form microemulsions, are receiving increased attention as a possible means to enhance the oral bioavailability of drug candidates (Zhang and Benet 2001, Yılmaz and Kadıoğlu 2004), and may provide a new approach for the oral delivery of anticancer drugs. However, the use of microemulsion is limited not only by drug loading capacity but also the amounts of excipients. Surfactants and cosolvents may have toxic effects at high doses, and result in the reduced uptake levels. Formulators aim to optimize microemulsion systems with maximum drug loading efficiency while using minimum amounts of surfactant and cosolvents (Ansari, Tingstedt et al. 2013).

1.4.4.2 Liposomes

Liposomes are artificial small vesicles composed of one or more phospholipid membrane bilayers surrounding aqueous inner phase. The reported sizes range is 15 nm to 10 µm (Allen and Everest 1983, Ingebrigtsen and Brand 2002, Ivić, Petrović et al. 2016). Liposomes are composed of biocompatible and biodegradable phosphate lipids similar to biological membrane (Figure 1-5).

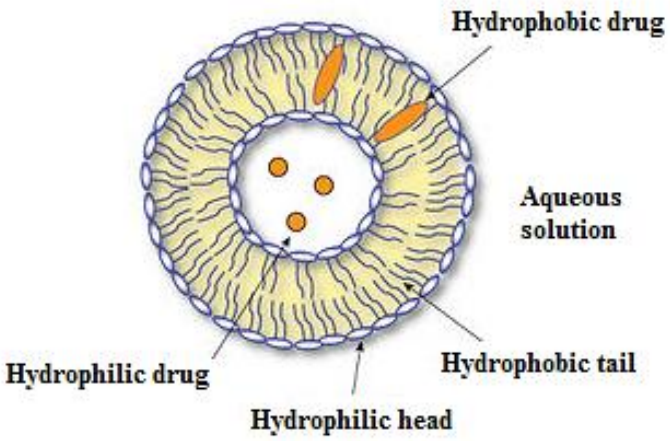

Figure 1-5. Basic liposome structure as drug carrier system.

Liposomes can be classified into six categories based on their size and numbers of bilayers as follow: small unilamellar vesicles (SUVs), large unilamellar vesicles (LUVs), multilamellar vesicles (MLVs), multivesicular vesicles (MVVs), oligolamellar vesicles (OLVs) and giant unilamellar vesicles (GUVs) (Figure 1-6) (Guetens, De Boeck et al. 2002, Grob and Barry 2004, Gali-Muhtasib, Roessner et al. 2006, Kirstein, Hassan et al. 2006, Pavia 2006, Teradal, Kalanur et al. 2012, Ivić, Petrović et al. 2016). Lipophilic molecules are embedded in the phospholipid layers while hydrophilic molecules are entrapped in the aqueous inner cavity. In this way, liposomes can carry both lipophilic and hydrophilic drugs concurrently.

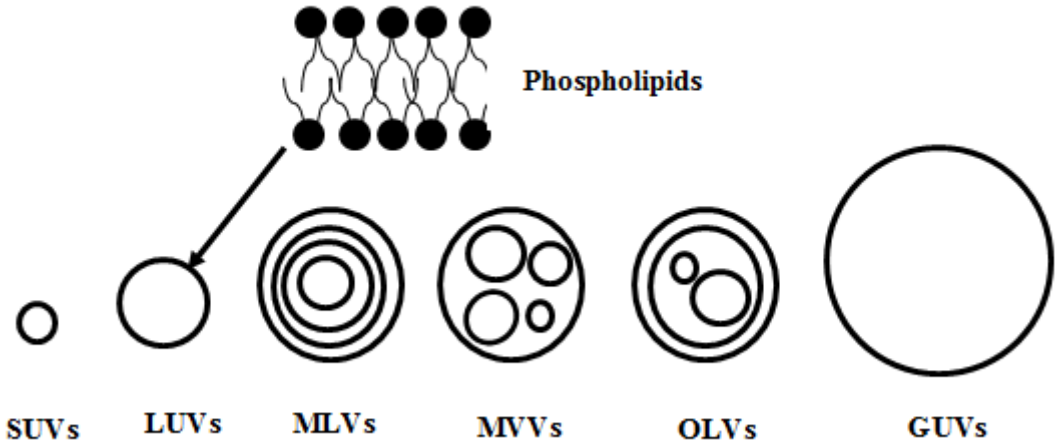

Figure 1-6. Different model membranes of liposomes. SUVs: small unilamellar vesicles; LUVs: large unilamellar vesicles; MLVs: multilamellar vesicles; MVVs: multivesicular vesicles; OLVs: oligolamellar vesicles; GUVs: giant unilamellar vesicles.

The amphiphilic nature of liposomes makes them suitable for many drugs delivery. The lipid bilayer can entrap lipid-soluble compounds whereas the aqueous core can dissolve water-soluble drugs. Due to the negatively charged properties of the intestinal epithelial membrane, cationic liposomes promote interaction with epithelial cell resulting in the enhanced cell uptake. Cationic liposomes have been used to encapsulate genetic materials to protect them from the extracellular environment and provide a mechanism for genetic materials transfer to target cell (Davis 1997). Coupling the liposomes with an antibody or a target ligand that will be recognized by cell surface receptors can induce specific uptake of the drug-loaded particles into the intestinal epithelial cells, after which the drug can be released into the systemic circulation. Liposomes can also be used as pH-sensitive carriers for delivery drugs to target tissues (e.g. a low pH in inflammatory tissues and tumours) (Alcon, Baca-Estrada et al. 2005). PEGylated immunoliposomes have been used to targeted transfect β-galactosidase and luciferase into the brain by oral delivery route (Shi, Zhang et al. 2001). Liposomes coated with PEG have been proven to prolong the blood circulating time and reduce clearance by liver metabolism. Liposomes have been considered for tumour targeting in several pathologies mostly through intravenous administration. Immordino, *et al* developed a liposome encapsulating lipophilic gemcitabine prodrugs, which showed a great protection of the drug from degradation in plasma, and elevated the drug plasma half-life (Salmaso). Paolino, *et al* have prepared a gemcitabine loaded PEGylated unilamella liposomes to treat cancer. Compared with the market drug GEMZAR®, the liposome delivery system has

improved the *in-vivo* drug biodistribution, drug pharmacokinetic profile, plasma half-life and effectively inhibited the tumour growth (Anton, Mojzisova et al. 2010).

Because of the nature of the compounds used for their preparation, liposomes are considered as biocompatible and biodegradable. The advantages of liposomes are relatively non-toxicity, specific targeting release, enhanced plasma half-life, and decreased clearance. However, the stability of this system is a main drawback to be concern. Most of studies have shown quite significant drug leakage from the developed liposomes (Salmaso , Sacchi, Gasparri et al. 2006). Furthermore, despite extensive studies in the technology, the good *in vitro* results are not related to the *in vivo* results. The ability to reproduce this formulation on an industrial scale with even uniformity is challenging and the commercial success of liposome technology is still limited (Lian and Ho 2001, Losa, Sierra et al. 2006).

1.4.4.3 Niosomes

Niosomes are non-ionic surfactant bilayered vesicles similar to liposomes which form spontaneously. Advantages of this approach include low cost, great stable, low toxicity due to their non-ionic nature, ease of storage, flexibility in their structural constitution, biocompatible and biodegradable, enhancement of drug uptake and controlled release at specific targeting site (Yoza, Ito et al. 1980, Carafa, Santucci et al. 2002). Dufes, *et al* have investigated the anticancer drug doxorubicin loaded glycol chitosan niosomes to treat cancer. The in-vitro studies have shown great drug uptake in the drug resistant tumour cells A2780AD cells and A431 cells, as well as a superior *in vivo* safety profile was obtained compared to the free drug (Sottani, Turci et al. 2007). Parthasarathi *et al*, were using non-ionic surfactant niosomes to encapsulate anticancer drug vincristine sulfate. The toxicity of drug candidate was reduced after niosome encapsulation and the anticancer activity was improved, which indicated its suitability for anticancer drug delivery (Ali, Haque et al. 2013). Vasoactive intestinal peptide (VIP) is an example of a drug which can be incorporated into glucose-bearing niosomes. The study suggested that encapsulation within glucose-bearing niosomes allowed a significantly enhanced oral administered VIP on intestinal drug uptakes (Dufes, Gaillard et al. 2004).

1.4.4.4 Nanoparticles

Nanoparticles (NPs) are well-defined, solid, colloidal particles, ranging in size approximately from 1 to 1000 nm (usually 200-300 nm) (Lin, Zeng et al. 2004). Therapeutic agents can be adsorbed to the surface of particles, or entrapped in the particles or covalently attached (Lockman, Mumper et al. 2002). The NPs can be categorized into capsule or sphere (Figure 1-7). Capsules are reservoir systems with a drug containing hollow core that is surrounded by a layer of polymer that acts as a diffusional barrier. Spheres, on the other hand, are polymeric matrix systems with drug being dispersed in it. Figure 1-7 is schematic presentation of different types of spheres and capsules (Brandau 2002, Costantino, Tosi et al. 2009).

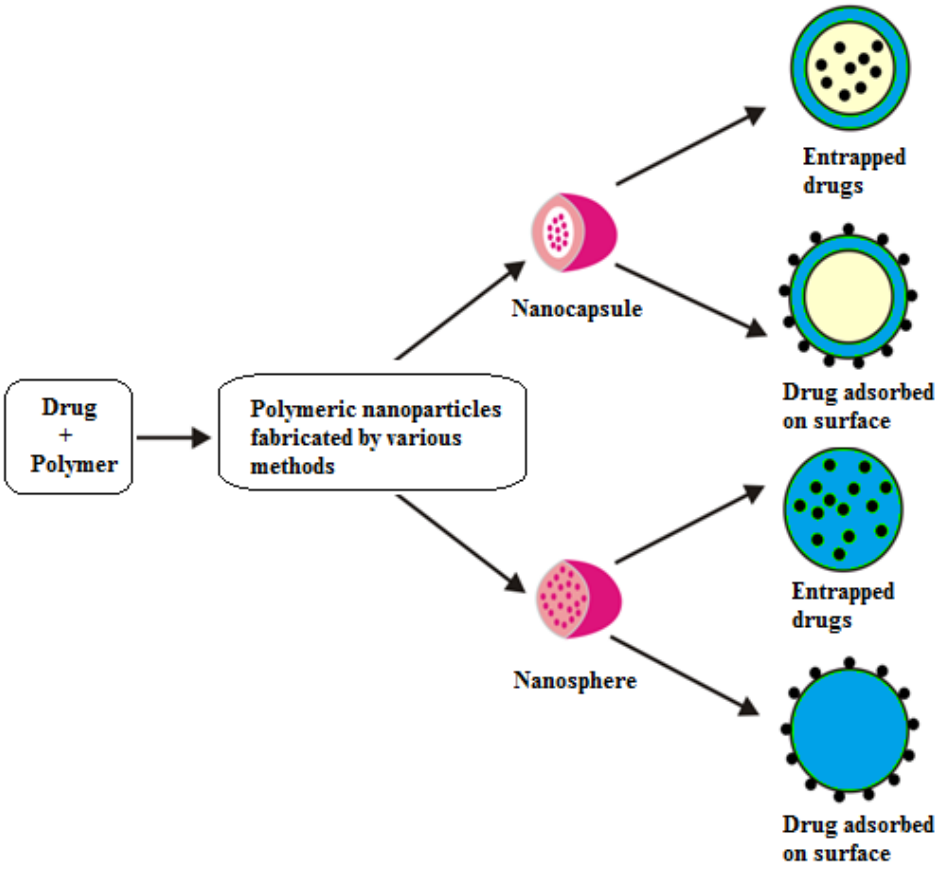

Figure 1-7. Schematic drawing of nanocapsules and nanospheres.

Polymeric NPs are suitable for delivering small molecular weight drugs and macromolecules by either localized or targeted delivery to the tissue of interest (Moghimi, Hunter et al. 2001). In addition, NPs allow the incorporation of either lipophilic or hydrophilic drug candidates into the cavity, thus allowing the delivery of a greater range of drug compounds. Polymeric

particles isolate the encapsulated drugs from the external medium in the gastrointestinal tract thereby protecting the drugs from chemical or enzymatic degradation thus improving the bioavailability. Various coatings such as chitosan and trimethyl-chitosan can be incorporated onto the surface of these particles to increase absorption of the NPs across the GIT (Aktaş, Yemisci et al. 2005, Lopedota, Trapani et al. 2007, Veltkamp, Jansen et al. 2008). The loaded drugs can be released in a controlled manner by desorption, diffusion through the NP matrix or polymer wall or NP erosion (Lockman, Mumper et al. 2002, Costantino, Tosi et al. 2009). Thereby, slow release of drug from the particles facilitates sustained levels of drug therapeutic concentrations.

Common polymeric materials used for formulation of NPs include poly lactic acids (PLA) (Abbruzzese, Grunewald et al. 1991), polyanhydride, poly(D,L-lactide-co-glycolide) (PLGA) (Kubicka, Rudolph et al. 2000), gelatin (Dintaman and Silverman 1999), or chitosan (Ma, Zheng et al. 2010). There are various methods for the preparation of NPs such as interfacial polymerization, solvent evaporation and phase separation (Lin, Zeng et al. 2004, Losa, Sierra et al. 2006). The solvent evaporation method is widely used due to its simplicity and high drug entrapment efficiency. A number of studies have demonstrated that NPs can enhance the oral bioavailability of encapsulated therapeutic drugs. For instance when calcitonin was incorporated in NPs, oral absorption was enhanced in rats and consequently calcium concentration in blood was decreased with oral administration of a calcitonin solution (Yu, Bridgers et al. 1999). Anticancer drugs have been encapsulated in PLA NPs (Youk, Lee et al. 2005), PLGA-polyvinyl alcohol composite NPs (Neuzil, Tomasetti et al. 2007) and gelatine NPs (Constantinou, Papas et al. 2008). Many insulin-loaded NPs of PLGA (Snyman, Hamman et al. 2003), PCL (Sahni, Chopra et al. 2008) and chitosan (Ma, Zheng et al. 2010) have been formulated and maintain the integrity of insulin for oral administration with high drug entrapment efficiency ranging from 70% to 96%. EL-Shabouri explored chitosan NPs to increase absorption of cyclosporia A (Sonavane, Tomoda et al. 2008). As mentioned earlier chitosan has mucoadhesive properties, and is able to adhere to the apical intestinal cell membrane. Its absorption enhancing properties are attributed to the ability to reduce the transepithelial electrical resistance by transiently opening tight conjunctions and allowing the passage of small electrolytes. When dextran sulfate is incorporated into chitosan NPs forming Chitosan-dextran sulfate NPs, longer times of the circulation of drugs have been reported to be due to the intrinsically hydrophilic properties (Jani, Halbert et al. 1990).

Bestpte.com

There are very few investigations into encapsulation of gemcitabine within NPs for oral delivery, but the tumour targeting ability of gemcitabine has been investigated as a ligand conjugated with NPs to construct a parenteral delivery system (Gasco 1993, Todokoro and Ezumi 1999, Beaucage, Kammler et al. 2004, Mu and Seow 2006, Phenrat, Kim et al. 2009, Van Eerdenbrugh, Vermant et al. 2009, Mondal, Halder et al. 2010). Win and Feng have developed a PLGA NPs for oral delivery of anticancer drug. The optimal formulation has shown great cellular uptake on human colon adenocarcinoma cells, indicating it is highly feasible for NPs of biodegradable polymers PLGA to be applied to promote oral chemotherapy (He, Hu et al. 2010).

1.4.5 Polymers

Polymeric particles could be fabricated from biodegradable or non-biodegradable polymers. Examples for non-biodegradable polymers are polyamide, polymethyl methacrylate and polystyrene. Biodegradable polymers are preferred as drug release rate from non-biodegradable matrix is very low. Biodegradable polymers would not lead to polymer accumulation in the body as the polymers are degraded to non-toxic metabolites that can be excreted from the body (Gad 2008).

1.4.5.1 Biodegradable Polymers

Biodegradable polymers are widely used in the controlled delivery systems because they can be degraded and expelled by human body and cause no harm to human. Biodegradable polymers can be categorized into synthetic and natural polymers. Chitosan, gelatine, collagen, bovineserum albumin (BSA) and human serum albumin (HAS) are natural polymers that have been studied for pharmaceutical applications. The disadvantage of natural polymers is their impurity. The synthetic polymers that have been used to formulate NPs are PLA, poly(ε-caprolactone), poly(amino acid), polyanhydride, PLGA and poly (alkyl cyanoacrylate). Synthetic polymers are preferred as they provided a more sustained drug release over a period of days to weeks compared to natural polymers. This is because synthetic polymers have a slow rate of degradation (Gad 2008). Other advantages of synthetic polymers are high product purity, less batch to batch variation and lack of immunogenicity (Pillai and Panchagnula 2001).

Although the number of biodegradable polymers is large, only a limited number of polymers are suitable for drug delivery applications. In general, the desirable biopolymer properties are film forming (coating), thickening (rheology modifier), gelling (controlled release), adhesion (binding), pH-dependent solubility (controlled release), solubility in organic solvent (taste masking), and barrier properties (protection and packaging) (Calvo, Remunan-Lopez et al. 1997, El-Shabouri 2002, Kumar, Bakowsky et al. 2004, Patil, Sandberg et al. 2007, Hunter 2013, Saberi, Fang et al. 2013). These biopolymers as drug carriers have been often presented as particulate spheres where the active molecules have been incorporated either inside the spheres or have been absorbed onto the surface or both. It is understood that while the drug is delivered at rates that maintain its optimum therapeutic activity at the active site, concurrently side effects should be minimized (Musumeci, Ventura et al. 2006). Thus delivering drugs using biopolymer systems are considered a primary choice when aiming to reduce adverse actions. Therefore, biopolymer materials have to be so chosen as to possess several characteristics that have been summarised as (1) Biocompatible and the ability to be eliminated from the body; (2) Enable hydrophobic drug encapsulation (e.g. formulated as micelles), favourably alter bio-distribution (e.g. formulated into nanoparticles) and prolong drug availability (e.g. formulated as hydrogels or microparticles) (Song, Zhao et al. 2008); (3) Processability, sterilizability and storage stability (Bala, Hariharan et al. 2004); (4) No inhibitory effects on drug therapies; and (5) The ability to target specific sites in the body.

Despite synthetic polymers offer the biggest advantage in that either homo- or co-polymers can be tailored uniformly to provide a wide range of properties, natural polymers extracted from abundant natural resources possess several inherent advantages such as bioactivity, the ability to present receptor-binding ligands to cells, susceptibility to cell-triggered proteolytic degradation and natural remodelling. Therefore, natural biodegradable polymers are considered as the first option. Proteins (e.g. gelation, collagen, and albumin) and polysaccharides (e.g. alginate, carrageenan, chitin/chitosan, trimethylated chitosan (TMC), starch and dextran) are examples of natural biodegradable polymers families that have been used in the production of drug delivery system (Budhian, Siegel et al. 2007, Song, Zhao et al. 2008, Song, Zhao et al. 2008, Yu, Zhao et al. 2011).

In this research, a biodegradable polymer PLGA and a polysaccharides polymer TMC are used as the bases to form NPs for oral delivery of gemcitabine.

BEST PFE.COM
List of research project topics and materials

1.4.5.2 Poly(lactide-co-glycolide) (PLGA)

For the biodegradable polymers, the most widely used polymers for NPs preparation is PLGA. Advantages of this polymer include biocompatibility, predictability of biodegradation kinetics, and ease of fabrication. PLGA has been approved for human use by the FDA (Mittal, Sahana et al. 2007). Both hydrophilic and hydrophobic drug molecules can be successfully encapsulated in the PLGA matrix. PLGA has been used for delivery drugs for both oral (Konstantinos 2004) and parenteral routes (Fonseca, Simões et al. 2002).

PLGA is a synthetic polymer that has been extensively studied for NPs preparation. PLGA is composed of lactic acid (PLA) and glycolic acid (PGA) monomers (Jalil and Nixon 1990). The polymer PLA itself is found in two stereoisoforms L-PLA and D, L-PLA (Jalil and Nixon 1990). The optically active form L-PLA exists in semi crystalline structures in nature due to compacting arrangements of polymer chain, while the optical inactive form D, L-PLA is an amorphous polymer due to irregular arrangement of its polymer chain structure. On the other hand, PLGA polymer is a highly crystalline structure. For this reason, the incorporation of D, L-PLGA is preferred as a better perfusion of the drug in the matrix structure of the polymer is possible (Cohen, Alonso et al. 1994). PLA is more lipophilic than PGA, thus, lactide-rich PLGA copolymers are less hydrophilic, absorb less water, results in slower degradation rate (Jalil and Nixon 1990, Cohen, Alonso et al. 1994). Both PLA and PGA have glass transition temperatures that are greater than 37ºC, which means that they are glassy and have high mechanical strength at room temperature. This is important as the polymers need to be mechanically strong enough to withstand the harsh processing conditions (Södergård and Stolt 2002). The mechanical strength, swelling behaviour, capacity to undergo hydrolysis, and subsequently the biodegradation rate are directly influenced by the crystallinity of the polymer (Wu 1995). The type of monomer and ratio of two monomers determine the total crystallinity (Jalil and Nixon 1990). The PLGA degradation rate is much faster when PLGA copolymers containing 50% lactic acid and 50% glycolic acid.

Figure 1-8 shows the degradation of PLGA occurs via a spontaneous hydrolysis of the ester linkages to yield individual non-toxic monomers of D,L-lactic and glycolic acid (Li 1999). The lactate will be converted into pyruvate and glycolate before entering the citric acid cycle where they will be degraded and is finally removed from the body as CO_2 and H_2O (Anderson and Shive 1997). The rate of this process is controlled by factors including the

polymer crystallinity, copolymer ratio, temperature, and pH (Couvreur, Blanco-Prieto et al. 1997). Because the rate of degradation is slow, the delivery carrier is expected to create and maintain a concentration gradient for 1-2 weeks and protect the drug from enzymatic and chemical degradation prior to release. Since the polymer degradation rate is slow, degraded products do not affect the normal functioning of the cell. Drug release rates can be modified by varying the polymer crystallinity, copolymer ratio, polymer molecular weight, and the porosity of the polymer matrix. Drugs entrapped in PLGA matrix not only protects drugs from enzymatic and chemical degradation but also allows modulating drug release from NPs. Thereby, slow release of drugs from particles facilitates sustained levels of drug concentration.

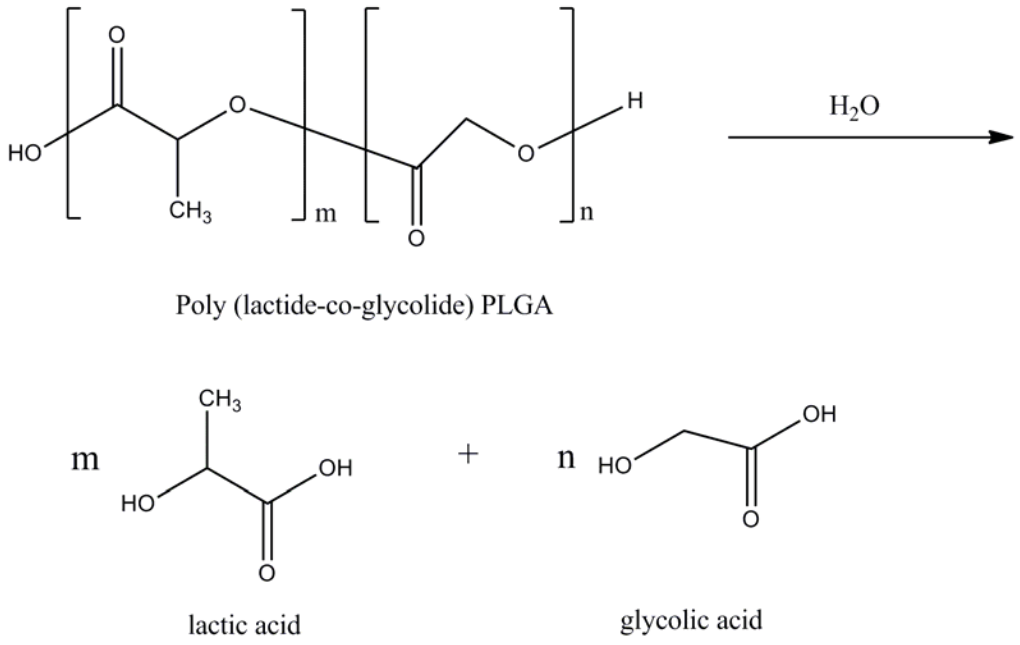

Figure 1-8. Schematic hydrolysis of PLGA into monomer units of lactic acid and glycolic acid.

1.4.5.3 Trimethylated chitosan (TMC)

The cationic characteristic of chitosan being based on the primary amino groups, which is responsible for many function roles, such as controlled drug release, absorption enhancing, and improving mucoadhesiveness properties. This linear polysaccharide derived by *N*-deacetylation of the natural polymer chitin. In nature, chitin is the second most abundant

naturally occurring polymer, which shows non-toxic, and has already been approved as a food additive in Japan. In addition, chitosan is a very outstanding polymer in drug delivery due to its high availability, high biodegradability and biocompatibility, as well as the ease of chemical modification. Thus it has been widely applied in both pharmaceutical and nutraceutical industries (Budhian, Siegel et al. 2007, Hung, Teh et al. 2010, Rouxel, Hadji et al. 2011). Although chitosan is widely studied as a potential permeation enhancer for drug delivery systems, the polymer is only soluble in an acidic environment, thus in body fluid, the solubility is very limited which lead to difficult in releasing the entrapped drug candidate. Therefore further chemical modification was done to chitosan.

N-trimethyl chitosan chloride (TMC), a soluble derivative of chitosan, which has attracted many formulation scientists recently, especially for the peroral drug delivery studies. Domard *et al,* first synthesised TMC (Murakami, Kawashima et al. 1997), then Kotzé et al further optimized the synthetic method based on Domard's method (Maa and Prestrelski 2000). TMC (Figure 1-9) is a partially quaternized derivative of chitosan which is generated by reductive methylation of the amino group on the chitosan with methyl iodide, sodium hydroxide and reacts over heat. The methylation also associates with catalyst to increase the formation step. The degree of quaternization can be improved by prolonging the reaction time (Robinson 1978, Pandey, Sharma et al. 2005)

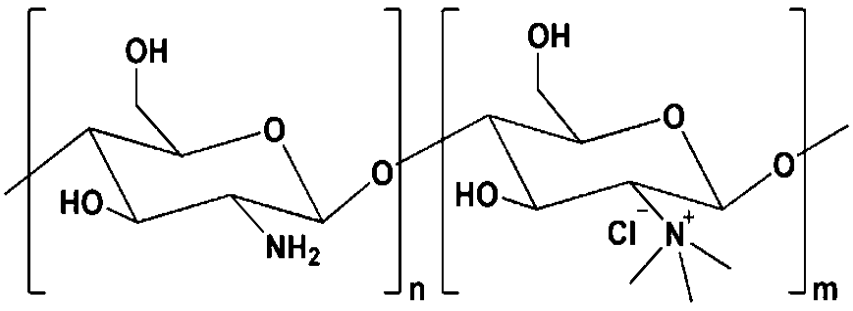

Figure 1-9. The chemical structure of TMC.

From the studies of Kotzé *et al* (Maa and Prestrelski 2000), chitosan was initially only soluble in acidic environment, but after methylation with methyl iodide, it became water soluble, and higher degree of the quaternization, better the solubility of the TMC in water. The increase in water solubility was attributed to the replacement of the primary amino group

on the C-2 position of chitosan with quaternary amino groups. (Figure 1-7). The increased solubility, either in acidic or basic environment, was even observed for a degree of quaternisation as low as 10%, which was determined by ^{1}H-NMR. A pronounced reduction in the TMC intrinsic viscosity during the synthesis process, compared to the initial chitosan was found, this phenomenon is attributed to the strong reaction conditions under which TMC is synthesised. Compare to chitosan salts, TMC is a derivative of chitosan that shows superior solubility in water and basicity character, even at low degrees of quaternization (Yamaguchi, Takenaga et al. 2002).

The molecular weights and polydispersity of the TMC polymers with different degrees of quaternization were previously determined with a multi-angle laser light scattering (MALLS), and a size exclusion chromatography (SEC). It was found the TMC molecular weight decreased with an increase degree of quaternization. In addition, the molecular weight of the TMC polymer chain increases during the reductive methylation reaction due to the addition of methyl groups to the amino group of the repeating chitosan monomers. However, a net reduction in the TMC molecular weight was found due to the polymer chain degradation caused by exposure to the specific reaction conditions such as heat during the synthesis process (Makadia and Siegel 2011).

As previously mentioned chitosan possesses mucoadhesive characteristic. The same is true for TMC. Snyman *et al* has conducted a study to investigate the TMC with various degrees of quaternization (ranging between 22% and 49%) for their mucoadhesive characteristics. It was found a lower intrinsic mucoadhesivity when compared to the chitosan, chitosan glutamate and chitosan hydrochloride. However, when compared to pectin, the reference polymer, TMC showed superior mucoadhesive features. The slight reduction in the mucoadhesion of TMC compared to the initial chitosan, which can be explained by a change in the conformation of the TMC due to interactions between the quaternary amino groups with a positive charge. Which possibly also reduces the flexibility of the polymer molecules. The interpenetration to the intestinal epithelial membrane by the TMC is influenced by a reduction in flexibility resulting in a subsequent decrease in intestinal mucoadhesivness (Yamaguchi, Takenaga et al. 2002, Qiao, Chen et al. 2005).

1.4.6 Methodologies for PLGA fabrication

1.4.6.1 Solvent evaporation/Emulsion evaporation

Solvent Evaporation is a most commonly used method for NP preparation, Polymer and drug are first dissolved in a non-miscible solvent such as ethyl acetate or dichloromethane (DCM). This is followed by the transfer of the organic phase to the aqueous phase containing a surfactant or stabilizers such as Polyvinyl Acetate (PVA) (Thanoo, Sunny et al. 1993), Tocopherol Polyethylene Glycol Succinate (TPGS) (Liu and Kiran 2008), chitosan (Jin, Song et al. 2012), poloxamer (Derakhshandeh and Fathi 2012), forming oil-in-water (O/W) emulsion. The mixture is subjected to high shear stress, which results in emulsion droplet size reduction. The term is derived when the organic solvent is eliminated by evaporation under vacuum and leading to the precipitation of polymer and NPs formation (Schoevaart, Wolbers et al. 2004).

The advantages of this method are 1) both hydrophilic and hydrophobic drugs are suitable for this method. 2) Additives such as PVA or chitosan can be incorporated to further reduce the size of the NPs. For disadvantages: 1) High energy consumption due to the requirements of high stress shear, thus results in shear-accelerated particle destruction. 2) Solvent evaporation leads to the solvent evaporated to the air causing aerosol hazards. 3) Time consuming process, more complex and labour-intensive method (Sonia and Sharma 2012). This method requires high energy input to reduce the particle size. There are various methods to reduce the particle size and they include probe sonication, homogenization, mechanical stirring and vortexing (Cafaggi, Russo et al. 2007). In this project, ultrasonicator was used.

1.4.6.2 Emulsion Diffusion

Organic phase containing the polymer and the drug are emulsified with the aqueous phase, lead to formation of oil-in-water (O/W) emulsion. A large amount of water is then added to the mixture resulting in the diffusion of the solvent from the emulsion droplet into the aqueous phase. The end result is the formation of NPs with the respective polymer of choice (Sandri, Bonferoni et al. 2010, Arya, Vandana et al. 2011).

The advantages of this method are: i) it is suitable for both hydrophobic and hydrophilic drugs; ii) The toxic solvent can be avoided to use; iii) Higher entrapment efficiency of lipophilic drug as a result; iv) Scale-up of the process can be accomplished easily. While for the disadvantages are: i) Large amount of water is required, thus the purity of the water should be aware of; ii) Hydrophilic drugs have the tendency to migrate to the external aqueous phase due to the polar solvent diffusion, resulting in low drug entrapment efficiency (Sondhi, Xu et al. 1998, Fan, Chen et al. 2014, Zhang, Zhu et al. 2014)

1.4.6.3 Nano-precipitation/ Solvent Diffusion

Polymer and the drug are first dissolved in a water soluble solvent. The mixture is then transferred drop-wise into the aqueous solution containing a surfactant or a stabilizer. Fast solvent diffusion into the aqueous phase occurs due to the solvent miscibility, which then leads to NPs formation and the solvent is eventually removed by rotatory evaporator (Kumar, Bakowsky et al. 2004, Dash, Murthy et al. 2010).

The advantages of this method are: i) Hydrophobic active drugs are commonly used with this method and it can be used for the preparation of particles that are present in the film formation of tablet formation; ii) The need for high toxic solvent is prevented; iii) Low energy consumption with regular stirring; iv) No high stress shear is required; v) It is a process which is easily to scale-up. For disadvantages: i) the process can be time consuming as solvent must be removed by evaporation. ii) Eliminating the residue of the solvent might also be difficult. iii) Hydrophilic drugs have lower loading efficiency since the poor hydrophobic interaction with the polymer (Sieval, Thanou et al. 1998, Barzegar-Jalali, Adibkia et al. 2008, Mourya and Inamdar 2009, de Britto, de Moura et al. 2012).

1.4.6.4 Salting out

The drug and the polymer are dissolved in an organic solvent, such as dichloromethane. This mixture will then be emulsified by strong mechanical shear stress in an aqueous phase containing the stabilizer and a high concentration of salting out agent. This forms oil-in-water (O/W) emulsion. NPs are subsequently formed when pure water is added immediately to this emulsion mixture. This occurs is due to the salting out agent effectively migrates to the aqueous phase. And salting out agent are then removed by cross-flow filtration,

centrifugation or washing (Mahler, Shuler et al. 2009, Hosseinzadeh, Atyabi et al. 2012, Zidan, Spinks et al. 2013).

The advantages are including: i) it is a common method to make latexes which can be used in film coating, granulating and also for controlled release preparations; ii) The method is less time consuming; iii) It reduces shear stress to the drug entrapped. The disadvantages are: i) Purification step which is the extensive washing steps is required to remove high amount of salting out agent; ii) It is not allowed to be used on lipophilic drugs (Huet, Sahuquillo-Merino et al. 1987, Yücel, Değim et al. 2013).

1.4.6.5 Coacervation

Forming a water-in-oil (W/O) emulsion by emulsifying an aqueous solution into a polymeric organic solution. Hydrophilic drugs are then dissolved in the aqueous solution and hydrophobic drugs are dissolved in the polymeric organic solvent. The organic nonsolvent such as silicone oil is added into the w/o emulsion and stirred. The polymer separates out from the organic solvent to form soft coacervate droplets containing the dispersed drug, then the mixtures are poured into a second nonsolvent organic solution such as heptane or hexan to harden the coacervate droplets giving rise to nanoparticles (Lesuffleur, Barbat et al. 1990, Wikman, Karlsson et al. 1993).

The advantages of this process are including: i) it is a commonly used method for both hydrophilic and hydrophobic drugs. Hydrophilic drugs are more preferred such as proteins, vaccines and anticancer drugs. The disadvantages are: i) It is difficult to scale up; ii) The production of nanoparticles tend to agglomerate; iii) Large amount of organic solvent are used and presence of residual solvents in the particles that are difficult to be removed (Marks, Belov et al. 1992, Wikman-Larhed and Artursson 1995, Walter, Janich et al. 1996).

1.4.7 Methodologies for trimethylate chitosan (TMC) nanoparticle fabrication

In particular, various methods have been developed for chitosan and TMC nanoparticle fabrication, mostly involving emulsification, various types of coacervation, or even slight modifications of these. More specifically, these methods are emulsion solvent diffusion (Hong, Yamauchi et al. 2011), reverse micellar method (Jin, Song et al. 2012), emulsion-

droplet coalescence (Behrens, Pena et al. 2002, Liang, Zhao et al. 2012), Emulsification and cross-linking (Sai, Kajita et al. 1998), and ionic gelation (Huang, Ma et al. 2002), whose particularities will be introduced in the following sections.

1.4.7.1 Emulsion solvent diffusion

The emulsion solvent diffusion method of preparing TMC NPs is an adaptation of the original procedure developed to produce PLGA-based NPs (Hilgendorf, Spahn-Langguth et al. 2000), setting its basis on the partial miscibility of an organic solvent with water. The specific method for preparation of TMC NPs involves the addition of an organic phase such as acetone containing the hydrophobic drug, to an aqueous solution containing TMC polymer and a stabiliser, such as lecithin and poloxamer, under stirring (Figure 1-10) (El-Shabouri 2002). This leads to the formation of an O/W emulsion which is then subjected to high pressure homogenisation. At this stage, organic solvent diffuses to the aqueous phase, decreasing TMC solubility and, thus, NPs are formed upon polymer precipitation. An additional amount of water is usually added in order to permit the complete diffusion of organic solvent. Finally, NPs are isolated by centrifugation. In spite of the limited number of studies available on the method, parameters such as TMC molecular weight, homogenisation rate and time for evaporation and diffusion, are expected to affect the final properties of the NPs. The presence of organic solvent was also reported as essential, since its rapid diffusion disturbs the organic/aqueous phase interface, which spontaneously produces a larger area and, thus, leads to the formation of much smaller droplets (El-Shabouri 2002). Particles produced without organic solvents presented sizes outside the submicron range (above 1.2 μm). Notwithstanding the ability of this method to produce effective NPs, it is important to highlight the need for harsh preparation conditions, such as high shear forces, which are absent in several other methods.

Bestpfe.com

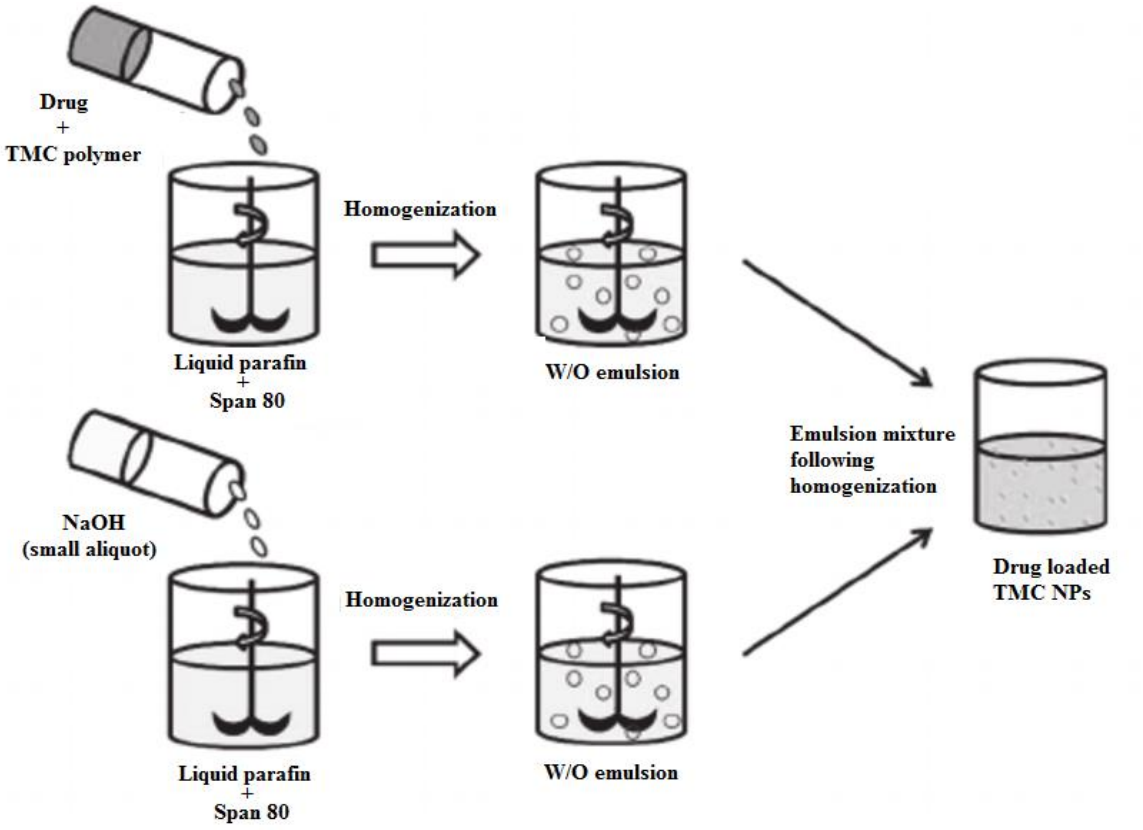

Figure 1-10. Schematic representation of the method of emulsion solvent diffusion.

1.4.7.2 Reverse micellization

The production of chitosan NPs from reverse micelles was first reported by Mitra *et al*, as a strategy for tumour targeted delivery. Reverse micelles are W/O droplets and thus form in a W/O system (Ho, Broze et al. 1997, Hu, Qiu et al. 2006), in contrast to conventional micelles that form in O/W environment. In this method of reverse micellisation, a W/O microemulsion is prepared using a lipophilic surfactant that is dissolved in an appropriate organic solvent such as n-hexane. Surfactants such as cetyl trimethylammonium bromide or sodium bis(ethyl hexyl) sulfosuccinate (AOT) have been used. An aqueous phase comprising TMC polymer, the drug and glutaraldehyde is then added over the organic phase under continuous stirring. As depicted in Figure 1-11, reverse micelles are produced at this stage. Thereafter, NPs are extracted following solvent evaporation (Mislick and Baldeschwieler 1996, Matsson, Pedersen et al. 2009). It is described that an increase in the crosslinking rate results in the production of larger particles (Rejman, Bragonzi et al. 2005, Matsson, Pedersen et al. 2009). As compared to other emulsion-based methods, the reverse micellization method has the

advantage of producing ultrafine NPs of around 100 nm or even less, with a narrower size range, in contrast to the larger NPs (> 200 nm) usually obtained by other emulsification techniques. Nevertheless, disadvantages such as the difficult isolation of NPs and the need for larger amounts of solvent, have been mentioned (Summers, Moore et al. 2004, Rejman, Bragonzi et al. 2005). Apart from the application in anticancer therapy, other authors have later used this method as a strategy for enzyme immobilisation (Summers, Moore et al. 2004) or to encapsulate oligonucleotides (Wang, Zhang et al. 2011).

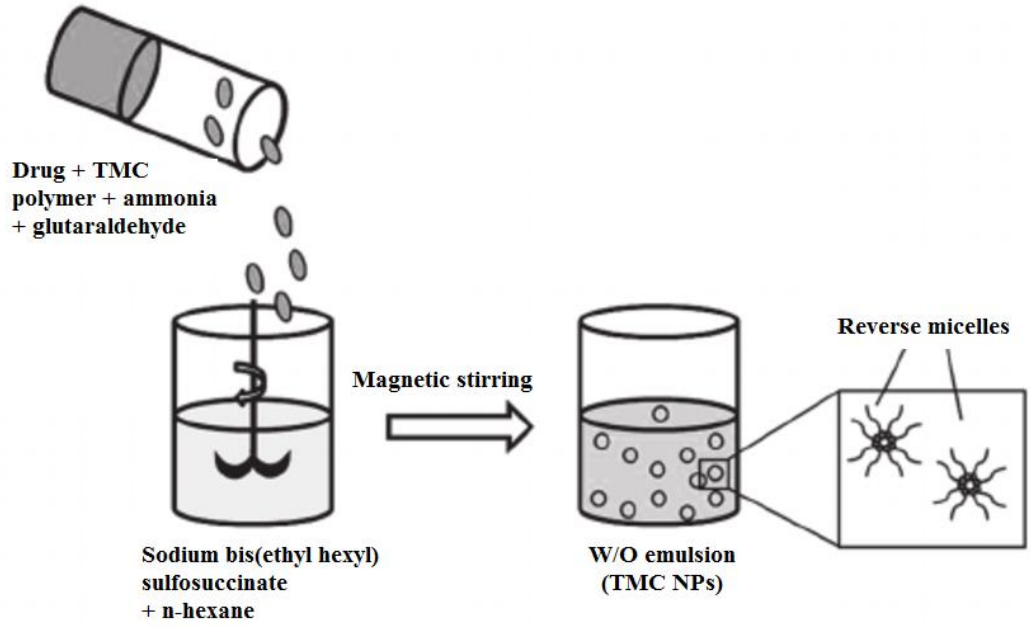

Figure 1-11. Schematic representation of the method of reverse micellization.

1.4.7.3 Emulsion droplet coalescence

This method first reported for microparticles preparation (Walgren, Lin et al. 2000). The same authors adapted the method later to prepare NPs loaded with gadolinium, as a strategy for neutron-capture therapy of cancer (Walgren, Lin et al. 2000). TMC is dissolved in the aqueous solution of gadolinium and a small aliquot of this is added to great amount of liquid paraffin containing sorbitan sesquiolate (Span® 83). The mixture is stirred with a high-speed homogeniser, thus forming a W/O emulsion (Figure 1-12). In parallel, another W/O emulsion is prepared by adding NaOH to a similar outer phase. Both emulsions are then mixed using a high-speed homogeniser, leading to droplet coalescence. This results in the solidification of

BEST PFE.COM
List of research project topics and materials

particles by action of NaOH, which acts as precipitating agent. Afterwards, a further set of washing and centrifugation steps is applied using toluene, ethanol and water (Walgren, Lin et al. 2000). A similar procedure was used in a different study to encapsulate 5-fluorouracil (Tomita, Hayashi et al. 1996). This method exploits the fact that, when two emulsions with equal outer phase are mixed together, droplets of each collide randomly and coalesce, resulting in final droplets with uniform content. The NPs are formed within the emulsion-droplets (Uchiyama, Sugiyama et al. 1999). Decreasing chitosan deacetylation degree was shown to increase particle size and to reduce NP capacity for drug association, as a consequence of the diminished capacity of ion-pair formation and de-swelling (Behrens, Pena et al. 2002). It was also found that varying polymer concentration between 0.5 and 2.5% affects 5-fluorouracil encapsulation efficiency and drug release profile (Tomita, Hayashi et al. 1996).

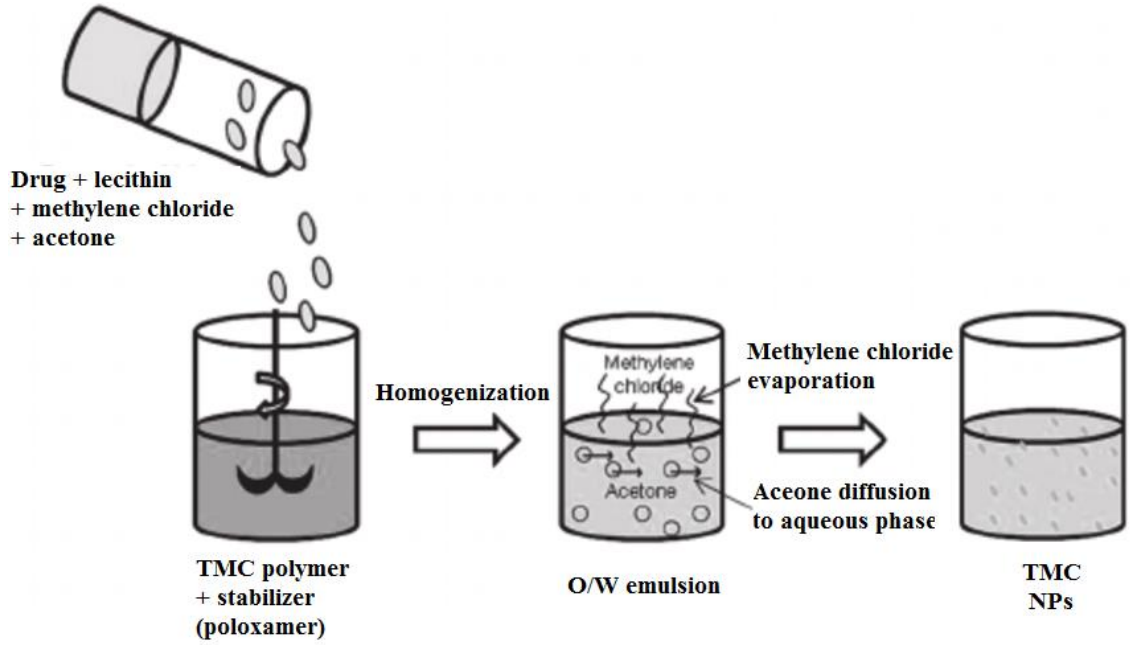

Figure 1-12. Schematic representation of the method of emulsion droplet coalescence.

1.4.7.4 Emulsification and cross-linking

Emulsification and cross-linking method was the first to be used to form TMC NPs and involves the preparation of a W/O emulsion (this first report described the emulsification of TMC aqueous solution in toluene, using Span 80® as emulsifier), with subsequent addition

of a cross-linking agent that has the function of hardening the formed droplets. The reactive amino groups of TMC undergo a covalent cross-linking with the aldehyde groups of glutaraldehyde (Figure 1-13), which is added after the emulsion formation and, consequently, after NP production (Hussain, Arnold et al. 2004). Those authors pioneered the production of NPs used to deliver 5-fluorouracil. Other authors used the method for the same purpose of drug delivery, but modified the oil phase composition to liquid paraffin and petroleum ether (Thanou, Verhoef et al. 2001). The final particle size was demonstrated to be highly dependent on stirring speed, as well as on the extent of cross-linking (Gupta 2011, Hauschild and King 2011). Several drawbacks have been progressively pointed out for this method, including the need of tedious procedures and the application of harsh cross-linking agents (Hauschild and King 2011). In fact, cross-linkers such as glutaraldehyde were found to cause overt toxicity and to compromise drug integrity, contributing to a progressive shift of interest towards less aggressive procedures (Randhawa 2009). Consequently, the application of this method to obtain TMC NPs was restricted to a few works.

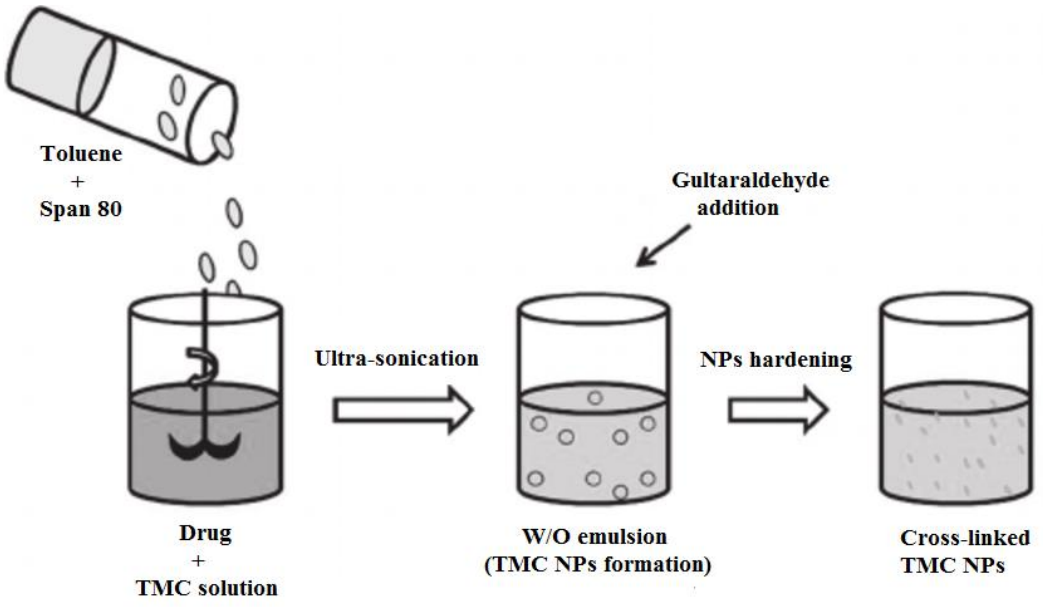

Figure 1-13. Schematic representation of the method of emulsification and cross-linking.

1.4.7.5 Ionic gelation

Ionic gelation method is a simple process derives from inter- and intramolecular cross-linkages mediated by the anionic molecules (Randhawa 2009) and has been used to produce

NPs very commonly. It should be noted that ionic gelation is the preferred term when polymer gelation is induced by small anionic molecules, such as phosphate, citrate, sulfate (Conroy, Desseigne et al. 2011). The latter approach is often referred to as complex coacervation or interfacial coacervation (von der Maase, Hansen et al. 2000, Oettle, Post et al. 2007). Ionic gelation method involves an ionic interaction between the positively charged amino groups of polymer and the polyanion tripolyphosphate (TPP), which acts as a crosslinker. NPs formation takes place immediately after the addition of a TPP solution to the polymer solution, under mild stirring, at room temperature (Figure 1-14). Stirring should be maintained for approximately 10 minutes to allow particle stabilisation and the obtained suspension centrifuged to separate the NPs from unreacted polymer and TPP. The resultant pellet of NPs is then resuspended in water (Win and Feng 2005).

Materials applied in the production of NPs using ionic gelation method include polymers such as sodium alginate (Blackstein, Vogel et al. 2002), dextran sulfate (Silverstein and Rodgers 2004), arabic gum (Brusa, Immordino et al. 2007), carrageenan (Yuan, Chesnutt et al. 2011), glucomannan (Freier, Koh et al. 2005), pectin (Bowman and Leong 2006), heparin (Hidaka, Ito et al. 1999), cyclodextrins (Boonyo, Junginger et al. 2008), and hyaluronic acid (Yien, Zin et al. 2012). One work reports the use of sodium lauryl sulfate (Dehousse, Garbacki et al. 2010). In some cases, both the aforementioned methods are combined to form NPs. Examples of these systems include the use of alginate/tripolyphosphate to form NPs by ionic gelation (Chow and Ho 2013), and NPs formation involving hyaluronic acid/tripolyphosphate (He, Yin et al. 2012).

The author's experience in the field and other works available in the literature, have demonstrated that the final properties of TMC NPs obtained through electrostatic interaction are dependent on several parameters inherent to the preparation method. In this sense, controlling the stirring pattern (speed and type of vial, most importantly) and the conditions of centrifugation (speed and duration), is of utmost importance (Win and Feng 2005), independently of the specific materials composing the NP matrix. Optimizing variables like materials concentration and mass ratios, as well as temperature of the reacting solutions and the volume of resuspension are also have significant influences (Konerding, James et al. 2002, Win and Feng 2005). It was reported that the production of NPs by ionic gelation resulted in smaller particles for higher amounts of cross-linker (Konerding, James et al. 2002, Gan and Wang 2007). A very recent work on TMC/TPP NPs has also established that the

concentration of TPP crosslinker and the temperature at which the crosslinking process occurs, strongly affect the polydispersity (PdI) of the obtained NPs (Konerding, James et al. 2002). In addition, TMC is the derivative of chitosan, and the type of chitosan used has also been reported as crucial. Chitosan exists under many different chemical structures, being available either as a base or a salt (different types of salts are also available, such as chloride, lactate, glutamate, etc). Moreover, distinct molecular weights and deacetylation degrees also exist. Several studies have established a relation between these features and the final characteristics of the resultant NPs (Vandenberg, Drolet et al. 2001, Pan, Li et al. 2002, Al-Qadi, Grenha et al. 2012), revealing that chitosan structure determines NPs preparation variables, as well as their final properties, such as size and zeta potential. The most important advantage claimed by those working with the methods of ionic gelation and polyelectrolyte complexation is the complete hydrophilic environment and the mild preparation conditions. In fact, the avoidance of organic solvents or high shear forces makes encapsulation of labile drugs an easier task (Tiyaboonchai 2003). Possibly for this reason, this methods are the most widely used to produce chitosan and TMC NPs. Importantly, through physical cross-linking mediated by an electrostatic interaction, instead of a chemical cross-linking with glutaraldehyde, those methods of chitosan nanoparticle production have improved cell viability and drug integrity (Katas and Alpar 2006). Therefore in this project, we use ionic gelation method to fabricate the TMC based NPs.

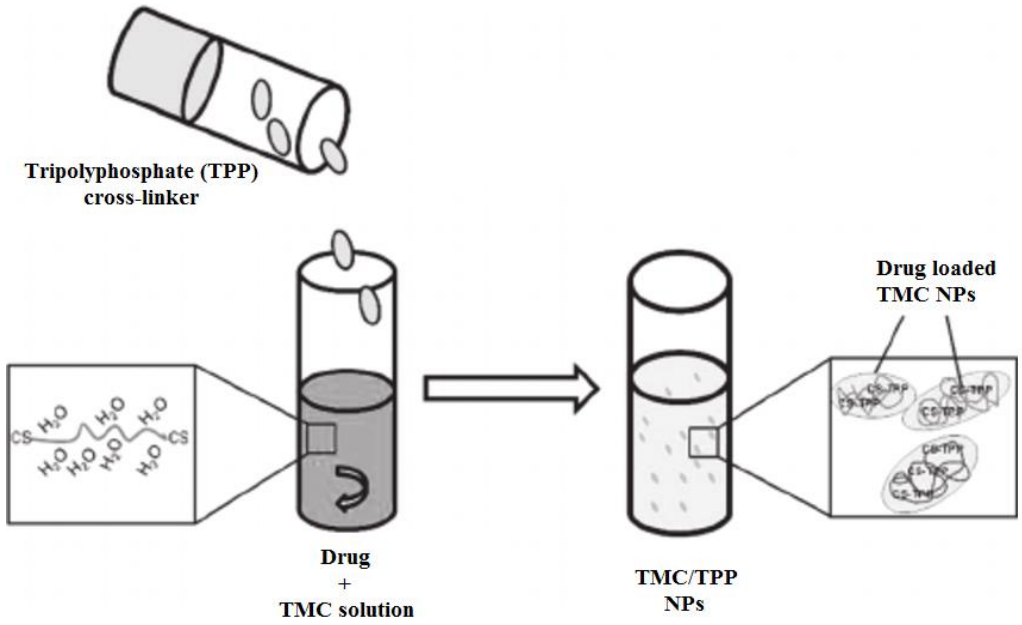

Figure 1-14. Schematic representation of the method of ionic gelation.

1.5 Characterisation of bioadhesive Nanoparticles

1.5.1 Particle size and size distribution

The particle size of NPs is a key parameter which influences half-life and bioavailability, tissue distribution, and clearance (in the following, particle size refers to the diameter). Hepatic uptake and accumulation and kidney excretion may depend heavily upon particle size. It was found that NPs within a particular size ($\leq$ 100-150 nm) were able to exit or enter fenestrated vessels in the liver endothelium or tumour microenvironment (Moghimi, Hunter et al. 2001). Table 1-2 shows the estimated pore size of capillaries in various organs. These capillary pore size data provide a context of why most NPs preparations of 50-200 nm do not easily escape from continuous blood capillaries in their intact form. Particles of 100-200 nm in diameter, may distribute to bone marrow, spleen, and liver sinusoids, and to some extent may escape through sinusoidal capillaries within these organs, whereas NPs in blood vessels do not easily escape out of capillaries that perfuse tissues such as the lung, brain, and kidney if they are within the diameter range of 100-150 nm. Therefore, when we developed our gemcitabine loaded NPs, particle size that falls between 100-200 nm in diameter is more ideally to avoid the anticancer drug loaded NPs to perfuse other healthy organs, which ensure the safety profile of the drug delivery systems to our body. In addition, due to the leaky nature of the vasculature at the breast tumour site, the appropriate particle size that would tend to permeate across the leaky pore of the blood vessel around tumour region, which leads to higher chance of drug loaded NPs to accumulate at the tumour site. This phenomenon is termed Enhanced Permeation and Retention (EPR) effect (Chen 1978, Lee, MacKay et al. 2005), which is the key feature that this project will be focussing in, for developing a promising nanoparticulate delivery system to encapsulate gemcitabine.

Literature has reported that small NPs are able to penetrate through the submucosal layers while the larger microparticles are predominantly localized in the epithelial lining (Desai, Labhasetwar et al. 1996). These findings suggest that cellular internalization: phagocytosis, macropinocytosis, caveolin- and clathrin-dependent endocytosis, and caveolin- and clathrin-independent endocytosis may also be related to particle size. Caveolin- and clathrin-dependent and caveolin- and clathrin-independent endocytosis is most relevant to particles of 50-150 nm in diameter (Wang, Byrne et al. 2011). Particles less than 10 nm undergo renal

filtration through the glomerular capillary wall and are not reabsorbed (Venturoli and Rippe 2005). Thus, to reduce the mononuclear phagocyte system (MPS) uptake and to prolong blood circulation time, most therapeutic NPs are designed within 50-100 nm diameters. For instance, reduction of particle size to 50 nm greatly reduced MPS mediated clearance and achieved a plasma half-life similar to those achieved with PEGylated NP of 100-150 nm in diameter (Baldeschwieler 1983, Beaumier and Hwang 1983). In addition, DaunoXome, a nanoparticular cancer therapeutic, consists of 45-80 nm diameter particles intended to reduce MPS uptake (Kraft, Freeling et al. 2014).

Size distribution can be used to predict whether a delivery system will retain structure and function during storage or processing as well as an indicator of particle stability. Ideally, polymeric particles should have a reproducible, homogeneous and narrow size distribution. The uniformity and distribution of polymeric particles are represented by the polydispersity index (PDI). PDI is close to zero for a monodisperse samples, smaller for narrower distribution, and larger for a wider distribution. Two methods are commonly used to determine size and size distribution of particulate delivery system. The first is direct visualization using electron microscopy. Several variations on electron microscopy such as negative staining, freeze-fracture transmission electron microscopy (TEM), scanning electron microscopy (SEM) and cryo-TEM, provide valuable information on particles since they yield a view of morphology and surface properties and can resolve particles of varying size. However, organic surface ligands are difficult to resolve owing to their low electron density, so the TEM determined size mainly reflects the size of the core. In addition, electron microscopy usually requires complicated sample preparation, can generate artefacts, induce shrinkage and shape distortion, and may be time consuming to obtain a representative size distribution of the population, thus electron microscopy is not always amenable to routine measurement (Wyatt and Villalpando 1997). The second is an indirect method, dynamic light scattering, also referred to as photon correlation spectroscopy (PCS). PCS measures the time dependent fluctuations of light scattered from particle exhibiting Brownian motion, which results from collisions between suspended particles and solvent molecules (Pecora 2013). As a result, it provides information on the mean size of the sample and on the width of the size distribution from aqueous suspensions of particles. However, this method suffers from low sensitivity toward small particles and possible interference from light-absorbing species (Filella, Zhang et al. 1997). PCS is not a suitable and precise technique for the characterization of inhomogeneous spheres. Ingebrigtsen and Brandl (2002) (Ingebrigtsen

and Brandl 2002) reported that PCS appeared to underestimate very small particles below 30 nm if a small proportion of larger particles were present. Therefore, a combination of dynamic light scattering and electron microscopy techniques is helpful to overcome the weakness of the single techniques.

1.5.2 Zeta potential

The overall net charge of the particles is typically expressed as surface or zeta potential. Zeta potential is the electrical potential at the plane of shear as particles move in an electrical field, providing an indication of the surface charge of the particles (Hunter 2013). Surface charge determines inter-particle interactions and hence contributes towards resistance to aggregation. Particles without charge have higher tendency to aggregate than those with same net charge. NPs with zeta potentials more positive than + 15 millivolt (mV) or more negative than - 15 mV are considered stable, when combined with steric stabilization, ± 20 mV is sufficient (Jacobs and Müller 2002). The zeta potential can also be used to determine whether a charged active material is encapsulated within the centre of the nanocapsule or adsorbed onto the surface. PCS may be combined within zeta potential measurement within the one instrument. For example, the zetasizer nano series from Malvern Instrument can measure both particle size and zeta potential.

In addition, the nature and density of the surface charge may impact pharmacokinetics, biodistribution, cellular affinity and drug internalization. Generally, the plasma membrane of cells is negatively charged. Hence, NPs with positive charges are easily adsorbed on negatively charged areas of cell membrane and further translocated into cytoplasm *via* direct penetration and various endocytosis pathways (Harush-Frenkel, Debotton et al. 2007). For example, Liu *et al.* (2012) revealed that the cell uptake of curcumin was greatly enhanced by encapsulating curcumin into cationic chitosan/PCL nanoparticles (Liu, Xu et al. 2012). Furthermore, Jiang *et al.* (2012) designed a cationic core-shell liponanoparticle by enveloping the plasmid-laden chitosan nanoparticle into a cationic lipid shell, showing that the cellular uptake increased up to 1.25-fold and 5-fold than that of chitosan NPs and lipid-coated chitosan NPs(Jiang, Gan et al. 2012). However, cationic charge is claimed to enhance cytotoxicity, and positive charge possess a membrane destabilizing and concomitantly destructive effect resulting from an interaction of positive charge and negative charge of membrane (Qi, Xu et al. 2005, Makhlof, Werle et al. 2011). Non-phagocytic cells, such as

those in the tumour, have a preference for NPs with slight negative charges (Kulkarni and Feng 2013). Moreover, negatively charged nanoparticles are cleared more slowly from the blood compared to positively charged NPs and retain in systemic circulation for longer time (Unger, Wittmar et al. 2007). Because cationic NPs with net positive charges have a tendency to interact with proteins in serum and lead to enhance uptake by the MPA and cause a faster clearance by the lung, liver or spleen (Plank, Mechtler et al. 1996). Furthermore, negatively charged had lower cytotoxicity compared with positively one and approved by FDA. In summary, both positive and negative zeta potential have their benefits. Therefore, the surface charge density of NPs should be optimized for minimal toxicity and effective intracellular delivery of encapsulated drug.

1.5.3 Drug entrapment efficiency and loading capacity

Ideally a successful nanoparticulate system should have a high drug-loading capacity thereby reduce the quantity of matrix materials for administration. Drug loading highly depend on the solid-state drug solubility in matrix materials, which is related to polymer composition, surfactant, drug molecular weight, or different preparation techniques (Govender, Stolnik et al. 1999, Panyam, Williams et al. 2004, Zhang, Tan et al. 2006). Drug entrapment efficiency (EE) and drug loading capacity are frequently used terms to express the successfulness of loading and the amounts of drugs in the particles. The EE (%) is the amount of the drug loaded into the particles divided by the total amount of the drug both inside and remaining outside the formulation (i.e. unsuccessfully encapsulated). The EE of drug into the particles can be determined directly or indirectly (Agnihotri, Jawalkar et al. 2006). In the direct way, the drug content is extracted by dissolving the particles in a suitable solvent and analysed for amount. In the indirect method, ultracentrifugation is utilized to separate efficiently the particles from the supernatant and the supernatant is analysed for the free drug concentration. Moreover, drug loading capacity (weight per weight) (w/w) shows the percentage of drug in relation to the dry particles which serves to estimate the effectiveness and ability of the particles to encapsulate and hold the drug (Snehalatha, Venugopal et al. 2008).

Bestpfe.com

1.5.4 Drug release profile

The kinetic profile of drug release may exhibit different profiles: such as zero-order, monophasic, biphasic, and triphasic, depending on the dynamics of any initial burst release, diffusion through the particle matrix and pores, and the stages of degradation and erosion (Fredenberg, Wahlgren et al. 2011). Zero-order release is desirable where a constant release rate is maintained, but a tri-phasic profile is probably most common (Möckel and Lippold 1993, Luan and Bodmeier 2006). The classic triphasic release profile is given in Figure 1-15.

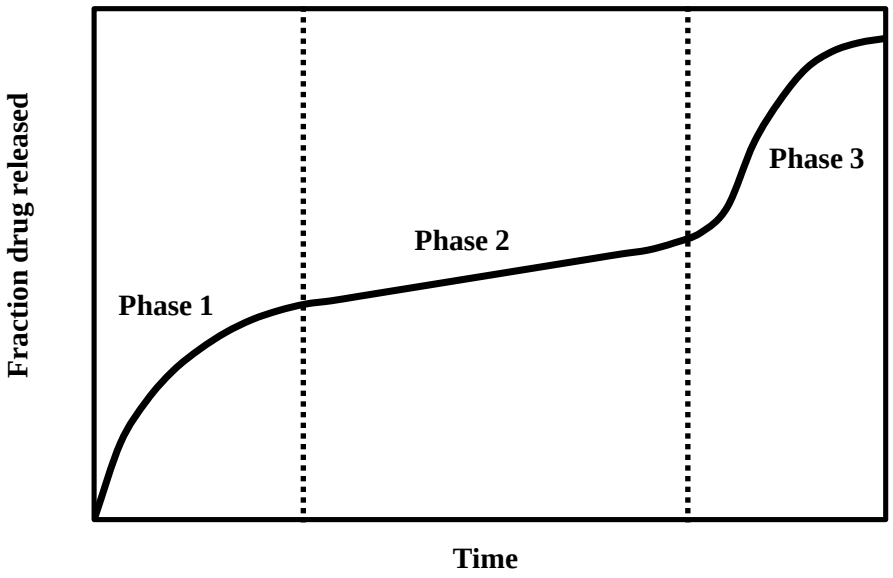

Figure 1-15. Tri-phasic release profile consisting of phase 1 (burst), phase 2 (sustain release) and phase 3 (Second burst).

Phase 1 is described as a burst release and is attributed to surface-bound (or very near surface) and poorly encapsulated drugs or rapid disintegration of the matrix (Wang, Wang et al. 2002, Lao, Venkatraman et al. 2008). Phase 2 shows a slow diffusion-controlled release manner which may be attributed to binding or entrapment of the drug within the particle matrix (Janoria and Mitra 2007). Phase 3 is due to erosion-controlled release which is usually a period of faster release, commencing at the onset of erosion (Loo, Tan et al. 2010). The release mechanisms are mainly based on the diffusion coefficient of the drug and biodegradation rate of polymeric matrix of particles. However, large particles often exhibit this tri-phasic release due to heterogeneous degradation, and small particles exhibit a bi-phasic release profile with a relative rapid second phase (Sansdrap and Moës 1997, Berchane,

Carson et al. 2007). Combining particles of different size has been shown to offer a means of altering the overall drug release profile, from a Fickian diffusion profile and a sigmoidal profile to a zero-order profile (Berkland, King et al. 2002). Moreover, if the polymeric NP is coated by another layer of polymer, the release is then controlled by diffusion of the drug from the NP core across the outer polymeric membrane. The membrane coating acts as a barrier to release, therefore, the solubility and diffusivity of drug in polymer membrane becomes determining factor in drug release (Manjunath and Venkateswarlu 2005). *In vitro* methods that have been commonly used to investigate release profiles include: side-by-side such as Ussing chambers or Franz-type diffusion cells with artificial or biological membranes (cell culture models and tissue preparations), dialysis bag diffusion or reverse dialysis set ups, ultracentrifugation or ultrafiltration (Vihola, Laukkanen et al. 2002, Chattopadhyay, Huff et al. 2006, Peltonen and Hirvonen 2008).

1.5.5 Stability

Stability of NPs is mainly related to either stability of encapsulated therapeutic drug in their nanoparticulate form, since they are more prone to degradation or coalescence. Besides the instability of drug in GIT, special care has to be taken since stability problems can easily degrade the drugs when exposed to various types of stress during formulating processes (Table 1-3).

BESTPFE.COM
List of research project topics and materials

Table 1-2. Main stress factors which potentially impede drug stability during particle fabrication and manufacturing (Lu, Kopečková et al. 1999, Kafka, Rades et al. 2010).

Stress Factor	**Encountered**
Elevated temperature	Rotary evaporation; Ultrasonication; Specific production processes (e.g. spray-drying)
Freezing, freeze-thawing	Accidental freezing during storage; Storage of frozen (bulk) material; Lyophilization
Mechanical stress	Production (pumping, filtration, stirring, and so on); Handling (e.g. shaking)
Light	Exposure to daylight or artificial light during production, storage or handling; UV detection during downstream processing
Oxidative stress	Contact with oxygen (air, dissolved O_2); Excipients (e.g. peroxide impurities in polysorbate); Metal ion traces from production equipment or excipients; Light; Vaporized sanitation agents (e.g. vaporized hydrogen peroxide); Cavitation
pH changes	Formulation; Dilution

Chemical degradation of a drug due to oxidation is the other primary degradation process that occurs, along with the hydrolytic reactions (Houchin and Topp 2008). Oxidation can occur during any stage of drug production, purification, formulation and storage. Even presence of less than 1% of atmospheric oxygen in the vial is sufficient to produce complete oxidation. Chemically degraded drugs are often monitored by high performance liquid chromatography (HPLC), and mass spectrometry (MS). In case of HPLC, reserve phase HPLC (RP-HPLC) is widely used for quantitation and separation of drug candidates. Due to the sensitivity of reversed-phase interactions with drug candidates, any changes in a drug compound result in a change in the retention time of that drug. By interfacing with MS, HPLC-MS further confirms the purity of each peak. There were various examples to study the integrity of drug candidates using HPLC-MS (Shire, Shahrokh et al. 2004).

Forced degradation studies have to go hand in hand with analytical characterization mentioned above. Because the outcome of these studies depends on not only the analytical methods included assessing stability, but also the conditions applied. The exposure to various extreme conditions summarized in Table 1-3 can be considered as a stress method to address the robustness of a drug loaded particulate delivery system during processing and formulation. Such conditions can have influences on changes in the average particle size and size distribution due to vesicle aggregation and fusion and loss of entrapped materials due to leakage, thus accelerating the chemical and physical degradation of entrapped drug compositions. As for oral drug delivery, the stability of drugs in intestinal digestive enzymes should be evaluated. The major digestive enzyme in the stomach is pepsin, and the main digestive enzymes in small intestine are trypsin and chymotrypsin. Thus the stability studies of the drug and drug loaded nanocarrier should be conducted interacting with enzymatic solution of pepsin, trypsin and chymotrypsin. The related stability studies of this project are introduced and discussed in Chapter 2.

1.5.6 Mechanism of cellular uptake and transport

The intestinal mucosal surfaces are covered with a mucus layer, in which mucins are the major component (Losa, Sierra et al. 2005). Mucins are highly glucosylated glycoproteins with a large peptide backbone and oligosaccharides as side chains. Their protein backbone is characterized by the presence of repeating sequences rich in serine, threonine and proline residues. Many of the O-linked oligosaccharide side chains are often terminated in sialic acid, sulfonic acid, or L- fructose. As a result, mucins are negatively charged at physiological pH (Bansil and Turner 2006). Mechanisms of adhesion of certain macromolecules to the surface of a mucous tissue are not yet fully understood**.** However, bioadhesive nanoparticular carrier systems possibly delivery a therapeutic drug at the tissue site by two steps, the contact stage and the consolidation stage (Figure 1-16).

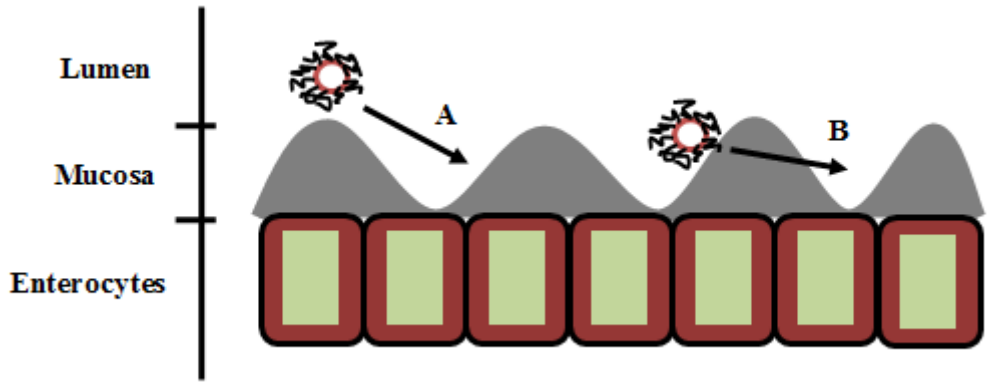

Figure 1-16. Mechanism of mucoadhesion. The mucoadhesion takes place in two stages. (A) Contact stage: Intimate contact between a bioadhesive and a membrane (wetting or swelling phenomenon). (B) Interactive stage: Penetration of the bioadhesive into the epithelial membrane or into the surface of the mucous membrane (interpenetration).

The first stage is characterized by the contact between the mucoadhesive and the mucous membrane, with spreading and swelling of the formulation, initiating its deep contact with the mucus layer (Devine and McKenzie 1992). In oral delivery, mucoadhesion can be promoted by peristalsis, the motion of organic fluids in the organ cavity, or by Brownian motion (Losa, Sierra et al. 2005). If the particle reaches the mucous surface, it will come into contact with repulsive forces such as osmotic pressure or electrostatic repulsion, and attractive forces such as van der Waals forces and electrostatic attraction (Smart 2005, Carvalho, Bruschi et al. 2010). For mucoadhesion to occur, the attractive interaction should be larger than nonspecific repulsion. In the consolidation step, the mucoadhesive materials are activated by the presence of moisture. Moisture plasticizes the system, allowing the mucoadhesive molecules to break free and to link up by weak van der Waals and hydrogen bonds (Smart 2005). Essentially, there are two theories explaining the consolidation step: the diffusion theory and the dehydration theory. According to diffusion theory, the mucoadhesive molecules and the glycoproteins of the mucus mutually interact by means of interpenetration of their chains and the building of secondary bonds (Smart 2005). For this to take place, the mucoadhesive device has features which favour both chemical and mechanical interactions. For example, molecules with hydrogen bonds building groups (-OH, -COOH), with an anionic surface charge, high MW, flexible chains and surface-active properties, which induct its spread throughout the mucus layer, can present mucoadhesive properties (Kumar, Dhawan et al. 2014). According to dehydration theory, materials that are able to readily gelify in an aqueous

environment, when placed in contact with the mucus can cause its dehydration due to the difference of osmotic pressure. The difference in concentration gradient draws the water into the formulation until the osmotic balance is reached. This process leads to the mixture of formulation and mucus and can thus increase contact time with the mucous membrane. Therefore, it is the water motion that leads to the consolidation of the adhesive bond, and not the interpenetration of macromolecular chains (Velmurugan, Ali et al. 2014).

Intestinal absorption is a vital process bridging digestive system and life of human. This process takes place right from the mouth to the stomach, small intestine and finally colon. There are four distinct mechanisms for molecules to cross the intestinal epithelial cell membrane: *via* paracellular, transcellular, carrier-mediated, and receptor-mediated transport, which were metnioned in section 1.3.2. The average size of aqueous pores created by epithelial tight junctions is approximately 7-9 nm for the jejunum, 3-4 nm for the ileum, and 8-9 nm for the colon in the human intestine (Tomita, Hayashi et al. 1988). This data suggests that solutes with a molecular radius exceeding 15 nm (approximately 3.5 kDa) cannot be transported *via* this route (Rubas, Cromwell et al. 1996). Furthermore, tight junctions comprise only about 0.01% of the total absorption surface area of the intestine (Pappenheimer 1987). For receptor-mediated transport, drug carriers require a receptor specific ligand for cell surface receptors or a receptor for cell surface ligands (King and Johnson 1985). Consequently, gemcitabine load NP across intestinal epithelia using paracellular transport, carrier-mediated transport and receptor-mediated transport is severely restricted. Transcellular transport occurs through the intestinal epithelial cells by transcytosis, a particular process by which particles are taken up by cells. This starts with an endocytosis process that takes place at the cell apical membrane. The membrane invaginates and pinches off to form enclosed vesicles. Then, particles are transported through the cells and released at the basolateral membrane. Particle uptake by the transcellular transport includes (A) Enterocytes transport and (B) M cell transport (Figure 1-17).

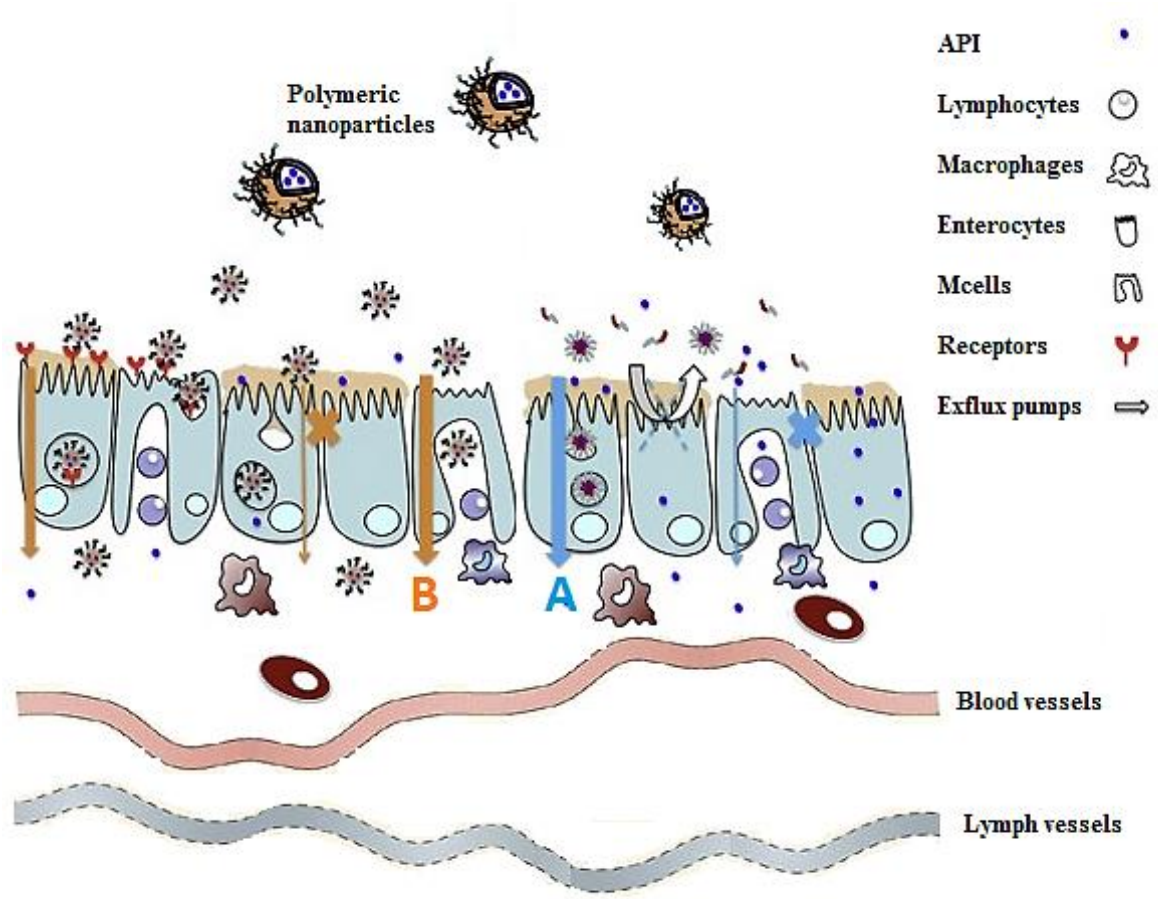

Figure 1-17. Absorption of NPs through various mechanisms of intestinal cellular uptake (A) Enterocytes absorption and (B) M cell uptake.

Enterocytes represent the majority of cells lining the GI tract and M cells are mainly located within the epithelium of Peyer's patches and represent a very small proportion of the intestinal epithelium (5 % of the human follicle-associated epithelium, i.e., about 1 % of the total intestinal surface) (Giannasca, Giannasca et al. 1999). M cells represent a potential portal for oral delivery of drugs due to their high endocytosis ability. M cells possess a high transcytotic capacity and transport a wide variety of materials, including NPs (Frey and Neutra 1997, Clark, Hirst et al. 2000). A study carried out by Yuan *et al.* (2007) reported that ~77.9 % of absorbed NPs was transported into systematic circulation *via* lymph through M cell uptake, which is the major transport pathway. The rest of the absorbed NPs were transported directly into blood through capillary vessel or intestinal epithelial cells by exploiting the enterocytes uptake (Yuan, Chen et al. 2007). In addition, Li *et al.* (2009) also showed the NPs could be absorbed in all GI tract segments with different percentage and pattern of absorption. The absorption of NPs was only 6 % from stomach while 82 % from

intestine and colon region (Li, Zhao et al. 2009). In addition, large intestinal surface for particle adhesion (presence of M cells in Peyer's patches) have benefit for oral uptake of NPs. Moreover, the use of mucoadhesive polymer coating enables the NPs to increase the chance for mucosal absorption into lymphatic circulation, especially by lactoeals (Porter and Charman 1997). Compounds absorbed by the intestinal lymphatics drain *via* the thoracic lymph and enter the systemic circulation at the junction of the left internal jugular vein and the left subclavian vein, thereby avoiding potential first-pass metabolism. Furthermore, the coincubation of Caco-2 cell and HT29-MTX-E12 cell membranes were used to model human intestinal absorption for testing different types of particles and have become a great tool for the predication of intestinal drug absorption and for mechanistic investigations of drug transport (Hilgers, Conradi et al. 1990, Wikman-Larhed and Artursson 1995, Collett, Sims et al. 1996, Behrens, Stenberg et al. 2001). Originally isolated from a human colon adenocarcinoma, Caco-2 cells undergo spontaneous enterocytic differentiation in culture to resemble epithelial cells of the small intestine (Artursson, Palm et al. 1996). With addition of HT29-MTX-E12 cell, which is an intestinal mucus-secreting cell (Walter, Janich et al. 1996). The co-cultured cell model simulates the complete intestinal epithelial membrane with all the essential features and properties. When the cells grown to confluence, cell polarity, mucus layer and tight junctions are established in the cell membranes and several active transport systems are expressed as in the walls of the human small intestine(Wilson, Hassan et al. 1990).

1.5.7 *In-vitro* cytotoxicity on cells

The cytotoxicity of oral drug delivery systems has been estimated by the (4,5-dimethylthiazol-2-yl)2,5-dyphenyltetrazolium bromide (MTT) assay, which assesses the mitochondrial function of the Caco-2 cells and HT29-MTX-E12 cells (Agullo, Gamet et al. 1994). Only live cells could react with the MTT reagent and the cell viability is detected at early stage. Other studies could be carried out to study different cytotoxic effects, such as the oxidative potential, i.e. the effect of peroxidation of the nanocarriers in cells (Yang, Lu et al. 1999). Polymeric nanocarriers are well tolerated in living systems because they are made of physiological compounds and therefore, metabolic pathways exist decreasing the risk of acute and chronic toxicity. For example, cytotoxicity of chitosan-coated nanoparticle was decreased towards Caco-2 cells (Yang, Geng et al. 2009). Nonetheless, the toxicity of components of

the aqueous phase, especially non-ionic emulsifiers and preservatives that have been used for stabilizing these particles, has to be considered.

1.5.8 Pharmacokinetics, oral bioavailability and safety

Pharmacokinetics is the study of the time course of the absorption, distribution, metabolism and excretion of a drug, which referred to as 'what the body does to a drug'. There are several pharmacokinetics parameters which are the useful in characterizing the *in vivo* disposition of a drug, including clearance, volume of distribution, half-life and bioavailability (Grit, Underberg et al. 1993). Almost all pharmacokinetics of drug delivery systems are based on quantification of drug remained in the blood or plasma over time following its application. However, plasma is more widely analysed than blood because sample preparation and analysis methods are easier for plasma than for blood.

To estimate pharmacokinetic parameters from plasma concentration versus time profiles, non-compartmental analysis is more commonly used than compartmental analysis due to requiring minimal a priori assumptions on the structure of the pharmacokinetic model. The non-compartmental approach is based on the area under the drug concentration versus time cure (AUC) and the mean residence time (MRT) (Grit and Crommelin 1993). From a pharmacokinetic perspective, the bioavailability is the fraction of an extravascular administered dose that reaches the systemic circulation. Bioavailability may be assessed by measurements intended to reflect the rate and extent to which the active drug become available at the site of action. A drug given by the intravenous route is considered to have an absolute bioavailability of 100%. Hence, to determine absolute oral bioavailability of a drug, a pharmacokinetic study must be done to obtain a plasma concentration vs time plot for the drug after both intravenous and oral administration. The absolute bioavailability is then determined by calculating the ratio of the dose-corrected AUC oral to AUC intravenous. Relative bioavailability (F_{bio} %) is employed to assess bioequivalence between two drug formulations, which similarly calculated as the ratio of the dose-normalized AUC of the test formulation to the dose-normalized AUC of the reference formulation. The MRT is the arithmetic mean of the duration that a compound resides in the body before being eliminated. Formulation of drugs in the polymeric NPs generally leads to enhanced MRT in the systemic circulation as well as in various tissues.

A true estimate of the total body or systemic clearance of a drug can be obtained from its concentration versus time profile after administration. This is because systemic clearance of a drug is defined as its rate of elimination from the body normalized to the concentration of the drug in the body fluid (plasma or blood) in which the drug is introduced. For oral delivery, C_{max} and T_{max} are critical to pharmacokinetics behaviours, C_{max} is the highest drug concentration after administration, and T_{max} is the time at which C_{max} is observed. The volume of distribution is a direct measure of the accumulation from the plasma to several tissue compartments including brain, kidneys, liver, spleen, lungs, heart, blood, and tumour if applicable (Wulff-Pérez, Barrajón-Catalán et al. 2014). In many studies, following oral administration of the nanocarriers, organs are harvested and analysed for nanoparticle and drug content using analytical techniques (e.g. HPLC) (Han and Wang 2005). And lastly, terminal half-life ($T_{1/2}$) is the time required to reduce the concentration in blood or plasma to one-half after equilibrium has been reached. This parameter can be determined from the slope of the terminal line of a semilogarithmic plot by regression analysis (Chiou 1978). This parameter is important for the selection of the type (matrix) of nanoparticulate delivery systems. The shorter the terminal $T_{1/2}$ the greater will be the amount of the drug that will be incorporated into the system.

1.6 Other factors to be considered for oral drug delivery

1.6.1 Physiochemical properties of the drug

Firstly, we need to consider the physiochemical characteristics of the drug itself before selecting the formulation and delivery route to be investigated. The solubility of a drug determines the dosage required to be loaded onto NPs to achieve a specific dose. The lower the solubility, the larger the dosage that will be required (Lipinski 2000). Drug permeability through the mucosal membrane is also a critical consideration for systemic delivery. pKa, LogP, and the molecular weight (MW) of the drug all affect the intestinal mucosal permeability (Davis, Little et al. 2006).

It has been shown that passive permeability correlates well with lipophilicity. To be absorbed by this route, drugs must be sufficiently lipophilic to penetrate the lipid cores of membranes. Lipophilicity is expressed by the octanol-water partition coefficient (logP) (Davis, Little et al.

2006). The more lipophilic molecular (more non-ionized) may permeate through the lipid epithelium membrane more efficiently (Prausnitz and Noonan 1998). Moreover, most drugs ionise in aqueous solution, and can therefore exist in a neutral or a charged state, depending on the pH of the local environment. Molecules are more lipophilic when neutral than when charged. Ionisation is expressed by the aqueous ionisation constant pKa (The pK_a of a molecule predicts the degree of ionisation the molecule will have at a particular pH) (Brechue and Maren 1993). Lipophilicity, pKa, and aqueous solubility are the three principal physicochemical parameters that must be considered to carry out drug permeability studies over the intestinal epithelial membrane. In addition, Drug with low permeability will need a large area for absorption, an increased loading dose, or the addition of permeation enhancers to optimize the transmucosal absorption (Williams and Barry 2012). Again, given the size limitation for patient compliance, the oral drug delivery is most suitable for drug with high permeability or relatively higher potencies (Hubatsch, Ragnarsson et al. 2007).

1.6.2 Pharmacological Aspects

For a drug delivery system intended to deliver drug systemically via oral route, drug is released from the NPs to the intestinal surface or the intact drug loaded NPs will perfuse to the mucosal surface, where it is absorbed through the mucosa to enter the systemic circulation. This type of drug delivery is advantageous as it allows direct drug or drug loaded NPs to enter the systemic circulation. However, the associate drawback for this type of drug delivery is the low permeability of intestinal epithelial membrane to many active ingredients, which needs to be overcome by enhancing drug absorption. Given the limits on the physical size of a carrier system that can be adhered to the intestinal mucosa (Amidon, Lennernäs et al. 1995). Moreover, other limitation such as the potential for drug loss by degradation in the GIT or by hepatic first-pass metabolism should be overcame (Zhang and Benet 2001).

1.7 Thesis aims and structure

This review Chapter has provided background knowledge and laid a foundation for the current research on the barriers for oral drug delivery and the rationales for using polymeric nanoparticulate delivery systems.

The aim of this thesis is to develop, formulate and characterise novel oral delivery nanoparticulate systems for improving oral bioavailability of gemcitabine *via* TMC modified PLGA-TPGS NPs and TMC-CSK NPs. To achieve this aim the following specific objectives were envisaged:

1. To develop and validate an HPLC analytical method for qualifying and quantifying gemcitabine for its stability and formulation screening test. Forced degradation studies of gemcitabine were monitored according to International Conference on Harmonisation (ICH) guideline, and its enzymatic degradation studies (Chapter 2).

2. To prepare gemcitabine loaded TMC modified PLGA-TPGS NPs using a modified solvent evaporation method. Subsequently the formulation was optimized by changing formulation parameters using central composite design. The characterization of the NPs such as particles size, size distribution, entrapment efficiency, zeta potential, stability, drug-polymer compatibility, drug release and *ex-vivo* permeation over epithelial membrane were determined, and selecting the optimal delivery system for further studies (Chapter 3).

3. Development of TMC-CSK NPs by ionic gelation method. Similar characterization as mentioned above was carried out for TMC-CSK NPs, and the optimal formulation was selected for further studies (Chapter 4).

4. To establish an *in-vitro* intestinal epithelial cell model of co-culture of Caco-2 cells and HT29-MTX-E12 cells. Subsequently, the cytotoxicity, cellular uptake and transport of optimal formulations by the co-cultured cells were studied. In addition, the cellular up take and transport mechanisms were investigated (Chapter 5).

BESTPFE.COM
List of research project topics and materials

5. *In vivo* pharmacokinetic and pharmacodynamics studies of gemcitabine control drug solution and gemcitabine in the presence or absence of the optimal drug delivery systems were carried out (Chapter 6).

6. The final chapter presents the general discussion and future directions arising from this work (Chapter 7).

Chapter 2

Analytical Method Development for Gemcitabine

Chapter 2 . Analytical method development for gemcitabine

2.1 Introduction

The quantitative determination of APIs in biological samples and pharmaceutical formulations has been accomplished using a variety of different analytical techniques such as spectrophotometry (Nagaraja, Murthy et al. 1998, Coello, Maspoch et al. 2000, Nagaraja, Vasantha et al. 2001, El-Dien, Zayed et al. 2005, Guo, Zhang et al. 2009), spectrofluorimetry (Takahashi and Fitzpatrick 1964, Johnson, Gold et al. 1973, Yang, Zhao et al. 1993, Liu, Yang et al. 2003), flow injection analysis (FIA) (Marcolino-Júnior, Teixeira et al. 2001, Pistonesi, Centurión et al. 2004), chemiluminescence (CL) (Deftereos, Calokerinos et al. 1993), capillary electrophoresis (CE) (Fanali, Pucci et al. 2000, Chen, Zhang et al. 2005), voltammetry (Badawy, Issa et al. 1996, Bergamini, Santos et al. 2005), gas chromatography (GC) (Doshi and Edwards 1981) and high performance liquid chromatography (HPLC) (Schieffer 1979, Kafil and Dhingra 1994, Wu 2000, Siddhuraju and Becker 2001, Cannazza, Di Stefano et al. 2005).

A great deal of literatures reported successfully quantitative analysis of gemcitabine from a variety of sample matrices using RP-HPLC (Losa, Sierra et al. 2005, S Bansal, Celia et al. 2013). Hence, RP-HPLC has been selected as the analytical method of gemcitabine in this study. An HPLC conditions was selected from those reported in the literatures as a preliminary analytical method for further HPLC method development (Abbruzzese, Grunewald et al. 1991, S Bansal, Celia et al. 2013).

Therefore, in this chapter, a rapid, simple, sensitive and reliable HPLC method was develop and validated for separation and quantification of gemcitabine. The application of the analytical method is also introduced.

2.1.1 Analytical techniques to determine gemcitabine

2.1.1.1 Spectrophotometry

Spectrophotometry is a method that measures the amount of light a sample absorbs. The use of spectrophotometric method for determination of an API is based on oxidation of API with

different oxidising agents to *o*-benzoquinone or oxidation followed by coupling with compounds having electron-donating groups. Nagaraja *et al* reported that the oxidation of catecholamine derivatives by N-bromosuccinimide followed by oxidative coupling with isoniazid will lead to formation of red-coloured products (Nagaraja, Murthy et al. 1998). Yilmaz and Kadioglu proposed a sensitive technique Spectrophotometry, gemcitabine was determined by means of zero-order derivative absorbance values (A) at 288 nm and from values from the second-order derivative absorbance values (^{2}D) at 285 nm, and demonstrating a great capability of the method to quantify gemcitabine (Yılmaz and Kadıoğlu 2004). Sacchi *et al* and Ansari *et al*, have used spectrophotometry to determine the amount of gemcitabine as well (Sacchi, Gasparri et al. 2006, Ansari, Tingstedt et al. 2013). These methods can measure gemcitabine concentration in either pharmaceutical formulation or biological samples (urine and blood). However, instability of coloured species, samples require heating or extraction and time consuming are examples of drawbacks of these methods.

2.1.1.2 Spectrofluorimetry

The spectrofluorimetric technique is based on the presence of a fluorophore in the compound of interest or an oxidizing agent is used to facilitate the formation of a fluorescent product. Spectrofluorimetry has been used to determine many APIs and their metabolites. Salmaso *et al* incubated human MCF-7 breast adenocarcinoma and murine MC3T3-E1 embryonic fibroblast cell lines with fluorescein labelled gemcitabine loaded liposomes. Subsequently, the cells were harvested by trypsin treatment and the gemcitabine content was analysed using a spectrofluorimetry (Salmaso). Anto *et al* have used spectrofluorimetry to analyse the gemcitabine elution using the 96-well plate. The excitation and emission light passes through band-pass filters at 485 ± 14 and 542 ± 13 nm, respectively. Moreover, fluorescent excitation and emission maxima in gemcitabine-micellar suspension in oil, are separately and precisely determined by spectrofluorimetry (Anton, Mojzisova et al. 2010). Nevertheless, the technique suffers from limitations for routine application due to various factors influencing the gemcitabine reaction which renders the standardization of the analytical procedure rather cumbersome.

2.1.1.3 Flow Injection Analysis

Flow injection analysis (FIA) coupled with, photometric (Marcolino-Júnior, Teixeira et al. 2001, Pistonesi, Centurión et al. 2004), chemiluminometric (Deftereos, Calokerinos et al. 1993), amperometric (Manuela Garrido, Lima et al. 1997), or fluorometric (Pérez-Ruiz, Martínez Lozano et al. 2007) techniques have been applied for the gemcitabine determination in pharmaceutical products. By using FIA, the samples and reaction reagents are simultaneously injected into the carrier streams which will merge inside a reactor. The reaction mixture was measured by the above mentioned detection systems. FIA significantly increase the sampling rate. Yoza *et al* and Sottani *et al* have reported using a FIA analytical method to determine gemcitabine (Yoza, Ito et al. 1980, Sottani, Turci et al. 2007). However, most of these proposals required the use of reagents in order to generate products that can be measured by the detection systems. The reagents concentrations used are critical and the coloured or fluorescent products are not stable.

2.1.1.4 Capillary Electrophoresis

Capillary electrophoresis (CE) is an efficient, low cost and low detection limit method for analysis of anticancer drugs. Beside it has been widely used to analysis different anticancer drugs in biological samples, environmental matrices and pharmaceutical preparations. It has also been used to detect different biomarkers in cancer patients. Analytes are separated based on different migration velocities of charged species in an electric field through an electrolyte-filled capillary in CE. The very narrow band widths make it much easier to obtain separation and therefore specificity. Ali *et al* have published a review of using CE to analysis various anticancer drug, such as nucleoside analogs, antimitotic agents, antibiotics and topoisomerase inhibitors, etc (Ali, Haque et al. 2013). Compared with the spectrophotometric methods, where a complexation step is needed, this method offers higher separation efficiency, shorter analysis times, cheaper running costs and robustness. In addition, it allows the simultaneous analysis of gemcitabine and carbidopa.

2.1.1.5 Voltammetric Analysis

Voltammetric analysis methods are powerful techniques to estimate the potency of pharmaceutical compounds that have electroactive functionality in their structure. Teradal *et al* have developed a novel, convenient, and sensitive differential pulse voltammetric method to determine gemcitabine in the concentration range of 5.0×10^{-8} to 3.0×10^{-4} M with a limit of detection (LOD) of 8.2×10^{-9} M. Moreover, the developed voltammetric method was successfully applied for the determination of gemcitabine in pharmaceutical formulations as well as spiked biological samples (Teradal, Kalanur et al. 2012). Also published a review of introducing voltammetric techniques combined with different spectrophotometric, chromatographic and spectroscopic methods in the different aspects to successfully analysis various anticancer drugs (Ivić, Petrović et al. 2016). However, the voltammetric techqniues require the use of reagents to clean up the electrode surface and complicated steps involving modified electrode construction. Bergamini *et al* (2005) used a gold screen-printing electrode as an amperometric sensor to determine drug candidates. A microflow cell system was developed to amplify the amperometric signal resulting in manifolds simplification of features and rapidity of analysis (Bergamini, Santos et al. 2005).

2.1.1.6 Gas Chromatography

Gas chromatography (GC) is a common type of chromatography for separating and analysing various compounds that can vaporize without decomposition. Generally, GC is sued to test the purity of the compound or to separate the different components of a mixture. Sometimes it can be used to help in identifying a compound, as well as to prepare pure compound from a mixture (Grob and Barry 2004, Pavia 2006). Although the use of GC to determine gemcitabine has not been reported in literature yet. The use of GC to analyse other anticancer drugs are widely reported. Guetens *et al* have introduced a capillary GC and mass spectrometry to analysis various anticancer agents (Guetens, De Boeck et al. 2002). Gali-Muhtasib *et al* used GC method to quantify the level of thymoquinone, which is a promising anticancer drug from natural sources (Gali-Muhtasib, Roessner et al. 2006). However, this method can hardly be considered as a simple, quick or inexpensive method. It is only justified in conditions necessitate a complete identification of all metabolites of drug candidates in biological tissues.

2.1.1.7 High Performance Liquid Chromatography

Chromatography is defined in the early 1900s by a Russian botanist, Mikhail S. Tsweet as "a method in which the components of a mixture are separated on an adsorbent column in a flowing system." (Berezkin 2001). The adsorbent material, or stationary phase, can be paper, thin layers of solids attached to glass plates, immobilized liquids, gels, and solid particles packed in column. The flowing component of the system, or mobile phase, can be liquid, gas or supercritical fluid. According to the nature of the mobile phase, chromatographic techniques can be classified into three classes: liquid chromatography (LC), gas chromatography (GC) and supercritical fluid chromatography (SFC) (Scott 1994).

High performance liquid chromatography (HPLC) is a liquid chromatography technique for the separation and determination of organic and inorganic solutes in samples, such as biological and pharmaceuticals samples, food, environmental matrices, and industrial chemicals. It has the ability to separate, identify, and quantitate the compounds that are dissolved in a liquid. HPLC is particularly suitable for the separation of compounds that are of high polarity and/or molecular weight, exhibit thermal instability and for compounds that have a tendency to ionize in solution (Hamilton and A. 1982). It can render itself to be a stability indicating assay.

Most HPLC separations of pharmaceutical compounds are carried out on surface reacted or chemically bonded organic stationary phase or bonded-phase chromatographic column (Snyder and Kirkland 1979). Polar adsorbent is used for normal phase HPLC (NP-HPLC) separating compounds of moderate to strong polarity, whereas non-polar adsorbent is used for reversed phase HPLC (RP-HPLC) separation of less polar compounds on the basis of their hydrophobicity (Lough and Wainer 1995). RP-HPLC coupled with different types of detection systems, is the most popular mode of chromatography for analysis of gemcitabine and related substances due to its higher stability, lower equilibration times, wider range of molecules being analysed, and higher retention time than NP-HPLC (Wainer 1985). RP-HPLC involves the use of a non-polar stationary and a polar mobile phase. When a non-polar drug is analysed by RP-HPLC, the decrease in the polarity of the mobile phase will result in a decrease in solute retention. Successful separations are achieved by partition, adsorption or ion-exchange process depending on the type of stationary phase and polarity of the mobile

phase used (Wainer 1985). The use of HPLC technique to separate and quantitate gemcitabine in different sample matrices is summarized in Table 2-1.

Bestpfe.com

Table 2-1. Summary of HPLC conditions for gemcitabine determinations from literature

Column	Sample matrix	Mobile Phase	Detection	Flow Rate	Reference
Waters Spherisorb 4.6 mm × 250 mm, 5 µm C18 column	Plasma and Tissue culture medium	10:90 (v/v) acetonitrile-aqueous buffer (50 mM sodium phosphate and 3.0 mM octyl sulfonic acid, pH 2.9)	UV wavelength set at 267 nm	1.0 ml/min	(Kirstein, Hassan et al. 2006)
Lichrospher C18 (250 mm×4.6 mm ID, 5 µm)	Plasma	40 mmol/L acetate ammonium buffer solution (pH 5.5)/ acetonitrile (97.5:2.5, v/v)	UV wavelength set at 268 nm	0.8 ml/min	(Lin, Zeng et al. 2004)
Tracer Excel ODSA C_{18} analytical column (100 mm × 4.6 mm, 3 µm particle size)	Plasma	KH_2PO_4 10 mM/TBACl 10 mM pH 7 with 0.25% methanol , and KH_2PO_4 250 mM/TBACl 10 mM pH 7:methanol (85:15, v:v)	UV wavelength set at 271 nm	1.2 ml/min	(Losa, Sierra et al. 2006)
µBondapack C_{18} analytical column (300 mm × 3.9 mm, 10 µm particle size)	Raw material, dosage forms	5 mM pentane-1-sulfonic acid pH 3.1/methanol (96:4)	UV wavelength set at 268 nm	1.5 ml/min	(Losa, Sierra et al. 2005)
Hypersil C8 column (150 × 4.6 mm, 5 µm particle size)	Human urine	0.1% aqueous formic acid and acetonitrile (98:2, v/v)	UV wavelength set at 270 nm	1.0 ml/min	(Sottani, Zucchetti et al. 2004)

2.1.2 Gemcitabine Degradation Pathway

Degradation of drugs may change their pharmacological effects, resulting in altered therapeutic efficacies as well as toxicological consequences (Yoshioka and Valentino J 2004). Hence, determining factors that have significant impact on the stability, degradation pathway and the degradation reaction rate of the drug is crucial. The chemical degradation pathways of drug substances include hydrolysis, dehydration, isomerisation and racemisation, decarboxylation and elimination, oxidation, photodegradation and drug-drug interaction (Yoshioka and Valentino J 2004). Various factors including temperature, pH, oxygen, light and moisture can significantly affect the extent of the drug degradation.

It is reported that less than 10% of the administered gemcitabine dose is transported unchanged to the blood circulation after oral administration (Veltkamp, Jansen et al. 2008). This low availability of gemcitabine in the circulation is mostly due to its sensitivity to chemical and enzymatic degradation as well as peripheral decarboxylation (Zorc, Ljubic et al. 1993). In general, most orally administered drug candidates will undergo extensive peripheral decarboxylation at the gut wall (first-pass metabolism) thus results in poor drug oral bioavailability (Blaschko and Chruściel 1960). For some particular drugs, over 90% of the drug content given orally is metabolised in the first passage before it can reach the circulation.

Gemcitabine is readily freely soluble. It is considered as a very hydrophilic compound with a log $P_{octanol/water}$ value of -1.4, and a pKa of 3.5 (Merck 2001). Oral administration of gemcitabine will inevitably expose the drug to the GI lumen that is known to have different pH and enzyme content depending on the location of the drug in the GIT. In a formulation study to improve oral bioavailability of gemcitabine, it is of great importance to develop a simple, efficient and sensitive HPLC analytical method that can separate the drug from its metabolites formed under various physicochemical and enzymatic conditions.

2.2 Aims of Studies

The aims of current studies in this chapter were to develop and validate a stability indicating method for gemcitabine determination using HPLC and to examine the metabolism behaviour of gemcitabine under different conditions using this validated HPLC method.

BESTPFE.COM
List of research project topics and materials

2.3 Materials

Table 2-2. All the chemicals listed for the study.

Chemicals	**Suppliers**	**Comments**
Gemcitabine hydrochloride	Sigma-Aldrich Inc, St Louis, USA	Drug candidate
Hydrochloric acid	Sigma-Aldrich Inc, St Louis, USA	Analytical grade, for Forced Degradation Studies
Sodium hydroxide	Sigma-Aldrich Inc, St Louis, USA	Analytical grade, for Forced Degradation Studies
Hydrogen peroxide	Sigma-Aldrich Inc, St Louis, USA	Analytical grade, for Forced Degradation Studies
Sodium dihydrogen phosphate monohydrate	Merck, Darmstadt, Germany	Analytical grade, used as mobile phase buffer
Poly lactic-co-glycolic acid (PLGA), MW 30,000-60,000	Purac Biochem, Lincoln, IL, USA	Used as polymer to make PLGA NPs
Polyvinyl alcohol (PVA), MW 125,000	Ajax Finechem, Germany	Used as stabilize to prepare PLGA NPs
Milli-Q water	Pharmacy laboratory, University of Auckland, New Zealand	Reverse osmosis using a Millipak® system (Millipore, 0.22 μm), resistivity ≥ 18 Ω cm.
Acetonitrile	Ajax Finechem Pty Ltd, New South Wales, Australia	HPLC grade, used as mobile phase component
Ethyl acetate	Merck, Darmstadt, Germany	Organic solvent to dissolve PLGA
Trifluoroacetic acid	Sigma-Aldrich, Switzerland	Used as ion-pairing agent in organic phase
Methanol	Merck, Darmstadt, Germany	Used for washing method

Instruments:

- GraceSmart RP C_{18} reversed phase column (250 × 4.6 mm, 5.0 µm particle size; GraceSmart, India. Lot NO. 45/077)
- C_{18} guard column (10 × 3.0 mm)
- The Agilent Techologies 1260 series HPLC system used for the assay is composed of :
    1. A vacuum degasser
    2. An autosampler
    3. A thermastatted column compartment
    4. A photodiode-array detector (PAD) (Victoria, Australia)

2.4 Methods

2.4.1 Chromatographic conditions and optimization

The HPLC instrument was used for method development, validation and degradation studies. For instrument control, data acquisition and processing, the chromatographic system is interfaced to Agilent Chemstation software (Agilent Technologies, Germany).

Various mobile phase components, combinations and pHs were investigated, screening the most suitable and simple combinations of reagents. The mobile phase was filtered through a 0.45 µm membrane and degassed prior to use. The column and samples temperature were maintained at 25ºC and 4°C, respectively. Other chromatographic conditions such as injection volume, flow rate and the detection wavelength were also investigated, in order to obtain a simple, efficient, and precise analytical method.

2.4.2 Stock solution preparation

Standard solutions from a range of 1-100 µg/mL were prepared by dilution of a stock solution (1 mg/mL) using mobile phase as solvent. Samples were stored at 4 °C and protected from light until use. The calibration standards in the range of 1-100 µg/mL with 5 replicates were determined by HPLC.

2.4.3 Method validation

The developed HPLC method was validated with respect to linearity, accuracy, precision (repeatability and intermediate precision), limit of detection (LOD), quantitation (LOQ), and robustness according to the International Conference on Harmonisation of technical Requirements for Registration of Pharmaceuticals for Human Use (ICH) guideline (2005).

The linearity of the method was validated over the concentration range of 5-100 µg/ml for gemcitabine. The calibration standards were injected into the HPLC column (5 replicates at each concentration), keeping the injection volume constant (15 µl). The regression lines for each compound were calculated by the peak areas under curves versus analyte concentrations. The gradient of the slope, y-intercept and linearity of the best fit line was obtained. The linearity was determined by linear regression and expressed as R^2. The particular range is derived from linearity studies and is established by confirming that the HPLC method is able to generate an acceptable degree of linearity (Chen, Svirskis et al. 2015).

Sensitivity of the HPLC method was evaluated by the limit of detection (LOD) and quantitation (LOQ) for gemcitabine, which were determined based on the slopes and standard deviations of the intercepts from the linear regression lines. The following expressions were used (Guideline 2005):

$$LOD = \frac{3.3\delta}{S}$$

Equation 2-1

$$LOQ = \frac{10\delta}{S}$$

Equation 2-2

Where σ is the standard deviation of the response and S is the slope of the calibration curve.

The intra-day accuracy and precision of the analytical method were determined by the analysis of 5 replicates of standard solutions containing 5 µg/mL, 40 µg/mL, and 100 µg/mL of gemcitabine to represent low, medium and high concentrations. The inter-day accuracy and precision were determined by preparation of same concentrations with 5 replicates and tested over three consecutive days, giving a total of 15 measurements. The precision of the

assay was determined in terms of percentage relative standard deviation (% RSD), while the accuracy was determined by comparing the measured concentrations against the true concentrations. Robustness measures the capacity of a developed HPLC method to remain unaffected by small but deliberate variations in method parameters. It helps evaluating the reliability of the HPLC method (Guideline 2005). In this study, the influence of different ratios of organic content in mobile phase (ACN : 1.38% w/v sodium dihydrogen phosphate buffer ratio of 9:91, 7:93, 5:95) were investigated, alongside variations in pH (pH 5 – 8) of the mobile phase, different injection volumes (10 – 30 µL), different flow rates (0.8 – 1.2 mL/min) and different temperature (15 – 25 ºC). The peak area, %RSD, theoretical plates and peak tailing were determined subject to these deliberate changes in the method (Guideline 2005, Chen, Svirskis et al. 2015).

2.4.4 Forced Degradation Studies and Peak Purity Assessment

Forced degradation studies were performed on gemcitabine to provide an indication on the stability indicating property and specificity of the proposed method (Bakshi and Singh 2002). All degradation studies were done at an initial gemcitabine concentration of 1.0 mg/ml. For acid and alkaline decomposition studies, degraded samples were prepared by treating standard solution with acid (1.0 N HCl) and base (1.0 N NaOH) over 7 days. For study in heat-stressed condition, gemcitabine (1 mg/mL) was stored in Binder Incubator KBF240 series (Binder, Germany) at 70 °C over 7 days. Oxidative conditions were obtained by mixing gemcitabine standard solution with 3% v/v H_2O_2 at room temperature over 7 days. Photolytic degradation of gemcitabine was tested by storing an aqueous solution of gemcitabine (1 mg/mL) in Binder Incubator KBF240 series (Binder, Germany), with exposed to artificial daylight illumination of 10000 lux. When gemcitabine was exposed to light, no significant degradation was observed over 7 days. Therefore, this particular condition was conducted over 2 weeks. The degradation experiments were terminated when samples were 5% - 20% degraded, compared to the initial samples, or after 14 days, whichever occurred first. After treatment all samples were filtered through a 0.2 µm filter and diluted with mobile phase to appropriate concentrations, the extent of degradation is reported as a percentage of the starting concentration (Bakshi and Singh 2002, Reynolds, Facchine et al. 2002, 2005).

2.4.5 HPLC peak purity test

To assess the purity of gemcitabine peaks in a mixture of stressed samples, a PAD was used. UV spectra were obtained at five points across the peak; two points before the peak apex (leading front), on point at the apex and two points after the apex (tailing front). The peak purity was determined by examining the similarity of the UV spectra obtained at these five points. When a degradation product co-elutes with the gemcitabine peak the five UV spectra obtained across the peak are not similar.

2.4.6 Preparation of gemcitabine-loaded PLGA nanoparticles

To evaluate the application of the HPLC analytical method on a gemcitabine loaded formulation. We used a gemcitabine loaded PLGA NP. These PLGA NPs were prepared by a solvent evaporation method. Aqueous drug solution (0.6 mL of 5% w/v) was added dropwise into 4 mL of ethyl acetate containing 8% w/v PLGA and sonicated at an output of 20 W for 60 sec by ultrasonicator (UP 200S model, Hielscher, USA) to form a w/o emulsion. The emulsion was then poured into 16 mL of 2% w/v PVA aqueous phase to form a w/o/w emulsion and emulsified by ultrasonicator at an output of 20 W for 300 sec. A rotatory evaporator (V-850 model, Buchi®. USA) was used to remove organic solvent for 4 hrs. Then the PLGA nanoparticles were extracted from the emulsion by ultracentrifugation at 138,288 G (Wx Ultra 80 model, Thermo Scientific®. USA). The obtained nanoparticles were washed thoroughly with 5% w/v sucrose water twice, and freeze-dried at -50 ^{0}C for 48 hrs using a freeze-drier (Model Freezone 6, Labconco®, USA).

2.4.7 Application of the analytical method to *in-vitro* release study of the gemcitabine-load nanoparticles

The validated HPLC method was applied to *in-vitro* release of gemcitabine from the nanoparticle formulation for 30 hrs using Franz diffusion cells (VTC 200, Logan, USA). The receptor chamber (12 mL) contained 1.38% w/v sodium dihydrogen phosphate buffer (pH 6.5). Drug loaded nanoparticles, equivalent to 30 mg of gemcitabine, were added to the receptor chamber, while the temperature was maintained at 37 ± 1 °C. An aliquot sample (0.5 mL) was withdrawn at different time intervals over 30 hrs, and replaced by 0.5 mL of fresh

medium. All the samples were filtered by Acrodisc® syringe filters (0.45 µm) before analysis with HPLC (Chen, Li et al. 2014)

2.4.8 Enzyme degradation studies using pepsin, α-chymotrypsin and trypsin

Pepsin is the major digestive enzyme in the human stomach (Mathialagan and Hansen 1996), while trypsin and α-chymotrypsin are the major digestive enzymes in the small intestine (Hayakawa, Kondo et al. 1980). In this study, pepsin (200 mg) was dissolved in 20 mL of pH 1.2 PBS. Gemcitabine encapsulated nanoparticles equivalent to containing 5 mg of gemcitabine were weighed out and added to 20 mL of pepsin solution which was maintained at 37 °C with slow shaking over 48 hrs. At 48 hr, proteolysis was stopped by addition of 1 mL of NaOH (6 M), as pepsin starts to lose activity above pH 4 (Mathialagan and Hansen 1996). Dichloromethane was added to degrade the PLGA capsule follow by a minute of ultrasonication to ensure the complete breakage of the PLGA capsule in order to extract the remaining drug. As a control, gemcitabine (5 mg) was added to 20 mL of the pepsin solution which was treated in the same manner without the dichloromethane addition step. The amount of gemcitabine remaining after 48 hrs was determined by the presented HPLC method. To investigate potential enzymatic degradation in the small intestine a mixed enzymatic solution was prepared by dissolving α-chymotrypsin of 60 mg and trypsin of 60 mg in 20 mL of pH 6.8 PBS. The study was conducted in a same format as for pepsin, except using 2 mL of 30% v/v acetic acid to terminate the proteolysis at 48 hr (Hayakawa, Kondo et al. 1980). To investigate the recovery of gemcitabine from dichloromethane, standards of 0.1 mg/ml, 0.25 mg/ml, 0.5 mg/ml and 1 mg/ml gemcitabine in dichloromethane were prepared and analysed by HPLC.

2.4.9 Data Analysis

All data reported are the mean of triplicate measurements ± standard deviation. Differences in % gemcitabine remaining between groups were determined using one-way ANOVA followed by Tukey's test. Probability estimates of $p < 0.05$ were considered to be significant. All analyses were carried out using MINITAB (version 17).

2.5 Results and discussion

2.5.1 Development and Optimization of the HPLC Method

An HPLC method was required to separate and quantify gemcitabine. The successful use of an HPLC method for a given compound requires the appropriated combination of operating conditions such as: column type, mobile phase composition and pH, injection volume, flow rate and detection system.

Based on the UV spectrum obtained for gemcitabine, a fixed UV wavelength was selected at 270 nm. The retention time (R_t) and shape of the gemcitabine peak were adjusted through modifying firstly, the flow rate and secondly, the composition of the mobile phase. The R_t shifted as anticipated with the change in flow rate. The change of the mobile phase composition will lead to change on the R_t of gemcitabine. The R_t of gemcitabine could be decreased (peak is eluted faster) by increasing the organic proportion in the mobile phase. The slight variations in the mobile phase composition did not change the chromatography observed. However, it will be noted that the R_t of gemcitabine peak was sensitive to the change in the amount of ACN in the mobile phase. At 1 ml/min flow rate, a composition of 4% ACN in mobile phase gave baseline separation for gemcitabine at around 4.70 min.

The optimal conditions for quantification of gemcitabine are reported in Table 2-3. Figure 2-2a shows an injection of a gemcitabine standard solution (100 µg/ml) with the drug eluting as a sharp peak at around 4.65 min.

Table 2-3. Optimized HPLC conditions

Column	Mobile phase	Detection	Injection Vol	Flow rate	Temperature
GraceSmart RP C_{18} column (250 × 4.6 mm, 5.0 µm particle size)	ACN and 1.38% w/v sodium dihydrogen phosphate buffer (pH 6.5) at the volume ratio of 7:93	270 nm	20 µl	1 ml/min	Column: 30°C Sample: 4°C

2.5.2 Validation studies

2.5.2.1 HPLC standard curve for gemcitabine

The standard curve of gemcitabine was prepared by plotting response area versus concentration (Figure 2-1). The slope was 35.416 ± 0.010 with a y-intercept of 4.2703 ± 0.351. The linearity of the best fit line was expressed regard to $R^2 = 0.9999$, which indicated a good linearity over the concentration range of 1-100 µg/mL detected.

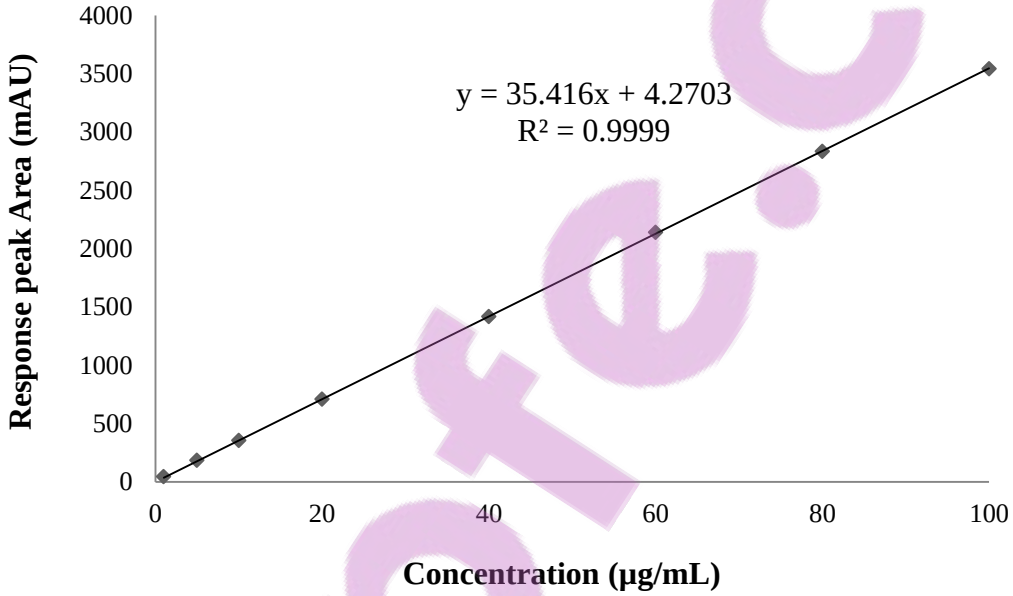

Figure 2-1. Gemcitabine standard curve achieved by using developed HPLC method. (Data points indicate mean ± SD, n = 5).

Bestpfe.com

Table 2-4. Intra- and inter-day accuracy and precision of the HPLC method.

Spiked concentration of gemcitabine (µg/mL)	Calculated concentration of gemcitabine (µg/mL)	Accuracy %	Precision (RSD) %
Intra-day			
5	5.09 ± 0.087	101.77	1.71
40	39.96 ± 0.182	99.91	0.46
100	99.96 ± 0.465	99.96	0.47
Inter-day			
5	5.04 ± 0.027	100.77	0.54
40	40.06 ± 0.271	100.16	0.68
100	100.04 ± 1.101	100.04	1.10

The data obtained from the precision experiments are shown in Table 2-4. LOD indicates the lowest concentration of analytes the HPLC method can detect (Armbruster, Tillman et al. 1994). The result indicated that LOD of 0.014 µg/mL and LOQ of 0.043 µg/mL was obtained from the equations, indicates the lowest concentration of analytes the HPLC method can be detected and quantified, respectively (Armbruster, Tillman et al. 1994, Shrivastava and Gupta 2011). Accuracy and precision results for intra-day and inter-day are presented in Table 2-4. These results indicate the excellent intra- and inter-day accuracy and precision, which are well within the ICH acceptance criteria (Guideline 2005, Li, Martini et al. 2012).

Table 2-5. Robustness data for the analytical method with different conditions.

Parameters	Optimized	Used	Mean peak Area	% RSD	Plate count	Tailing
Mobile phase ACN : phosphate buffer	7 : 93	9:91	3618.57	1.61	10748	0.97
		7:93	3575.77	1.55	12057	1.13
		5:95	3564.33	1.25	8746	1.01
pH (± 1.5)	6.5	5	3520.73	1.39	10949	0.97
		6.5	3575.77	1.83	12057	1.13
		8	3765.64	1.10	11841	0.97
Injection volumes (± 10 µL)	20 µL	10 µL	3567.07	1.16	11694	0.98
		20 µL	3575.77	0.99	12057	1.13
		30 µL	3553.87	1.64	12913	1.16
Flow rates (± 0.2 mL/min)	1 mL/min	0.8 mL/min	3643.77	1.25	11539	1.06
		1.0 mL/min	3575.77	1.83	10436	1.13
		1.2 mL/min	3739.47	1.07	10729	1.16
Temperature (± 5 °C)	20°C	15°C	3569.30	1.09	11380	1.19
		20°C	3575.77	0.99	12057	1.13
		25°C	3545.00	0.73	14377	1.14

BESTPFE.COM
List of research project topics and materials

Variations of pH in the mobile phase, injection volume, organic phase ratio and flow rate to test robustness. It was observed that the deliberate changes have no significant impact on the peak area, %RSD $\leq$ 1.83 in all cases. The system suitability was found to meet pre-established criteria at all the conditions and the %RSD in peak area was less than 2.0% for all conditions tested (Guideline 2005).

The higher the plate numbers indicates the method is more efficient, that is, it generates a narrower peak at a given retention time than a method with a lower plate count (Kirkland, Yau et al. 1977). Our results also showed significant high plate count of >8000, they all met the ICH acceptance criteria, which indicated sharper peaks, and smaller amount of overlap that occurred between them.

The peak tailing is defined as the distance from the front slope of the peak to the back slope divided by twice the distance from the centre line of the peak to the front slope (Dongre, Shah et al. 2008). A good peak shape can be defined as a symmetrical peak and poor peak shape can include both peak fronting and tailing, the ICH guideline indicates a good peak shape can be defined by a tailing factor of no greater than 2 (Guideline 2005, Sistla, Tata et al. 2005). From Table 2-5, the tailing factor obtained with all the changed conditions meets the ICH acceptance criteria for robustness study as per protocol.

All these parameters indicate a promising system with specificity, precision and column stability ensuring the method is robust. Although when different percentage of organic content in the mobile phase were tested, various elution time of the peaks were observed, with higher ratios of organic solvent leading to quicker elution of the gemcitabine peak. However the eluting peaks were clearly detectable with satisfactory resolution, USP plate count, tailing factor and excellent purity of the peaks. Therefore, it indicated the reliability of the developed method, and ensured the method need not be revalidated (Blessy, Patel et al. 2014).

2.5.3 Forced Degradation of gemcitabine

Many factors may affect the chemical stability of drug substances including the molecular structure of the drug itself and environmental factors, such as temperature, pH, buffer species, ionic strength, light, oxygen, and moisture (Yoshioka and Valentino J 2004). Forced

degradation studies of gemcitabine conducted under different stress conditions suggested the following degradation behaviour.

2.5.3.1 Acid and Basic Conditions

According to ICH guidelines, degradation of gemcitabine (1 mg/mL) was forced in 1 N HCl, with 6.5 ± 0.7% (mean ± SD, n=3) of gemcitabine degraded over 7 days, resulting in degradation peaks eluting at 1.804 and 2.761 min (Figure 2-2b).

When subjected to the basic condition of 1 N NaOH, with 7.3 ± 1.4% of the drug degraded over 7 days forming several degradation products (Figure 2-2c), degradation of the drug at alkaline conditions resulted in the formation of degradation products that were eluted at 2.839, 2.904, 3.799, 4.142, 6.040 and 6.484 min.

The results from the forced degradation studies in acid and base demonstrate that gemcitabine is relatively stable in strong acidic and strong basic environments, indicating pH does not significantly affect the stability of gemcitabine.

2.5.3.2 Oxidative Conditions

Upon treating the drug with 3% v/v H_2O_2 at room temperature for 24 h, slight fall in the drug peak area was observed. With 13.2 ± 2.1% of gemcitabine degraded over 7 days, and a major degradation product observed at elution time 2.652 min, and two additional peaks at 3.096 and 4.095 min (Figure 2-2d). This shows a relatively greater extent of degradation observed in oxidative stress condition.

2.5.3.3 Heat-stressed Conditions

Under 70 °C condition, 14.5 ± 2.0% degradation was observed over 7 days, with the degradation product shown at the peak eluted at 4.650 min, with a major degradation product eluted at 6.757 min (Figure 2-2e). Purity assessment revealed that the UV spectra of the drug were similar across the peak. This indicted that gemcitabine eluted as a pure compound without interference from any degradation product.

2.5.3.4 Photolytic Conditions

When gemcitabine was exposed to artificial daylight illumination of 10000 lux, there was less than 5% drug degradation over 7 days, to achieve more than 5% degradation and to determine if the gemcitabine peak remained pure with adequate resolution from any degradation peaks the experiment was extended to 2 weeks. The results show a 5.2 ± 1.5% of gemcitabine degraded under light over 2 weeks, with a degradation product eluted at 3.669 min (Figure 2-2f). The concentration of the test solution remained unchanged. Gemcitabine seemed to be stable under photolytic conditions. The gemcitabine peak was adequately resolved from all degradation peaks, which ensuring the acceptability of this analytical method.

In addition, the degradation peaks were not identified in this study, as they have been previously reported by others. Naga M *et al* reported gemcitabine was degraded under oxidative stress to a predominant degradation component identified as 4-amino-1-(2-deoxy-2,2-difluro-a-D-erythro-pentofuranosyl) pyrimidin-2(1H)-one (Naga Malleswararao, Suryanaryana et al. 2012). Jansen *et al* investigated the degradation products under thermal stress by nuclear magnetic resonance (NMR). Thermal degradation caused gemcitabine to undergo deamination to uridine derivatives, thus the possible peak of the degradant from Figure 2e can be identified as 2'-deoxy-2',2'-difluorouridine (Jansen, Akers et al. 2000).

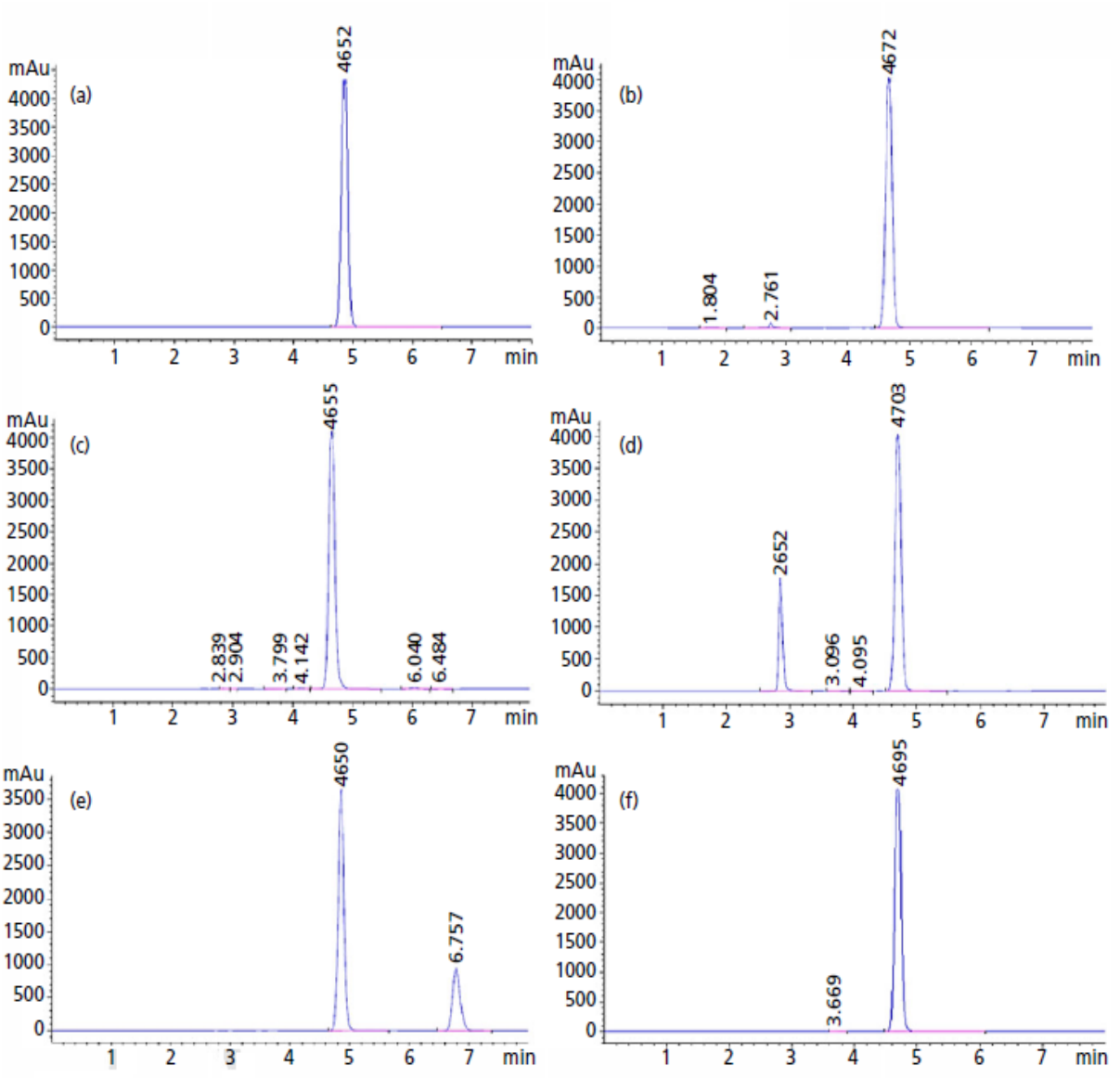

Figure 2-2. Chromatograms of gemcitabine (1 mg/mL) with a retention time of 4.8 min; a) standard, b) following exposure to HCl (1 N) over 7 days, c) following exposure to NaOH (1 N) over 7 days, d) following exposure to H_2O_2 (3% v/v) over 7 days, e) following exposure to 70 °C over 7 days, f) following exposure to light over 2 weeks. Peak purity of five overlaid UV spectra (inset) at five time points across the gemcitabine was shown homogeneity, confirming the purity of the peaks are acceptable.

2.5.4 Application of the HPLC method to determine *in-vitro* drug release from PLGA NPs

The *in-vitro* drug release study of the drug-loaded NPs exhibited an initial burst of release with 14.60 ± 0.48 % of gemcitabine releasing in the first hr. This burst release of gemcitabine from the NPs which may result from drug adsorbed or close to the surface of NPs and the large surface to volume ratio of the NPs due to their size. In addition, following addition of the formulation to the dissolution medium, the water soluble drug could partitioned quickly into the medium accounting for the burst release phase (Magenheim, Levy et al. 1993). This was followed by sustained release with a total of 72.40 ± 0.16 % of drug being released over 30 hrs (Figure 2-3). There was a secondary increase in release rate observed around the 6 hr sampling point and can be attributed to PLGA polymer erosion, follow by diffusion of the dissolved drug within the core of the PLGA NPs into the dissolution medium gradually (Saab, Magda et al. , Magenheim, Levy et al. 1993). Depending on the desired application, the drug release rate from polymeric matrix could be adjusted by modifying the concentration of polymers. Increasing the concentration of the polymer in the delivery system would be expected to slow release of the incorporated drug, whereas comparatively low concentrations of polymer would result in a quicker drug release phenomenon (Saab, Magda et al.).

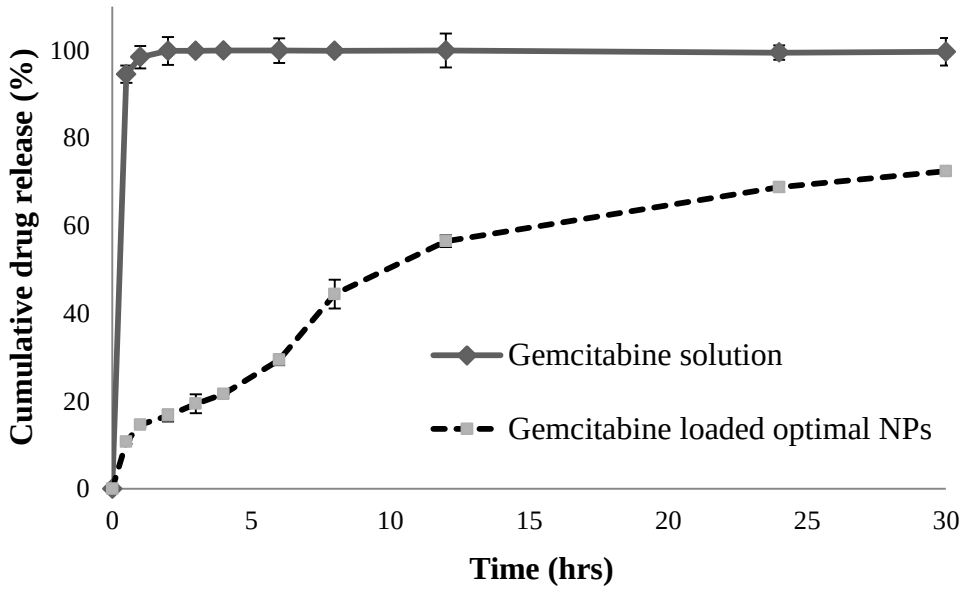

Figure 2-3. *In-vitro* drug release profile of gemcitabine-loaded PLGA NPs. (Mean ± SD, n=3).

2.5.5 Enzyme degradation studies

The stability of the gemcitabine encapsulated NPs was studied in the presence of pepsin, trypsin and α-chymotrypsin to simulate their exposure to both gastric and intestinal enzymes following oral delivery (Marschütz and Bernkop-Schnürch 2000, Borisagar, Patel et al. 2012). Figure 2-4 shows that in the presence of pepsin, trypsin and α-chymotrypsin, the drug solution underwent enzymatic degradation, with over 95% of the drug degraded over a 48 hr period. In contrast, the drug encapsulated NPs were incubated with the digestive enzymes for 48 hrs, with 34.01 ± 2.21% and 22.72 ± 3.12% of drug remaining in the pepsin solution, and the combined trypsin and α-chymotrypsin solution, respectively. These results demonstrate that a significant level of protection against digestive enzymes is afforded by encapsulating gemcitabine in PLGA NPs, $p = 0.0011$ between the encapsulated and free drug groups. The gemcitabine peaks on the HPLC chromatograms remained pure in all situations with no additional peaks observed due to enzymes, solvents or degradation products. The Analysis of gemcitabine standards in dichloromethane at 0.1 mg/mL, 0.25 mg/mL, 0.5 mg/mL and 1 mg/mL gave recoveries of 98.23 ± 2.68%, 99.88 ± 1.75%, 100.01 ± 1.41% and 98.91 ± 3.21%, respectively.

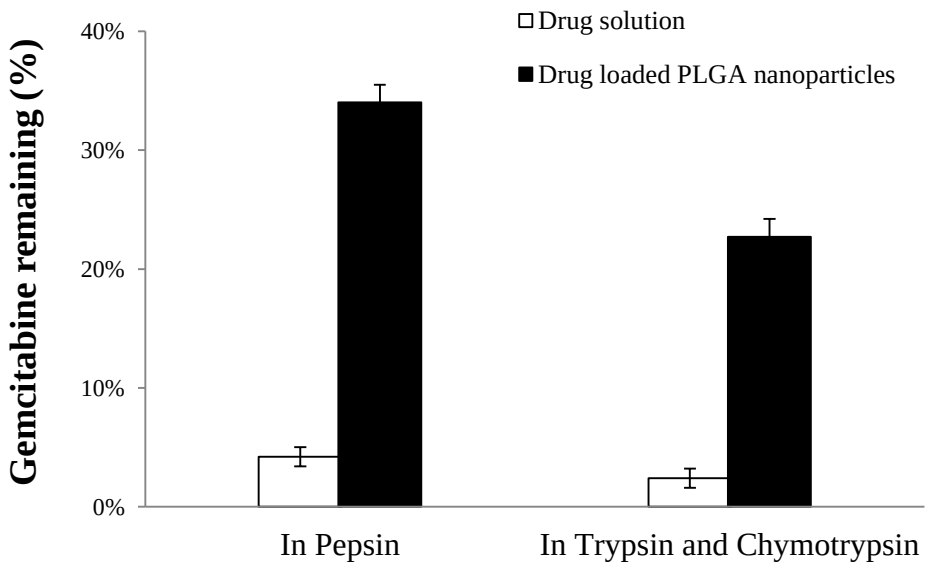

Figure 2-4. Enzymatic degradation of gemcitabine solution and gemcitabine loaded PLGA nanoparticulate delivery system in pepsin, trypsin and α-chymotrypsin enzymatic environment over 48 hrs (Mean ± SD, n=3).

The results from the stability studies of enzymatic degradation of gemcitabine drug solution and gemcitabine loaded PLGA NPs showed a stabilizing effect of encapsulation in PLGA polymer since drug degradation was reduced significantly compare to the naked drug solution without the carrier system. The formulation protects drug from secreted digestive proteases as these enzymes must first penetrate into the polymeric network of the carrier matrix before they can degrade the embedded drug (Lopedota, Trapani et al. 2007). Referring back to the *in-vitro* drug release studies, after 30 hrs, 72.40 ± 0.16 % of drug was released from the formulation, which is in the same range as the 30% of drug that remained after 48 hrs of incubation in the enzymatic mixture. In future work it would be interesting to more closely investigate the timing between release from the formulation and enzymatic degradation. However, In order to improve this protective effect of the carrier matrix from enzymatic degradation, the incorporation of enzyme inhibitors to the nanoparticular carrier system can be applied in the future studies, enzyme inhibitors such as soybean trypsin inhibitors, chromostatin and aprotinin, etc (Marschütz and Bernkop-Schnürch 2000). The protective properties of the nanoparticulate delivery system can be significantly advanced by these simple polymer modifications.

2.6 Conclusion

An isocratic RP-HPLC method for the quantification of gemcitabine was developed and validated showing good linearity and reasonable sensitivity with high accuracy and precision. Therefore, this method is suitable for its intended purpose. Results of robustness, however, reveals that extra care should be taken during preparation of the mobile phase as the method is very sensitive to change in the ratio of ACN and buffer. The change of aqueous phase pH also significantly affects the elution time and the peak shape of gemcitabine. The optimal chromatographic conditions were determined and were used for the future studies. Following forced degradation, all the gemcitabine peaks were adequately resolved from the degradation products, which ensured the acceptability of this analytical method. This analytical method was applied in *in-vitro* drug release studies, generating a sustained release profile from the drug-loaded nanoparticulate delivery system. Finally, this analytical method was applied to enzymatic degradation studies. The enzymatic metabolism studies demonstrated that gemcitabine can be metabolised by the digestive enzyme to some extent, and the results also demonstrated that gemcitabine, following encapsulation in PLGA NPs, was protected from metabolism. Therefore, in order to improve the bioavailability of gemcitabine,

sustained/controlled release drug delivery systems that can protect the drug from chemical and enzymatic metabolism would be desirable. The formulation and characterization of nanoparticulate drug delivery systems are described in Chapter 3. From all these studies, it can be concluded that this isocratic HPLC method is a promising analytical method in the overall performance of gemcitabine containing formulations.

Bestpfe.com

Chapter 3

Development and Optimization of TMC Modified PLGA-TPGS Nanoparticles

Chapter 3. Development and optimization of TMC modified PLGA-TPGS nanoparticles

3.1 Introduction

As discussed in Chapter 1 and 2, gemcitabine is a very effective drug for the treatment of breast cancer. However, gemcitabine has a very short plasma half-life of approximately 12 min (Campbell and Hasinoff 1989, Abbruzzese, Grunewald et al. 1991). It undergoes peripheral decarboxylation by AADC and first-pass metabolism resulting in limited amount of the given gemcitabine dose is transported unchanged to the breast cancer site after oral administration (Zorc, Ljubic et al. 1993). Due to limited transport across the GIT to the blood circulation, gemcitabine has to be administered at high dose continuously with administration of a peripheral decarboxylase inhibitor such as carbidopa (Whitney 2007). However, it is potentially toxic if a large amount of gemcitabine is ingested in combination with an AADC inhibitor. These toxic side effects include cholangiocellular, carcinomas, nausea, neutropenia, hair lost, and gastrointestinal disturbances such as vomiting and anorexia (Pahwa and Koller 1998, Kubicka, Rudolph et al. 2000, Whitney 2007). In addition, gemcitabine can also undergo auto-oxidation and enzymatic oxidation to generate toxic metabolites (Parsons 1985) because as described in Chapter 2, gemcitabine can be oxidized relatively easy (Siddhuraju and Becker 2001).

A promising approach to circumvent such limitations and increase its bioavailability is to encapsulate the gemcitabine in a suitable nano-sized carrier and to specifically target breast cancer via oral drug delivery route. This aim in using PLGA based NPs is to improve gemcitabine bioavailability by protecting gemcitabine against peripheral decarboxylation, enzymatic degradation and promote the permeation of the drug across the GIT to the blood circulation. PLGA was selected for formulation of polymeric NPs due to its biodegradability and biocompatibility as well as high permeability across the GI tract.

D-α-tocopheryl polyethylene glycol 1000 succinate (TPGS) is a hydrophilic derivative of natural vitamin E, which is formed by esterification of vitamin E succinate with polyethylene glycol (PEG) 1,000. TPGS could improve drug permeability through intestinal epithelial cell membranes by inhibiting P-glycoprotein, a drug efflux pump. Thus elevate drug absorption as

BEST-THESIS.COM
List of research project topics and materials

well as reducing P-glycoprotein-mediated multidrug resistance in tumour cells (Dintaman and Silverman 1999, Yu, Bridgers et al. 1999, Ma, Zheng et al. 2010). In addition, it was reported that TPGS could also inhibit the human lung cancer cells effectively. This was confirmed from *in-vitro* cell culture studies and *in-vivo* studies on lung cancer bearing mice (Youk, Lee et al. 2005). The superior anticancer effect of TPGS is associated with its ability to induce cancer cells apoptosis and not due to its increased cell uptake into cells (Youk, Lee et al. 2005, Neuzil, Tomasetti et al. 2007, Constantinou, Papas et al. 2008). Synergistic anticancer effects can be also obtained by using vitamin E isomers or derivatives combining other antitumor agents (Constantinou, Papas et al. 2008). Furthermore, TPGS can be also used as a stabilizer for NPs preparation. TPGS-emulsified drug loaded NPs have shown great drug encapsulation capability as well as sufficient cellular uptake, enhanced drug half-life and improving anticancer effects compared to those emulsified by PVA stabilizer, which is a widely used stabilizer in PLGA NPs preparation (Ma, Zheng et al. 2010). Therefore we were inspired to develop a PLGA-TPGS NPs formulation and stabilized by TPGS emulsifier for gemcitabine.

TMC, a derivative of chitosan, which has been widely applied in various pharmaceutical formulations due to its many benefits such as great stability, enhanced solubility in physical pH, and most importantly, it allows to increase the mucoadhesion to the intestinal epithelial membrane, thus facilitating drug permeation across the intestinal epithelial membrane (Snyman, Hamman et al. 2003, Sahni, Chopra et al. 2008). Bearing with this in mind, TMC is considered as a great option to encapsulate PLGA-TPGS NPs as an outer coating. Therefore it will further protect the inner PLGA-TPGS NPs from harsh GIT environment as well as enhancing the drug loaded NPs to permeate through the intestinal epithelial membrane which attributed by its great mucoadhesion property. Therefore in this project, we develop a novel TMC modified biodegradable PLGA-TPGS random copolymer NPs for oral delivery of gemcitabine to treat breast cancer.

Several techniques to fabricate PLGA based NPs have been reported in the literature (Astete and Sabliov 2006). Selection of a particular method of encapsulation depends on the drug solubility and molecular stability. The commonly employed techniques for NPs preparation are emulsion evaporation, emulsion diffusion, solvent displacement and salting out (Astete and Sabliov 2006). The most widely used technique for hydrophilic drug encapsulation in NPs is the double emulsion method. As it is difficult to entrap a hydrophilic molecule within

a hydrophobic polymer, this technique takes advantage of high energy mixing. By using this technique, a primary water-in-oil (W_1/O) emulsion of hydrophilic drug and polymer is formed, and the secondary water-in-oil-in-water ($W_1/O/W_2$) emulsion is formed by dispersion of the primary emulsion in an aqueous phase. Subsequently, polymeric particles were precipitated upon removal of the organic solvent. The drawback of double emulsion solvent evaporation is the low entrapment efficiency of the hydrophilic compounds due to the hydrophilic molecules are easily diffusing out of the inner W_1 phase to outer W_2 phase.

Taking advantage of the polymeric NPs, the main focus of the present study was on the development of TMC modified PLGA-TPGS NPs (Figure 3-1), that will allow oral delivery of gemcitabine to cross GIT, thus achieving the ultimate goal of this research: to enhance oral bioavailability of gemcitabine.

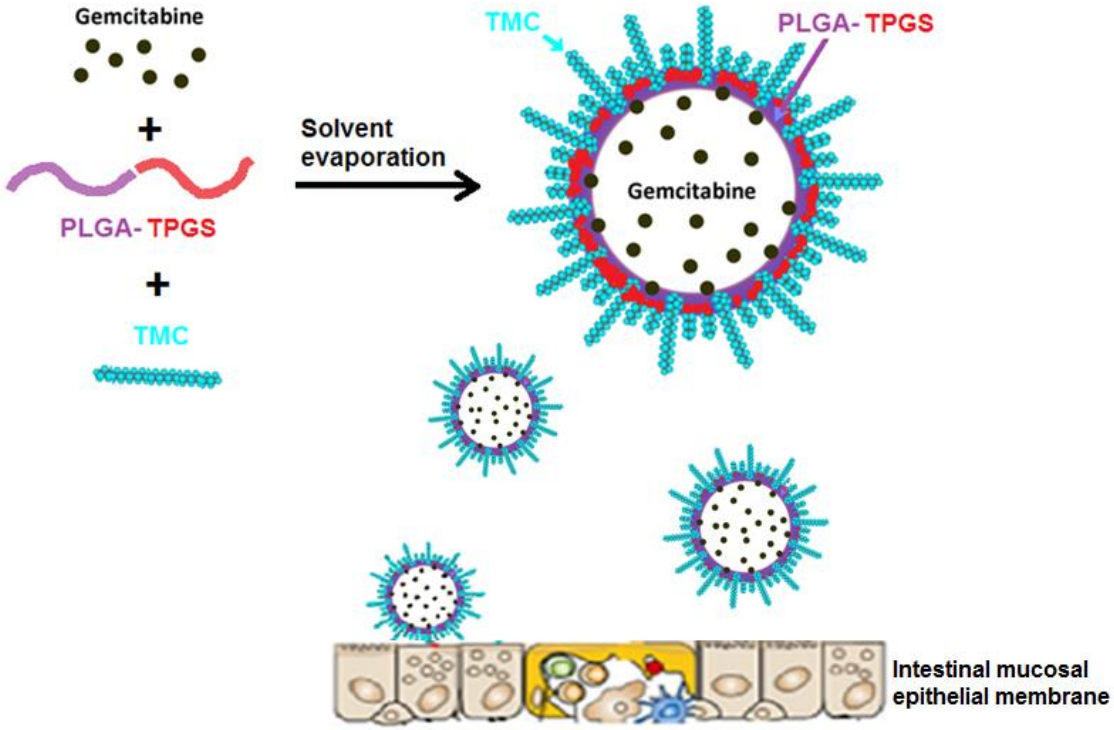

Figure 3-1. A schematic layout of the formulation design to enhance the oral bioavailability of gemcitabine.

To fabricate this drug delivery system, the chemical conjugation of PLGA-TPGS copolymer was predominately prepared. Subsequently the gemcitabine-loaded PLGA-TPGS NPs was fabricated with a double emulsion solvent evaporation technique. Finally, to address the TMC outer coating by further suspend the NPs in the TMC solution. The NP formulations were then characterized for their particle size, size distribution, zeta potential, morphology, drug entrapment efficiency, drug release and long-term stability. The process and formulation variables were optimized to produce nano-scale particles with high drug entrapment efficiency based on a factorial design and response surface methodology (RSM).

3.2 Materials

Poly(D,L-lactide-co-glycolide) (PLGA: L/G = 50/50, MW 7,000 - 17,000) was provided by Purac Biochem, Lincoln, IL, USA. D-α-tocopheryl polyethylene glycol 1,000 succinate [TPGS, $C_{33}O_5H_{54}(CH_2CH_2O)_{23}$], gemcitabine (purity ≥ 98%), stannous octoate [Sn(OOCC7H15)2], 3-(4,5- dimethylthiazol-2-yl)-2,5-diphenyltetrazolium bromide (MTT), trifluoroacetic acid (HPLC grade, purity ≥ 99.0%), fluorescein isothiocyanate (FITC) conjugation kit, *N*-hydroxysulfosuccinimide (NHS), *N*-(3-Dimethylaminopropyl)-*N*'-ethylcarbodiimide hydrochloride (EDC), were obtained from Sigma-Aldrich (St. Louis, MO, USA). Dichloromethane (DCM, AR grade) and pyridine were purchased from Scharlau Chemie S.A (Barcelona, Spain). Acetonitrile (HPLC grade) and toluene (HPLC grade) were supplied by Merck (Auckland, New Zealand). Distilled, deionised water was used throughout and was obtained from a Millipore water purifier (Milli-Q water gradient, resistivity ≥ 18 Ω cm). All other chemicals used were reagent grade.

3.3 Methods

3.3.1 Formulation development

To prepare the gemcitabine-loaded TMC modified PLGA-TPGS NPs, the modified water-in-oil-in-water ($W_1/O/W_2$) emulsion solvent evaporation technique was used (Blanco and Alonso 1997, Davda and Labhasetwar 2002).

3.3.1.1 PLGA-TPGS copolymer synthesis

First, a copolymer of PLGA-TPGS conjugation is synthesised. PLGA-TPGS random copolymers were synthesized from PLGA and TPGS in the presence of stannous octoate as a catalyst via ring opening polymerization (Ma, Zheng et al. 2010) (Figure 3-2). Briefly weighted amounts of PLGA, TPGS (weight ratio 1:1) and 0.5% w/w stannous octoate (in distilled toluene) were added in a flask. The mixture was heated to 145°C and allowed to react for 16 hr. Synthesis was carried out under an oxygen and moisture free environment. The product was dissolved in dichloromethane and then precipitated in excess cold methanol to remove unreacted PLGA polymers and TPGS. The final product was collected by filtration and vacuum dried for 24 hr to remove organic solvent residues.

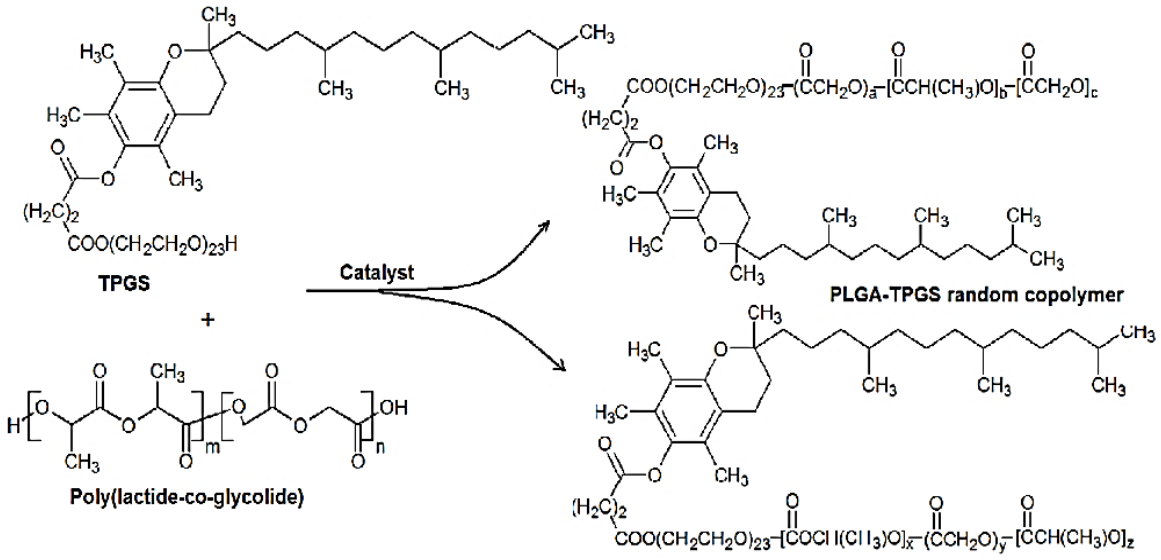

Figure 3-2. Schematic description of the synthesis of PLGA-TPGS random copolymer.

3.3.1.2 Fourier transform infrared (FTIR) spectroscopy

The molecular structure of PLGA-TPGS copolymer was determined by using a FTIR spectrophotometer with a Tensor 37 FTIR Spectrometer (Bruker Optics, Ettlingen, Germany) equipped with an attenuated total reflection Ge crystal cell in the reflection mode. In brief, the random copolymer samples for FTIR analysis were placed on the measuring stage, and a testing probe was pressed to contact the sample and conduct the measurement. Background signals were recorded and subtracted automatically from the sample reading. Each sample was scanned 64 times from 400 to 4000 cm^{-1} with a resolution of 4 cm^{-1}.

3.3.1.3 PLGA-TPGS NPs preparation

0.6 ml aqueous solution of gemcitabine 25 mg/ml (prepared in Milli-Q water) was emulsified in 4 ml of dichloromethane (DCM), an organic phase, containing 1% w/v PLGA-TPGS, by means of sonication using a microtip probe sonicator (UP 200S, Hiescher, Germany) at an output of 20 W for 90 sec to form a primary W_1/O emulsion. The primary emulsion was further emulsified in 16 ml of TPGS solution (0.6%, w/v) by sonication for 150 sec at 20 W to obtain a double $W_1/O/W_2$ emulsion. The resultant double emulsion was then stirred at a rate of 600 rpm for 5 hrs at room temperature on a magnetic stirring plate to evaporate organic solvent. After 5 hrs of stirring, the resultant suspension was transferred to a rotary evaporator (Buchi Rotavapor R-215, Switzerland) and dichloromethane was further evaporated by reduced pressure until the bubble formation ceased. The resulting NPs suspension was kept at 4ºC overnight to allow hardening of the PLGA-TPGS membrane by allowing the dichloromethane to fully partition to the external aqueous phase. NPs were recovered by ultracentrifugation (Sorvall WX Ultra80 Centrifuge, Thermo scientific, USA) at 173210 g for 1 hr at 4ºC. The supernatant was removed and NPs sediments were washed twice with sucrose solution to remove free drug and excess surfactant, and further suspended in 16 mL of 0.5% w/v TMC solution, with gentle stirring to allow TMC fully adsorb on the surface of PLGA-TPGS NPs, the resultant suspension were ultracentrifuged at 173210 g for 1 hr at 4ºC, the sediments TMC modified PLGA-TPGS NPs were then lyophilized (Labconco, USA) for 2 days. The lyophilized NPs were stored at 4 °C until needed. A schematic diagram for the preparation of the drug-loaded PLGA NPs using double emulsion solvent evaporation technique is shown in Figure 3-3.

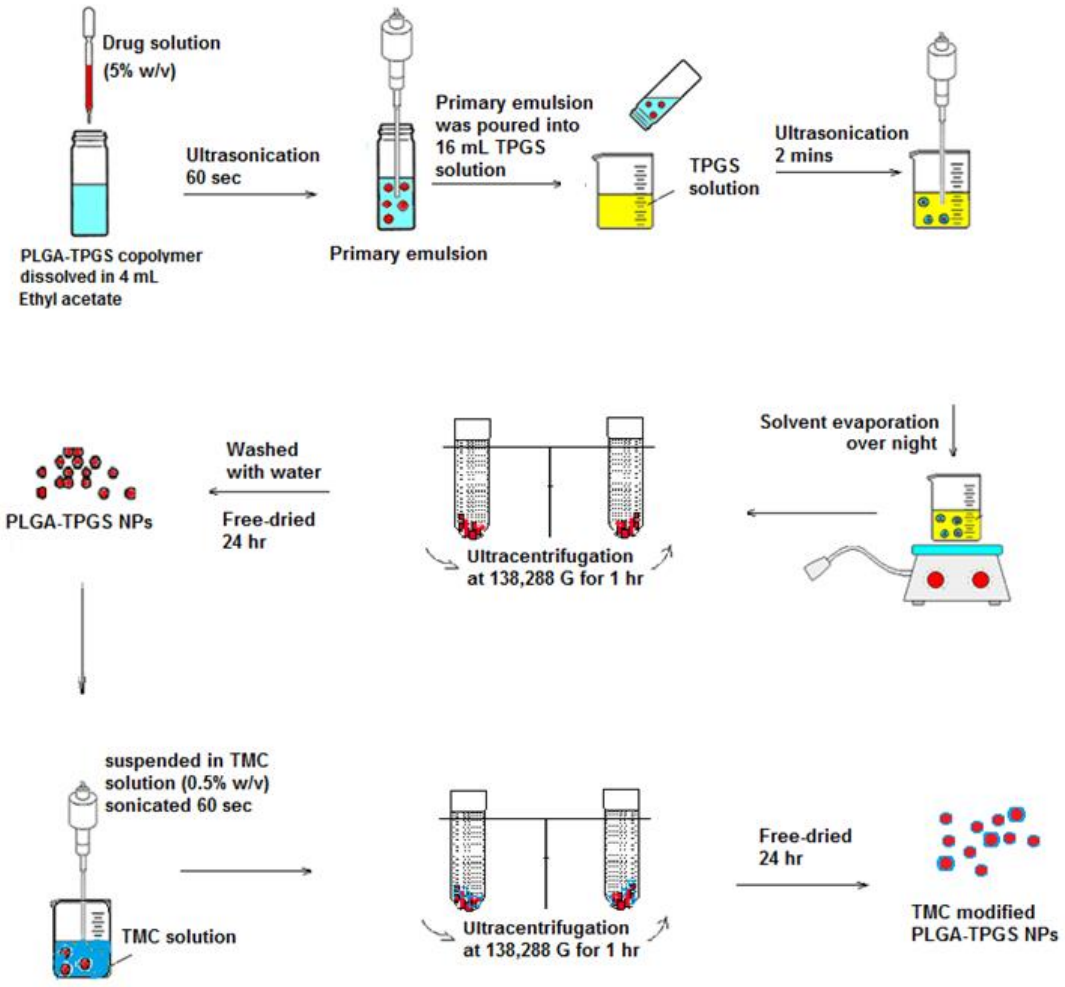

Figure 3-3. Schematic diagram for the preparation of NPs using the double emulsion solvent evaporation technique.

3.3.1.4 Evaluation of the effect of different glucose and sucrose used in the NPs washing step

In order to produce NPs with narrow size distribution and better redispersity, various concentrations (1, 3 and 5% (w/v)) of glucose and sucrose were investigated during NP washing procedure. After ultracentrifuge, NPs pellets were redispersed in a glucose/sucrose solution and votex for a mintue to wash off the drug on the NPs surface and further stabilize the NPs. The suspension was then kept in freezer overnight, ultracentrifuged and followed by freeze-dried for 2 days. The lyophilized particles were subjected to appearance observation and particle size analysis to determine the most suitable concentration of sucrose solution to be used to wash the NPs.

3.4 Factorial design

Traditional pharmaceutical formulation is developed by changing one variable while keeping the other variables constant at a time. However, it is difficult to evaluate an ideal formulation using this method since the combined effects of the variables are unknown. When there are two or more variables involved in an experiment, we want to know not only whether there is an effect of each variables alone but also whether there is an interaction between them (one variable affects the response of the experiment to the other). Therefore, it is important to use statistical tools to understand the complexity of a pharmaceutical process. In addition, we would also want to predict a response based on the knowledge of the way a response depends on the input variables. Furthermore, we would also want to optimize the pharmaceutical process to yield a maximum or minimum response based on the relationship between controllable (independent) variables and dependent variables (responses). Response Surface Methodology (RSM) is a collection of mathematical and statistical techniques that can be used to develop, improve or optimize products. RSM typically is used for the modelling and analysis of problems in which a response of interest is affected by several variables the objective is to optimize this response (Myers, Montgomery et al. 2009).

A typical RSM comprises three steps: design of experiment, modelling and optimization. Each of these is described below.

3.4.1 Design of experiment

Design of experiment (DOE) is defined as the strategy for setting up experiments in such a manner that the information required is obtained as efficiently and precisely as possible (Fu, Ping et al. 2005). There are many designs reported in the literatures such as factorial design, central composite design, extreme vertices design, simplex design, evolutionary operations, etc (Stetsko 1986). Factorial design is one of the experiment designs that is widely utilized in the investigation of pharmaceutical formulation to characterize multivariable processes (Box, Hunter et al. 1978). It allows separation of the important factors, and identification of any possible interactions between those factors. A full factorial experiment consists of two or more factors, each with discrete possible levels, and the whole experimental units take on all combinations of the experimental factor levels.

Bestpfe.com

A *k* factor, *n* level, full experimental design involves n^k experiments. Two-level (2^k) factorial design is the most popular design in pharmaceutical development due to its saving of experimental time and materials.

For each factor in a 2^k design, the low and high value of the low and high level can be transformed to dimensionless coded variables with -1 and 1 sign, respectively. A coded value can be translated to an uncoded value using a general equation as follow:

$$X_{actual} = X_{(-1)} + \frac{(X_{coded} + 1)}{2} x (X_{(+1)} - X_{(-1)})$$

Equation 3-1

Where X_{actual} is the actual value, $X_{(+1)}$ and $X_{(-1)}$ were the actual high and low values (corresponding to +1 and -1 coded value), and X_{coded} was the coded value to be translated.

A full factorial design can be set out in a design matrix. Table 3-1 illustrates a 2^3 experimental design as guidance for any 2^k design. The design matrix is highlighted in grey colour, showing all the possible combinations of high and low values.

Table 3-1. A 2^3 factorial design model matrix and responses

Run	Design Matrix *D*			Matrix of Independent Variables *X*							Response *Y*
	X_i	X_j	X_k	X_i	X_j	X_k	X_{ij}	X_{ik}	X_{jk}	X_{ijk}	
1	-	-	-	-	-	-	+	+	+	-	Y_1
2	+	-	-	+	-	-	-	-	+	+	Y_2
3	-	+	-	-	+	-	-	+	-	+	Y_3
4	+	+	-	+	+	-	+	-	-	-	Y_4
5	-	-	+	-	-	+	+	-	-	+	Y_5
6	+	-	+	+	-	+	-	+	-	-	Y_6
7	-	+	+	-	+	+	-	-	+	-	Y_7
8	+	+	+	+	+	+	+	+	+	+	Y_8

In a design matrix (columns marked in grey), the signs of "-" and "+" denote the low and high levels of a factor, respectively. The first column on the left of Table 3-1 shows a run

order called the standard order. This 2^3 design matrix with standard run order can be expanded to any 2^k full factorial designs. The first (X_i) column starts with "-" and alternates in sign for all 2^k runs. The second (X_j) column starts with "-" repeated twice, then alternates in sign twice until all 2^k places are filled. The third (X_k) column starts with '-" repeated 4 times, then 4 repeats of "+" and so on. In general, the n-$_{th}$ column (X_n) starts with 2^{n-1} repeats of "-" followed by 2^{n-1} repeats of "+".

To obtain a clear view, the 2^3 factorial design can also be graphically represented on a cube as shown in Figure 3-2. In the case of 2^k ($k > 3$) full factorial design, because there are more factors than axes on a 3D-graph of a single cube, the different samples can be represented on the corners of 2^{k-3} cubes.

Figure 3-4, geometrically, the eight runs form the corners of the cube. "-1" and "1" denote the low and high levels of a factor, respectively. The arrows show the direction of increase of the factors. The numbers "1" through "8" at the corners of the design box represent the standard order of runs.

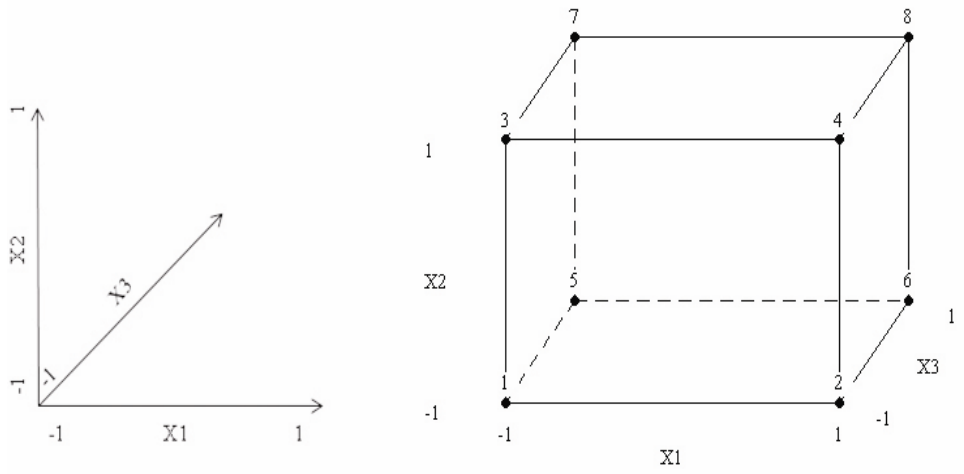

Figure 3-4. A 2^3 full factorial design scheme.

When all the responses have been measured following the design, the main effect of a specific factor and the interaction effect between factors can be calculated. A main effect is the effect of one independent variable on the dependent variable, ignoring the effect of all other independent variables (Montgomery 1999). A significant interaction effect shows the influence of an individual factor on the response is highly dependent of the other factors.

BESTPDF.COM
List of research project topics and materials

Table 3-2. The equations used to determine the effects of individual factors and interactions between factors.

	Equations	Abbreviations	Comments	References
Equation 3-2	$E_x = \overline{y_{(+)}} - \overline{y_{(-)}}$	$\overline{y_{(+)}}$ is the average response when the factor *X* is at its high (+) level; $\overline{y_{(-)}}$ is the average response when the factor *X* is at its low (-) level.	The effect of a factor is defined to be the change in response produced by a change in the level of the factor. The main effect of the individual factor in the factorial design of experiments can be calculated using this equation.	(Box, Hunter et al. 1978).
Equation 3-3	$Ex_i = \frac{Y_2 + Y_4 + Y_6 + Y_8}{4} - \frac{Y_1 + Y_3 + Y_5 + Y_7}{4}$	X_i: individual factor; X_iX_j: an interaction between X_i and X_j; Y: responses	The main effect of individual factor X_i, and interaction effects between factors (X_iX_j) can also be obtained by applying these equations.	(Montgomery 1999).
Equation 3-4	$Ex_1x_j = \frac{Y_1 + Y_4 + Y_5 + Y_8}{4} - \frac{Y_2 + Y_3 + Y_6 + Y_7}{4}$			

3.4.2 Central composite design

This 2^k factorial design allows a first-order polynomial to be obtained. However, the information obtained from a two-level design is not sufficient to determine the linearity of factor effects. To evaluate experimental error and to determine curvature effects in a two-level design, one should include a number of centre points (Montgomery 1999). A centre point is an experiment where all factors are kept at an intermediate level – half way between the low and high levels values for a two-level design, which is coded 0. The added centre point replications in the design allow minimizing the risk of missing non-linear relationships in the centre of the design (Agnihotri, Mallikarjuna et al. 2004). If the value of the response for the centre point differs much from the mean value of the other experiments, it will be necessary to adjust the response surface by second-order non-linear polynomials (Agnihotri, Mallikarjuna et al. 2004). For this purpose, one can expand a two-level design to three levels, but this would extensively increase the number of the experiments. An alternative way is to conduct central composite design (CCD).

CCD also known as Box-Wilson design, was introduced by Box and Wilson in 1951 (Box and Wilson 1951). It is an augmented factorial design and is appropriate for calibrating the full quadratic models in RSM. The CCD is composed of two-level factorial design with axial points and centre points. The axial points are positioned on the coordinate axes of factorial space at a distance α from the centre point (González 1993). A schematic layout of this CCD is presented in Figure 3-4.

3.4.3 Formulation Optimization Using Central Composite Design

The optimization of the variables affecting the drug loaded NPs were carried out following the central composite design. The response measured, Y_1 was particle size, and Y_2 was entrapment efficiency. The variables chosen were PLGA-TPGS copolymer concentration (X_1), TPGS stabilizer concentration (X_2) and 2nd ultrasonication time during NP preparation (X_3). First block of the design was to perform a three levels full factorial design. The levels of each factor were chosen based on the preliminary experiments. Table 3-3 shows the levels of variables and their corresponding actual values. Observed responses were fitted to second-order polynomial model and main effects as well as interaction effects were calculated.

Desirability functions were calculated using Equation 3-10. The optimized formulations were obtained by contour plot and desirability function, which will be discussed in the result section.

Table 3-3. Independent variables, their actual and coded values

	Independent variables		
Coded value	**PLGA-TPGS Concentration (%, w/v) (X_1)**	**TPGS Concentration (%, w/v) (X_2)**	**Sonication time (Sec) (X_3)**
Low (-1)	1	0.1	90
Moderate (0)	3	0.3	180
High (1)	6	0.6	270

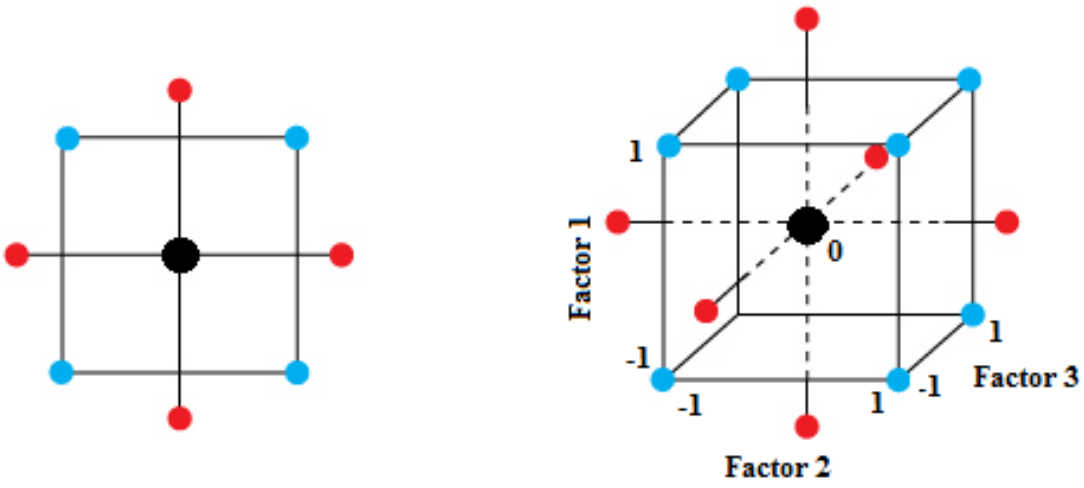

Figure 3-5. Schematic layout of CCD for 3 factors. Coded values "-1", 0 and "1" denote the low, intermediate and high levels of a factor, respectively. The design consists of factorial points (signs of ●) representing all combinations of coded values $X_i = \pm 1$, and axial points (signs of ●) from the centre point, and a centre point (sign of ●) with coded value of 0 for each X_i.

3.4.3.1 Modelling

It is useful to consider the factor response relationship in terms of a mathematical model. The use of variance analysis and factorial design of experiments allows us to express relationship of factors and responses as a polynomial model. By using the generated mathematical polynomial model, each experimental response can be predicted in relation to changing independent variables levels (Table 3-4).

Table 3-4. Mathematical polynomial model to predict experimental response in relation to changing independent variables levels.

	Equations	Abbreviations	Comments	References
Equation 3-5	$y = b_0 + b_1X_1 + b_2X_2 + b_3X_3 + b_{12}X_1X_2 + b_{13}X_1X_3 + b_{23}X_2X_3 .....$	where y is the observed response, X_i is the coded values of i-th factor, b_0 is the constant coefficient, b_i is the coefficient of the linear terms and represents the main effect of X_i, b_{ii} is the coefficient of the quadratic terms and represents the non-linearity effect of X_i, and b_{ij} is coefficient of the interaction terms representing the first order interaction effect between X_i and X_j ($i < j$).	In a two-level factorial design, linear first-order model is used to fit the experimental data (coded values) in the form.	(Agnihotri, Mallikarjuna et al. 2004)
Equation 3-6	$y = b_0 + b_1X_1 + b_2X_2 + b_3X_3 + b_{11}X_1^2 + b_{22}X_2^2 + b_{33}X_3^2 + b_{12}X_1X_2 + b_{13}X_1X_3 + b_{23}X_2X_3 .....$		In central composite design, a statistical second-order model incorporating interactive and polynomial terms is used to fit the data (coded values)	(Agnihotri, Mallikarjuna et al. 2004)
Equation 3-7	$t_i = \frac{\lvert b_i \rvert}{S(b_i)}$	where $\lvert b_i \rvert$ is the absolute value of coefficient of a factor X_i and $S(b_i)$ is the standard error on the coefficient. The replicates of the centre point are used to estimate $S(b_i)$. The calculated test statistic t_i is compared to a tabulated t-value at a significance level of 95% ($\alpha = 0.05$). If the calculated t-value is higher than the tabulated t-value the effect is deemed to be significant.	Once the mathematical model is established, the coefficients are tested for significance with a student t-test according to the following equation	(González 1993)

Furthermore, the models are analysed using analysis of variance (ANOVA) and regression coefficients are calculated. Turkey *F* test is performed to test the adequacy of the models. Significance of the regression models are judged by determining if the probability that model *F* value calculated from the data exceeds a theoretical tabulated *F* value. The probability decreases as the value of *F*-statistic increases. If this probability is less than 0.05 ($P_{\text{model}} > F_{\text{tab}}$ less than 0.05), the full model is significant. The goodness of fit of the model is checked by the adjusted coefficient (adjusted R^2) (Konan, Gurny et al. 2002).

3.4.3.2 Optimization

In formulation optimization, two or more response variables are being studied. It is unlikely that optimizing one response will lead to the best outcome for the other. For this reason, 'optimization' is defined as finding experimental conditions that will fulfil the overall desirable formulation properties where the different responses are most satisfactory (Lewis, Mathieu et al. 1999). Optimization can be performed using mathematical (numerical) or graphical (contour plot) approaches. The desirability function is used as a numerical optimization method for up to 6 factors multiple responses (Montgomery 1999). Each response Y_i is associated with its own partial desirability function d_i that varies over the range of $0 \leq d_i \leq 1$. If the response Y_i is at its goal target, then $d_i = 1$, and if Y_i is outside of an acceptable range, the $d_i = 0$. For the optimization purpose, some responses with minimum outcomes may be desired (e.g. particle size). In contrast, some responses with maximum outcomes may be of interest (e.g. entrapment efficiency).

For the particle size, we expected to obtain particle with size as small as possible. The partial desirability function for response Y_1 can be calculated as follow:

$$d_1 = \frac{Y_{\max} - Y_i}{Y_{\max} - Y_{\min}}$$

Equation 3-8

Where d_1 is the partial desirability of particle size. The values of Y_{max} and Y_{min} are for the maximum and minimum particle size, respectively, and Y_i is the measured result.

For drug entrapment efficiency, we would like as high a value as possible. The partial desirability function, d_2, for Y_2 can be calculated using the equation:

$$d_2 = \frac{Y_i - Y_{\min}}{Y_{\max} - Y_{\min}}$$

Equation 3-9

The two individual desirability functions are then combined together to obtain the overall desirability function (D) and can be calculated using Equation 3-10.

$$D = (d_1 \times d_2)^{1/2}$$

Equation 3-10

3.5 Characterization of TMC modified PLGA-TPGS nanoparticles

3.5.1 Particle size, size distribution and zeta potential analysis

The mean particle size (Z-average) and polydispersity index (PDI) of NPs was determined by dynamic light scattering using the photon correlation spectroscopy (PCS) technique (Zetasizer nano series, Malvern instrument, UK). A dilute suspension of the freeze-dried NPs was prepared with Milli-Q water at a concentration of 1 mg/ml and sonicated at 20 W for 30 sec. Size measurements were performed in triplicate once the NP suspension was preparation.

The zeta potential (ζ), is an indicator of particle surface charge, which may arise from the adsorption of a charged species and/or from ionization of groups that at the surface of the formed particles. It determines particles stability in dispersion. To measure zeta potential of NPs, 1.0 mg of the lyophilized samples was dispersed into Milli Q water (pH 7) and the suspension was then sonicated on an ice bath for 30 sec prior to measurement (in triplicate) using the Malvern Zetasizer Nano series.

3.5.2 Drug entrapment efficiency and loading capacity

The amount of gemcitabine in supernatant and wash medium was measured with HPLC (Agilent LC1200) after particle separation by centrifugation. The concentration of gemcitabine in supernatant and wash medium represented the gemcitabine not associated with the NPs. The entrapment efficiency (EE) of gemcitabine was obtained as the mass ratio between entrapped amount of gemcitabine in the NPs and the total amount of gemcitabine used in the preparation. The following equation was used:

$$EE\% = \frac{\text{total amount of gemcitabine added - free gemcitabine detected in supernatant}}{\text{total amount of gemcitabine added}}$$

Equation 3-11

The exact amount of gemcitabine present within the particles was also analysed by extraction technique to courter check the EE with the following procedures. Twenty mg of NPs were dissolved in 1 ml of DCM and 3 ml of Milli Q water was added. Gemcitabine was extracted by vortexing for 15 min. The aqueous phase containing gemcitabine was separated by centrifugation at 12,000 rpm for 15 min. The solution was subjected to gemcitabine concentration determination by HPLC. The loading capacity (LC) was calculated using the following equation:

$$LC\% = \frac{\text{total amount of gemcitabine added - free gemcitabine detected in supernatant}}{\text{Mass of nanoparticles}}$$

Equation 3-3

3.5.3 Morphology of nanoparticles

Morphological characterization of the NPs revealed the shape, surface, structure and possible degree of aggregation. Surface morphology of the NPs was assessed by scanning electron microscopy (SEM). Ten mg of lyophilized NPs was suspended in 2 ml of Milli Q water. Two hundred µl of the NPs suspension was added on top of a conductive double-sided adhesive tape mounted on an aluminium stub. The samples were dried overnight in air and then sputtered with platinum using a sputter coater (Polaron SC 7640). Samples were then observed under a condition of high vacuum and at a temperature of less than -120ºC using Philips XL30S FEG scanning electron microscope at 25 kV.

3.5.4 *In vitro* release of gemcitabine from nanoparticles

In vitro release studies for up to 48 hrs were carried out using Franz diffusion cells (FDC-6, Logan instrument Corp, USA) to obtain the release profile of gemcitabine loaded NPs. Briefly, aliquot of 2.5 mL of the drug loaded NP suspension was added to the upper donor chambers of the Franz diffusion cells. Drug solution containing the equivalent amount of gemcitabine was added in the donor as a control group. A 12 mL aliquot of PBS (pH 6.5) was filled in the receptor chamber. The temperature of the donor was maintained at 37 ± 0.5°C. The upper and downer chambers were divided by a single layer of synthetic cellulose

membranes (12000-14000 wt cut-off, pre-soaked in the release medium overnight). At time intervals (0, 15, 30 min and 1, 2, 3, 4, 6, 8, 12, 24, 30 and 48 hr), the aliquot of 400 μL samples was taken from the receptor chambers and replaced with same amount of the medium. The amount of gemcitabine released in supernatant was analysed with the validated HPLC analysis as described in Chapter 2.

3.5.5 Drug release kinetics

The release kinetics was evaluated using four different models including zero orders, first order, Higuchi equation and Korsmeyer-Peppas equation to characterize the mechanism of drug release from the NPs. Selection of model was based on the best fit of model. For the different models, data obtained were plotted in the following manner: zero order as cumulative percentage of drug release versus time, first order as log cumulative percentage of drug remaining versus time, Higuchi's model as cumulative percentage of drug released versus square root of time, and Korsmeyer-Peppas model as log cumulative percentage of drug released versus log time.

Zero order kinetics (Costa and Sousa Lobo 2001, Sinko 2006):

Drug dissolution from its dosage form follows Fick's law (assuming that area does not change) can be expressed by the following equation:

$$Q_t = Q_0 + K_0 t$$

Equation 3-4

Where Q_t is the amount of drug released in time t, Q_0 is the initial amount of drug in the release medium (it is usually zero), and k_0 is the zero-order release constant. Under zero order kinetic, the rate of drug release is independent of time and the concentration of drug within a dosage form. A graph of cumulative drug released versus time would yield a straight line with a slope equal to k_0. Zero order mechanism ensures that a steady amount of drug is released over time.

BESTPFE.COM
List of research project topics and materials

First order kinetics (Costa and Sousa Lobo 2001, Sinko 2006):

$$Q_t = Q_0 e^{-k_1 t}$$

Equation 3-5

Where Q_t is the amount of drug released in time t, Q_0 is the initial amount of drug in the solution and k is the first order release constant. This equation can be expressed in decimal logarithms:

$$\log Q_t = log\, Q_0 + \frac{k_1 t}{2.303}$$

Equation 3-6

Equation 3-6 can be simplified and expressed as:

$$\log Q_t = log\, Q_0 + k_1 t$$

Equation 3-7

Where k_1 is the first order release constant.

The first order model describes the release of drug from its dosage form is concentration dependent and the rate of drug release is proportional to the amount of drug remaining in its dosage form. Hence, a linear graph will be obtained when plotting decimal logarithm of the released amount of drug versus time.

Higuchi model (Higuchi 1963, Costa and Sousa Lobo 2001):

Higuchi's well known model, which has traditionally been applied to describe the release of non-swellable and non-erodible drug loaded nano/microspheres, neglects the effects of the finite drug dissolution rate and assumes that a depletion layer extending inward leaches drugs. The dissolution of drug from a planar heterogeneous matrix system, where the drug concentration is lower than its solubility and the release occurs through pores in the matrix, can be expressed as:

$$Q_t = \sqrt{\frac{D\varepsilon}{\tau}(2C - \varepsilon C_s)C_s t} = k_h t^{1/2}$$

Equation 3-8

where Q_t is the amount of drug released in time t by surface unity, C is the initial concentration of the drug, ε is the matrix porosity, τ is the tortousity factor of the capillary system, C_s is the drug solubility in the matrix/excipients media, D is the diffusion constant of the drug molecules in that liquid, k_h is the Higuchi dissolution constant. It can be found from the above equation, the dissolution rate is related to the matrix porosity and the tortousity of the system. The amount of drug released is proportional to the reciprocal of the square root of time.

Korsmeyer-Peppas model (Korsmeyer, Gurny et al. 1983, Costa and Sousa Lobo 2001):

The Korsmeyer-Peppas model is used to analyse the release of polymeric dosage form, when the release mechanism is not well known or when more than one type of release phenomena could be involved.

$$Q_t = k_k t^n$$

Equation 3-9

Where Q_t is percentage cumulative amount of drug release at time t, t is the release time, k_k is a kinetic constant characteristic of the drug/polymer system, and n is an exponent that characterizes the mechanism of release. If the exponent n = 0.5, then the drug release mechanism is Fickian diffusion, and if $0.5 < n < 1$, then it is non-Fickian or anomalous diffusion. This equation is the analytical solution by the Fickian equation to get rid of the error term, so the equation is only applicable to the release of drugs in a shorter time, which is $Q_t < 0.6$. Therefore, data for the first 60% of drug release were plotted as log cumulative percentage of drug released versus log time, and the exponent n was calculated through the slope of the straight line, while Y intercept provided k_k.

3.5.6 *Ex-vivo* permeation studies over porcine epithelial membrane

Ex-vivo permeation of gemcitabine loaded NPs were determined in Franz cells by substituting the cellulose membrane for porcine intestinal epithelial membrane. Porcine mucosal tissue was previously soaked in pH 7.4 PBS overnight. After the accumulative drug amount was determined by HPLC and plotted over time, the apparent permeation coefficient (P_{app}) was also calculated. P_{app} is the rate at which a drug will cross the intestinal wall and enter the portal circulation (Youdim, Avdeef et al. 2003), and was calculated using Equation 3-19.

$$P_{app} = \frac{dXr}{dt} \times \frac{1}{A.Co}$$

Equation 3-19

Where Xr is the cumulative drug amount (µg), A is area of the permeation membrane (cm^2), C_0 is the initial concentration in the donor compartment (µg/mL) and dX_r/dt is the flux which is the gradient of the best fit line when cumulative amount of drug permeated in µg is plotted against time in hrs (Chen, Bunt et al. 2015).

3.5.7 Physical and chemical stability of the nanoparticles

The optimal drug loaded NPs were studied for their physical and chemical stability. The optimal NPs were stored in screw-capped amber vials at three different temperatures (4, 25 and 40 °C) for 3 months. Samples were withdrawn at 0, 1, 2 and 3 months and evaluated for:

i) Changes in size by measuring the particle size and PDI as previously mentioned.

ii) The amount of drug retained in the NPs by measuring the residual EE% as previously described.

In the control groups, drugs with the equivalent to that entrapped in the NPs were used, and the drug solution was subjected to the 3 temperatures and the drug retained was examined at the end of each month during the 90-day storage.

3.5.8 Data Analysis

Data are presented as mean ± S.D, and statistical differences between groups were tested by SigmaStat 3.5 (Systat Software, Inc, USA) using a two-tailed unpaired Student's *t*-test or One-way analysis of variance (ANOVA) followed by Tukey-test. Values of $p < 0.05$ were considered statistically significant. Fisher *F* test is performed to test the adequacy of the polynomial model.

3.6 Results and discussion

3.6.1 Determination of glucose and sucrose effects on particle size

In the preliminary study, NPs freeze-dried in water were found to form aggregates and could not be suspended evenly in aqueous medium. Glucose and sucrose can act as spacing matrix between particles during particle washing process, by keeping the colloidal particles separated and hence preventing aggregation (Konan, Gurny et al. 2002). From Table 3-5, particle size of lyophilized NPs decreased when there was addition of glucose and sucrose during washing step. As the concentration of sucrose or glucose increased, the mean particle size of NPs decreased, indicating that they effectively prevented particles from aggregation. In addition, there have different effects on the preservation of particle size at different concentrations. When 3% (w/v) of sucrose was added, the size of NPs showed smallest change compared with water and glucose at any concentrations. This demonstrates that sucrose causes better redispersibility effects than glucose. The sucrose with concentration of 3% (w/v) showed the best protection effects of PDI of 0.11, indicating the great uniformity of particle distribution. The low PDI of 0.16 was also achieved in the presence of 5% sucrose, confirming sucrose is a suitable material to be added during NP washing step. Hence, 3% (w/v) of sucrose was selected to prepare lyophilized PLGA NPs in all the future works.

Table 3-5. Effect of cryoprotectants on the mean particle size and polydispersity (PDI), results expressed as mean ± SD (n = 3)

Dispersant	Concentration (%, w/v)	Particle size (nm)	PDI
Water		745.13 ± 280.13	0.52 ± 0.12
Glucose	1	571.20 ± 55.46	0.70 ± 0.04
	3	348.83 ± 19.52	0.39 ± 0.03
	5	337.00 ± 34.60	0.42 ± 0.01
Sucrose	1	401.07 ± 22.15	0.36 ± 0.04
	3	208.17 ± 11.40	0.11 ± 0.01
	5	225.80 ± 14.88	0.16 ± 0.03

3.6.2 FTIR Characterization for PLGA-TPGS conjugation.

The PLGA-TPGS random copolymer was synthesized in this research study using a stannous octoate as catalyst. The reaction of synthesis is schematically described in Figure 3-6. To confirm the success of conjugation of the two polymers, the structure of the copolymers were determined using FTIR spectroscopy. The PLGA functional groups can be characterized as C=O stretching of ester at 1741 cm^{-1}, C-H stretching of CH_2 and CH_3 at 2850-3000 cm^{-1}, C-O stretching of ester at 1181 cm^{-1}, and O-H stretching at 3200-3500 cm^{-1}. The hydroxyl end of TPGS served as initiator to selectively cleave acyl oxygen chain of lactide or glycolide of PLGA. The FTIR spectra of the PLGA-TPGS random copolymer and TPGS were showed in Figure 3-4. The carbonyl band of TPGS appears at 1730 cm^{-1}. For the synthesized random copolymer, the carbonyl band was shifted to 1754 cm^{-1}. Overlapping of the C-H stretching band of PLGA at 2945 cm^{-1} and that of TPGS at 2880 cm^{-1} was observed. In the PLGA-TPGS copolymer, the C-H stretching band of TPGS was decreased. The absorption band at 3400–3650 cm^{-1} is attributed to the terminal hydroxyl group and that at 1045–1500 cm^{-1} is due to the C–O stretching (Liu and Kiran 2008). The FTIR spectrum results confirmed the PLGA polymer and TPGS polymer were conjugated, which were subsequently used for NPs preparation.

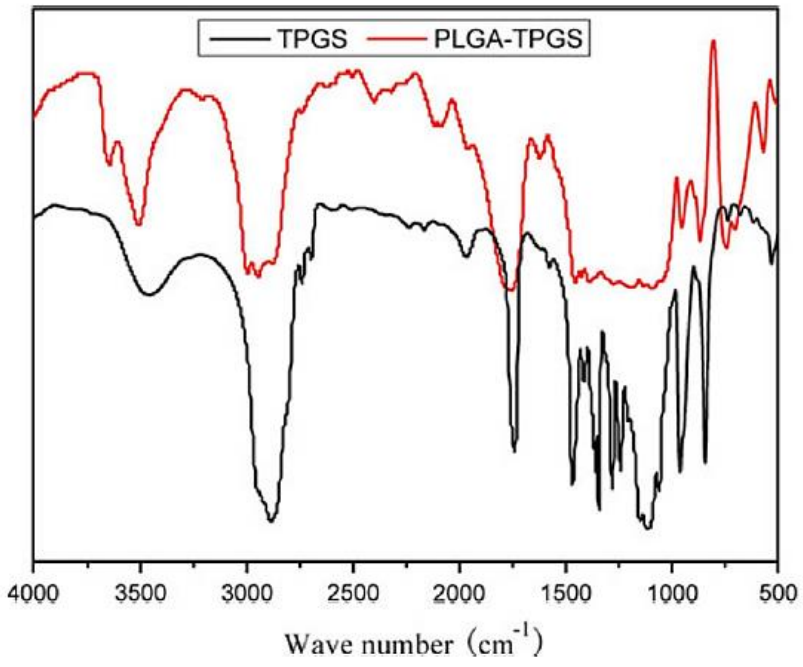

Figure 3-6. FTIR spectra of PLGA-TPGS random copolymer and TPGS.

3.6.3 Optimization of formulations from factorial design

The optimization of gemcitabine loaded NPs was carried out using central composite design. The aim of this study was to develop the nanoparticulate delivery system with acceptable nano-size as well as high drug encapsulation. The three independent variables (factors) investigated were concentration of PLGA-TPGS (X_1), TPGS stabilizer (X_2) and the 2nd ultrasonication time (X_3). The response variables observed were particle size (Y_1) and drug entrapment efficiency (Y_2). The ultimate goal was to determine how these factors influenced the properties of the NPs prepared and to find the set of factor that produce the 'most desired' response.

3.6.3.1 Two-level full factorial design with centre point

Twenty batches of formulations (3 factors, 2 levels with centre point, and 2 responses) were prepared according to the design as illustrated in **Error! Reference source not found.**. The particle size and drug entrapment efficiency were subsequently determined, and the results were then submitted back to the Factorial design system. Finally, the system automatically analysed the data and interpreted the experimental results from the joint effects of the three independent variables on the responses are shown and discussed in the following section. The Desirability was expressed based on the responses of smaller particle size and higher drug entrapment efficiency.

3.6.3.2 Factors affect the response of particle size

The mean particle size of the prepared NPs varied from 201.1 to 315.2 nm, thus, a control of particle size can be achieved by combining the three independent variables. The smaller particle size is desired, results are presented graphically in a Normal Probability plot (Figure 3-7). The higher probability of all the tested NPs are shown as green colour points which indicates the mean particle size is around 250 nm (median of 201 and 315).

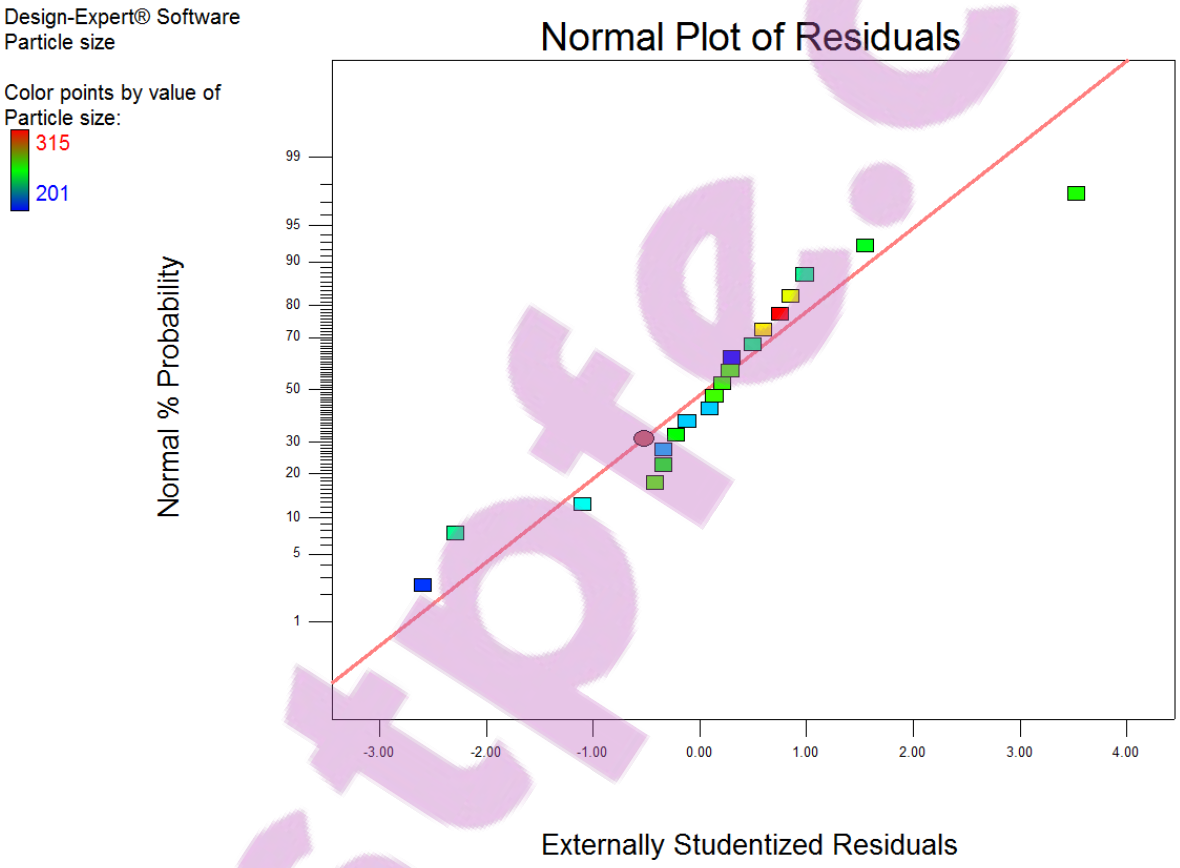

Figure 3-7. Normal Probability plot of the three factors affecting the particle size by using Design-Expert software.

Bestpfe.com

From Figure 3-8. It is a model graph showing the interaction effect of PLGA-TPGS concentration and TPGS concentration on particle size of NPs, when the 2nd ultrasonication time was 180 sec. As we can see, the particle size increase from 220 nm to 260 nm, PLGA-TPGS concentration increase from 1% w/v to 4% w/v, and the concentration of TPGS decrease from 0.5% w/v to 0.1% w/v. Therefore we can conclude that the PLGA-TPGS concentration increases and the concentration of TPGS decreases, will lead to increase the particle size.

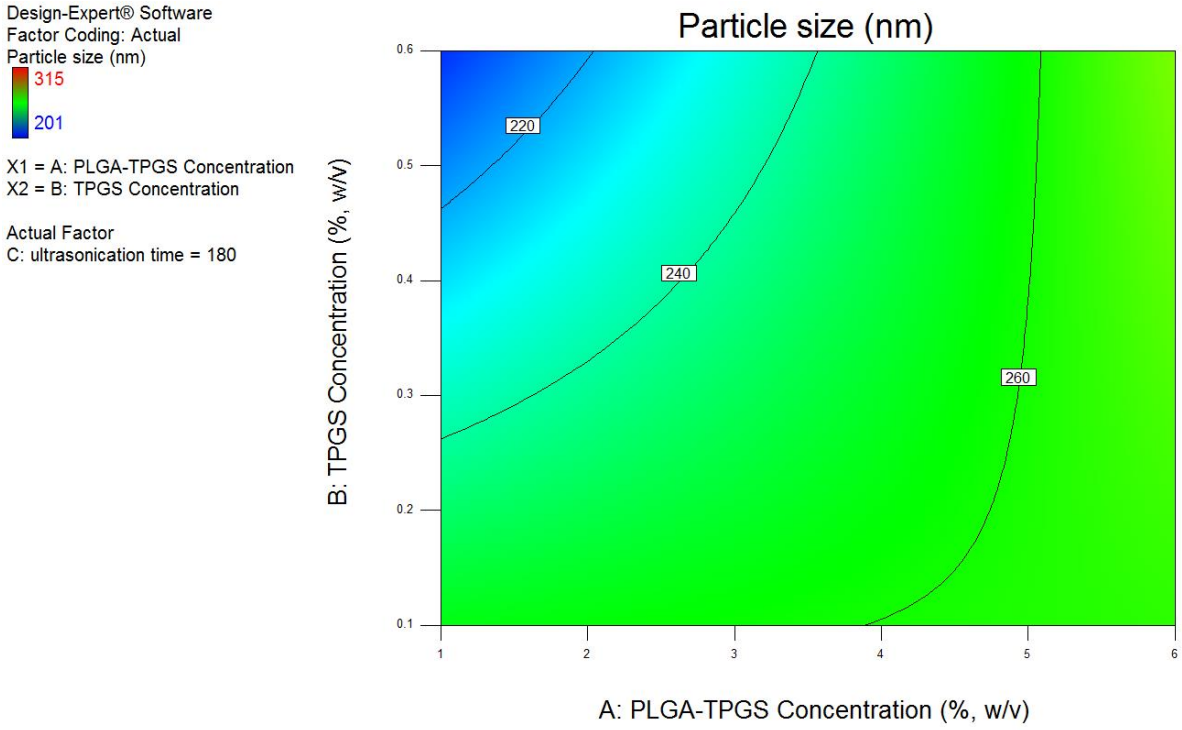

Figure 3-8. A model plot showing the interaction effect of PLGA-TPGS Concentration and TPGS concentration on particle size when the 2nd ultrasonication time was 180 sec.

The statistical differences were assessed using ANOVA test to prove these results. From Figure 3-9, the *F*-value of the model is 9.51 indicating the statistical model is significant. The *F*-test results confirmed that all three factors had significant effect on particle size ($p < 0.05$) (Cochran and Cox 1957, Box, Hunter et al. 1978). Among all the variables, different 2nd ultrasonication time has the most significant influence on particle size of NPs. The effect of these three variables on the particle size can be arranged in the sequence 2nd ultrasonication time > PLGA-TPGS concentration > TPGS concentration.

Response 1 Particle size

ANOVA for Response Surface 2FI model

Analysis of variance table [Partial sum of squares - Type III]

Source	Sum of Squares	df	Mean Square	F Value	p-value Prob > F	
Model	12197.36	6	2032.89	9.51	0.0004	significant
A-PLGA-TPGS Concer	*3501.68*	*1*	*3501.68*	*16.38*	*0.0014*	
B-TPGS Concentration	*1047.59*	*1*	*1047.59*	*4.90*	*0.0453*	
C-ultrasonication time	*7151.85*	*1*	*7151.85*	*33.46*	*< 0.0001*	
AB	*1292.07*	*1*	*1292.07*	*6.05*	*0.0287*	
AC	*39.75*	*1*	*39.75*	*0.19*	*0.6733*	
BC	*490.60*	*1*	*490.60*	*2.30*	*0.1537*	
Residual	2778.39	13	213.72			
Lack of Fit	*1916.23*	*8*	*239.53*	*1.39*	*0.3732*	*not significant*
Pure Error	*862.17*	*5*	*172.43*			
Cor Total	14975.75	19				

The Model F-value of 9.51 implies the model is significant. There is only a 0.04% chance that an F-value this large could occur due to noise.

Values of "Prob > F" less than 0.0500 indicate model terms are significant.
In this case A, B, C, AB are significant model terms.
Values greater than 0.1000 indicate the model terms are not significant.
If there are many insignificant model terms (not counting those required to support hierarchy), model reduction may improve your model.

Figure 3-9. Design Expert software output of the statistical differences of the three factors that were assessed using ANOVA *F-test*. Indicating the three factors affect the particle size significantly.

BESTPFE.COM
List of research project topics and materials

3.6.3.3 Factors affect the response of drug entrapment efficiency

In order to diminish polymer toxicity, a polymeric nanoparticulate delivery system must be made with the minimum possible amount of polymers yet able to entrap as much drug as possible. Hence an optimal ratio between the entrapped drug and the polymer amount for the highest entrapment efficiency must be obtained (Illum, Khan et al. 1986). Obtaining the maximum drug entrapment within the NPs, requires information about the effects of formulation variables on the NPs properties. Data describing the relationship between the percentage of entrapment efficiency and the independent variables are determined by factorial design.

From Figure 3-10, we can see the percentage of gemcitabine entrapped in the NPs varied from 69.4 to 81.5%. The orange colour points at higher probability region indicating most of the NPs drug entrapment efficiency are above 75% (median between 69 and 81).

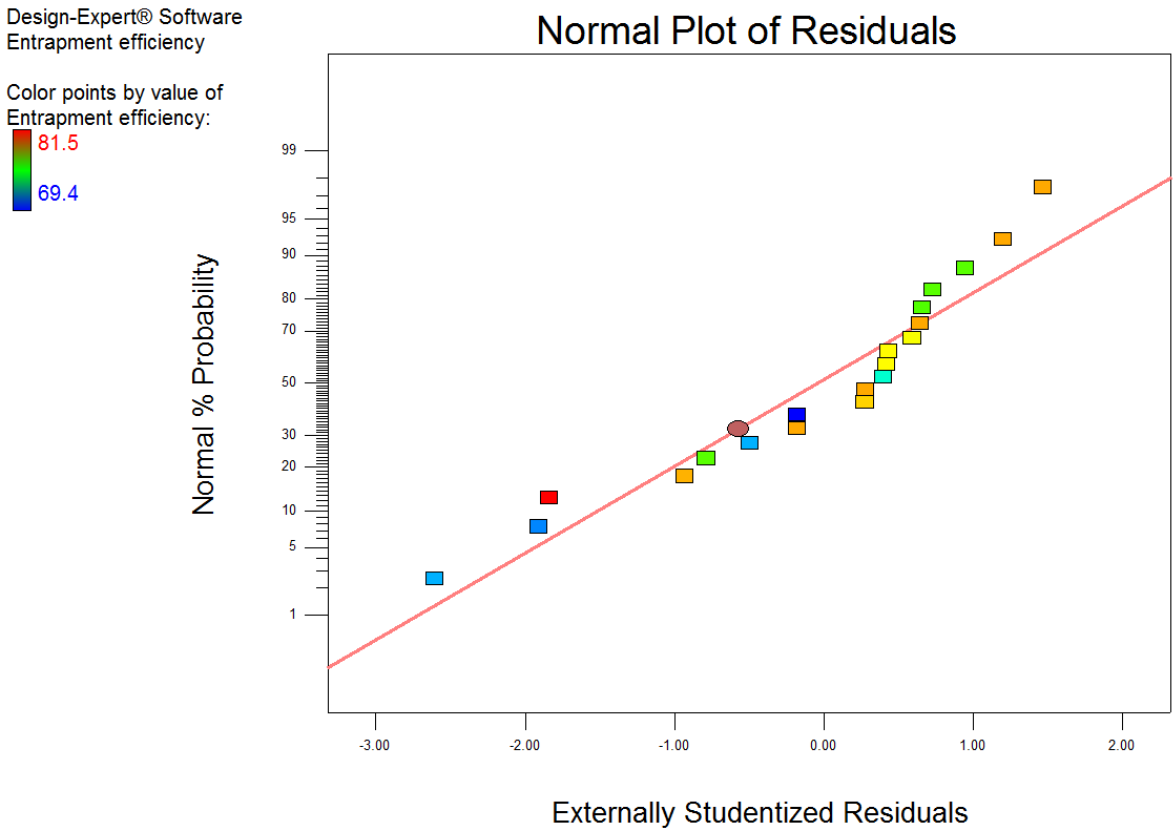

Figure 3-10. Normal Probability plot of the three factors affecting the drug entrapment efficiency by using Design-Expert software.

Figure 3-11 demonstrates all three investigated factors were positively affected the drug entrapment efficiency of the NPs. The drug entrapment efficiency increases from 72 to 78%, when the PLGA-TPGS concentration increases from 1 to 6% w/v, and TPGS concentration increases from 0.1 to 0.6% w/v, when the 2nd ultrasonication time was 180 sec. Therefore we can conclude that the drug entrapment efficiency of the NPs is increased when the PLGA-TPGS concentration and TPGS concentration are elevated.

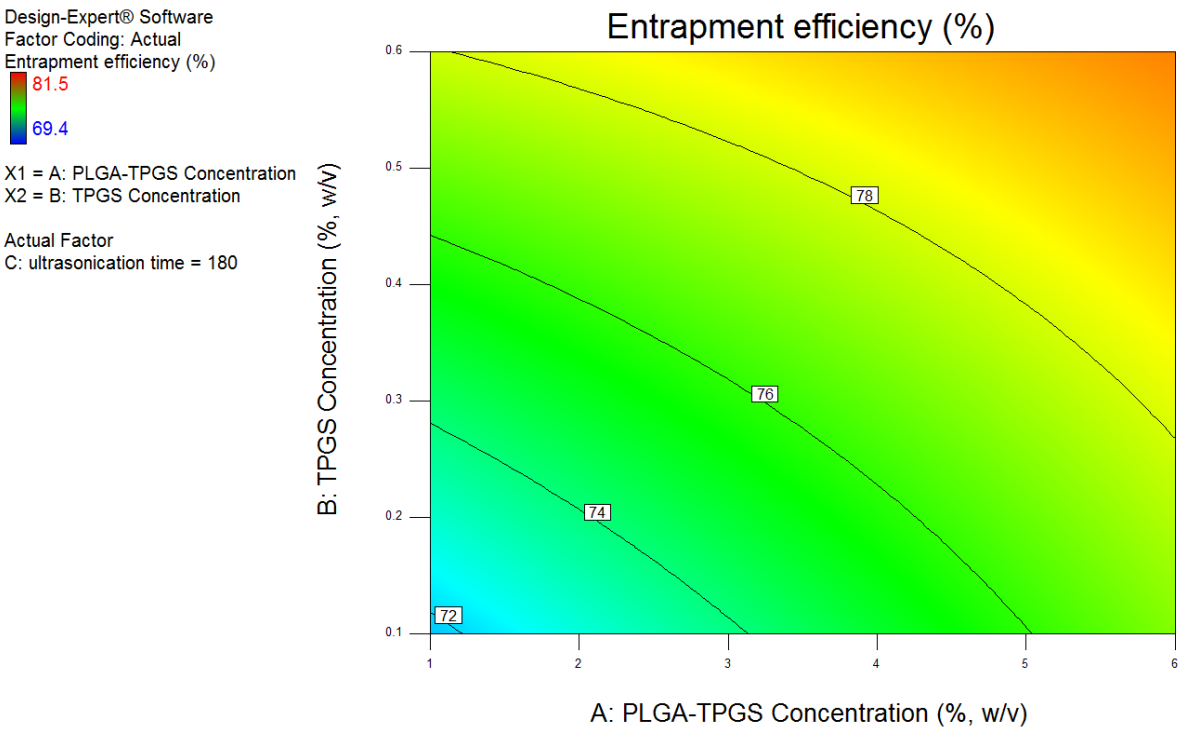

Figure 3-11. A model plot showing the interaction effect of PLGA-TPGS Concentration and TPGS concentration on drug entrapment efficiency when the 2nd ultrasonication time was 180 sec.

Figure 3-12 shows the statistical model with a *F*-value of 31.55 which implies the model is significant. Additionally, it demonstrates the ANOVA test proves the significance of the factors, as all the investigated factors shows their *p*-values of less than 0.05. The effect of the three factors on the drug entrapment according to the level of impact is 2nd ultrasonication time > TPGS concentration > PLGA-TPGS concentration. *F*-test confirms that the curvature effect is significant ($p < 0.01$) (Cochran and Cox 1957, Box, Hunter et al. 1978).

Response 2 Entrapment efficiency

ANOVA for Response Surface Linear model

Analysis of variance table [Partial sum of squares - Type III]

Source	Sum of Squares	df	Mean Square	F Value	p-value Prob > F	
Model	203.49	3	67.83	31.55	< 0.0001	significant
A-PLGA-TPGS Concer	*42.93*	*1*	*42.93*	*19.97*	*0.0004*	
B-TPGS Concentration	*53.99*	*1*	*53.99*	*25.11*	*0.0001*	
C-ultrasonication time	*86.12*	*1*	*86.12*	*40.06*	*< 0.0001*	
Residual	34.40	16	2.15			
Lack of Fit	*29.16*	*11*	*2.65*	*2.53*	*0.1577*	*not significant*
Pure Error	*5.24*	*5*	*1.05*			
Cor Total	237.89	19				

The Model F-value of 31.55 implies the model is significant. There is only a 0.01% chance that an F-value this large could occur due to noise.

Values of "Prob > F" less than 0.0500 indicate model terms are significant.
In this case A, B, C are significant model terms.
Values greater than 0.1000 indicate the model terms are not significant.
If there are many insignificant model terms (not counting those required to support hierarchy), model reduction may improve your model.

The "Lack of Fit F-value" of 2.53 implies the Lack of Fit is not significant relative to the pure error. There is a 15.77% chance that a "Lack of Fit F-value" this large could occur due to noise. Non-significant lack of fit is good -- we want the model to fit.

Figure 3-12. Design Expert software output of the statistical differences of the factors that were assessed using ANOVA *F-test.* Indicating only the concentration of TPGS and 2nd ultrasonication time had significant effect on drug entrapment efficiency.

3.6.4 Optimization of the drug loaded NPs with maximum desirability

Due to the existence of curvature, the 2^3 factorial design plus centre point was expanded to central composite design. The added axial points allow the determination of the response surface by second-order non-linear polynomials. Results for the whole CCD, the optimal formulation with highest 'Desirability', as well as its components are presented in Figure 3-13 and Figure 3-14.

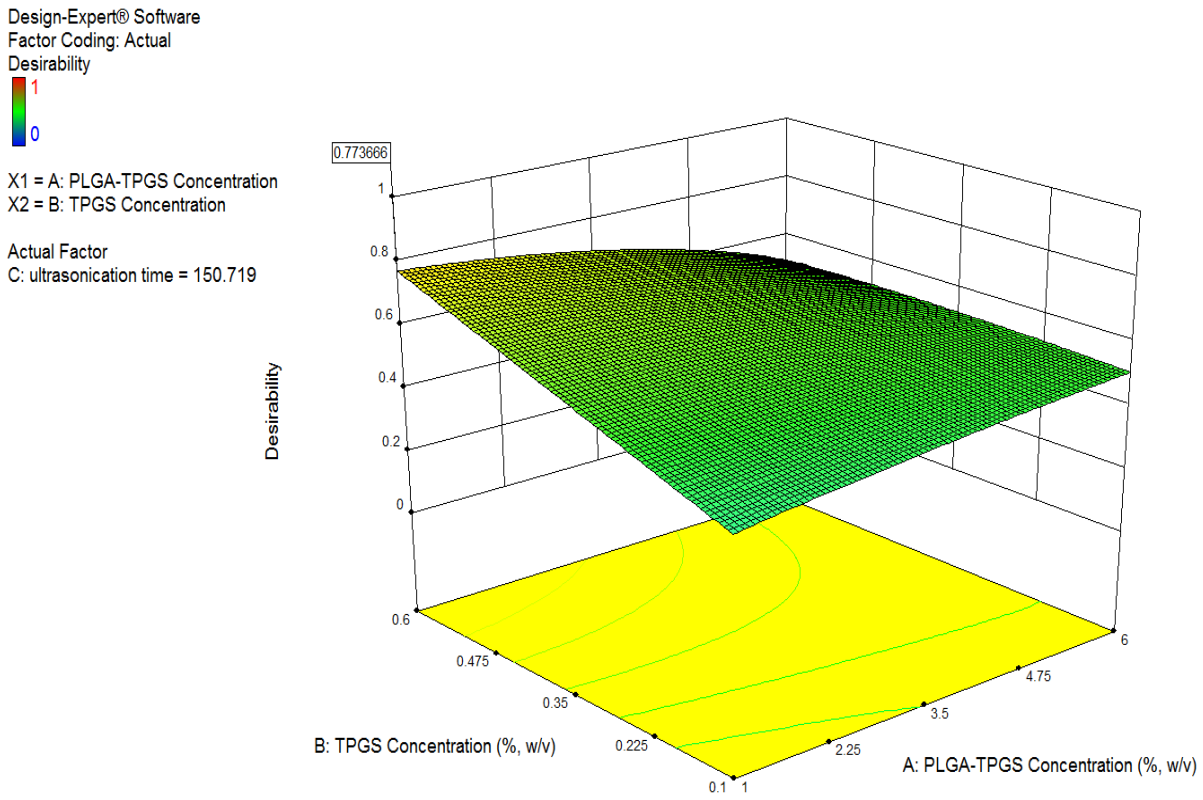

Figure 3-13. Three-dimensional surface plot for overall desirability as a function of the formulation variables: (A) PLGA-TPGS concentration; (B) TPGS concentration; (C) 2nd ultrasonication time.

From Figure 3-13, the 3-dimensional surface plot shows an overall effect of the factors with various conditions, on the final desirability of minimum particle size and maximum drug entrapment efficiency. The desirability is in range from 0 to 1. The highest desirability was calculated as 0.774 with all the optimal conditions predicted by factorial design.

The optimal 2nd ultrasonication time was predicted as 150 sec, and we can see to reach the highest desirability (the top left spot), higher TPGS concentration (closer to 0.6% w/v) and lower PLGA-TPGS concentration (closer to 1% w/v) should be combined. Another interesting finding shall be mentioned, when PLGA-TPGS concentration is at the highest and TPGS concentration at the lowest, it also have a relatively high desirability. Furthermore, two conditions should be avoided, which are lower concentration of both PLGA-TPGS and TPGS concentration, as well as highest concentration of both PLGA-TPGS and TPGS concentration, the figure shows these two spots have lowest desirability.

From Figure 3-14, the factorial design statistically predicted the optimal formulation with all the optimal conditions of the investigated factors. We can see that the optimal formulation with highest overall desirability value of 0.774 was achieved by 1% w/v PLGA-TPGS, 0.6% w/v TPGS and 150 sec 2nd ultrasonication time. The resulting NPs showed the best response to drug entrapment efficiency of 77.82% and optimum smaller particle size of 216.97 nm.

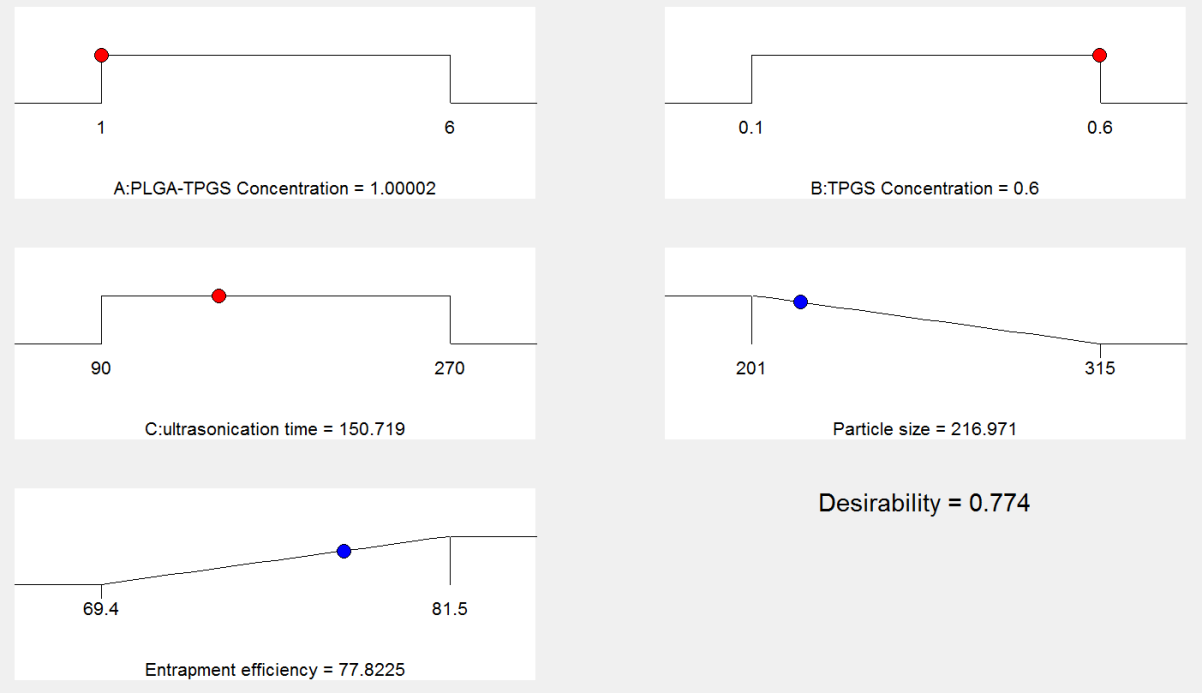

Figure 3-14. The factorial design statistically predicted the highest desirability formulation with all the optimal condition of the investigated factors.

3.7 Characterization

The optimal formulation (1% w/v PLGA-TPGS, 0.6% w/v TPGS and 150 sec 2nd ultrasonication time) predicted from factorial design was further subjected to the characterisation step so that comprehensive information about the formulation can be obtained.

3.7.1 Particle size, zeta potential and size distribution

Particle size is the key factors influencing the rate and extent of permeation across the cell membrane as well as the stability of the formulation. Narrow particle size distribution has advantages in permeation and avoiding aggregation or drug leakage issues. Large particle size distribution might lead to aggregation (Sonavane, Tomoda et al. 2008, He, Hu et al. 2010). Generally, after sonication, spherical NPs of narrow size distribution will be obtained (Jani, Halbert et al. 1990).

The results obtained of particle size of optimised NPs were summarised in Table 3-7. The particle size of the optimal NP had a vesicle size of 243.21 ± 21.72 nm, and a PDI of 0.27 ± 0.03. PDI values were lower than 0.5 indicating a relatively narrow size distribution. Particle sizes ranging from 100 to 500 nm were measured for all the formulations prepared according to factorial design output.

Usually, for small size NPs, there is a tendency for the NPs to aggregate during the freeze-drying procedure, resulting in the formation of aggregates, which is a major drawback of freeze-drying process (Mondal, Halder et al. 2010). TPGS is used as a great stabilizer for PLGA-TPGS NPs formation, as it helps to stabilize the emulsion by lowering the surface tension and allowing development of interfacial tension gradients that impede the flow of liquids along the interface. Moreover, the concentration of stabilizer will change the total surface area of the NPs which can also affects the particle size (Sansdrap, P *et al*., 1993). For most NP formulations, the increase of the TPGS stabilizer concentration, particle size decreases. During the removal of organic solvent, stabilizers can avoid the coalescence of droplets and lead to form NPs with smaller size. After the removal of organic solvent, more TPGS stabilizers can be physically incorporated onto the surface of NPs and a large number

of hydroxyl groups extending into the continuous phase could be hydrated, hence forming a hydrated layer at the surface to hinder NP aggregation (Mu and Seow 2006).

Since NPs were formed from the emulsion droplets after solvent evaporation, their size is dependent on the size and stability of the emulsion droplets. Smaller droplets resulted in smaller particles. In addition, if there were sufficient TPGS covering the droplets surface, coalescence of particles during the solvent evaporation process could be avoided. The relationship of TPGS stabilizer concentration and the particles size can be understood through droplet dynamics. The emulsion droplet deformation and breakup are controlled by two groups, capillary number (Ca) which is the ratio of viscous to capillary force, and viscosity ratio (M) of the droplet phase to the continuous phase.

$$Ca = \frac{\gamma \eta_s \alpha}{\Gamma}$$

Equation 3-20

$$M = \frac{\eta_d}{\eta_s}$$

Equation 3-21

where γ is the shear rate, α is the droplet size, and Γ is the interfacial tension between the droplet and continuous phase, η_d and η_s is the viscosity of droplet and continuous phase, respectively (Larson 1999). Therefore, increase the TPGS concentration resulted in the increase of continuous phase viscosity (η_s) and the decrease of interfacial tension (Γ), thus leading to a high Ca or low M that favour droplet deformation (Heslinga, Mastria et al. 2009). Hence, the size of NPs decreased with an increase in the TPGS concentration which is preferred. However, the high amount of stabilizer used might lead to toxicity which needs to be concerned (Van Eerdenbrugh, Vermant et al. 2009).

Furthermore, the discrepancy in the size of NPs can be determined by the dynamic light scattering method, and gives the hydrodynamic diameter rather than the actual diameter of NPs, therefore a comparison of the particle size with other techniques as well is worthwhile (Todokoro and Ezumi 1999).

Table 3-6. Results of particle size and zeta-potential of the optimised NPs (means ± SD; n=3).

	Particle size (d.nm)	PDI	Zeta-potential (mV)
Optimal drug loaded NPs	243.21 ± 21.72	0.27 ± 0.03	+14.70 ± 1.31

From Figure 3-15, it was the size distribution output graph from Zetasizer of the optimal formulation. The peak has shown relatively narrower, and higher intensity compared to the size distribution output peaks of other formulations, which demonstrated the good uniformity, and well dispersed of the particles of our optimal formulation (Gasco 1993, Phenrat, Kim et al. 2009). In addition, The PDI describes variation in sizes. The higher the PDI values, means the wider the particle size distribution. Thus lower PDI is preferred as it represents the level of uniformity of particle sizes (Beaucage, Kammler et al. 2004, Saberi, Fang et al. 2013). For this formulation, we can see rather low PDI value which indicating the good quality and uniformity of the particles.

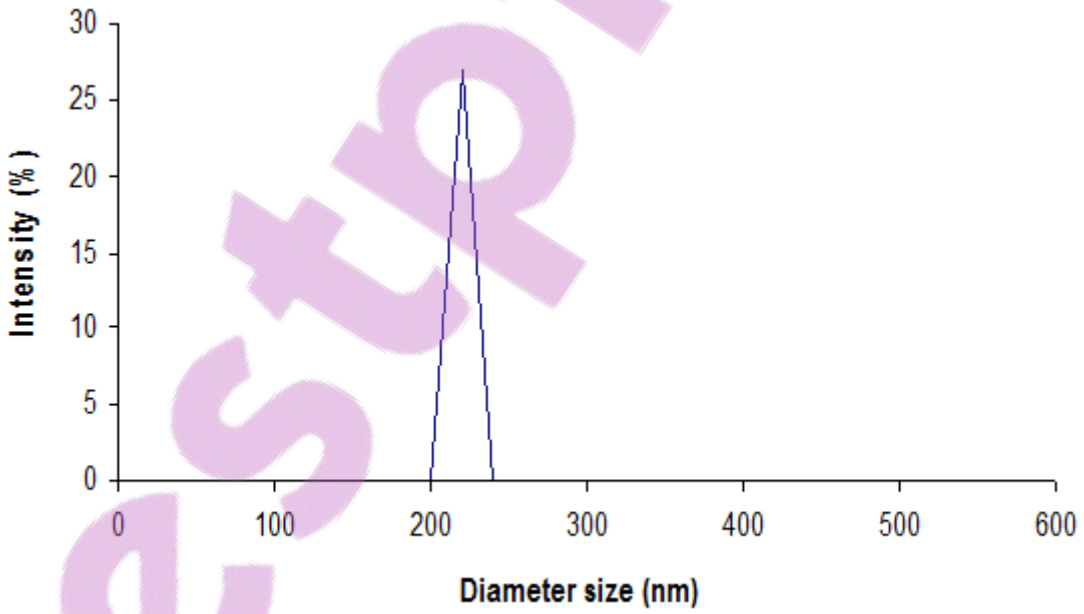

Figure 3-15. Size distribution output of the optimal formulation from Zetasizer. (PDI: 0.27 ± 0.03).

Bestpfe.com

Zeta potential is defined as the potential at the shear plane in the Stern model (Myers 1999) and it is considered as an important stability and mucoadhesivity parameters for dispersed particles. It is due to the fact that zeta potential represents the stability of the colloidal dispersion and the extent of repulsion between NPs. The higher the zeta potential between the NPs, which indicates the less likely of aggregation, this is due to the presence of the same charge layer which will repel the NPs away from each other (Patil, Sandberg et al. 2007, Hunter 2013). Zeta potential values in the range of |15| mV to |30| mV are common for well stabilized particles. (Geys, Coenegrachts et al. 2006, Kesisoglou, Panmai et al. 2007). Furthermore, the surface charge can be used to determine how the particles would adhere to, and interact with cells whose membranes are negatively charged in nature (Feng 2004). Intestinal epithelial membrane of GIT has shown to carry negative charges (Vorbrodt 1987). Cationic particles would disrupt the tight junction of intestinal epithelial membrane by the inter-endothelial routes opening (Lockman, Koziara et al. 2004) or undergo absorptive-mediated transcytosis across the membrane (Xu, Lu et al. 2009).

From Table 3-6. We can see our optimal formulation has a zeta-potential of +14.70 ± 1.31 mV. According to the literature, this value demonstrates a reasonable good physical stability of the optimal NPs. Although in order to further enhance the physical stability of the colloidal particles, its zeta potential shall be elevated. However, when the particle zeta potential presents very high positive charge, it might also trigger irritations and toxicity to the intestinal mucosal tissue (Calvo, Remunan-Lopez et al. 1997, El-Shabouri 2002). Therefore, bearing both of the concepts in mind, the zeta potential of the optimal formulation is considered as promising result.

Generally, the zeta potential values for the PLGA based NPs are in the negative range, it's due to the fact that PLGA containing high proportion of carboxyl and hydroxyl groups in its chemical structure, therefore it creates a negative shell layer surrounding the NPs (Kumar, Bakowsky et al. 2004, Musumeci, Ventura et al. 2006). However, with an outer coating of TMC, which is has a cationic property, therefore it leads to the TMC coated PLGA-TPGS NPs shows positive surface charge. Additionally, this phenomenon also confirms the successful coating of TMC around the PLGA-TPGS NPs.

3.7.2 Drug entrapment efficiency and loading capacity

Entrapment efficiency is determining the amount of the drugs in relation to the initial amount of the drug used in the formulation of the NPs (Song, Zhao et al. 2008). From the results, the optimal drug loaded NP shows a drug entrapment efficiency of 76.43 ± 0.21%, and a loading capacity of 5.32 ± 0.12% (Table 3-7).

Table 3-7. Results of drug entrapment efficiency and loading capacity of the optimised NPs (means ± SD; n = 3).

	Entrapment efficiency (%)	Loading capacity (%)
Optimal drug loaded NPs	76.43 ± 0.21	5.32 ± 0.12

Concentration of PLGA-TPGS has showed significant influences on entrapment efficiency. This is due to the increase of PLGA-TPGS concentration will lead to expansion of the internal water droplets, there will be a point whereby the internal water droplets are too large that the polymeric layer encapsulating the former would rupture leading to loss of drug into the external aqueous phase causing reduced encapsulation efficiency (Yu, Zhao et al. 2011). The semipermeable polymeric organic layer that acts as a barrier for drug diffusion to the external aqueous phase becomes thinner as the internal water droplets expand. As the organic barrier becomes thinner, more drugs can diffuse out to the external aqueous phase during the second emulsification step leading to decrease entrapment efficiency (Budhian, Siegel et al. 2007, Song, Zhao et al. 2008). Another explanation is that increasing the PLGA-TPGS concentration may result in alterations in the internal structure and surface morphology of the particles. The internal water droplets in the particle would form internal pores (Song, Zhao et al. 2008) and the entry channels of water into the particles would give rise to surface pores once the particles are freeze dried. Particles with more porous surface and larger internal pores would release more drug leakage during the solvent removal step (Song, Zhao et al. 2008).

BESTPFE.COM
List of research project topics and materials

In contrast, the loading capacity was decreased as the increase of PLGA-TPGS concentration. This was because the increase amount of drug loading was not proportional to the increase of the amount of polymer.

In addition, it is found that there is a trend of increasing entrapment efficiency when the TPGS concentration used increases. A possible explanation for this phenomenon is that the coherent with the findings reported by Bala *et al*, that increase in stabilizer concentration may result in increase in the viscosity of the external water phase. This in turn could increase the difficulty for drug to diffuse out into the external water phase. Therefore, this led to increase drug retention in the particle and thus increased entrapment efficiency (Bala, Hariharan et al. 2004). However, the excess use of stabilizer has its drawback. Feng *et al* found that the use of excessive stabilizer results in increasing drug adsorption to the particle surface and thus causes drug loss during the NPs washing steps (Feng, Mu et al. 2004).

Another phenomenon was found that when the 2^{nd} ultrasonication time decreased, the entrapment efficiency increased. From 90 sec to 450 sec for 2^{nd} sonication duration time, EE was reduced about 5%. Thus we can deduce that increasing the duration of second sonication step has more or less effects on drug entrapment efficiency, the observation in this case could be explained by with increasing sonication time might lead to breakage of the particles, and result in drug leakage, thereby a lower entrapment efficiency (Rouxel, Hadji et al. 2011).

Furthermore, there are a few of other evidence can be used to explain the drug loss in entrapment efficiency studies. Such as the precipitation of PLGA-TPGS droplets was not fast enough that the drug diffuses into the outer aqueous phase. It is known that the amount of drug entrapped into particles is dependent on the speed of polymer precipitation from the organic phase (Hung, Teh et al. 2010). Gemcitabine is very soluble in the outer aqueous phase, and this property couples with the concentration gradient between the inner and outer aqueous phases drive gemcitabine to diffuse out into the outer aqueous medium via the organic layer (Budhian, Siegel et al. 2007). Moreover, a certain amount of the gemcitabine was released from the harden particles during the long duration solvent removal step as well as the overnight storage in the fridge for hardening process. Subjecting the particles for centrifugation to participate the particles from the supernatant could also cause the release of some active drugs during the process. Moreover, the lack of sufficient time to allow PLGA-

TPGS to undergo polymerization could account for less gemcitabine entrapment in the particles (Murakami, Kawashima et al. 1997).

3.7.3 Morphology of the optimal nanoparticles

Surface morphology is important in determining the drug release kinetics of NPs. Under scanning electron microscope (SEM), the morphology of the optimal drug loaded NPs were shown nearly spherical in shape with irregular and porous outer surface (Figure 3-16A). The particle size showed in a range of 200 to 500 nm. This result correlates to the particle size measurement by Zetasizer. However, a slight increase in particle size may be attributed by the freeze-drying process. Freeze-drying method may lead to certain degree of particle aggregation (Maa and Prestrelski 2000).

In addition, it was observed that particles adhered to each other even after ultrasonication. Some surface pores were found, and the surface porosity could be attributed to the solvent evaporation during particle hardening. This pore nature of the NPs is important as it is responsible for the controlled release manner of the NPs. According to the Higuchi model, the release of entrapped drug from polymeric particles is dependent on the porosity of the particle matrix. As the evaporation rate of organic solvent increase, more and more pores form on the surface of the particles, through which release buffer could easily penetrate into the particles.

Moreover, an increase in temperature could result in the fast evaporation rate. In order to obtain NPs with slow release profile, evaporation temperature should be controlled not too close to organic solvent boiling point. Therefore, the evaporation of dichloromethane in this study was carried out at room temperature of about 20°C.

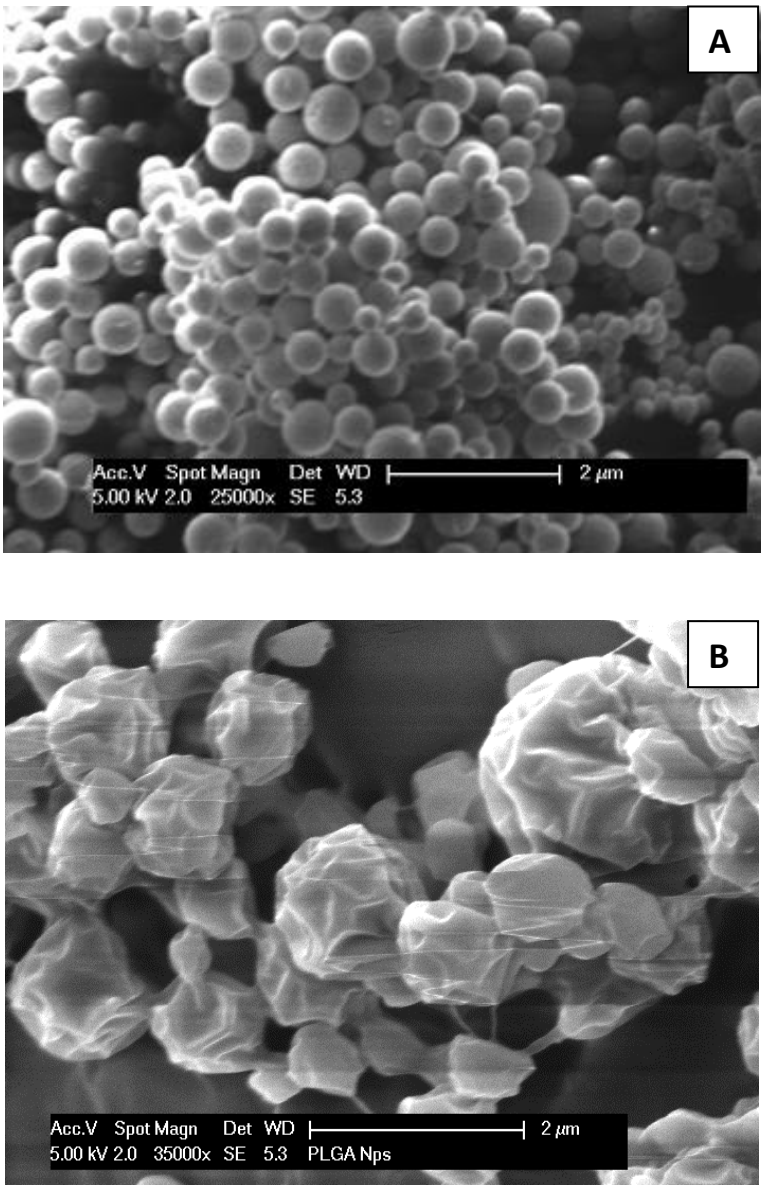

Figure 3-16. SEM images of drug loaded optimal NPs (A); A long beam exposure at a high voltage setting over time produced heating that make the particles shrink and crack (B).

3.7.4 *In vitro* drug release

The release profile of gemcitabine-loaded PLGA NPs and gemcitabine solution (control groups) is presented in Figure 3-17. The control group shows a fast drug release over cellular membrane of 94% gemcitabine released over 2 hrs. On the other hand, the optimal drug loaded NPs showed a biphasic gemcitabine release profile exhibiting a burst release followed by slow and steady release of gemcitabine.

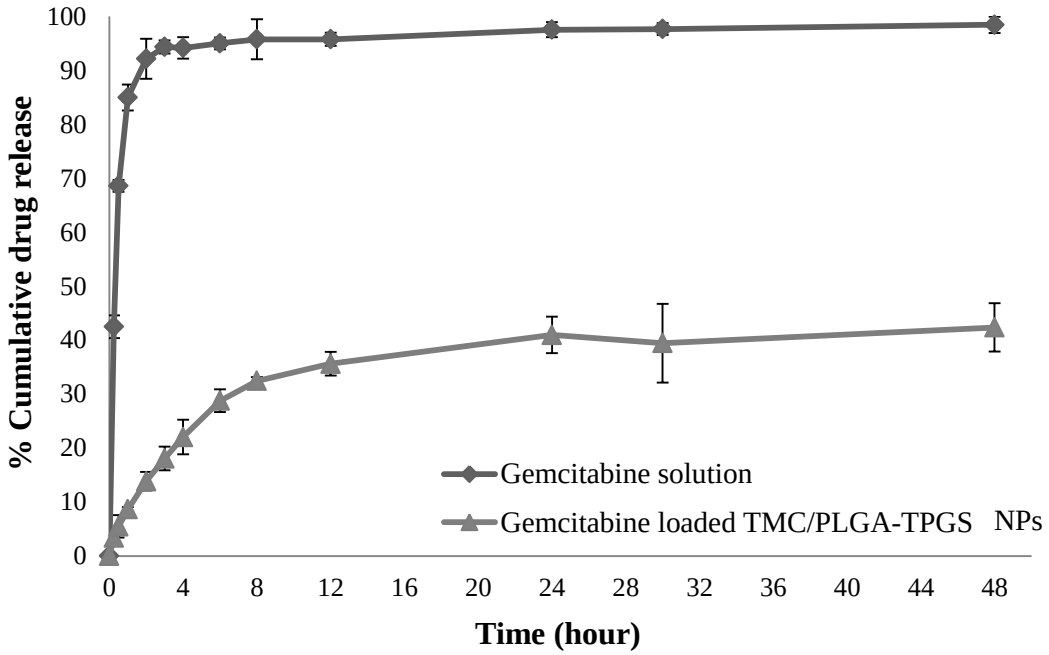

Figure 3-17. *In-vitro* release of gemcitabine loaded TMC modified PLGA-TPGS NPs versus gemcitabine solution using Franz diffusion cells. (Mean ± SD, n=3).

The first phase is an initial rapid burst release phase which is indicating the release of drug from the particle surface or in the pockets that are close to the surface of the particle (Agnihotri, Mallikarjuna et al. 2004). The figure shows an approximate 22% of drug was rapidly released over first 6 hrs. This burst release of the formulation may be also due to the particles with more porous the surface as the external volume was increased (Faisant, Siepmann et al. 2002). Solvent at the surface of the particles diffuses rapidly during the second emulsification step (The 2nd the sonification duration time), thus the longer the duration of 2nd sonification time, the smaller the particles as a result and increase the stability of the emulsion. At the same time, water would counter-diffuse into the oil droplets to occupy the space on the particle surface left behind by the solvent. Once the sample was freeze dried,

the water droplets would be evaporated, leaving behind pores on the particle surface. (Faisant, Siepmann et al. 2002, Yamaguchi, Takenaga et al. 2002). Particles with high surface porosity would release drugs at a higher rate giving rise to a higher burst release (Faisant, Siepmann et al. 2002).

The second phase is the lag phase which is characterized by a slow release rate that is due to the slow diffusion of entrapped drug through aqueous pores into the external release medium. From the figure, we can see there was 42.36% of gemcitabine released from the NPs over 48 hrs. This prolonged release in the later stage can be attributed to the slow degradation of PLGA particles through the hydrolytic process and the slow diffusion of gemcitabine from the polymer matrix. Another reason may be due to the presence of the oily phase within the double emulsion NPs, whereby it may have failed to degrade in the buffer medium during the *in-vitro* drug release study. Therefore, majority of the drug encapsulated within the nanoparticles were not released (Qiao, Chen et al. 2005, Makadia and Siegel 2011). In addition, gemcitabine release rate gradually decreased, reflecting less and less amount of entrapped drug are being released over time (Jain 2000, Costa and Sousa Lobo 2001, Panyam and Labhasetwar 2003). The release profile of a formulation influences the frequency the formulation has to be administered. Thus, a formulation that releases the drug over a prolonged period of time is preferred (Robinson 1978).

In addition, the method of conducting the *in-vitro* release study involves centrifugation of the nanosuspension for 40 minutes to separate the particles from the supernatant to harvest NPs. During the period of centrifugation, gemcitabine continued releasing out of NPs and the wash of NPs with sucrose solution might also cause gemcitabine to leak out into the medium (Faisant, Siepmann et al. 2002). Centrifugation also causes aggregation of particles, which increases the size of the particles (Schoevaart, Wolbers et al. 2004). Change in particle size affects the drug release characteristics of the particles. Large particles have smaller surface area will have slower drug release rate. In contrast, smaller particles with larger surface area leads to faster release rate (Thanoo, Sunny et al. 1993). Therefore, all these factors may contribute to the inaccuracies of the *in-vitro* release profile.

Furthermore, from the *in-vitro* drug release study, it demonstrates the magnitude of burst phase is considerably smaller for nanoparticles compared to the control. From the figure, we can see that over period of 48 hrs, 42.36% of the drug was released, which in the other hand

indicated about approximately over 57% of the drug preserving drug within the NPs after 48 hrs. This is an advantage for oral anticancer drug delivery, as it will provide the NPs with greater entrapped drug amount to reach the systemic circulation, and allow the release of the remaining drug molecules into the systemic circulation gradually (Pandey, Sharma et al. 2005). In addition, the TMC coating with high mucoadhesive characteristic, which leads to greater drug loaded NPs being absorbed over the GIT, thereby elevates the overall oral bioavailability of gemcitabine.

3.7.5 *In vitro* release kinetic modelling

In vitro release of optimal gemcitabine loaded NPs was evaluated as per the method described in Section 3.5.4. In previous section, we can see the drug release profile showed an initial burst releases followed by a sustained release manner for the formulation. The data obtained from the drug release was fitted to different kinetic models to understand the drug release mechanism and kinetics. The modelled kinetic parameters are reported in Table 3-8. The release data was subjected to goodness of fit test (r^2) by linear regression analysis according to the selected release kinetics models. (Figure 3-18).

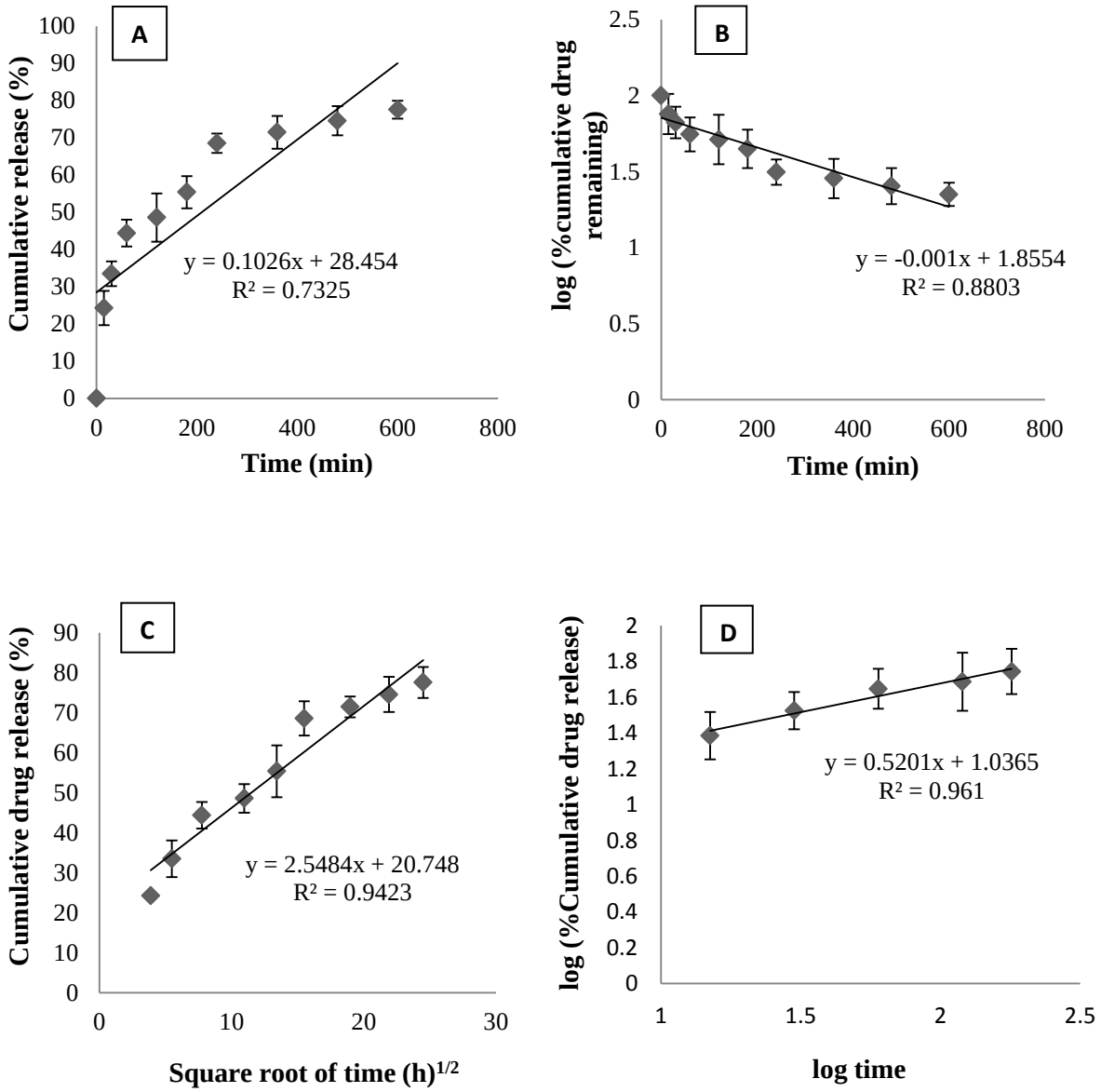

Figure 3-18. Drug release fitted to (A) zero-order, (B) first-order, (C) Higuchi model and (D) Korsmeyer-Peppas models (mean ± SD, n = 3).

Table 3-8. Release kinetic parameters of gemcitabine loaded NPs.

	Zero order		First order		Higuchi model		Korsmeyer-Peppas model		
Drug loaded NPs	r^2	k_0	r^2	k_1	r^2	k_h	r^2	n	k_k
	0.73	28.45	0.88	1.86	0.94	20.75	0.96	0.52	1.04

Zero order release describes the systems where the drug release is independent of its concentration. Under the zero order kinetic, drug diffuse out in a controlled manner from a dosage form with a defined area which doesn't disaggregate (Costa and Sousa Lobo 2001). Figure 3-18A shows the cumulative amount of gemcitabine release *vs* time for zero order kinetics. The r^2 value for the zero order kinetics was 0.73 for drug loaded NPs. This suggests the drug release didn't comply with zero order.

The first order release describes the release from systems where the rate of release is concentration dependent and the release follows Fickian diffusion mechanism (Costa and Sousa Lobo 2001). Figure 3-18B shows the first order release profile by plotting logarithm of cumulative percentage drug remaining *vs* time. This model did not provide a high r^2 for the optimal NP formulation, indicating that gemcitabine release occurred independently of the amount of drug remaining in the formulation.

Higuchi model describe the release of drug from an insoluble matrix, taking into account the volume of the dosage form accessible to the dissolution media changes with time (Higuchi 1963). This model can be analysed by plotting the amount of drug released *vs* square root of time (Figure 3-18C). It is typical for systems where drug release is governed by pure diffusion. Penetration of the media into the dosage form is depended on the matrix porosity and polymer relaxation. The high r^2 value for our drug loaded NPs indicates gemcitabine release from the NPs complies with Higuchi model very well. The release rate is highly dependent on the porosity of the particle matrix.

A Korsmeyer-Peppas model can be obtained by plotting log cumulative percentage of drug released versus log time for the first 60% drug (Figure 3-18D). The diffusional release exponent (n) in the model gives an indication of the diffusion mechanism. When n = 0.45, Fickian diffusion is expected. Diffusion is affected by a solvent moving with constant

velocity into the DDS. If n = 1.0, zero order release is seen, with release occurring independently of concentration. If $0.45 < n < 1$, then it is non-Fickian or anomalous diffusion as a mixture of Higuchi and zero order type diffusion (Korsmeyer, Gurny et al. 1983). Based on the results, gemcitabine release from the NPs followed Korsmeyer-Peppas model and the goodness fit test was satisfied (r^2 = 0.96). The release exponent n was 0.52 for the drug loaded NPs, which indicates the drug release governed by diffusion through the NPs matrix as well as matrix erosion – so called anomalous diffusion. This anomalous diffusion is evidence that gemcitabine released from the NPs was controlled by more than one process.

3.7.6 *Ex-vivo* permeation studies

The *ex-vivo* permeation studies on porcine intestinal epithelial membrane showed that the higher drug permeation rate was observed in the presence of NPs compare to the plain drug solution (Figure 3-19). A total of 45.1 ± 3.8% gemcitabine permeated through the epithelial membrane from the drug loaded NPs compared to 28.1 ± 4.2% from drug solution over 24 hrs. The results also showed the flux of drug released from the NPs across the epithelial membrane was significantly higher than the control ($p < 0.05$). The apparent partition coefficients (P_{app}) were calculated using Equation 3-19, this allows to compare more specifically the permeability of the two subjects. The flux (dX_r/dt),that is the gradient of the best fit line, it is shown that drug loaded NPs and drug solution have the flux of 31.74 and 19.14 respectively, using the linear part of the permeation curve from time 0 to 12 hrs. The surface area A is 1.77 cm^2 and C_0 is 5000 µg/mL. The P_{app} of drug solution and drug loaded NPs were determined as $(2.17 \pm 0.26) \times 10^{-3}$ cm/s and $(3.59 \pm 0.22) \times 10^{-3}$ cm/s, respectively, ($p < 0.05$). Larger P_{app} is expected to correlate with elevated oral absorption, which results in higher oral bioavailability (Grès, Julian et al. 1998), thereby this corresponds to the later pharmacokinetic results.

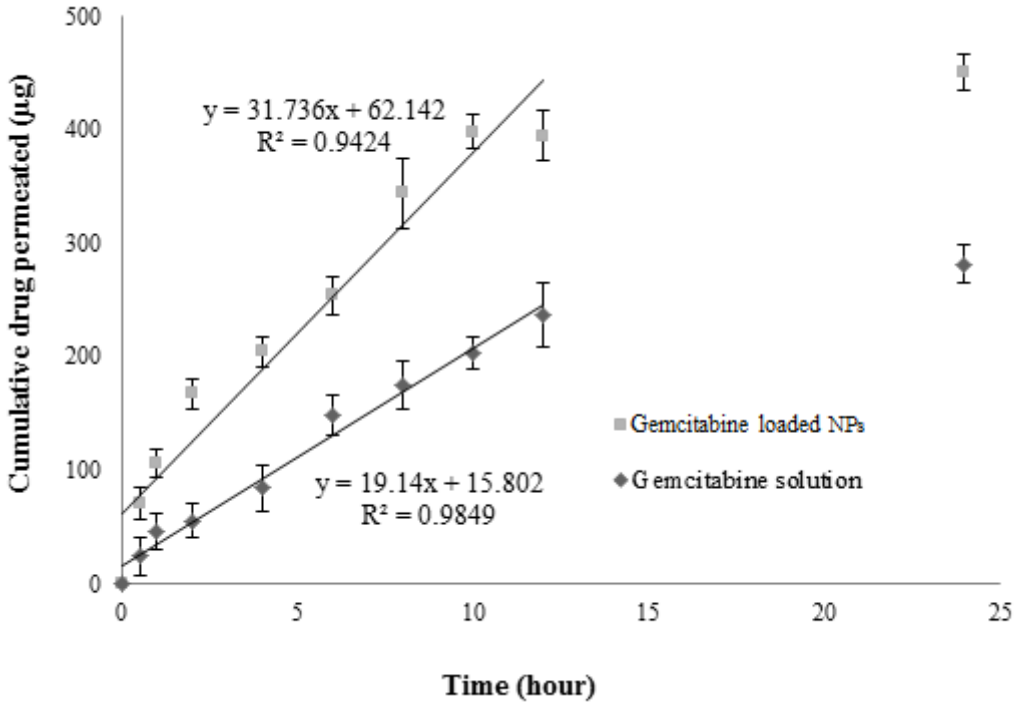

Figure 3-19. *Ex-vivo* permeation studies of gemcitabine loaded NPs and gemcitabine solution through porcine intestinal epithelial membrane (Mean ± SD, n=3).

BESTPPE.COM
List of research project topics and materials

3.7.7 Stability of gemcitabine-Loaded NPs

The optimized formulations were studied for their stability at different conditions and time intervals. The results of physical stability of lyophilized NPs formulation and chemical stability of gemcitabine on such NPs are shown in Table 3-9 and Table 3-10. As seen from the particle size analysis data in Table 3-9, the particle size of the NP formulation was very stable at 4°C for up to 3 months, for 2 months at 25°C conditions. The increase of particle size at high temperature and moisture may cause particle aggregation, which can be seen in 40°C, 75% RH group.

Table 3-10, it was observed that the initial drug content of drug loaded NPs analysed after 1, 2 and 3 months of storage at 4°C and 25°C were similar indicating there were no significant changes in the chemical properties of the NPs ($p > 0.05$). At 40°C/75% RH, a relatively significant change was observed in the drug content for NPs after 1 month storage. Drug content was reduced to approximate 91% in the third month.

Based on the observation, lyophilized drug loaded NPs should be stored at 4°C, where they remained stable in terms of both particle size and drug content.

Table 3-9. Influence of storage conditions on the particle size of lyophilized NPs (mean ± SD, *n* = 3)

Batch #	Storage conditions	Particle size (d.nm)			
		0 Month	1 Month	2 Month	3 Month
Drug loaded NPs	4°C	236.2 ± 12.95	224.5 ± 13.18	249.5 ± 10.07	241.9 ± 8.22
	25°C	236.2 ± 12.95	247.8 ± 10.36	247.2 ± 7.70	271.1 ± 21.76
	40°C, 75% RH	236.2 ± 12.95	270.6 ±11.19	304.9 ± 31.16	291.0 ± 21.04

Table 3-4. Influence of storage conditions on the chemical stability of gemcitabine on lyophilized NPs (mean ± SD, *n* = 3)

Batch #	Storage conditions	Amount of gemcitabine (% of initial amount)			
		0 Month	1 Month	2 Month	3 Month
Drug loaded NPs	4°C	100	101.7 ± 0.47	101.5 ± 1.51	99.8 ± 0.65
	25°C	100	100.3 ± 1.33	99.1 ± 1.31	97.2 ± 1.20
	40°C, 75% RH	100	94.4 ± 2.91	93.9 ± 0.35	91.8 ± 2.23

3.8 Conclusion

In this chapter, a novel gemcitabine loaded TMC modified PLGA-TPGS NP was developed and studied. Firstly, FTIR revealed the chemical structure of the synthetic copolymer, and the conjugation of PLGA and TPGS polymers was confirmed. The PLGA-TPGS was subsequently used to fabrication the NPs. This nanoparticulate delivery system incorporating gemcitabine were prepared by w/o/w double emulsion solvent evaporation technique. Effects of different concentration of polymers, stabilizer and the process variables on the NPs physiochemical properties were examined followed by a central composite design analysis. By means of this experimental design, the NPs can be prepared to obtain predetermined characteristics since the variables affecting these characteristics were determined and quantified. According to the studied factors, the selected optimal formulation was that prepared with PLGA-TPGS concentration (1%, w/v) and TPGS stabilizer concentration (0.6% w/v) accompanied by a 2^{nd} ultrasonication time (180 sec). Under such process conditions, the optimal drug loaded NPs can be produced with acceptable size in nano scale (243.21 ± 21.72) and high drug entrapment efficiency (76.43 ± 0.21%). *In vitro* release of selected factorial formulation showed 97.5% released over 24 hrs. The release showed biphasic profile exhibiting a burst release followed by a sustain release. The kinetic studies showed that gemcitabine released from NPs followed Korsmyer release kinetics. The mechanisms include desorption of the surface bound/adsorbed drug, dissolution diffusion of the drug from the matrices and matrix erosion resulting from polymer degradation (Le Corre, Rytting et al. 1997, Matsumoto, Matsukawa et al. 1997). The *ex-vivo* permeation studies on porcine intestinal epithelial membrane showed that the drug loaded NPs had a higher permeation rate (with 1.5-fold increase in permeation coefficient) compared to plain drug solution. Furthermore, NPs were washed and lyophilized for storage after particles were formed. Upon the stability studies, the optimal NPs were stable when stored at 4°C for up to 3 months.

In general the results show that the optimal TMC modified PLGA-TPGS NP is a promising carrier system for oral delivery of gemcitabine to maximize its oral bioavailability, and leads to a good clinical application potential.

Chapter 4

Development and Optimization of CSKSSDYQC Peptide Conjugated N-trimethyl Chitosan Nanoparticles

Chapter 4. Development and optimization of CSKSSDYQC peptide conjugated N-trimethyl chitosan nanoparticles

4.1 Introduction

In Chapter 3, a novel nanoparticulate delivery system of TMC modified PLGA-TPGS NP was developed and optimized, in order to enhance the oral bioavailability of gemcitabine. In this chapter, another approach to increase oral bioavailability of gemcitabine was investigated. A CSKSSDYQC (CSK) peptide modified TMC NPs was developed using TMC polymer to fabricate NPs via ionic gelation method, with conjugation of CSK peptide on the carrier system which will further enhance the intestinal mucoadhesion and elevate the particle permeation across the GIT to systemic circulation, and thereby improves the oral bioavailability of gemcitabine.

Chitosan (Figure 4-1A) is the second most abundant polymer on Earth and is obtained from insect and crustacean shells via treatment with sodium hydroxide (Derakhshandeh and Fathi 2012, Jin, Song et al. 2012). Chitosan is a linear polysaccharide composed of randomly distributed β-(1-4)-linked D-glucosamine (deacetylated) and N-acetyl-D-glucosamine (acetylated) units (Sandri, Bonferoni et al. 2010). It is highly compatible and easily degradable within the body, making it ideal for human administration (Jin, Song et al. 2012). Greater drug encapsulation and improved mucoadhesion has been shown for chitosan when compared to other NP polymers in prior research for oral drug administration (Sonia and Sharma 2012). In addition, chitosan has the ability to open intercellular tight junctions through interactions with anionic tight junction proteins (via cationic molecular groups), therefore enhancing permeability over intestinal epithelial membrane (Sonia and Sharma 2012). Tight junctions are ubiquitous throughout the GIT, making this an attractive characteristic of a polymer when considering oral drug delivery. At physiological pH, however, these properties are lost as a result of deprotonation, and chitosan becomes progressively insoluble as pH is increased (Cafaggi, Russo et al. 2007, Jin, Song et al. 2012). TMC (Figure 4-1B) is a partially quaternised chitosan derivative. More specifically, the amino function group of chitosan was substituted by a methyl group undergoes methylation to form TMC, and it has the capacity to overcome the limitations of chitosan (Jin, Song et al.

2012). Unlike chitosan, TMC is soluble at neutral and basic environments, promoting a greater potential anatomical area for NP uptake within the gut (Sandri, Bonferoni et al. 2010, Jin, Song et al. 2012). TMC also shows superior absorption relative to chitosan through increased contact with intestinal epithelium and mucoadhesion. Further, it promotes both transcellular and paracellular absorption (Sandri, Bonferoni et al. 2010).

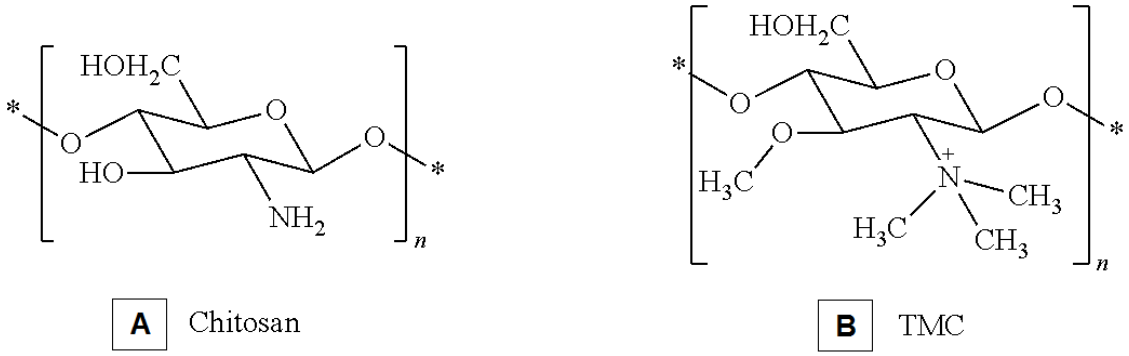

Figure 4-1. The chemical structure of chitosan (A); and TMC (B).

An approach of TMC conjugated to a ligand with high affinity for intestinal epithelial cells to enhance the drug permeation is demanded. An example of one of these ligands is CSKSSDYQC (CSK), a naturally occurring peptide that actively targets goblet cells, the second most common cell type of the intestinal epithelium (Jin, Song et al. 2012). CSK is also called tyrosin-protein kinase CSK, which has shown capability in ATP binding; protein C-terminal binding; protein phosphatase binding; metal ion binding; receptor binding and kinase activity (Sondhi, Xu et al. 1998, Fan, Chen et al. 2014, Zhang, Zhu et al. 2014). Zhang *et al* found that CSK target to receptor of intestinal epithelial goblet cells, and open up tight junction with the adjacent cells. The opening of tight junction is related with the transmembrane claudin-4, which is the principal barrier-forming protein of tight junction and interacts directly with the adaptor proteins. The distributions of claudin-4 on co-cultured cell membranes after the treatment of CSK modified NPs were investigated with immunofluorescence staining. As a result, after the treatment CSK modified NPs, claudin-4 staining at cell−cell contact sites became segmented and discontinuous, and the fluorescence signal became much weaker, indicating loss of tight junction function (Zhang, Zhu et al. 2014). In addition, CSK conjugation potentiates targeted NP uptake through adsorptive-mediated endocytosis and caveolae as well as clathrin mediated endocytosis over intestinal epithelial membrane. (The uptake mechanism was confirmed in Chapter 5, and demonstrated

CSK increases the uptake of NPs significantly). Moreover, CSK has shown great affinity to the intestinal mucosa and enhance the drug permeation in many other previous studies. Jin *et al* used HT29-MTX cell lines and *in vivo* rat studies, where insulin loaded CSK modified NPs resulted in a 1.7 increase in ileal permeation and a 1.5 fold increase in oral bioavailability compared to NPs without CSK conjugation (Jin, Song et al. 2012).

Taking advantage of the TMC polymer and CSK peptide, therefore we develop a second formulation approach of gemcitabine loaded TMC-CSK NP as a novel oral drug carrier system, in order to enhance oral bioavailability of gemcitabine. Figure 4-2 briefly shows a schematic layout of the formulation design for this study. (Details will be introduced in the Method section). Figure 4-3 shows the TMC-CSK NPs combines the TMC mucoadhesion characteristic and CSK goblet cells targeting properties, thus enhance the mucoadhesion on intestinal epithelial membrane and facilitate the endocytosis of drug loaded NPs across the GIT.

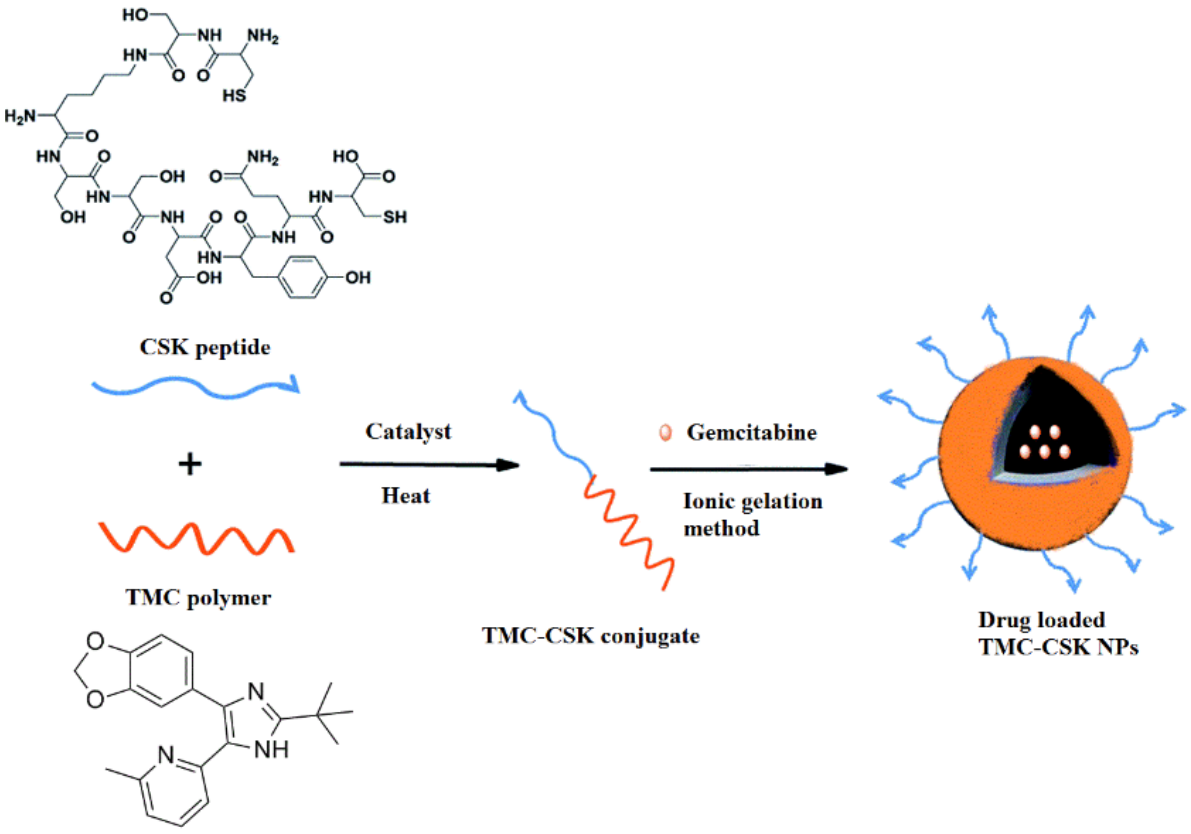

Figure 4-2. A schematic layout of the TMC-CSK NPs design to enhance the oral bioavailability of gemcitabine.

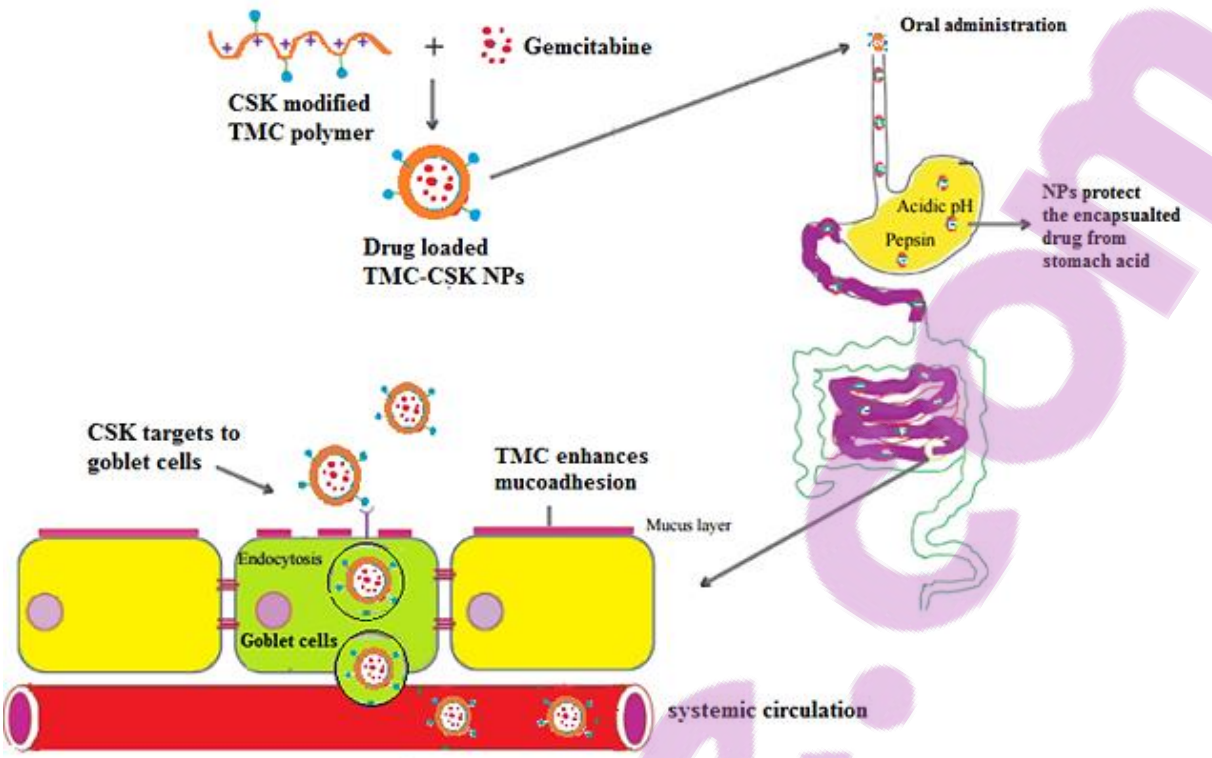

Figure 4-3. A schematic layout of the drug loaded TMC-CSK NPs with great mucoadhesion and goblet cell targeting characteristic to facilitate drug permeation across the GIT.

To fabricate this drug delivery system, TMC polymer was predominately synthesized from chitosan by using a new 2-step quanternization method. The conjugation of synthetic TMC and CSK peptide was subsequently prepared. Finally, the conjugated TMC-CSK polymer was used to fabricate gemcitabine loaded TMC-CSK NPs by using ionic gelation technique. The TMC-CSK NPs were then characterized for their particle size, zeta potential, morphology, drug entrapment efficiency and loading capacity, *in-vitro* drug release, *ex-vivo* drug permeation and long-term stability.

Bestthesis.com

4.2 Materials

Table 4-1. List of Materials.

Material	Batch Number	Manufacturer
TMC synthesis		
Chitosan 90% deacetylated	20140622	Comwin Fine Chemical, Changzhou, China
Sodium hydroxide mini-pearls	120524	ECP Ltd, Auckland, New Zealand
Ethanol	K44958183340	Merck, Auckland, New Zealand
Milli-Q water	0760	Millipore (0.22 µm filtered), Millipak 40, Germany.
Diethyl ether	12904006	Scharlau, Barcelona, Spain.
NaOH pellets (reagent grade)	84779	Scharlau, Barcelona, Spain.
Chitosan 75% deacetylated	077K0023	Sigma-Aldrich, St. Louis, MO, USA
Iodomethane solution (methyl iodide)	SHBD4382V	Sigma-Aldrich, St. Louis, MO, USA
N-methylpyrrolidone	SHBD6168V	Sigma-Aldrich, St. Louis, MO, USA
Sodium Iodide	MKBP2457B	Sigma-Aldrich, St. Louis, MO, USA
TMC collection		
Dialysis bag	2087	Membra-cel, MO, USA
Acetic acid (glacial analytical grade)	13630804	Scharlau, Barcelona, Spain.
Sodium Chloride	14806602	Scharlau, Barcelona, Spain.
Sodium hydrogen carbonate	55801	Scharlau, Barcelona, Spain.
Ethylenediaminetetraacetic acid disodium (EDTA-2Na)	085K00291	Sigma-Aldrich, St. Louis, MO, USA

TMC-CSK conjugation		
CSK	CM1100276	Chinese Peptide Company, Sichuan, China
N-hydroxysuccinimide (NHS)	BCBB3130	Sigma-Aldrich, St. Louis, MO, USA
N-(3-Dimethylaminopropyl)-N′-ethylcarbodiimide hydrochloride (EDC.HCL)	080M14582V	Sigma-Aldrich, St. Louis, MO, USA
Nitrogen (N_2) (gas)	N/A	University of Auckland, New Zealand
Nanoparticle synthesis		
Chitosan 90% deacetylated	20140622	Comwin Fine Chemical, Changzhou, China
Gemcitabine	20130501	Comwin Fine Chemical, Changzhou, China
Acetic acid (glacial analytical grade)	13630804	Scharlau, Barcelona, Spain.
Sodium tripolyphosphate (TPP)	12321JIV	Sigma-Aldrich, St. Louis, MO, USA
Polysorbate 80 (Tween 80) d	BCBJ7603V	Sigma-Aldrich, St. Louis, MO, USA

BESTPFE.COM
List of research project topics and materials

4.3 Methods

4.3.1 TMC Synthesis

4.3.1.1 One-Step Synthesis

Briefly, chitosan (2 g) and sodium iodide (4.8 g) were dissolved in n-methylpyrrolidone solvent (80 mL) and stirred magnetically (500 rpm) for 45 minutes. The reaction was refluxed in the dark at 60 °C in a water bath. Sodium hydroxide 15% solution (15 mL) and methyl iodide (11.5 mL) were added, and the mixture stirred (500 rpm) for 120 minutes. The product was collected via vacuum filtration and dialysed.

4.3.1.2 Two-Step Synthesis

The above procedure was carried out identically to the point of product collection (see Figure 4-4). The reaction mixture was instead poured into ethanol (200 mL) and centrifuged at 10376 g for 10 minutes. The ethanol was removed by washing the mixture with diethyl ether (60 mL) on a glass filter. The filtered product was dissolved with sodium iodide (4.8 g) in (n-methylpyrrolidone) solvent (80 mL) and magnetically stirred (500 rpm) under reflux conditions in the dark, over a water bath at 60 °C for 45 minutes. Sodium hydroxide 15% w/v solution (11 mL) and methyl iodide (7 mL) were added and the reaction continued for 60 minutes at 60 °C. Methyl iodide (2 mL) and sodium hydroxide pellets (0.6 g) were then added and the reaction was continued for 60 minutes. The final product was collected via vacuum filtration and dialysed as above.

4.3.2 TMC Collection

4.3.2.1 Vacuum Filtration

The synthesis product mixture was added to sodium chloride 10% solution (40 mL) and magnetically stirred (500 rpm) for 30 minutes. The resulting solution was added to ethanol (200 mL) and centrifuged at 10376 g for 10 minutes. The product was washed with diethyl ether (60 mL) on a glass filter and collected.

4.3.2.2 Dialysis

First, the dialysis bag was immersed in water and boiled for ten minutes in a solution of Milli-Q water (500 mL) containing sodium hydrogen carbonate (10 g) and EDTA (186.6 mg). The bag was then boiled in pure Milli-Q water (500 mL) for 10 minutes. The collected synthesis product was poured into ethanol (200 mL) and centrifuged at 10376 g for 10 minutes. The supernatant was discarded and the precipitate dissolved in Milli-Q water (15 mL), which was placed into the dialysis bag. The dialysis bag was placed in Milli-Q water (2 L) containing sodium chloride (15 g) and to dialyse for two days. The dialysis bag was then placed in Milli-Q water (2 L) for two days. The supernatant was removed and the product freeze-dried to remove any remaining water (Figure 4-4).

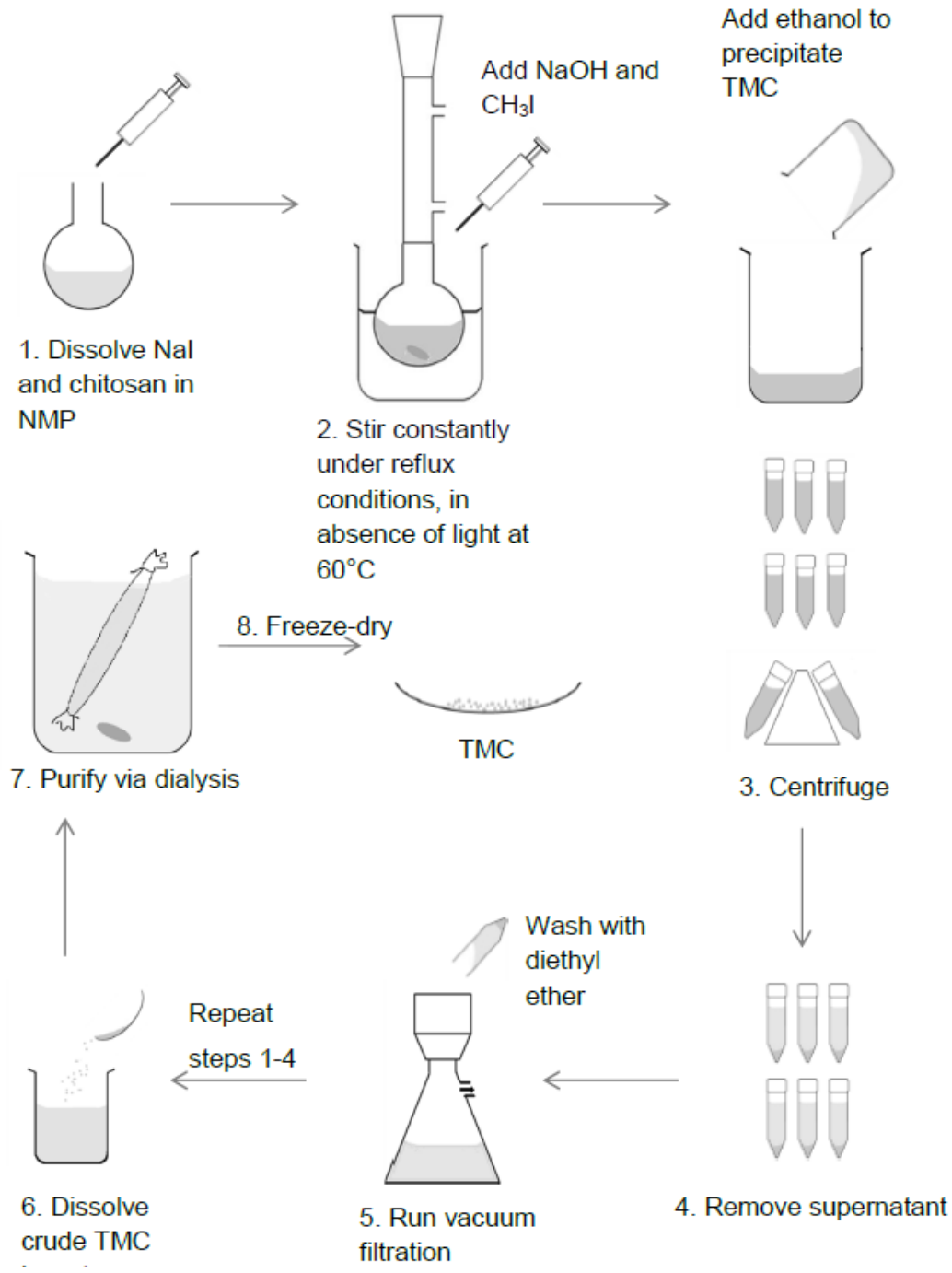

Figure 4-4. Schematic diagram of two-step quanternization method for TMC syntheses.

Quaternization was then identified by FTIR (Bruker Corporation, Billerica, MA, US). Methylation results when the spare pair of electrons presents on the primary amine residue of deacetylated glucosamine units constituting chitosan attack the relatively δ+ methyl group of the methyl iodide, and the methyl-iodine link is simultaneously broken via standard SN2 kinetics. This leads to the formation of a positively charged secondary ammonium ion. Subsequent deprotonation mitigates this charge and forms water, and the reaction can now repeat. (Figure 4-5). These two steps are repeated twice, resulting in trimethylated chitosan with an overall positive charge. The use of a two-step synthesis method facilitates a greater reagent contact time, increasing the likelihood of full amine methylation and results in higher yield of the product (Sieval, Thanou et al. 1998).

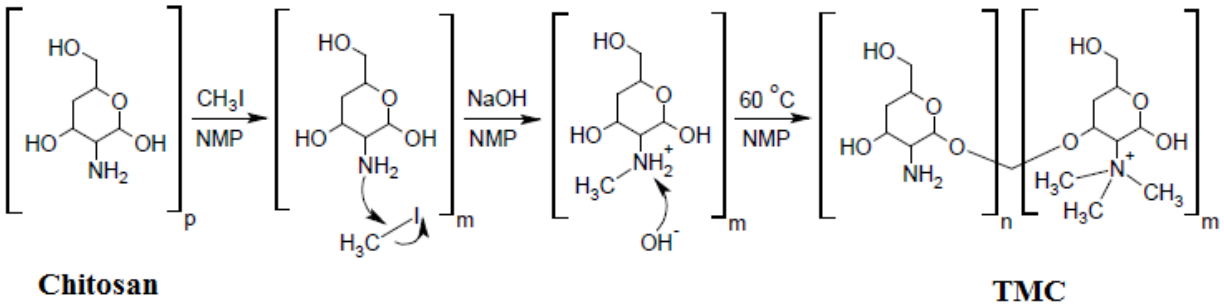

Figure 4-5. Schematic diagram of reaction mechanism for the synthesis of TMC polymer from chitosan.

4.3.3 TMC-CSK Conjugation

Following synthesis, TMC (200 mg) was dissolved in Milli-Q water (36 mL). EDC.HCL (380 mg) and NHS catalyst (228 mg) was added and stirred (500 rpm) to dissolution. Air was then removed under vacuum until all bubbles disappeared. CSK peptide (120 mg) was dissolved in Milli-Q water (4 mL) and transferred to the air-free flask via a needle and syringe. A balloon was filled with nitrogen gas and attached to the flask with a needle, to allow the transfer of nitrogen into the flask. The reaction was left to stir (500 rpm) for three days. The resulting TMC-CSK product was collected via dialysis in blank Milli-Q water (2 L) for three days using the above method. The dialysed product was then freeze-dried for two days to remove any remaining water (see Figure 4-6).

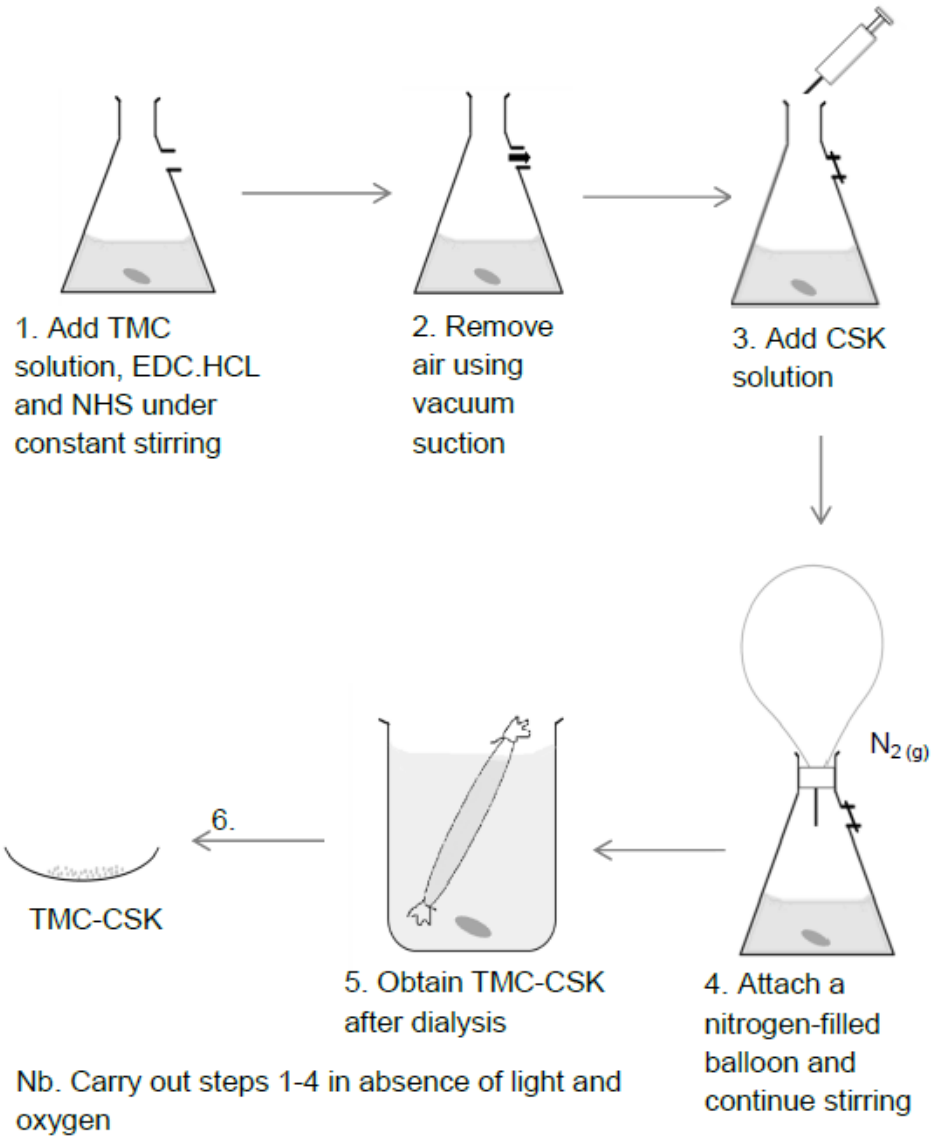

Figure 4-6. Schematic diagram of method for TMC and CSK conjugation.

TMC was subsequently conjugated with CSK via amide bonds formed between the carboxyl groups on CSK and the residual primary amino groups on TMC (Zhang, Zhu et al. 2014). The δ- hydroxyl group in CSK attacks the δ+ carbon atom in the carbodiimide group in EDC which is a coupling agent. The resulting electron rearrangement and subsequent nucleophilic attack by the amino group in TMC results in cleavage of the ester link in the EDC-CSK complex, and results in amide bond formation between TMC and CSK (Zarifpour, Hadizadeh et al. 2013, Zhang, Zhu et al. 2014). (Figure 4-7). Conjugation was identified by FTIR (Bruker Corporation, Billerica, MA, US).

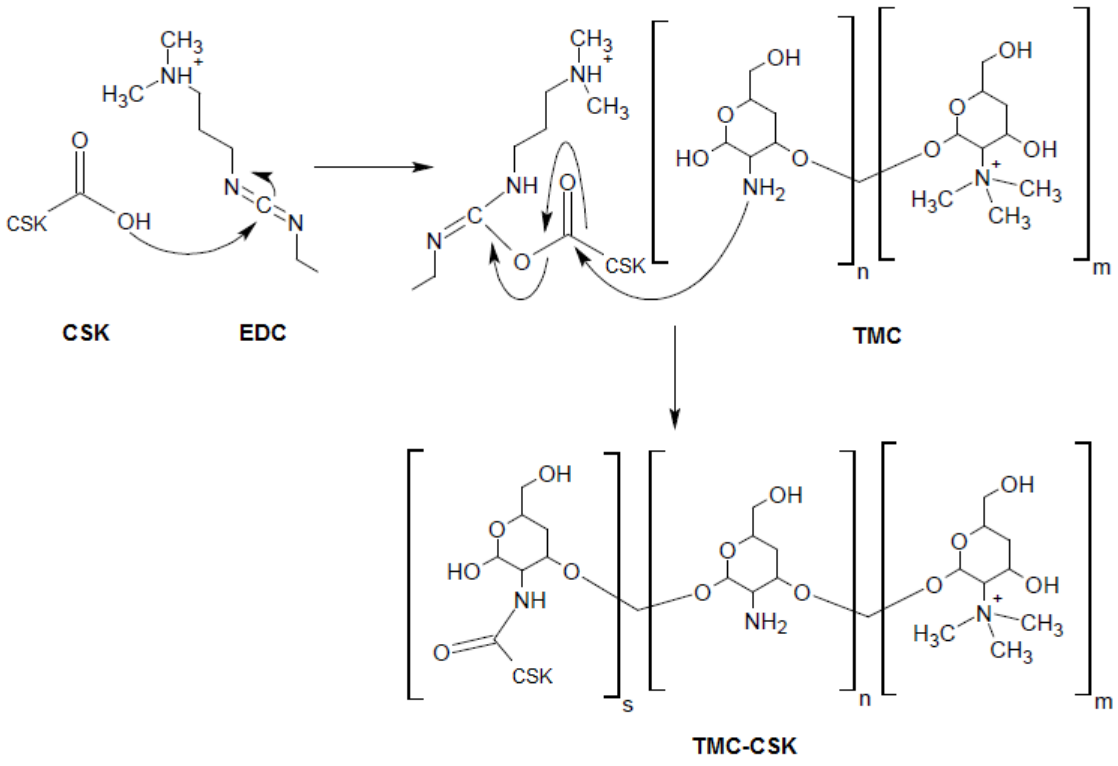

Figure 4-7. Schematic diagram of reaction mechanism for the EDC mediated conjugation of TMC and CSK.

4.3.4 Nanoparticle Preparation

Chitosan, TMC and TMC-CSK NPs were prepared using an ionic gelation method. Chitosan, TMC or TMC-CSK was dissolved in a 1% w/v gemcitabine solution. Acetic acid 99.8% (0.4 mL) was added to the chitosan solution to allow chitosan to be fully dissolved. Tween 80 (0.07mL) was added and thoroughly mixed with 2 mL of TPP solution of various concentrations were added drop-wise and the mixture stirred for 1 hr at room temperature during which time NPs precipitated. Weight ratio of TMC : TPP were varied from 1 : 1 to 6 : 1. The resultant suspension was ultracentrifuged at 173210 g for 30 minutes at 4 °C (Wx Ultra 80 model, Thermo Scientific®. US), the NPs collected, lyophilized and stored for further use (Zarifpour, Hadizadeh et al. 2013). A schematic diagram for the preparation of the drug-loaded TMC-CSK NPs using ionic gelation technique is shown in Figure 4-8.

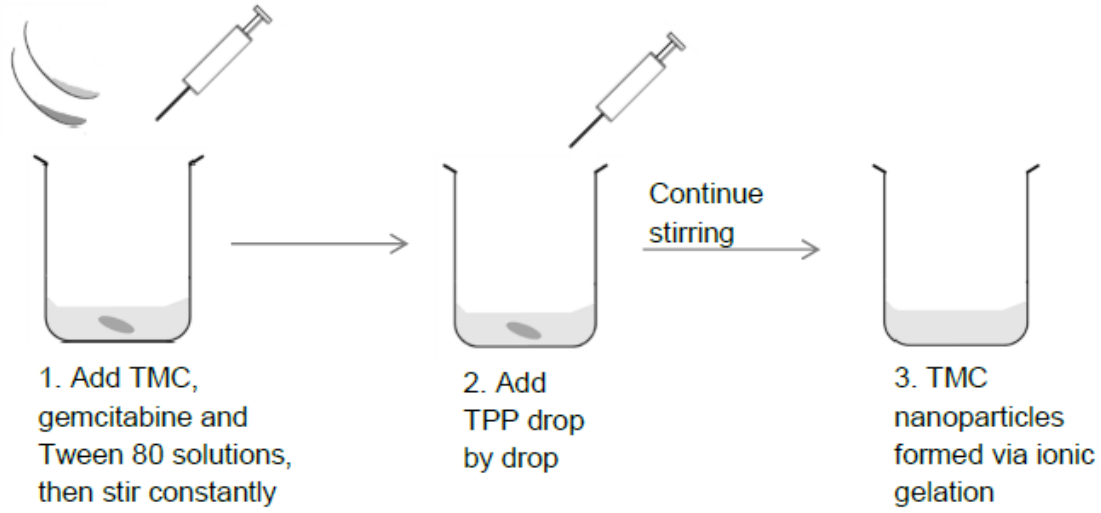

Figure 4-8. Schematic diagram of ionic gelation method for TMC NPs fabrication. Preparation of TMC-CSK NPs was used TMC-CSK polymer instead of TMC polymer in this case.

4.3.5 Formulation optimization TMC and TMC-CSK NPs

In order to develop an optimal drug loaded TMC and TMC-CSK NPs. The NPs were prepared by various weight ratios of TMC and TPP (Table 4-2), and characterization of these NPs were subsequently carried out.

TMC (quantity shown in Table 4-2.) and gemcitabine (50 mg) was dissolved in Milli-Q water (5 mL). Tween 80 (0.07 mL) was added and the mixture magnetically stirred (450 rpm). TPP solution of various concentrations (see Table 4-2) were made by dissolving TPP in Milli-Q water. Respective TPP solutions (2 mL) were added dropwise and the mixture stirred for 1 hr at room temperature. All nanoparticle suspensions were characterized for particle size and zeta potential, and drug entrapment efficiency. The optimal formulation was selected for further *in vitro* drug release and *ex-vivo* drug permeation studies as well as long term physical and chemical stability.

Table 4-2. Formulation parameters for nanoparticle synthesis.

Formulation	[TMC] (mg/mL)	TMC (mg)	[TPP] (mg/mL)	TPP (mg)	**TMC : TPP weight ratio**
A	5.00	25.0	4.17	8.33	**3:1**
B	6.00	30.0	5.00	10.0	**3:1**
C	7.00	35.0	5.83	11.7	**3:1**
D	8.00	40.0	6.67	13.3	**3:1**
E	7.00	35.0	2.92	5.83	**6:1**
F	8.00	40.0	3.33	6.67	**6:1**
G	4.00	20.0	3.33	6.67	**3:1**
H	7.00	35.0	17.5	35	**1:1**

Bestpfe.com

4.4 Characterization of the drug loaded nanoparticles

4.4.1 Fourier transform infrared spectroscopy

FTIR spectra were analysed using a Bruker FTIR tensor 37 (Bruker Optics, Ettlingen, Germany) at 4 cm^{-1} resolution between 400 and 4000 cm^{-1} to determine the chemical structure of chitosan, TMC polymers as well as to confirm the conjugation of TMC polymer and CSK peptide.

Briefly, the samples were placed on the FTIR measuring plate, and a testing probe was pressed down to contact the sample and measured. Background signals were recorded and subtracted automatically from the sample reading. Each sample was scanned 64 times and the average results were interpreted in peaks with different wavelength to represent different functional groups. To identify the function groups from the peak, an IR spectrum table as reference was used.

4.4.2 Particle size, polydispersity index and zeta potential

The size, Polydispersity Index (PDI), and zeta potential of the drug loaded NPs were measured in triplicate using a Malvern Zetasizer Nano-ZS (Malvern Instruments Ltd., Malvern, UK).

4.4.3 Drug entrapment efficiency and loading capacity

Entrapment efficiency (EE) was determined indirectly using a reverse phase HPLC analytical method (Chen, Svirskis et al. 2015). The conditions of this HPLC analytical method was introduced in Chapter 2.

Briefly, NPs containing gemcitabine (50 mg) were centrifuged at 10376 g at 20^0C for 10 minutes. Two mL of supernatant of each sample was removed and centrifuged at 10376 g at 20^0C for a further 30 min. HPLC was then used to determine the amount of gemcitabine in the supernatant which represent the non-entrapped drug amount. More specifically, the EE of the NPs was determined by subtracting the non-entrapped gemcitabine from the amount of

gemcitabine added to the NPs and expressed as a percentage (Chen, Li et al. 2014). (Equation 3-11). Using the same method to determine the loading capacity of the NPs, and loading capacity is calculated by using the Equation 3-12 in Chapter 3.

4.4.4 Morphology of nanoparticles

Samples were then observed under a condition of high vacuum and at a temperature of less than -120ºC using Philips XL30S FEG scanning electron microscope at 25 kV.

The surface morphology of the NPs revealed the shape, surface, structure and possible degree of aggregation. The morphology study was carried out using a scanning electron microscopy (SEM) (Phillips XL305 Field Emmsion Gun, Netherlands). Freeze-dried NPs were placed onto metal plates and sputter coated in platinum (Quorum Q150R S rotary pump sputter coater). Samples were then observed under a condition of high vacuum and at a temperature of less than -120ºC using Philips XL30S FEG scanning electron microscope at 25 kV. The morphology of TMC, and TMC-CSK NPs were evaluated.

4.4.5 *In vitro* release of gemcitabine from nanoparticles

In-vitro release of drug loaded TMC NPs and drug loaded TMC-CSK NPs were studied using a Franz diffusion apparatus (FDC-6, Logan, New Jersey, US). Gemcitabine solution of 1% w/v concentration and equivalent drug amount of gemcitabine loaded TMC NPs and TMC-CSK NPs were added to the donor compartment of the Franz diffusion cell, with a cellulose membrane (MW 12,000, Membra-Cel ®, Viskase, US) sandwiched between the donor and receptor chambers. PBS (pH 7.4) was used, and the temperature was maintained at 37 ± 1°C. Aliquots (500 µL) were withdrawn at pre-determined time points (15 min, 30 min, 1 hr, 2 hr, 3 hr, 4 hr, 6 hr, 8 hr, 12 hr and 24 hr) and replaced with fresh PBS (500 µL). The samples were centrifuged at 10376 g for 15 min, and this amount of gemcitabine released in the supernatant was filtered (0.22 µm) and analysed with the validated HPLC analysis as described in Chapter 2.

4.4.6 *Ex-vivo* permeation studies over porcine epithelial membrane

BESTPFE.COM
List of research project topics and materials

Ex-vivo permeation of gemcitabine loaded TMC and TMC-CSK NPs was determined in Franz cells by substituting the cellulose membrane for porcine intestinal epithelial membrane.

The apparent permeation coefficient (P_{app}) is the rate at which a drug will cross the intestinal wall and enter the portal circulation (Youdim, Avdeef et al. 2003), and was calculated using Equation 3-19 which mentioned in the previous chapter. Data was obtained from the *ex vivo* permeation curve of chitosan, TMC and TMC-CSK NPs using the first eight hrs to model initial linear permeation.

4.4.7 Physical and chemical stability of the nanoparticles

The optimal drug loaded NPs were studied for their physical and chemical stability. The optimal NPs were stored in screw-capped amber vials at three different temperatures (4, 25 and 40°C) for 3 months. Samples were withdrawn at 0, 1, 2 and 3 months and evaluated their physical stability by looking at their particle size and PDI. The chemical stability profile was evaluated by measuring the amount of drug retained in the NPs as previously described.

In the control groups, drugs with the equivalent to that entrapped in the NPs were used, and the drug solution was subjected to the 3 temperatures and the drug retained was examined at the end of each month during the 90-day storage.

4.4.8 Data analysis

Statistical data analyses were performed using Microsoft Excel 2010 software (Redmond, WA). Following primary exclusion, secondary exclusion was carried out on all data points outside two standard deviations from the mean. Results are shown as mean ± SD. Data comparisons were conducted using regression analysis, ANOVA tests, two-tailed t-tests, correlation coefficients, residual outputs and plots. A p-value ≤ 0.05 was pre-defined as the minimum level of significance. Primary and secondary exclusion processes were also undertaken.

4.5 Results and discussion

4.5.1 Pre-formulation studies

4.5.1.1 TMC synthesis

FTIR analysis was carried out to differentiate the TMC methylation product from chitosan, as well as to compare the TMC generated by using one-step synthesis method and two-steps synthesis method (Figure 4-9). For TMC prepared via both methods, peaks occur at 1425 and 1473 cm^{-1}. These are associated with N-CH_3 axial stretching and asymmetric angular deformation of C-H bonds respectively (Mourya and Inamdar 2009, de Britto, de Moura et al. 2012). Peaks evident at 1645 cm^{-1} are assigned to the quaternary ammonium salt native to TMC, and are absent from chitosan (Mourya and Inamdar 2009).

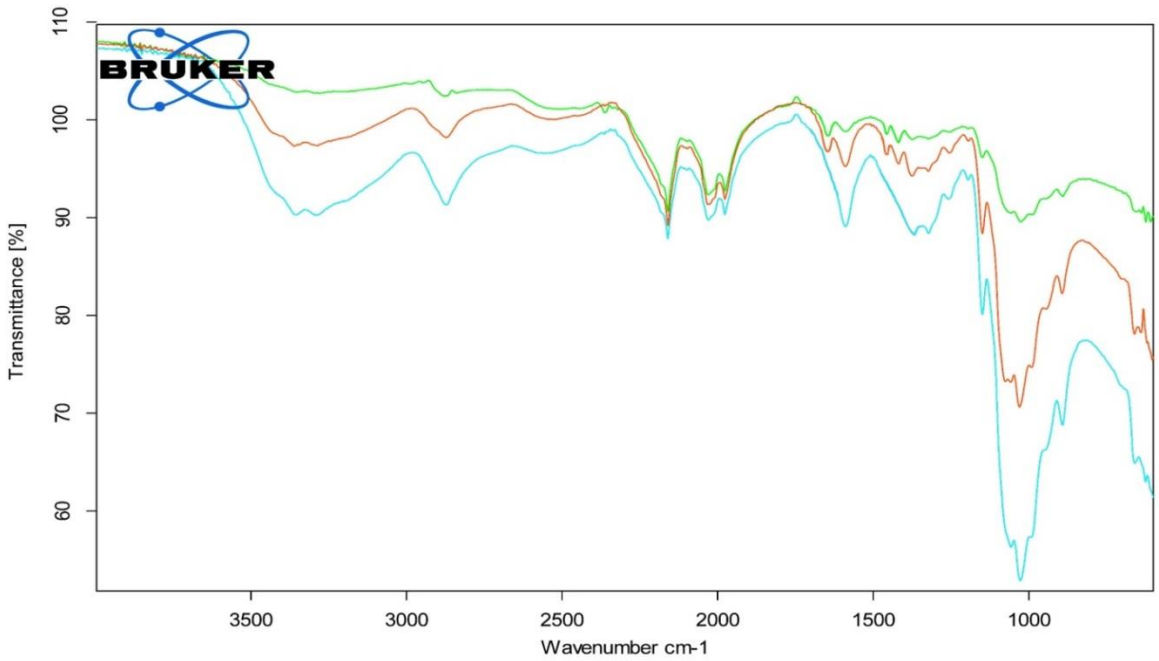

Figure 4-9. FTIR spectra of chitosan (-----), one-step synthesis of TMC (-----), two-step synthesis of TMC (-----)

There are reductions in certain peaks in both the one-step and two-step TMC spectra when compared to chitosan. Namely, a reduction at 1591 cm^{-1} shows the presence of an amino group (de Britto, de Moura et al. 2012), indicating the amino group being methylated. Further, a peak reduction between 3080 and 3360 cm^{-1} is attributed to the axial stretching of O-H and

N-H bonds, and peaks assigned to O-H bonds at 1000 - 1070 cm^{-1} consistent in all three spectra (Mourya and Inamdar 2009). The structures of chitosan and TMC are given in Figure 4-1.

4.5.1.2 TMC product yield

Initial TMC synthesis was conducted using 75% deacetylated chitosan. However, this did not allow for synthesis of TMC in quantities sufficient for characterisation and also demonstrated poor water solubility. Poor water solubility is associated with a low degree of chitosan methylation as un-methylated chitosan exhibits poor water solubility (Sieval, Thanou et al. 1998). The water insolubility of the synthesised TMC indicates the degree of methylation is not high enough to generate sufficient quantity of TMC product. For these reasons, it was excluded from further studies. By comparison, TMC yield improved dramatically when chitosan with more than 90% deacetylation was substituted, and thus the over 90% deacetylation chitosan was used for TMC synthesis.

The one-step synthesis method produced a TMC yield of 43%. By contrast, the two-step method produced a TMC yield of 89%, and TMC-CSK conjugation yield was 76% (Table 4-3). Therefore the two-step methylation method shows higher quanternization of TMC as well as greater product yield was used to synthesis TMC.

Table 4-3. Yield of One-Step Synthesis TMC, Two-Step Synthesis and TMC-CSK.

	Original material and weight (mg)	**Final material and weight (mg)**	**Percentage yield (%)**
One-step Synthesis	Chitosan: 200	TMC: 86	43
Two-step Synthesis	Chitosan: 200	TMC: 178	89
	TMC: 200 + CSK: 120	TMC-CSK: 242	76

4.5.1.3 TMC-CSK conjugation

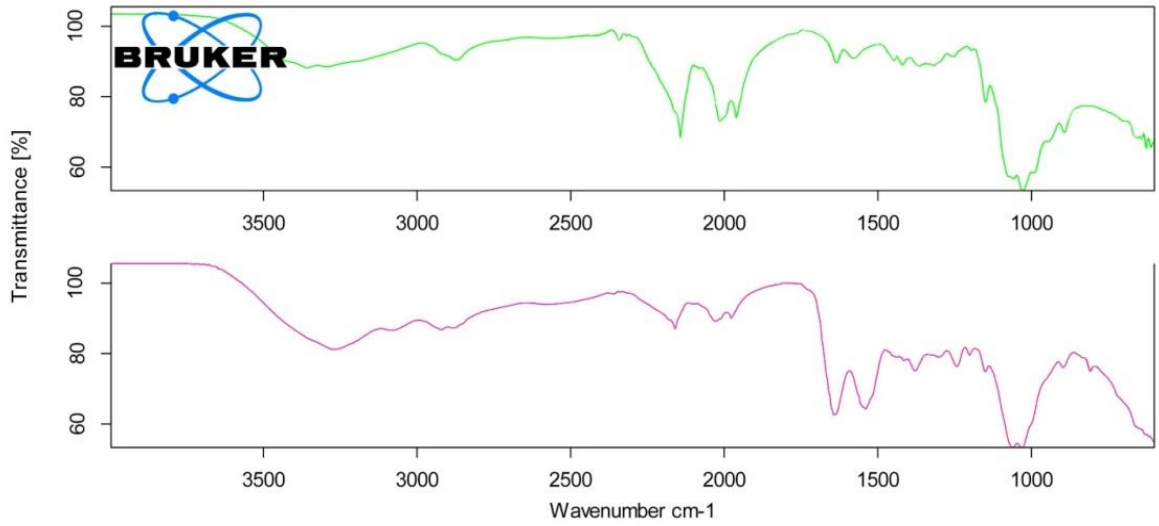

Figure 4-10. FTIR spectra of Two-Step Synthesis TMC (-----) and conjugation of TMC-CSK (-----)

FTIR analysis of TMC-CSK demonstrated conjugation between TMC and CSK (Figure 4-10.) A peak at 1515 cm^{-1} is due to a benzene ring of tyrosine in CSK, and distinguishes TMC-CSK from TMC alone (Abo-Riziq, Grace et al. 2011). In addition, a peak at 1651 cm^{-1} indicates the presence of an amide bond, confirming conjugation of TMC with CSK (Liao, Lien et al. 2002).

4.5.1.4 FTIR analysis peaks of chitosan, TMC and TMC-CSK nanoparticles

The FTIR of the synthesised NPs shows the appearance and modification of several significant peaks. The peak due to the amino group at 1590 cm^{-1} present in the spectra of all polymers (see Figure 4-9, and Figure 4-10.) was shifted to 1550-1560 cm^{-1} in the spectra of the synthesised NPs (see Figure 4-11.) (Arya, Vandana et al. 2011, Hosseinzadeh, Atyabi et al. 2012). The peak due to the axial stretching between O-H and N-H at 3452 cm^{-1} also became sharper when compared to chitosan, TMC or TMC-CSK alone (see Figure 4-9. and Figure 4-10.) (de Britto, de Moura et al. 2012). The peak due to angular deformation of the

C-H bond at 1473 cm^{-1} in the TMC spectrum decreased in size, though this result was not seen in either the chitosan or TMC-CSK NPs spectra. A peak at 740 cm^{-1}, due to the angular deformation of P-O, was also observed for all three spectra. For TMC and TMC-CSK, the peak due to the quaternary amine salt at 2050 cm^{-1} disappeared in the FTIR of the TMC and TMC-CSK NP formulations (Möckel and Lippold 1993). In both the TMC and TMC-CSK NP formulations, the peak at 1425 cm^{-1} became broader and the peak at 1645 cm^{-1} disappeared. These changes are attributed to interactions between gemcitabine and the respective polymers (Hosseinzadeh, Atyabi et al. 2012). These two differences however, were not seen in the chitosan spectrum. The C-H peak was seen at 1743 cm^{-1} across all three spectra. The TMC and TMC-CSK NP spectra also show a peak at 1374 cm^{-1} which was attributed to gemcitabine (Arya, Vandana et al. 2011, Hosseinzadeh, Atyabi et al. 2012).

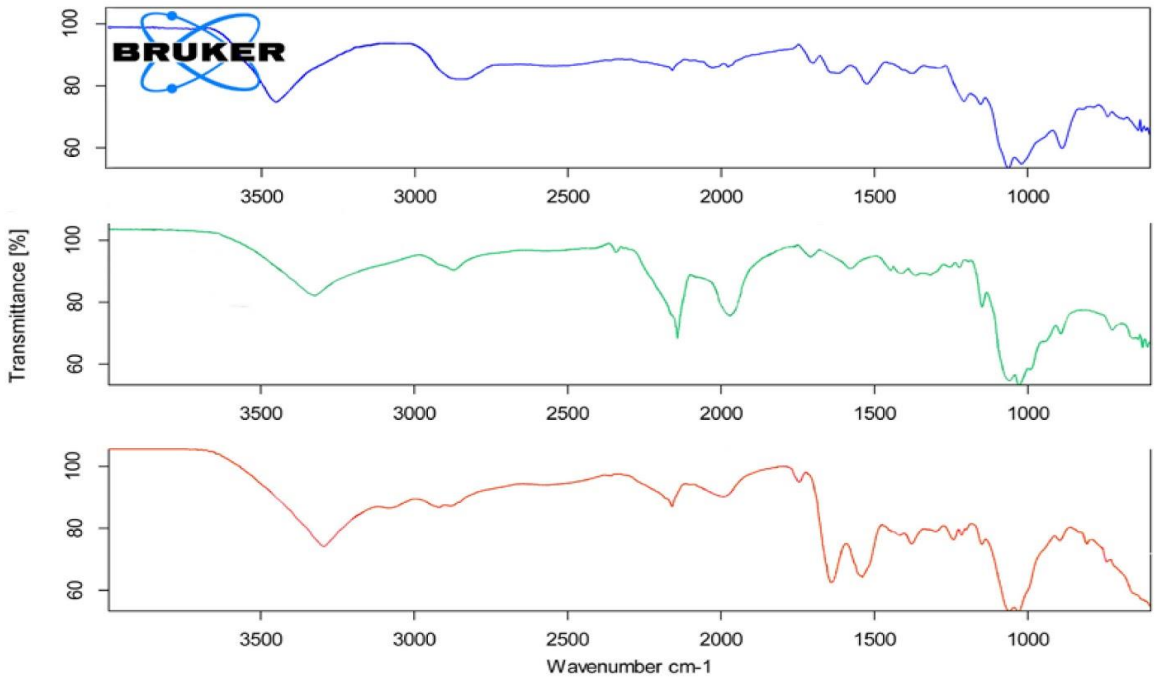

Figure 4-11. FTIR Spectra of chitosan NPs (-----), TMC NPs (-----) and TMC-CSK NPs (-----)

4.5.2 Characterization

All the drug loaded TMC NP formulations from A-H in Table 4-2 were prepared and characterized for particle size, PDI, zeta potential and drug entrapment efficiency. The overall optimal formulation was selected and prepared the drug loaded TMC-CSK NPs. Finally, the optimal TMC NPs and TMC-CSK NPs are further characterized for their surface morphology, *in-vitro* drug release, *ex-vivo* drug permeation, and long term stability studies.

4.5.2.1 Particle size

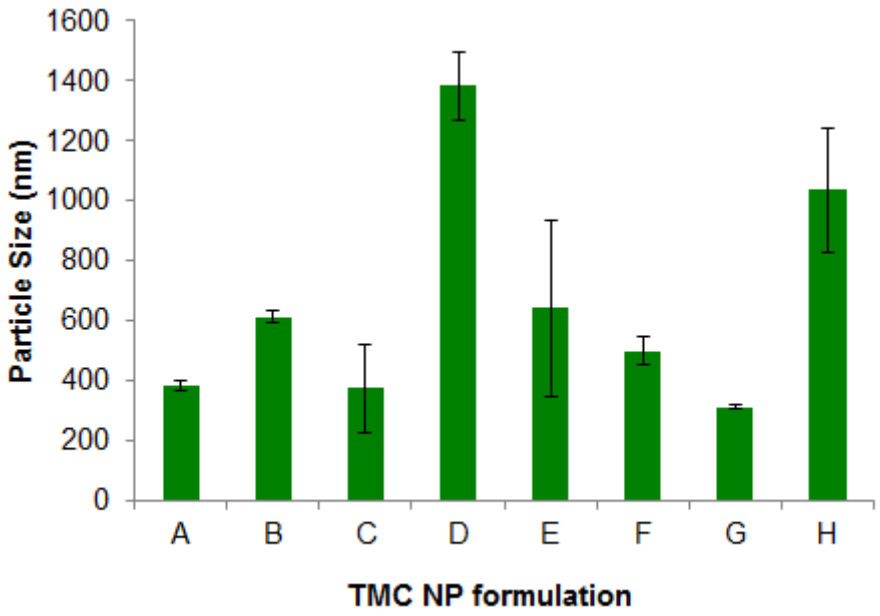

Figure 4-12. Particle size of TMC NP formulations from A-H groups (mean ± SD, n = 3).

All formulations were in the nanometre range (300-1000 nm) except for formulations D and H, which were sized at 1384 ± 113.8 and 1035.5 ± 207.7 nm respectively. Formulations A, C and G had the smallest particle size of 382.9 ± 18.2, 371.9 ± 146.8 and 310.9 ± 5.4 nm respectively. There was an increase in particle size with increasing TMC concentration ($p < 0.05$). Although formulation C had the smallest particle size, clear overlap between formulation C and A meant that there was no statistical difference between the particle size of formulations A and C (formulation G had an even smaller particle size but was excluded due to insufficient yield).

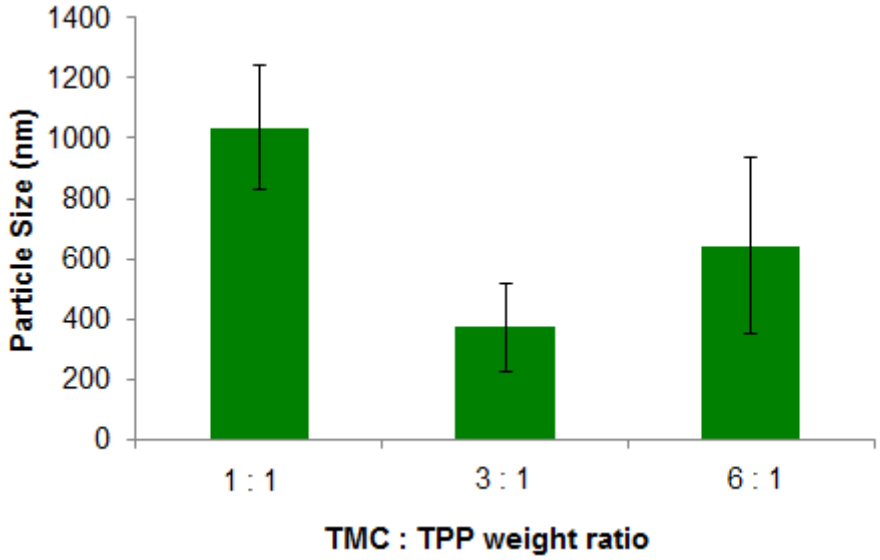

Figure 4-13. Particle size of TMC NP formulations with different TMC : TPP weight ratios (mean ± SD, n = 3).

From Figure 4-13, only the TMC : TPP weight ratio of 1:1 was not within the nanometre range, and was sized at 1035.5 ± 207.7 nm. A weight ratio of 3:1 yielded the smallest particle size of 371.9 ± 146.8 nm. Only the difference between 3:1 and 1:1 ratios was statistically significant ($p < 0.05$).

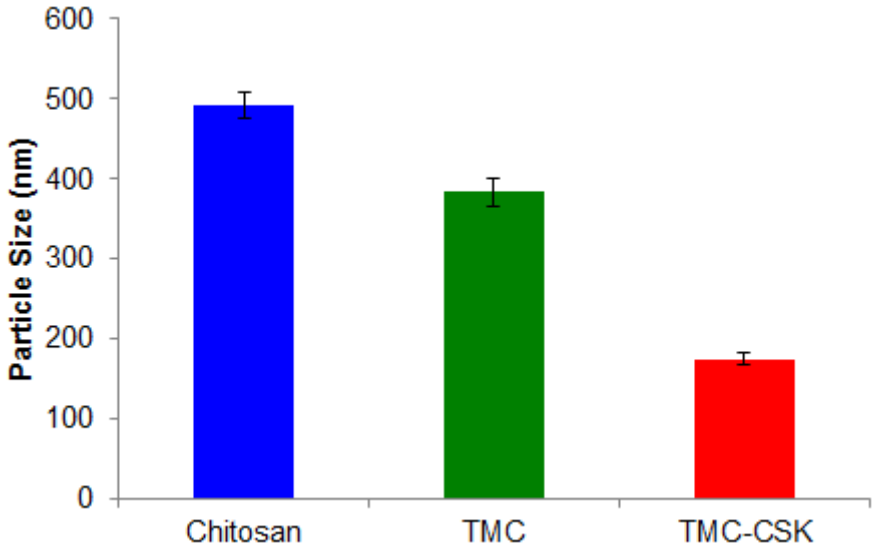

Figure 4-14. Particle size of chitosan, TMC, and TMC-CSK NPs prepared with 4.17 mg/mL TPP and 5 mg/mL of polymer (mean ± SD, n = 3).

From Figure 4-14. The particle size of all formulations was in the nanometre range. TMC-CSK NPs exhibited the smallest particle size, followed by TMC and then chitosan NPs (173.6 ± 7.7, 393.0 ± 18.2 and 492.1 ± 13.6 nm respectively). The differences between the NPs prepared by different polymers were statistically confirmed ($p < 0.05$).

4.5.2.2 Polydispersity Index

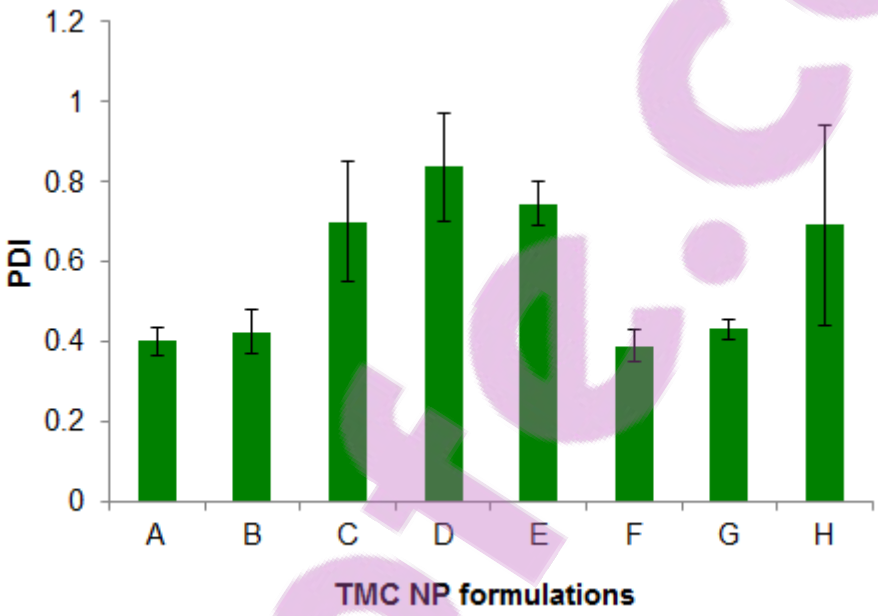

Figure 4-15. PDI of TMC NP formulations A-H (mean ± SD, n = 3).

From Figure 4-15, Formulations A, B, F and G had PDI values less than 0.5 (PDI values of 0.399 ± 0.033, 0.424 ± 0.054, 0.389 ± 0.042 and 0.43 ± 0.027 respectively). PDI was observed to increase as TMC concentration increased and this was statistically confirmed ($p = 0.01$).

Bestpdf.com

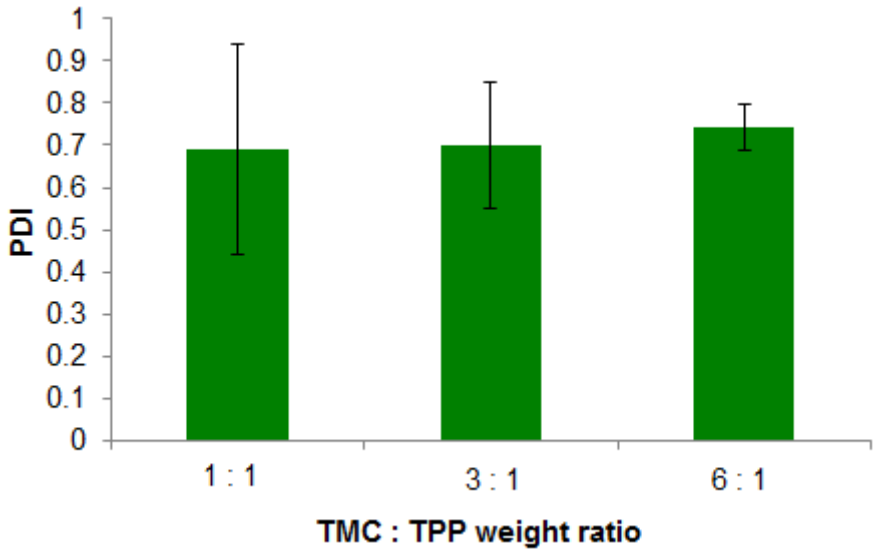

Figure 4-16. PDI of TMC NP formulations with different TMC : TPP weight ratios (mean ± SD, n = 3).

Figure 4-16 shows the PDI values varied by 0.053 across all weight ratios and all were $p > 0.5$. A TMC : TPP weight ratio of 6 : 1 had the least homogeneity (PDI = 0.744 ± 0.048) and a weight ratio of 1 : 1 had the most (PDI = 0.691 ± 0.220). The differences between the different formulations with various weight ratios were not statistically significant ($p > 0.05$).

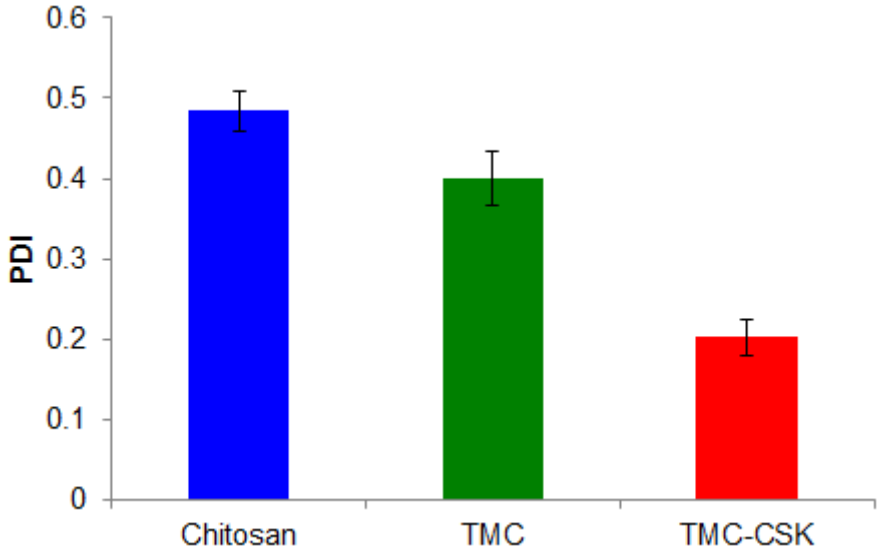

Figure 4-17. PDI of chitosan, TMC and TMC-CSK NPs prepared with 4.17 mg/mL TPP and 5 mg/mL of polymer (mean ± SD, n = 3).

PDI was < 0.5 for all three polymers, with TMC-CSK NPs showing the lowest PDI of 0.202 ± 0.022 which is preferred. Chitosan groups showed a highest PDI of 0.484 ± 0.026. The differences between all polymers was statistically confirmed significant ($p < 0.05$).

4.5.2.3 Zeta potential

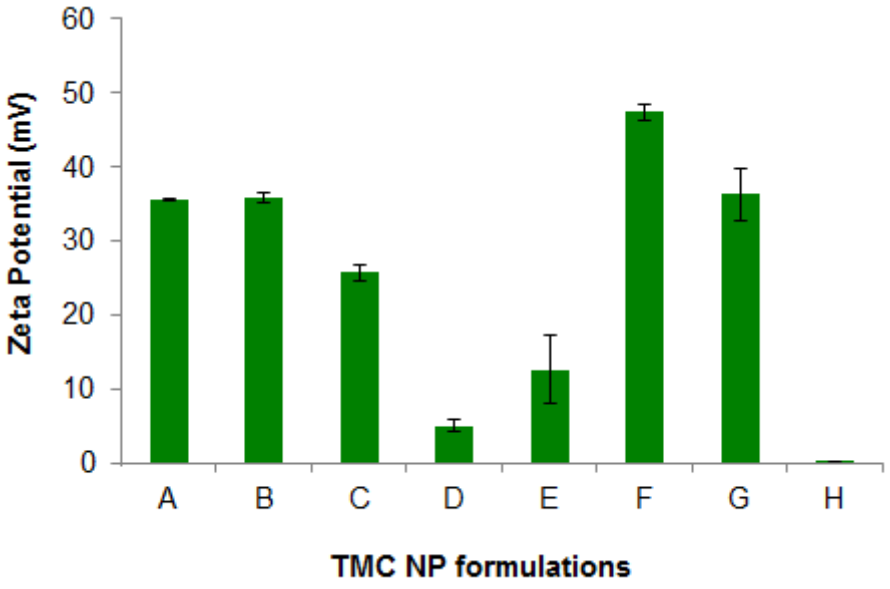

Figure 4-18. Zeta potential of TMC NP formulations A-H (mean ± SD, n = 3).

Figure 4-18 shows Formulations C and E had the ideal zeta potential values of between + 10 and + 30 mV with zeta potentials of + 25.7 ± 1.0 and + 12.6 ± 4.6 mV respectively. Formulations D and H had zeta potentials below this (+ 5.070 ± 0.863 and + 0.119 ± 0.134 mV respectively). Formulations A, B, F and G all had zeta potentials greater than + 30 mV. The zeta potential was observed to decrease with increasing TMC concentration.

BESTPFE.COM
List of research project topics and materials

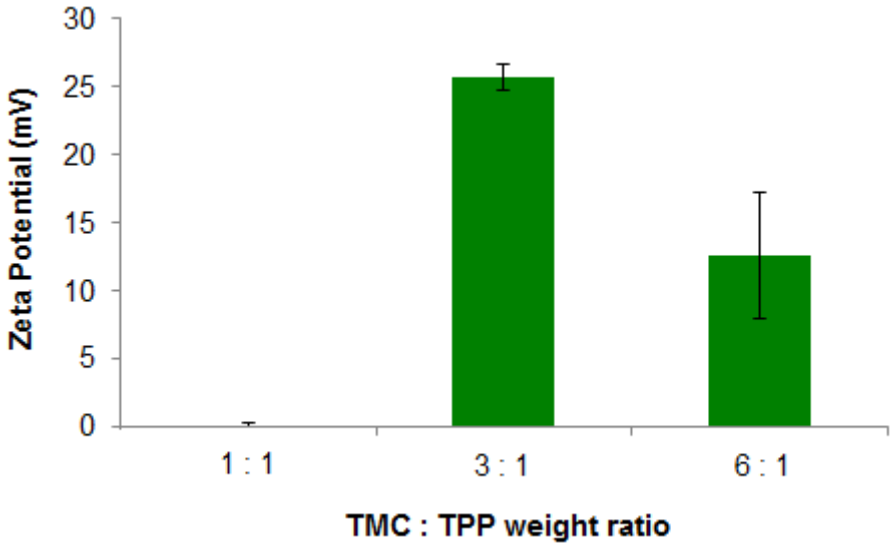

Figure 4-19. Zeta potential of NP formulations with different TMC : TPP weight ratios (mean ± SD, n = 3).

From Figure 4-19, we can see only the TMC : TPP weight ratio of 1 : 1 formulations did not display a zeta potential within the ideal range of +10 and +30 mV, with a zeta potential of +0.119 ± 0.134 mV ($p < 0.05$). The TMC : TPP weight ratio of 3 : 1 had the highest ideal zeta potential (+25.700 ± 1.018 mV compared to the +12.563 ± 4.907 mV of 6 : 1 weight ratio formulations) ($p < 0.05$).

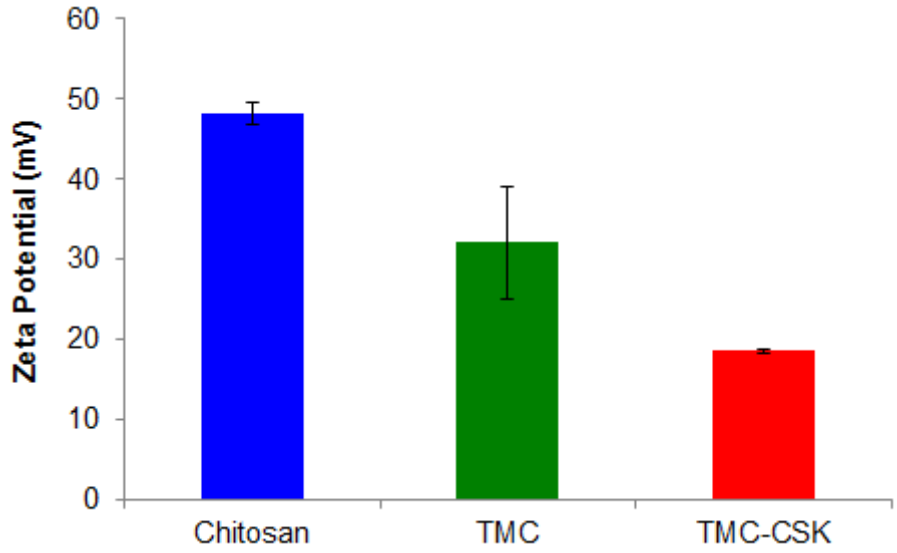

Figure 4-20. Zeta potential of chitosan, TMC, and TMC-CSK NPs prepared with 4.17 mg/mL TPP and 5 mg/mL of polymer (mean ± SD, n = 3).

From Figure 4-20, only TMC-CSK NPs had a zeta potential within the ideal range of between + 10 and + 30 mV with a zeta potential of + 18.5 ± 0.2 mV. Of the remaining two, TMC was closer to the ideal range than chitosan (+ 32.033 ± 6.994 m compared to + 48. 67 ± .3 2 mV) ($p < 0.05$)

4.5.2.4 Entrapment efficiency

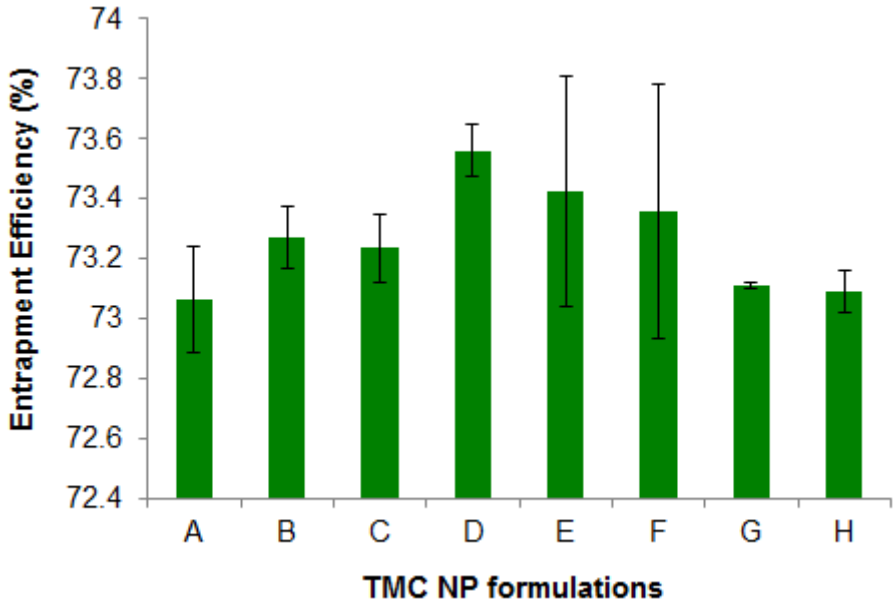

Figure 4-21. EE values of formulations A-H, each prepared with 50 mg of gemcitabine (mean ± SD, n = 3).

All formulations had EE > 70% (mean EE of 73.3%). Formulation D had the highest EE value (73.6 ± 0.9%) and formulation A had the lowest (73.1 ± 0.2%). Increasing TMC concentration had the overall effect of increasing EE ($p < 0.05$). However the differences between formulations A, B and C could not be statistically confirmed ($p > 0.05$)

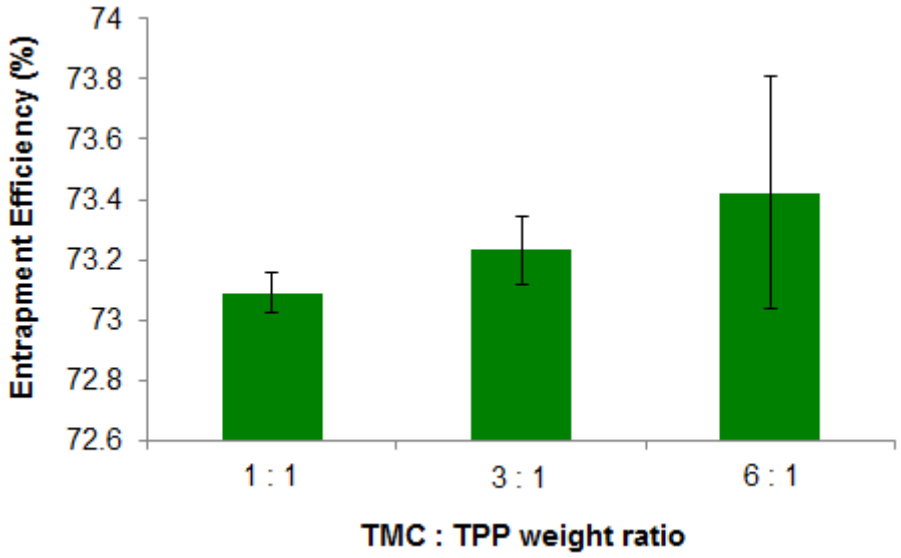

Figure 4-22. EE values of NP formulations with different TMC : TPP weight ratios (mean ± SD, n = 3).

All ratios displayed EE values > 70 %. The highest EE observed was the 6 : 1 TMC : TPP weight ratio with an EE value of 73.4 ± 0.4%. The differences between all groups with various weight ratios were not statistically confirmed ($p > 0.05$).

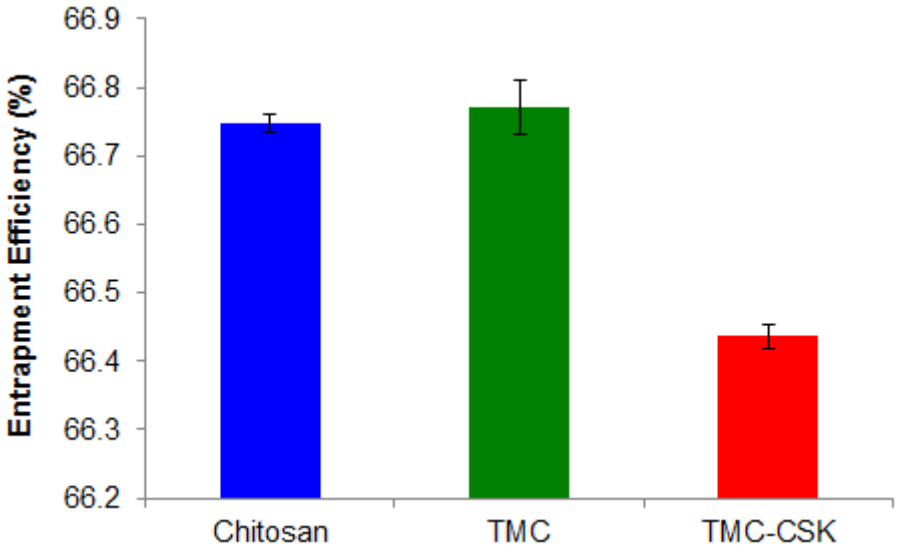

Figure 4-23. EE values of chitosan, TMC and TMC-CSK NPs, each prepared with 50 mg gemcitabine, 4.17 mg/mL TPP and 5 mg/mL of polymer (mean ± SD, n = 3).

All polymers displayed EE values > 65 %. TMC-CSK NPs displayed less EE than TMC or chitosan NPs by a margin of 0.3%, (66.437 ± 0.017 vs 66.770 ± 0.039 and 66.747 ± 0.013% for TMC and chitosan respectively. ($p < 0.05$)). TMC NPs yielded better EE than chitosan NPs by 0.03% ($p = 0.33$).

Overall, Formulation A exhibited the most favourable combination of particle size of 382.9 ± 18.2 nm, PDI of 0.399 ± 0.033, zeta-potential of + 35.60 ± 0.20 mV and an EE of 73.1 ± 0.2%. It was thus selected as the model formulation to investigate the differences between TMC and TMC-CSK NPs. Formulations D and H were excluded from further characterisation on the basis of size. Formulation G showed favourable characteristics but low yield. This low yield prevented drug release and SEM studies from being conducted on formulation G. Formulation G was deemed inefficient to manufacture and was excluded for this reason.

4.5.3 Further characterization of optimal formulations

4.5.3.1 Particle size, zeta potential and entrapment efficiency

Table 4-4 displays the size, zeta potential and entrapment efficiency of TMC and TMC-CSK NPs. The TMC-CSK NPs (173.60 ± 6.82 nm) are around half the size of TMC NPs (382.97 ± 18.20 nm). Additionally, it was found that increasing the ratio of TMC and TPP concentration, the particle size was reduced significantly ($p < 0.05$). A theory supported by Ing *et al*. who claimed that TMC NPs had small particle size due to the strong electrostatic interactions with polyanionic TPP (Dehousse, Garbacki et al. 2010, Yien, Zin et al. 2012). Particle size is important in delivering chemotherapeutic agents because of its implications for permeation and retention (Chow and Ho 2013). According to He *et al.*, NPs with diameters under 300 nm have an improved ability to penetrate the mucus layer resulting in better absorption and increased systemic distribution (He, Yin et al. 2012). Win *et al*, demonstrated that polymeric NPs sized 100-200 nm are appropriate for receptor-mediated endocytosis (Win and Feng 2005).

Both TMC and TMC-CSK NPs had positive surface zeta potentials, + 35.60 ± 0.20 and + 18.50 ± 0.22 mV, respectively. The TMC-CSK NPs had a suitable zeta potential fall in the range of between + 10 and + 30 mV to promote physical stability (Hunter 2013). TMC synthesis involves methylation of the primary amino groups present in chitosan, and methylation has been shown to lower the zeta potential of molecules (Biggs, Cosgrove et al. 2008). CSK conjugation caused a 2.5-fold reduction in zeta potential, which is attributed to the anionic character of CSK (Jin, Song et al. 2012).

Entrapment efficiency is determining the amount of the drugs in relation to the initial amount of the drug used in the formulation of the NPs (Song, Zhao et al. 2008). Both TMC and TMC-CSK NPs show similar entrapment efficiencies of 66 - 67%. The highest EE observed was the 6 : 1 of TMC : TPP ratio with an EE value of 75.4 ± 0.4%. Gemcitabine loading into TMC is attributable to ionic interactions between the positive carboxyl groups of TMC and the available hydroxyl groups on the drug (Pan, Li et al. 2002, Hosseinzadeh, Atyabi et al. 2012). Increased TMC concentration leads to greater interaction during ionic gelation process, increasing the drug entrapment (Vandenberg, Drolet et al. 2001).

Table 4-4. Particle size, zeta potential and entrapment efficiency of the drug loaded TMC and TMC-CSK NPs (mean ± SD, n=3).

	Particle size (d.nm)	PDI	Zeta potential (mV)	Entrapment Efficiency (%)
TMC NPs	382.97 ± 18.20	0.40 ± 0.03	+ 35.60 ± 0.20	73.10 ± 0.20
TMC-CSK NPs	173.60 ± 6.82	0.20 ± 0.02	+ 18.50 ± 0.22	66.43 ± 0.13

4.5.3.2 Surface morphology

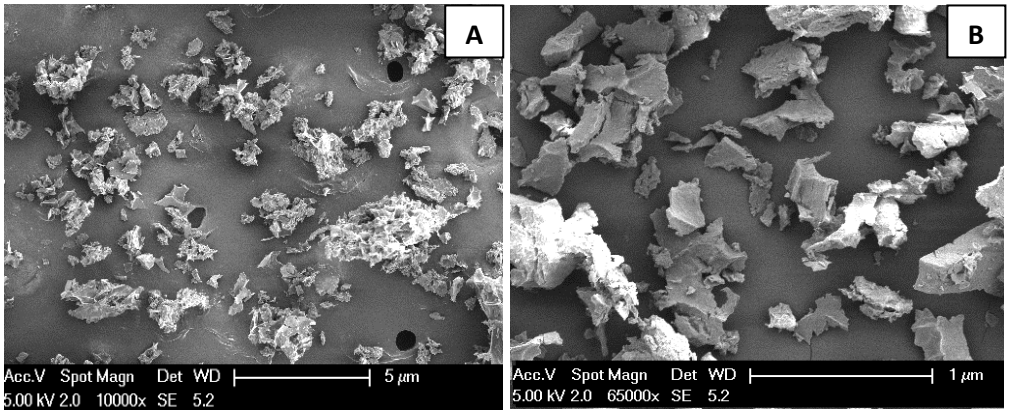

Figure 4-24. Surface morphology of (A) TMC NPs; and (B) TMC-CSK NPs.

On SEM imaging (Figure 4-24), we can see all SEM micrographs showed particles within the nano-meter range. However, a slight increase in particle size observed under SEM may be attributed by the freeze-drying process. Freeze-drying method may lead to certain degree of particle aggregation (Maa and Prestrelski 2000). Additionally, both the TMC and TMC-CSK NPs had rough surfaces and irregular shapes when prepared via ionic gelation. The freeze dried NPs appeared fragmented. This has previous been reported for freeze dried samples as evidenced by the rough surfaces (Choi, Briancon et al. 2004).

4.5.3.3 *In vitro* drug release

The *in-vitro* drug release profiles of gemcitabine loaded TMC NPs, gemcitabine loaded TMC-CSK NPs and plain drug solution (control group) are presented in Figure 4-25. Gemcitabine solution moved quickly through the cellulose membrane with 94.2 ± 2.0% of drug detected in the receptor compartment within the first four hrs and 98.4 ± 1.4% within 24 hrs. The gemcitabine loaded TMC NPs and TMC-CSK NPs demonstrated sustained release over 24 hrs, with 66.1 ± 2.4% released from TMC-CSK NPs compared to 58.4 ± 3.4% released from TMC NPs. This sustain release phase can be attributed to the slow degradation of polymeric particles through the hydrolytic process and the slow diffusion of gemcitabine from the polymer matrix. The release profile of a formulation influences the frequency the formulation has to be administered. The sustain drug release profile of our optimal formulations are beneficial as drug loss in the stomach due to acid degradation is minimised

(Chen, Svirskis et al. 2015), thus ensures most of the entrapped drug will transit to the small intestine where absorption can occur. Any NPs absorbed intact (Wang and Huang 2003) will circulate in the blood for some time promoting drug accumulation at the tumour sites via the EPR effect (Natarajan, Nugraha et al. 2014).

Furthermore, change in particle size affects the drug release characteristics of the particles. Large particles have smaller surface area will have slower drug release rate. In contrast, smaller particles with larger surface area leads to faster release rate (Thanoo, Sunny et al. 1993). In this case, TMC-CSK NPs shows slight smaller in particle size compare to TMC NPs, thus more amount of drug was release from TMC-CSK NPs over 24 hr period compared to TMC NPs.

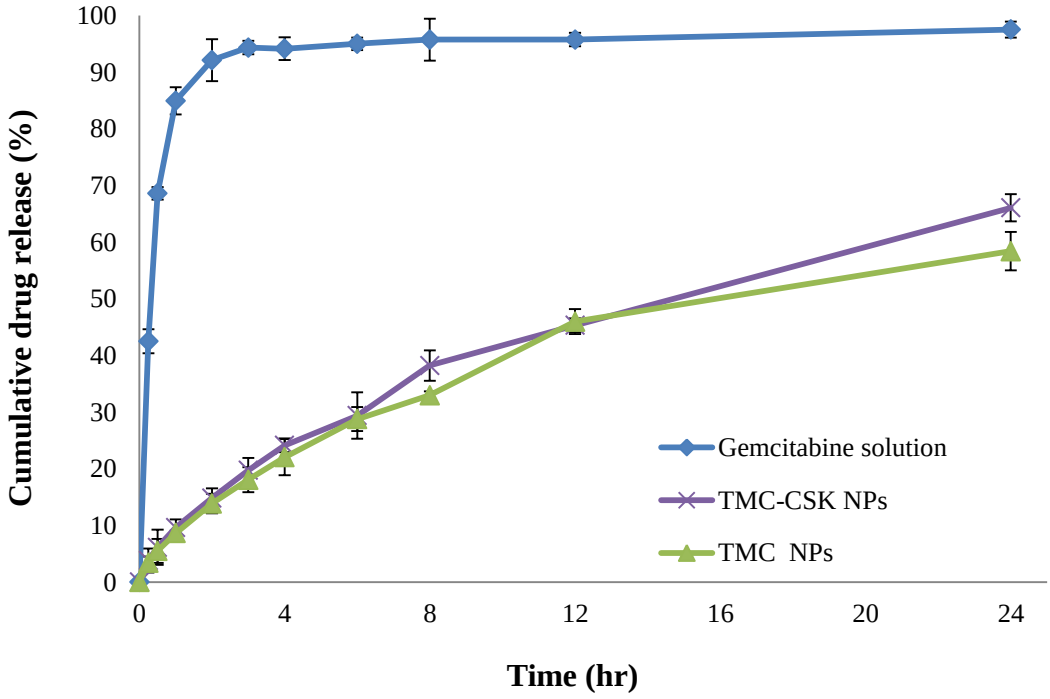

Figure 4-25. *In-vitro* release of gemcitabine solution and gemcitabine loaded TMC and TMC-CSK NPs (mean ± SD, n = 3).

4.5.3.4 *Ex-vivo* permeation studies

The *ex-vivo* permeation studies demonstrated that TMC-CSK NPs had a higher rate of permeation compared to TMC NPs. (Figure 4-26). After 48 hrs 81.2 ± 4.2% of gemcitabine had permeated from the TMC-CSK NPs compared to 52.6 ± 3.2% from TMC NPs through the porcine intestinal epithelial membrane.

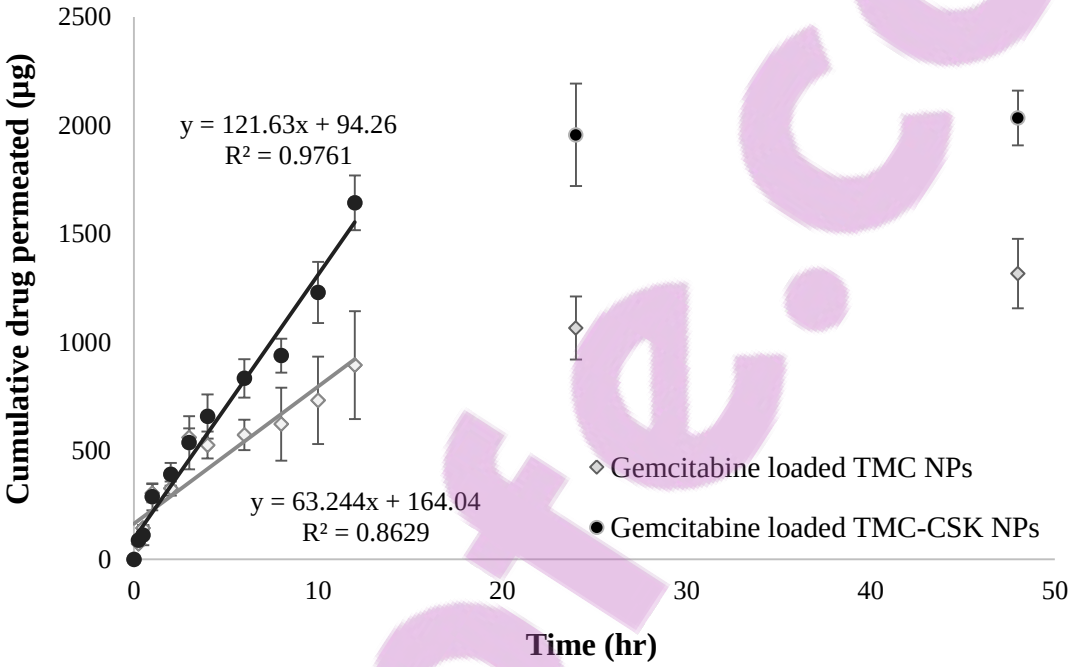

Figure 4-26. *Ex-vivo* permeation studies of gemcitabine formulated into TMC, and TMC-CSK NPs through porcine intestinal epithelial membrane (mean ± SD, n=3).

To allow for comparison the permeability of the two delivery systems, the apparent partition coefficients (P_{app}) were calculated using Equation 3-19. The value of dX_r/dt, the flux that is the gradient of the best fit line, 121.63 and 63.24 were obtained for gemcitabine loaded TMC-CSK NPs and gemcitabine loaded TMC NPs, respectively, using the linear part of the permeation curve between 0 and 12 hrs. The surface area A was 1.77 cm^2 and C_0 was 2500 µg/mL. The P_{app} of drug loaded TMC-CSK NPs and drug loaded TMC NPs were significantly different at $(2.75 \pm 0.36) \times 10^{-2}$ cm/s and $(1.43 \pm 0.12) \times 10^{-2}$ cm/s, respectively, ($p < 0.05$). These results support the hypothesis that TMC-CSK NPs would have a higher P_{app} than TMC due to the ability of CSK to target goblet cells, thus promoting the NPs uptake. Larger P_{app} is expected to correlate with enhanced oral absorption (Grès, Julian et al. 1998).

In this study set up, the mucus layer was present. The drug loaded TMC and TMC-CSK NPs were applied on the apical epithelial membrane, they may adhere to mucin fragments and be trapped in the mucus, or may penetrate through the mucus layer for possible uptake into goblet cells (Jin, Song et al. 2012). TMC has been reported to increase drug permeability due to a combination of increased mucoadhesion, promoting residency time, as well as the ability to open tight junctions (Schipper, Olsson et al. 1997). There are contrasting opinions regarding the effect of mucous on TMC NPs permeation. Behrens *et al* reported increased permeation with increased mucous presence (Behrens, Pena et al. 2002), directly contrasting other observations that the mucous layer hindered TMC NPs permeation (Schipper, Vårum et al. 1999). Bowman and Leong had investigated the inconsistent relationship between permeation and the mucous layer and suggested reasons for both phenomena (Bowman and Leong 2006). The observed increased permeation is attributed to ionic attraction between TMC and mucous. This attraction increases drug concentration in the extracellular environment and produces a gradient which according to Fick's Law, is favourable for drug permeation (Sherwood 2015). Decreased TMC permeation is attributed to the mucous layer preventing TMC NPs from reaching the intestinal cell surface, consequently preventing the NPs from opening tight junctions, thus limiting permeation. TMC-CSK demonstrates superior permeation to TMC, consistent with other literature. CSK binds to goblet cells promoting clathrin and caveolae endocytosis (Kang, Woo et al. 2008).

4.5.3.5 Stability of gemcitabine-loaded optimal formulations

The optimized TMC NPs and TMC-CSK NPs were studied for their stability at different conditions and time intervals. Over the 90-day storage period, the optimal formulations were withdrawn and evaluated for size, and retained drug amount. The results of physical and chemical stability of the two optimal nanoparticulate formulations are shown in Table 4-4 and Table 4-5.

As seen from the particle size analysis data (Table 4-4), the particle size of the NP formulation was stable at 4°C for up to 3 months, for 2 months at 25°C conditions. The results revealed that storage temperature had a noticeable effect on the stability. At higher temperatures, the NPs showed quicker aggregation than at cold temperature. This might be due the thermal energy imparted to vesicles causing both the rate and force of collision between vesicles to increase. The collision and aggregation led to the increased particle size.

These findings suggest that the storage temperature of choice of 4°C for prepared NPs showed minimal changes in particle sizes over 3 months.

Table 4-5. Influence of storage conditions on the particle size of lyophilized optimal NPs (mean ± SD, *n* = 3)

Batch #	**Storage conditions**	**Particle size (d.nm)**			
		0 Month	**1 Month**	**2 Month**	**3 Month**
Drug loaded TMC NPs	4°C	382.9 ± 18.2	388.9 ± 28.2	382.9 ± 8.2	392.9 ± 11.4
	25°C	382.9 ± 18.2	392.9 ± 24.1	402.1 ± 24.2	407.9 ± 22.0
	40°C, 75% RH	382.9 ± 18.2	402.1 ± 17.0	441.5 ± 19.1	452.9 ± 27.8
Drug loaded TMC-CSK NPs	4°C	173.6 ± 6.8	168.6 ± 11.2	183.6 ± 2.9	178.6 ± 12.1
	25°C	173.6 ± 6.8	175.6 ± 16.4	183.0 ± 7.7	198.5 ± 4.5
	40°C, 75% RH	173.6 ± 6.8	201.4 ± 15.4	244.5 ± 26.1	257.2 ± 13.3

Another stability parameter to determine is the drug leakage from the prepared NPs over the 90-day storage period. The percentages of drugs retained in NPs were measured for three months at the three different temperatures; 4, 25 and 40°C. The effects of storage temperatures on drug amount retained in the NPs over the 90-day period are presented in Table 4-6. The table shows the initial drug content of the optimal NPs analysed gradually reducing over time, indicating the temperature has significant effect on the particle stability. Particularly, at 40°C/75% RH, a relatively significant change was observed in the drug content for both TMC NPs and TMC-CSK NPs over 3 months storage. Drug content was reduced to approximate 83% and 74% for TMC NPs and TMC-CSK NPs, respectively in the

BESTPPE.COM
List of research project topics and materials

third month. Reduce of drug content at high temperature and moisture may be caused by the polymer degradation at such conditions (Dunne, Corrigan et al. 2000).

Table 4-6. Influence of storage conditions on the chemical stability of gemcitabine on lyophilized optimal NPs (Mean ± SD, *n* = 3)

Batch #	**Storage conditions**	**Amount of gemcitabine (% of initial amount)**			
		0 Month	**1 Month**	**2 Month**	**3 Month**
Drug loaded TMC NPs	4°C	100	102.1 ± 4.2	97.1 ± 2.2	103.1 ± 2.0
	25°C	100	93.4 ± 6.2	86.1 ± 3.7	87.4 ± 6.6
	40°C, 75% RH	100	85.7 ± 8.5	91.1 ± 2.2	83.1 ± 4.8
Drug loaded TMC-CSK NPs	4°C	100	99.2 ± 5.2	98.1 ± 3.4	91.4 ± 2.6
	25°C	100	87.4 ± 5.3	92.1 ± 5.1	90.3 ± 2.6
	40°C, 75% RH	100	83.7 ± 8.5	78.1 ± 12.2	74.1 ± 11.8

Based on the observation, the drug loaded TMC NPs and TMC-CSK NPs should be stored at 4°C, where they remained stable in terms of both particle size and drug content.

4.6 Conclusion

In this study, a novel gemcitabine loaded TMC-CSK NP formulation was developed successfully via ionic gelation method, and characterization studies were carried out. This foundation work has served to synthesize TMC via a modified two-step method, which leads to a TMC polymer with greater quaternization and product yield. TMC was conjugated with CSK, and prepared the TMC and TMC-CSK NPs via ionic gelation technique. From the characterization of the TMC NPs, they show smaller and more stable than chitosan NPs, a favourable characteristic when considering oral drug delivery. Comparing the particle size of TMC-CSK NPs with TMC NPs alone and basic chitosan NPs, the TMC-CSK NPs were 2.8-fold and 2.2-fold smaller than chitosan NPs and TMC NPs, respectively. The TMC-CSK NPs also show promising characteristic of zeta potential which was within optimal zeta potential range for drug delivery system, as well as a promising drug entrapment efficiency of 66.43 ± 0.13%. In addition, the optimal TMC-CSK NPs show a sustained drug release profile and a significant high *ex-vivo* permeation through porcine intestinal epithelial membrane.

The results of our research suggest that TMC-CSK NPs confer favourable properties for oral gemcitabine delivery, though our studies are strictly preliminary in nature. TMC is most favourably synthesised from chitosan using a two-step process. However CSK conjugation must occur under controlled conditions to ensure optimal yield of TMC-CSK. In conclusion, the present study of this novel TMC-CSK NPs can be used as a preliminary groundwork for future studies with the ultimate aim of creating an oral drug delivery system of gemcitabine that can used in both a clinical and community setting.

Chapter 5

Evaluation of Gemcitabine Uptake and Transport across Co-cultured Model in the Absence or Presence of Optimal Nanoparticles

Chapter 5. Evaluation of gemcitabine uptake and transport across co-cultured model in the absence or presence of optimal NPs

5.1 Introduction

In Chapter 3 and 4, a gemcitabine loaded TMC modified PLGA-TPGS NPs and a gemcitabine loaded TMC-CSK NPs were developed and optimized. They have shown great physicochemical characteristics of nano-size, positive zeta potential, and promising drug entrapment efficiency, a sustain drug release profile, a great *ex-vivo* drug permeation over intestinal epithelial membrane as well as good long term physical and chemical stability. Both optimized formulations are considered as great potential carrier delivery systems for oral delivery of gemcitabine, in order to maximize the oral bioavailability of gemcitabine. However, the behaviour of the safety, cellular uptake and transport as well as their associate mechanisms of the two developed nanoparticulate delivery systems have not been evaluated.

Nanoparticles must be able to travel across the cellular barriers upon oral administration in order for absorption to occur. The efficiency of the two novel nanoparticulate delivery systems depends on their readiness for internalization into, and sustained retention inside the intestinal epithelial cells. Cellular uptake efficiency is an important factor in drug delivery because it is related to the therapeutic efficiency as well as the toxicity effect of drug-loaded NPs (Zaro and Shen 2003). Hence, it is necessary to study how different factors can influence their cellular uptake.

Before cellular uptake, particle must adhere/bind to the lipid bilayer cell membrane. The Brownian motion of particles of less than 1 μm provides the force for random motion and diffusion through a media (Sinko 2006). Once in contact with the cell surface, the absorption of particles can take place. Such process is mediated through passive diffusion or active endocytosis governed by particle-cell surface interactions. Passive diffusion occurs through the aqueous pores between the tight junctions of cell membrane (paracellular) which requires no energy. Transportability of the particles, however, is limited due to the size and small surface of these water-filled pores (Brahma N and Kwon H 2007). Particles "kneading" between the intestinal epithelial cells are due to their extremely small size (< 50 nm).

Endocytosis is an active transport pathway that includes processes such as phagocytosis, pinocytosis (fluid phase) or receptor-mediated endocytosis (Foster, Yazdanian et al. 2001). Particles with a size smaller than 500 nm can be absorbed by intestinal enterocytes through endocytosis. Particles can also be internalized into cells via lymphatic uptake in which particles with size of larger than 500 nm can be absorbed by M cells of the Peyer's patches (Sanders and Ashworth 1961, Warren, Green et al. 1997). M cells are specialized epithelial cells overlaying the lymphoid tissue of the intestinal epithelium. This type of cells has lower proteolytic activity in its transport vehicles. However, the low number of M cells in the intestinal epithelium reduces the possibility of using these cells as general pathway for epithelial drug transport (Artursson, Palm et al. 2001). Most of the polymeric carriers follow the endocytic pathway to be internalized into intestinal epithelial cells and transport across this intestinal epithelial membrane.

In this chapter, the human adenocarcinoma cell line Caco-2 co-cultures with mucus secreting cell HT29-MTX-E12 has been developed as a model to explore the drug uptake and transport mechanism (Mahler, Shuler et al. 2009, Yücel, Değim et al. 2013, Zidan, Spinks et al. 2013). Caco-2 cells, which originates from a human colonic carcinoma (Fogh, Fogh et al. 1977), is the most commonly used as *in vitro* cellular model for the studies of oral drug uptake, transport and toxicity. Caco-2 cells can undergo spontaneous differentiation to polarized, columnar enterocytes under conventional cell culture condition, and thus resemble small intestinal epithelium (Artursson and Magnusson 1990). In addition, Caco-2 cell membranes are considered fully differentiated 25 days after confluence. After full differentiation, Caco-2 cells display well-defined brush border with high density of microvilli on the apical surface and tight junctions (Peterson and Mooseker 1993).

In recent years, several mucus-secreting goblet cell sublines have been established from human intestinal HT29 cells (Huet, Sahuquillo-Merino et al. 1987, Lesuffleur, Barbat et al. 1990). It could also be shown that goblet cells can be grown in cell membranes and be used for cellular uptake and drug transport studies (Wikman, Karlsson et al. 1993). Previous studies on co-cultures of Caco-2 and HT29 cells have shown that both cell types form cell membranes with tight junctions when well grown together in culture (Wikman-Larhed and Artursson 1995, Walter, Janich et al. 1996). Wikman-Larhed and Artursson tested the influence of co-cultured HT29-H cells on the permeability of paracellularly drug compounds and postulated the mucus layer as a potential barrier for drug permeation. The principal use of

co-cultures in drug absorption studies was investigated with various compounds, revealing correlation between permeability and absorption in humans (Wikman-Larhed and Artursson 1995, Walter, Janich et al. 1996).

Furthermore, the co-incubation of Caco-2 and HT29-MTX-E12 cell membrane simulates a complete intestinal epithelium, as it exhibits morphological characteristics similar to the intestinal enterocytes, they have effective tight junctions and contain a number of active transporters and metabolic enzymes. Several active transport systems which are located in the intestinal epithelium, such as peptide, amino acid, bile salt, sugars, and nucleoside transporters, as well as P-glycoprotein (P-gp) and Multi-drug resistance protein (MRPs) (Hu 1993, Saito and Inui 1993, Delie and Rubas 1997). The existence of P-gp and MRPs allows researchers to examine the active efflux of drug across cell membrane (Gan and Thakker 1997). In summary, a co-incubation of Caco-2 and HT29-MTX-E12 cell membrane represents a useful tool to assess cellular uptake and carrier-mediated drug transport (Delie and Rubas 1997, Sambuy, De Angelis et al. 2005).

Our objectives in this chapter, therefore, were to investigate the interactions between the optimal nanoparticulate delivery systems and biological membranes using a Caco-2 cell co-cultured with HT29-MTX-E12 cell membrane model as a platform. Firstly, preliminary evaluation of cytotoxicity using MTT assay was carried out to illuminate the safety of the NPs as an effective oral delivery system. Then, cellular uptake studies were performed as an approach to investigate the active absorption of gemcitabine and its delivery systems as well as the associated cellular uptake mechanisms. Finally, by using various absorption inhibitors and penetration enhancers to explore the transport mechanisms in the absence or presence of optimal NPs under various conditions.

5.2 Materials

Dulbecco's Modified Eagle Medium (DMEM) with high glucose, Hank's Balanced Salt Solution (HBSS), Phosphate-Buffered Saline (PBS), Non-Essential Amino Acid Solution (NEAA), heat inactivated Fetal Bovine Serum (FBS), penicillin-streptomycin, trypsin-EDTA, Molecular Probe® CellTracker™ Red CMTPX, 4'6-diamindino-2-phenylindole (DAPI) were purchased from Invitrogen (Auckland, New Zealand). Gemcitabine hydrocholoride, Fluorescein isothiocyanate (FITC), *N*-(3-Dimethlaminopropyl)-*N*'-ethylcarbodiimide hydrochloride (EDC), pyridine, *N*-hydroxy succinimide (NHS), 3-(4, 5-dimethyl-thiazol-2-yl)-2, 5-diphenyl tetrazolium bromide (MTT), fluorescein sodium salt, sodium azide, verapamil, MK-571 sodium salt hydrate and EDTA were purchased from Sigma Aldrich (St. Louis, MO, USA). Mill Q water was used throughout the studies and all other reagents were of analytical grade.

5.3 Methods

5.3.1 Analysis of gemcitabine

Gemcitabine concentration in μg range was determined by a previously reported RP-HPLC method in Chapter 2. Briefly, compounds were separated on a C18 HPLC column of GraceSmart RP C_{18} column (250 × 4.6 mm, 5.0 μm particle size) fitted with a security C18 cartridge (10 × 3.0 mm). Mobile phase A consisted of ACN and 1.38% w/v sodium dihydrogen phosphate buffer (pH 6.5) at the volume ratio of 7:93. The mobile phase was filtered through a 0.22 μm nylon membrane and degassed prior to use. A constant flow rate of 1 mL/min was used. The injection volume of the analysed samples was 20 μL and the column temperature was maintained at 30 °C. Absorbance was measured at the wavelength 270 nm. The elution time of gemcitabine is at 4.7 min.

5.3.2 Preparation of optimal drug loaded NPs

The method to prepared drug loaded TMC modified PLGA-TPGS NPs were mentioned previously in chapter 3. Both delivery systems were prepared with their optimal conditions as previously investigated. Briefly, 0.6 ml aqueous solution of gemcitabine 25 mg/ml was emulsified in 4 ml of DCM, containing 1% w/v PLGA-TPGS, by means of sonication using a microtip probe sonicator (UP 200S, Hiescher, Germany) at an output of 20 W for 90 sec to form a primary W_1/O emulsion. The primary emulsion was further emulsified in 16 ml of 0.6%, w/v TPGS solution, followed by sonication for 150 sec at 20 W to obtain a double $W_1/O/W_2$ emulsion. The resultant double emulsion was then stirred at a rate of 600 rpm for 5 hrs to evaporate organic solvent. To ensure the complete evaporation of organic solvent, a rotary evaporator (Buchi Rotavapor R-215, Switzerland) was used to further evaporate DCM by reduced pressure until the bubble formation ceased. The resulting NPs suspension was kept at 4ºC overnight to allow hardening of the PLGA-TPGS membrane. NPs were recovered by ultracentrifugation (Sorvall WX Ultra80 Centrifuge, Thermo scientific, USA) at 173210 g for 1 hr at 4ºC. The free gemcitabine in the supernatant was analyzed by RP-HPLC method to calculate the EE using Equation 3-11 as mentioned in Chapter 3. The EE of gemcitabine was 76.43 ± 0.21%. After ultracentrifugation, the NPs sediments were washed twice with sucrose solution to remove free drug and excess surfactant, and further suspended in 16 mL of 0.5% w/v TMC solution, with gentle stirring to allow TMC fully adsorb on the surface of PLGA-

TPGS NPs, the resultant suspension were ultracentrifuged at 173210 g for 1 hr at 4ºC, the sediments TMC modified PLGA-TPGS NPs were then lyophilized (Labconco, USA) for 2 days prior to use.

To prepare the optimal drug loaded TMC NPs. Briefly, following synthesis of TMC, the optimal TMC NPs were prepared using an ionic gelation method. TMC (0.5% w/v) was dissolved in a 1% w/v gemcitabine solution. Tween 80 (0.07 mL) was added and thoroughly mixed with 2 mL of 0.4% w/v TPP solution, and the mixture was added drop-wise to the TMC-drug solution, stirred for 1 hr at room temperature to allow NPs forming. Here the optimal weight ratio of TMC : TPP is 3 : 1. The resultant suspension was ultracentrifuged at 173210 g for 30 min at 4°C. Free gemcitabine in supernatant was correlated to the EE. The EE was calculated using the same method as mentioned previously showing a 73.10 ± 0.20% EE for the optimal TMC-CSK NPs. Finally, the NPs were collected, lyophilized. To prepared drug loaded TMC-CSK NPs, following conjugation of TMC and CSK, the TMC-CSK polymer was used to prepare the NPs via same ionic gelation method as TMC NPs preparation, only substituting TMC polymer by TMC-CSK polymer in this case, and the EE was determined as 66.43 ± 0.13% for TMC-CSK NPs. The dried samples were stored in a dry container at 4ºC before analysis. The storage conditions were subjected to the long term stability study conducted previously.

5.3.3 Preparation of FITC-conjugated NPs

FITC-labelled PLGA-TPGS was prepared by covalently conjugating FITC to the EDC-activated carboxylic terminal groups of PLGA polymers using modified carbodiimide method (Weissenboeck, Bogner et al. 2004, Kim, Jeong et al. 2005, Harfouche, Basu et al. 2009). EDC is a catbodimide commonly used to mediate the formation of amide linkages between a carboxylate and an amine. EDC can react with a carboxylic group of PLGA polymer to form a highly reactive *O*-acylisourea intermediate. These active intermediates are able to couple with amine-containing molecules such as NHS to form a stable amide bond (Hermanson 2008). The amide bond can further react with FITC to form a FITC conjugated PLGA-TPGS copolymer.

Briefly, 1000 mg of PLGA-TPGS (100 µl) was dissolved in 5 ml DCM and activated using 80 mg NHS and 100 mg EDC. The reaction mixture was incubated with constant end-over-

end rotation by Revolver^{TM} rotator (Labnet international, Inc. Woodbridge, NJ, USA) for 2 h at room temperature. Next, 38.9 mg of FITC (100 µl) was dissolved in a mixture of DCM (500 µl) and pyridine (500 µl). FITC solution was then added to the activated PLGA-TPGS solution at a molar ratio of 1:1 and the reaction mixture was incubated in the dark over night at 4°C. The unreacted FITC was removed by repeated washings with 5 mM HCl until the aqueous layer remained clear followed by precipitation with methanol for 2 h at 4°C. The polymer was centrifuged at 3,220 g for 30 min. The supernatant was discarded and the polymer was washed thoroughly by Milli-Q water and lyophilized. The FITC labelled NPs were prepared by blending pure PLGA-TPGS and FITC-labelled PLGA-TPGS at a 50/50 weight ratio and fabricated as per the protocol described at section. The lyophilized FITC-PLGA-TPGS NPs were stored in the dark at 4°C.

To determine the FITC content in the FITC labelled PLGA-TPGS NPs by using a fluorescein spectrophotometer (Perkin Elmer Precisely, USA, λ_{ex} 495, λ_{em} 525 nm), after dissolving the particles in 0.5% Triton X-100/1 M NaOH solution. A calibration curve was constructed by dissolving a series of different concentrations of FTIC-PLGA NPs in the same solvent.

5.3.4 Stability of gemcitabine loaded NPs in DMEM and HBSS

To investigate the stability of drug loaded TMC modified PLGA-TPGS NPs and the drug loaded TMC-CSK NPs in the incubation media of HBSS and DMEM medium, 2 mg lyophilized NPs were suspended in 2 ml HBSS and DMEM separately, and incubated at 4 or 37°C for up to 8 h. After centrifugation, the supernatant was removed and the TMC modified PLGA-TPGS NPs were dissolved in 1 ml of DCM with 2% acetic acid and 3 ml of Milli-Q water, while the TMC-CSK NPs were dissolved in 4 ml 0.2% acetic acid. Gemcitabine was extracted by vortexing for 15 min and ultrasonicated for 15 minutes. The aqueous phase containing gemcitabine was separated by centrifugation and gemcitabine concentration was determined using HPLC.

BESTPFE.COM
List of research project topics and materials

5.4 Cytotoxicity, drug uptake and transport studies

5.4.1 Cell culture

The Caco-2 cell line was obtained from the American Type Culture Collection (Manassas, USA). Cells were routinely maintained in complete DMEM medium in T-75 tissue culture flasks (Corning, New York, USA) at 37 °C in an atmosphere of 5% CO_2 and 95% relative humidity. Complete DMEM medium was prepared by adding 10% fetal calf serum, 1% penicillin-streptomycin-glutamine, and 1% nonessential amino acids to sterile DMEM and its pH adjusted to 7.4. Culture medium was changed every 3 days until cells grew to 90% confluence. Viable cells were determined by trypan blue exclusion method based on the fact that trypan blue dye can diffuse through the cell wall of dead cells only. For subculturing, the cells were dissociated with 0.25% trypsin-EDTA, split in a ratio of 1:3.

The HT29-MTX-E12 cell line was purchased from Sigma Aldrich (St. Louis, MO, USA). They are cultured using the same medium as Caco-2 cells (DMEM medium supplemented with 10% heat inactivated FBS, 1% NEAA, penicillin-streptomycin (100 U/ml and 100 µg/ml, respectively) and 2 mM L-glutamine), and cultured in the same environment of humidified atmosphere (5% CO_2, 95% relative humidity) at 37°C and exchange for fresh medium every 3-4 days.

When both Caco-2 cells and HT29-MTX-E12 cells grew to 90% confluence in T-75 culture flasks, Caco-2 and HT29-MTX-E12 with ratio of 3 : 1 were added into a new T75 flask for further co-culturing of both cells. The co-cultured cells generally reach their 90% confluence in approximate 3 weeks. For subculturing the cells were dissociated with 0.25% trypsin-EDTA, split in a ratio of 1:3.

5.4.2 Cytotoxicity studies

Prior to carry out the drug uptake and transport studies, the concentrations of the drug candidate must be within the safety dosage range for the cells. Therefore, a cytotoxicity of the drug and drug loaded formulations on the cells should be investigated. The cytotoxicity of gemcitabine and gemcitabine loaded TMC modified PLGA-TPGS NPs and gemcitabine loaded TMC-CSK NPs toward the Caco-2 and HT29-MTX-E12 co-cultured cells were

examined by a 3-(4, 5-dimethyl-thiazol-2-yl)-2, 5-diphenyl tetrazolium bromide (MTT) assay for the assessment of cells viability (Marks, Belov et al. 1992). Briefly, 1×10^4 cells/cm^2 per well were subcultured into 96-well plates (Corning, New York, USA). Subsequently, the cell membrane of cells was formed after 24 hr incubated at 37 °C, the medium was replaced with serum-free medium containing various concentrations (by serial dilution) of drug, drug loaded TMC modified PLGA-TPGS NPs and drug loaded TMC-CSK NPs, respectively, while cells treated with serum-free medium were used as control. After the 8 hr incubation, 20 μL of MTT (5 mg/mL in the serum-free medium) was added to each well and then the cells were incubated for another 4 hr at 37 °C. The supernatants were decanted and the formazan precipitates were solubilized by the addition of 200 μL of dimethyl sulphoxide (DMSO) and placed on a shaking plate for 15 min. Thus, the MTT assay assessed cell viability by measuring the enzymatic reduction of yellow tetrazolium MTT to a purple formazan at 540 nm using a SepctraMax Plus 384 (Molecular Devices, Sunnyvale, USA) (Hong, Yamauchi et al. 2011). Percentage of cell activity was calculated as: Cell activity = $(Ab_{exp} - Ab_{neg}) / (Ab_{con} - Ab_{neg}) \times 100$ %, where Ab_{exp} is the value of experiment group absorbance at 540 nm; Ab_{neg} is the value of blank group absorbance at 690 nm; Ab_{con} is the value of control group absorbance at 540 nm. The cell vability of the sample was expressed as the IC_{50}, which is defined as the concentration in mg of material per mL that inhibits the cell viability by 50%. Concentrations within the safety range were applied in the following drug uptake and transport studies.

5.4.3 Uptake of PLGA NPs by Caco-2/HT29-MTX-E12 cells

5.4.3.1 Quantitative analysis of the uptake of gemcitabine and gemcitabine loaded NPs

For the uptake studies, 5 mL of Caco-2/HT29-MTX-E12 cells suspension at a density of 1×10^5 cells/cm^2 were seeded onto 60 mm petri dishes (Corning, New York, USA), fed complete DMEM every 3 days and incubated at 37 °C in an atmosphere of 5% CO_2 and 95% relative humidity to allow cells attachment and proliferation. On reaching 90% confluence, the culture medium was replaced with 2 mL of HBSS. After 30 min of incubation at 37 °C, the medium was replaced with 1 mL suspensions of gemcitabine solution at 100, 300 and 500 μg/mL, gemcitabine loaded TMC modified PLGA-TPGS NPs at 100, 300 and 500 μg/mL of gemcitabine in HBSS and gemcitabine loaded TMC-CSK NPs at 100, 300 and 500 μg/mL of gemcitabine in HBSS and incubated for 2 hr at 4 °C and 37 °C, respectively, to study the

effect of incubated temperature and drug concentrations on particle uptake. For time-dependent uptake experiments, the medium was replaced with 1 mL 500 μg/mL suspensions of free drug and drug loaded NPs in HBSS per well and the plate was incubated for 0.5, 1, 1.5, 2, 3, and 4 hr at 37 °C, respectively.

Then the cells were washed with cold sterile PBS (pH 7.4) for eight times and the Caco-2/HT29-MTX-E12 cells were then scraped off using cell scraper (BD Biosciences, CA, USA) and transferred to a microcentrifuge tube containing 1.0 ml lysis medium (ACN/MeOH (3:1, v/v) mixed with 2% acetic acid, followed by ultrasonication at 20 W for 15 min. Finally, 25 μL of the cell lysates from each well were subjected to BCA protein assay (Thermo Scientific, Waltham, USA) for determining the amount of protein in the cells. The exposed NPs in the remainder of the cell lysates were subjected for quantitative measurement. Cell-associated NPs were quantified by analysing the cell lysate using fluorescein spectrophotometer (Perkin Elmer Precisely, USA, λ_{ex} 495, λ_{em} 525 nm). The Amount of cell-associated NPs was calculated from the calibration curve. The extent of uptake was expressed as the amount of NPs (μg) uptaken per mg cell protein (μg/mg protein).

5.4.3.2 Confocal microscopy analysis

Confocal Laser Scanning Microscope (CLSM) was used to examine whether NPs were indeed taken up and localized intracellularlly or were simply adsorbed onto the cell surface. Caco-2/HT29-MTX-E12 cells were transferred into 2-well chamber slides (BD Falcon, USA) at a density of 2×10^5 cells/well (5×10^4 cells/cm^2) and grown in complete DMEM culture medium. Two ml of gemcitabine-loaded FITC-PLGA NPs suspension at the specified concentrations were incubated with cells for 2 h at 37°C or 4°C. After 2 hrs, the transfer buffer and excess NPs were removed and cells were washed with ice-cold HBSS. Cells were incubated with serum-free DMEM for 15 min. After equilibrium, incubation medium was replaced with pre-warmed CellTracker dye (Invitrogen, New Zealand) with concentration of 5 μM in serum-free DMEM and cells were incubated for 30 min at 37°C. After cytoplasm staining with CellTracker, the Caco-2/HT29-MTX-E12 cells were then washed with PBS followed by fixation with a freshly prepared 3% w/v paraformaldehyde solution for 30 min at room temperature. The slides were then rinsed twice with PBS followed by nuclei staining with DAPI (100 nM in PBS) (Invitrogen, New Zealand) at room temperature for 3 min. After removing the culture chambers, slides were thoroughly washed with PBS and mounted with

CITI-Fluor (a medium used to decrease photobleaching during observation under CLSM). Coverslips were placed on top of the slides and sealed with nail polish. The slides were stored at 4°C and protected from light.

Slices were visualized by CLSM (Olympus FV1000; Olympus, Heidelberg, Germany). Samples were excited with 488 nm (green), 543 nm (red) and 405 nm (blue) laser lines. Images were captured with a 60 × 1.35 oil immersion lens. A step motor was used to image 3D sections of the cells and images were processed using FluView 2.0b software (Olympus, Heidelberg, Germany). The intercellular localization of FITC-NPs can be confirmed by the visualization of the cells at different planar sections.

5.4.3.3 Investigation of cellular uptake mechanisms

With the purpose of identifying the possible internalization mechanism of optimal NPs by Caco-2/HT29-MTX-E12 cells, the cells were incubated in different conditions or treated with specific agents. (I) To study the effect of temperature on cellular uptake, cells were incubated with test samples at 4 °C and 37 °C for 2 h. (II) To test the effect of sodium azide, an active transport inhibitor, 100 mM sodium azide was dissolved in the NPs suspension and incubated with cells for 2 h at 37 °C. (III) To study the effect of protamine treatment, an adsorptive-mediated endocytosis inhibitor, 1 mM protamine sulfate was dissolved in the NPs suspension and incubated with cells for 2 hr at 37 °C. (IV) To examine the effects of chlorpromazine and filipin, which were the clathrin and caveolae endocytosis inhibitors, cells were incubated with 10 μg/ml chlorpromazine or 1 μg/ml filipin dissolved in NPs suspension and treated for 2 hr at 37 °C. In addition, the drug loaded NPs (control) were conducted at 37 °C for 2 hr without any treatment, and the results of the inhibition tests were presented as the percentage of that internalized in control (Mislick and Baldeschwieler 1996, Rejman, Bragonzi et al. 2005, Jin, Song et al. 2012).

5.4.4 Drug transport studies over the co-cultured cell membrane

5.4.4.1 Quantitative analysis of the transport of gemcitabine and gemcitabine loaded NPs

Caco-2/HT29-MTX-E12 cells at a density of 1×10^5 cells/cm^2 were seeded on Transwell® inserts (0.4 μm pore diameter, 1.13 cm^2 area, Corning, New York, USA) (Figure 5-1). Cells were incubated at 37 °C in an atmosphere of 5% CO_2 and 95% relative humidity in complete DMEM. The medium was replaced every 3 days with 0.5 mL medium in the apical side and 1.5 mL in the basolateral side. The integrity of the cell membrane was checked by monitoring transepithelial electrical resistance (TEER) (Liang, Zhao et al. 2012).

TEER was measured using a Millicell-ERS Volt-Ohm meter connected to a pair of chopstick electrodes (Millipore Corp, USA). The electrodes were sterilized by 70% ethanol for 15 min and air-dried for 15 sec followed by immersing in a way that shorter electrode was in the apical side and longer electrode in the basolateral side. Care was taken that the electrodes did not touch the cells membrane. The TEER measurements were performed at 3 days intervals until the TEER values exceeded 350 Ω·cm^2 (after approximate 24 days post seeding in this study). TEER = $(R_{cells} - R_{blank}) \times A$, where R_{cells}, R_{blank} and A, are measured TEER value, TEER value of the blank transwell and the membrane surface area of transwell (1.13 cm^2), respectively. Caco-2/HT29-MTX-E12 cell membranes with TEER values above 350 Ω·cm^2 were considered as indicative of a confluent Caco-2/HT29-MTX-E12 cell membrane for the transport study.

Prior to the transport experiments, Caco-2/HT29-MTX-E12 cell membranes were equilibrated with HBSS for 30 min and removed by aspiration. All transport studies were conducted at 37°C. One mL suspensions of gemcitabine, and gemcitabine loaded NPs (500 μg/mL in HBSS) were added on the apical side while the basolateral side of the inserts containing 1.5 mL of HBSS. After 0.5, 1, 1.5, 2, 3 hr of incubation, 200 μL was withdrawn from the basolateral receiving chamber and was immediately replenished with an equal volume of prewarmed HBSS (37 °C). The concentration of gemcitabine in the transport medium was analysed by HPLC, thus the cumulative amount of gemcitabine transported across the cell membrane was determined.

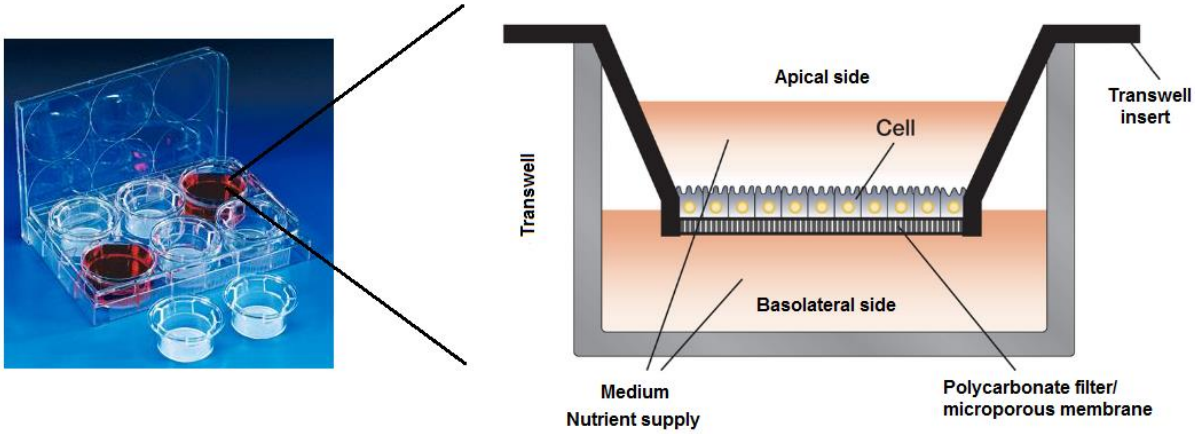

Figure 5-1. A schematic diagram of Transwell compartments and the Transwell insert.

5.4.4.2 *Investigation of drug transport mechanisms*

To further investigate the transport mechanisms of the drug loaded NPs across the epithelial cells and the influence of mucus on the targeting recognition, the co-cultured cell membrane was incubated for 21 days after being seeded on the Transwell® inserts, mimicking the intestinal epithelium with both epithelial cells and mucus layer. Subsequently, intestinal mucosa negative surface inhibitor, and two different efflux pump inhibitors as well as an absorption enhancer were added and carry on the transport studies to investigate the effects of these efflux inhibitors and absorption enhancers on the drug transport process.

Cell membrane is negatively charged due to the presence of heparin sulfate proteoglycans and glycosaminoglycan. Heparinase is an inhibitor of glycosaminoglycan sulfatation and could hydrolyse proteoglycans (Ho, Broze et al. 1997), therefore with presence of heparinase, it can neutralize the negative charge of the cell surface, and eliminate the electrostatic interaction between the positive charge particles and negative charge cell surface.

Two major cell efflux pumps, P-gp and multidrug resistance-associated protein 2 (MRP2), which can transport most of the APIs from intracellular matrix back to extracellular lumen (Hu, Qiu et al. 2006, Matsson, Pedersen et al. 2009). Verapamil and MK-571, are the two common used inhibitors that could block these two major efflux pumps P-gp and MRP2, respectively (Walgren, Lin et al. 2000, Summers, Moore et al. 2004). Therefore, with addition of the verapamil and MK-571, if any changes in the drug transport compare to

control group, which indicates these efflux pumps are affecting the transport process of these drug loaded NPs (Wang, Zhang et al. 2011).

An absorption enhancer, EDTA is able to activate the cellular protein kinase C (PKC) by depletion of extracellular calcium via chelation, resulting in tight junction opening. The open of tight junction will cause expansion of paracellular route, thus leads to facilitate the transport of the components through paracellular pathway (Tomita, Hayashi et al. 1996). Therefore in many studies, EDTA has been applied in the drug delivery system in order to enhance the drug uptake over the GIT (Uchiyama, Sugiyama et al. 1999, Thanou, Verhoef et al. 2001, Hussain, Arnold et al. 2004).

In this study, mucosal surface negative charge inhibitor (50 μM Heparinase), permeability glycoprotein (P-gp) inhibitor (100 μM verapamil), multidrug resistance-associated protein 2 (MRP2) inhibitor (100 μM MK-571), and absorption enhancer (10 mM EDTA) were added to the apical side with 1 mL 500 μg/mL suspensions of gemcitabine loaded NPs. All inhibitors were dissolved in DMSO and diluted with HBSS. The transport characteristics of gemcitabine loaded NPs through Caco-2/HT29-MTX-E12 cell membranes were expressed as percentage of relative cellular transport. The group without any addition of inhibitors or enhancer was set as a control group. In addition, the TEER values of the cell membranes were measured at 1 hr interval during experimental period, ensuring the integrity of the cell membranes.

5.4.5 Statistical analysis

Results are presented as mean ± SD of at least three replicates. Both student's *t* test and one-way ANOVA followed by Turkey-test were used to evaluate significance of differences between the groups (SigmaStat 3.5, Systat Software, USA), with the level of significance set at $p < 0.05$, as appropriate.

5.5 Results and discussion

5.5.1 Stability of NPs in HBSS incubation medium

The results of recoveries of gemcitabine from TMC modified PLGA-TPGS NPs and TMC-CSK NPs after incubation with HBSS and DMEM at 4 or 37°C for 8 h are presented in Table 5-1. The recoveries results show the NPs recoveries are in the acceptable range in the HBSS and DMEM, and the gemcitabine is very stable in both HBSS and DMEM medium. However, the loss of gemcitabine from the fabricated NPs was mainly due to the detachment of gemcitabine from the surface of the NPs.

Table 5-1. Stability of drug NPs after 8 hr incubation with HBSS (mean ± SD, n = 3).

	Recoveries in HBSS (%)		Recoveries in DMEM (%)	
	4°C	37°C	4°C	37°C
Drug loaded TMC modified PLGA-TPGS NPs	92.2 ± 8.4	89.7 ± 2.8	101.6 ± 6.8	95.2 ± 5.9
Drug loaded TMC-CSK NPs	88.9 ± 13.1	92.8 ± 4.5	92.6 ± 11.4	93.3 ± 7.2

5.5.2 *In vitro* cytotoxicity

Caco-2/HT29-MTX-E12 cells were exposed to gemcitabine (12.5-300 μg/mL) and equivalent drug amount of gemcitabine loaded TMC modified PLGA-TPGS NPs as well as gemcitabine loaded TMC-CSK NPs for 8 hrs. As showed in Figure 5-2, the cells retained more than 67% viability 91% viability and 86% viability when treated with gemcitabine solution, gemcitabine loaded TMC modified PLGA-TPGS NPs, and gemcitabine loaded TMC-CSK NPs, respectively. Indicating the NPs have greater protection of the entrapped gemcitabine from exposing to the intestinal epithelium, thus lower the toxicity toward the intestinal epithelium. Among the two optimal nanoparticulate delivery system, TMC modified PLGA-TPGS shows greater protection of entrapped gemcitabine from exposing to the intestinal epithelial Caco-2/HT29-MTX-E12 cells compared to TMC-CSK NPs. With the concentration of 25 μg/ml of gemcitabine and larger, all the formulations groups showed significant

Bestpfe.com

different from the control groups in percentage of cell viability ($p < 0.05$). In addition, The TMC, TMC-CSK, PLGA-TPGS polymers showed no significant cytotoxicity after 8 hrs of incubation indicating the biocompatibility of these polymers with Caco-2/HT29-MTX-E12 cells.

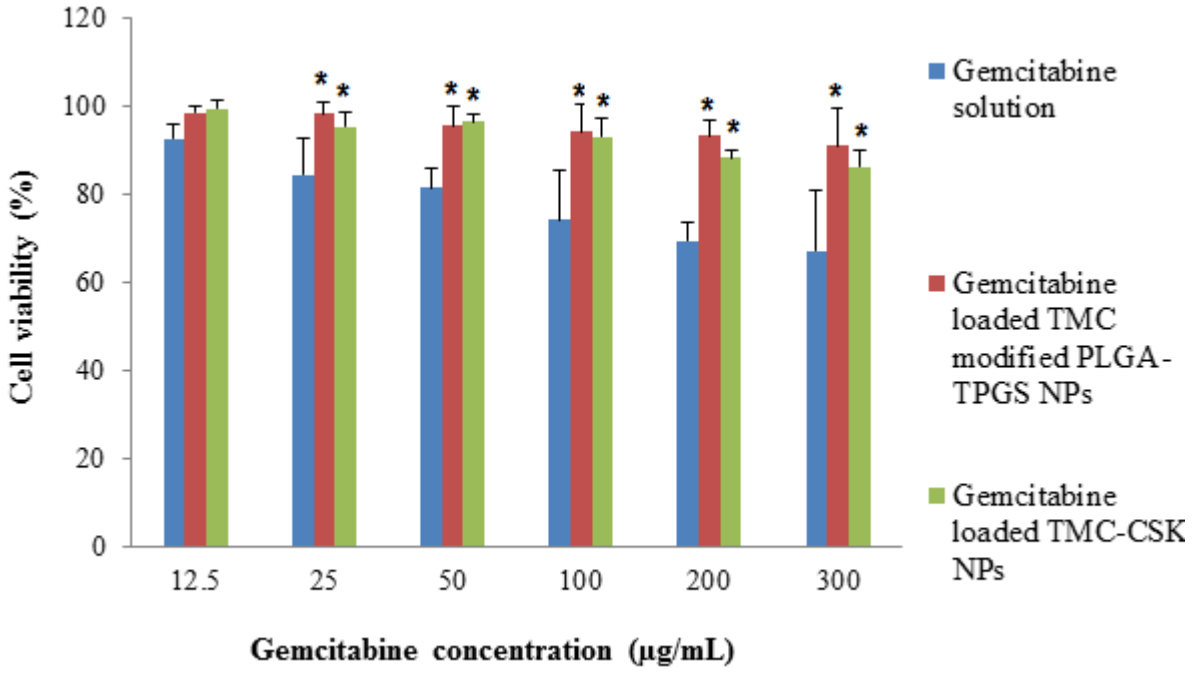

Figure 5-2. Cytotoxicity assay of gemcitabine and gemcitabine loaded TMC modified PLGA-TPGS NPs as well as gemcitabine loaded TMC-CSK NPs (12.5-300 µg/mL) on Caco-2/HT29-MTX-E12 cells for 8 hrs (mean ± SD, n = 3, *$p < 0.05$ significant different compared with control gemcitabine)

The gemcitabine solution, gemcitabine loaded TMC modified PLGA-TPGS NPs and gemcitabine loaded TMC-CSK NPs all demonstrated some dose dependent cytotoxicity over 8 hrs in the MTT study. The IC_{50} values were subsequently calculated. The IC_{50} of gemcitabine solution, gemcitabine loaded TMC modified PLGA-TPGS NPs, and gemcitabine loaded TMC-CSK NPs were of 529.4 ± 67.2 $\mu g.mL^{-1}$, 1881.4 ± 51.5 $\mu g.mL^{-1}$ and 1682.4 ± 27.9 $\mu g.mL^{-1}$, respectively. Both drug loaded NP formulations had higher IC_{50s} than gemcitabine solution which can be attributed to the drug being encapsulated in the NPs, and less exposure to the intestinal epithelium, thus higher the IC_{50s} were obtained.

5.5.3 *In vitro* cellular uptake of gemcitabine and gemcitabine loaded NPs

The cellular uptake was investigated quantitatively by HPLC and BCA assay. The *in vitro* uptake results (Figure 5-3, Figure 5-4 and Figure 5-5) showed that the uptake of either gemcitabine or gemcitabine loaded TMC modified PLGA-TPGS NPs, and gemcitabine loaded TMC-CSK NPs on Caco-2/HT29-MTX-E12 cells were time -, temperature - and concentration - dependent.

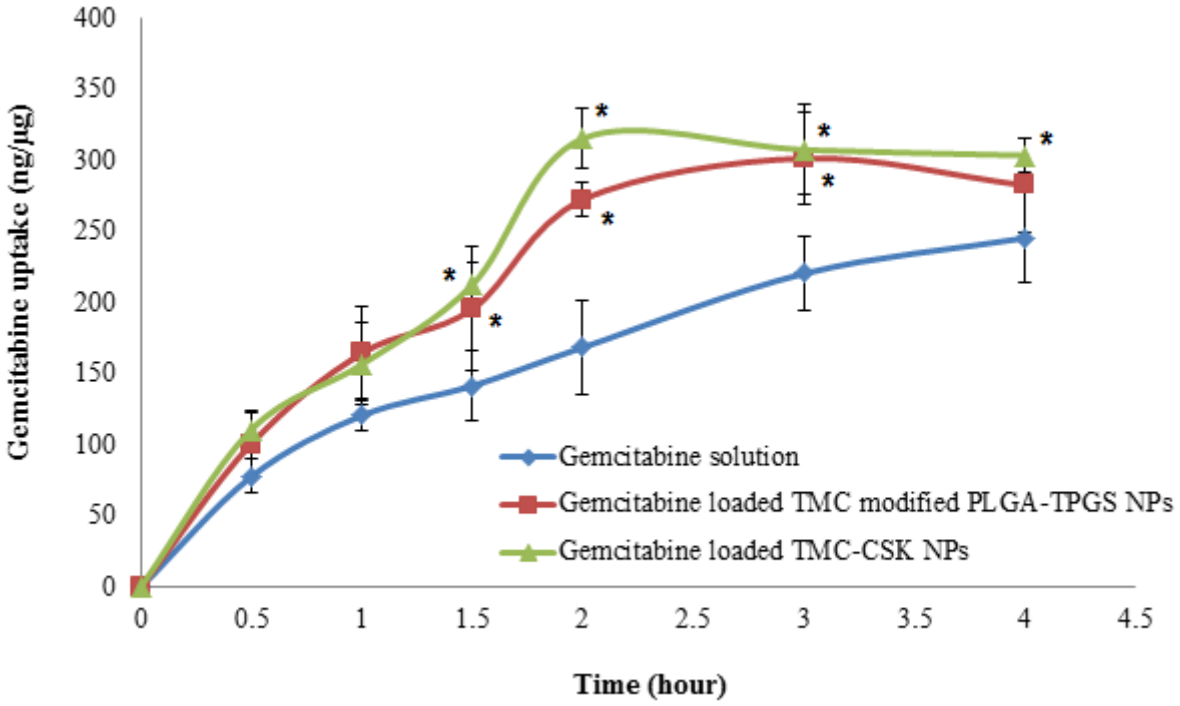

Figure 5-3. Time - dependent uptake of 500 µg/mL of gemcitabine solution, gemcitabine loaded TMC modified PLGA-TPGS NPs, and gemcitabine loaded TMC-CSK NPs after 0, 0.5, 1, 1.5, 2, 3 and 4 hr at 37 °C (mean ± SD, n = 3, *p < 0.05 significant different compared with control gemcitabine).

From Figure 5-3, the uptake of 500 µg/mL of gemcitabine and gemcitabine loaded NPs at 37°C increased with increasing the incubation time. The uptake amount of encapsulated gemcitabine were 246.6 ± 32.2 ng/µg for gemcitabine solution, 283.7 ± 33.0 ng/µg for gemcitabine loaded TMC modified PLGA-TPGS NPs, and 304.1 ± 12.7 ng/µg for gemcitabine loaded TMC-CSK NPs. From the results, we can see the drug loaded TMC-CSK

BESTPFE.COM
List of research project topics and materials

NPs had a greatest drug uptake compared to drug solution and TMC modified PLGA-TPGS NPs during 4 hr incubation (*p < 0.05 compare to gemcitabine solution group). This might be due to the CSK goblet cells-targeting capability, thus greatly enhance the drug uptake.

Figure 5-3 also shows that the uptake of the TMC modified PLGA-TPGS NPs and TMC-CSK NPs first increased and reached a plateau after about 2 hr exposure to cells and then decreased when the exposure time increased. Results indicated that the uptake of both nanoparticulate delivery systems was in a time-dependent manner and there was a saturation limit in exposure time. Fewer NPs were internalized into the cells after approximate 2 hr incubation suggesting that they could be lost via exocytosis by P-glycoprotein (P-gp) which transports NPs from the serosal to mucosal direction (Cartiera, Johnson et al. 2009). Thus, the optimal exposure time of 2 hr was selected for all other uptake studies.

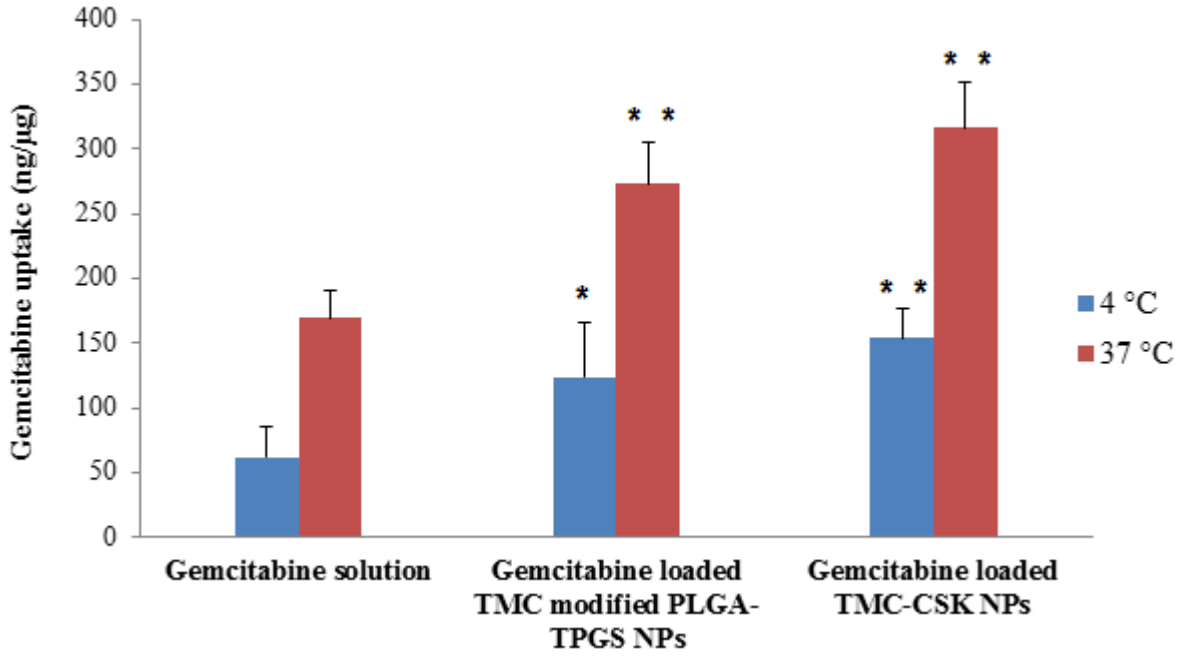

Figure 5-4. Temperature - dependent uptake of 500 µg/mL of gemcitabine solution, gemcitabine loaded TMC modified PLGA-TPGS NPs, and gemcitabine loaded TMC-CSK NPs after 2 hr at 4 °C and 37 °C (mean ± SD, n = 3; Significant difference from control, *p < 0.05, **p < 0.01).

From Figure 5-4, different temperature of 4 °C and 37 °C were applied for the drug uptake studies. The uptake amounts from gemcitabine solution, gemcitabine loaded TMC modified PLGA-TPGS NPs, and gemcitabine loaded TMC-CSK NPs after 2 hr under 37 °C were much higher than that under 4 °C, suggesting that the uptake was energy dependent. In addition, the gemcitabine loaded TMC-CSK NPs had a significant greater drug uptake amount compared to gemcitabine solution in both 4 °C and 37 °C ($p < 0.01$), and also shows a slight greater drug uptake amount compare to gemcitabine loaded TMC modified PLGA-TPGS NPs.

Moreover, the experiments performed at 37°C showed 2.1-fold greater uptake than that at 4°C for drug loaded TMC-CSK NPs, and 2.2-fold for drug loaded TMC modified PLGA-TPGS NPs. Endocytosis, an energy dependent process, is blocked at low temperature. Upon incubation at 37°C, the cells are metabolically active and energy consuming uptake can occur. In contrast, at 4°C the metabolism is reduced so that binding of NPs to the cell membrane is reduced. Our results provided evidence that both the TMC modified PLGA-TPGS NPs and TMC-CSK NPs cellular uptake are mediated by endocytosis. This is in accordance with a previous research which demonstrated that endocytosis is the main mechanism of PLGA based NPs and TMC based NPs uptake by Caco-2 cells and Caco-2/HT29 cells (Desai, Labhasetwar et al. 1997, Jin, Song et al. 2012).

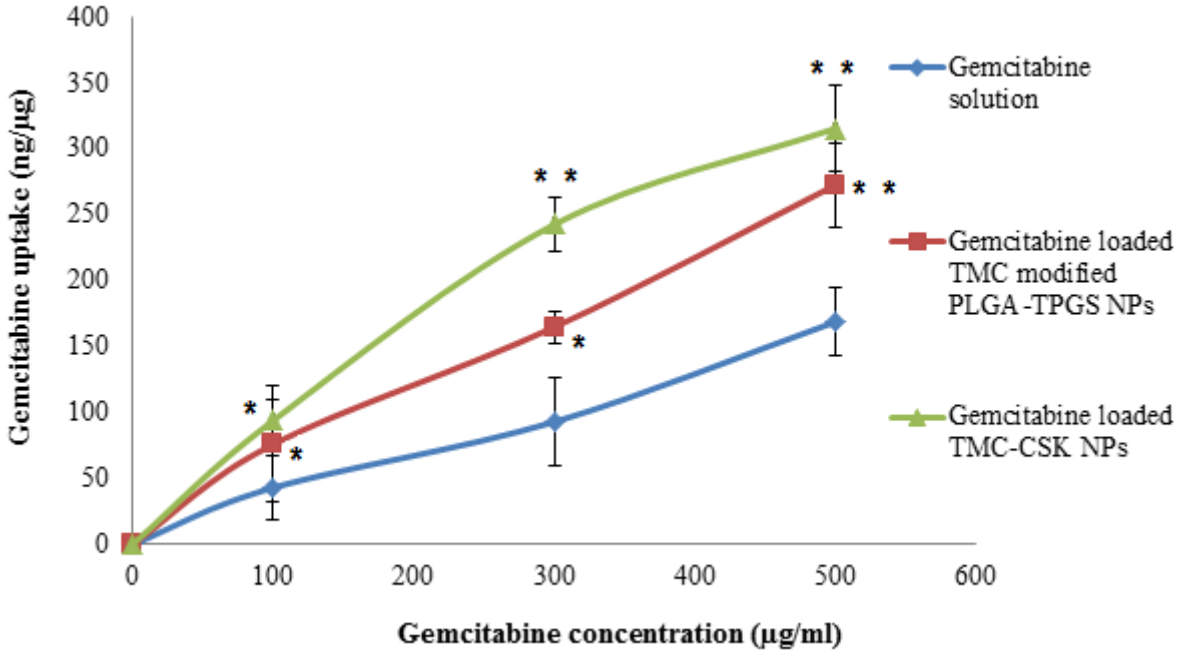

Figure 5-5. Concentration - dependent uptake of various concentration of gemcitabine solution, gemcitabine loaded TMC modified PLGA-TPGS NPs, and gemcitabine loaded TMC-CSK NPs after 2 hr at 37 °C (mean ± SD, n = 3; Significant difference from control, *p < 0.05, **p < 0.01).

Figure 5-5 shows the drug uptake is also in a concentration - dependent manner when the cells were exposed to gemcitabine solution, gemcitabine loaded TMC modified PLGA-TPGS NPs, and gemcitabine loaded TMC-CSK NPs with the concentrations of 100, 300, and 500 µg/mL. The drug uptake increase with increasing drug concentration when incubated with cells at 37°C for 2 h. Similarly, the gemcitabine uptake amount of drug loaded TMC-CSK NPs appeared to be higher than those of the free gemcitabine and gemcitabine loaded TMC modified PLGA-TPGS NPs at all three concentrations under 2 hr incubation at 37 °C ($p < 0.01$ at 100 µg/mL, $p < 0.01$ at 300 and 500 µg/mL). For gemcitabine loaded TMC-CSK NPs, concentration at 500 µg/ml had a 1.3-fold greater uptake compared to that at 300 µg/ml, and a 3.4-fold to that at 100 µg/ml. For gemcitabine loaded TMC modified PLGA-TPGS NPs, concentration at 500 µg/ml had a 1.7-fold greater uptake compared to that at 300 µg/ml, and a 3.6-fold to that at 100 µg/ml.

5.5.4 Investigation by confocal laser scanning microscope

The uptake of the FITC-labelled TMC modified PLGA-TPGS NPs by Caco-2/HT29-MTX-E12 cells at the concentration of 500 µg/ml with incubation time of 2 hr was visualized using confocal laser scanning microscope (CLMS). CLMS allows a 3-D cross-sectioning image of cells to be observed and gives information on the localization of particle. Labelling the cells with Tracker Red and DAPI resulted in the extracellular membrane and nuclei as well as the fluorescence labelled NPs being clearly visualized.

Figure 5-6 shows the distribution of green FITC labelled NPs within Caco-2/HT29-MTX-E12 cells after 2 hr incubation. The image indicates that NPs were clearly distributed throughout the cytoplasm and perinuclear region when particles were incubated with cells at 37°C, which confirmed the drug loaded NPs had been truly internalized into the cells and were not only adsorbed onto the cell membrane.

In addition, some residual attachment and internalization can be observed at some extent even after several washes of cells to remove the excess formulation. This suggested that the NPs are tightly bound to the cells. Adherence of a particle to the cell membrane is known as the precondition step leading to internalization (Foster, Yazdanian et al. 2001). Hence, the drug loaded NP which are tightly bound to the surface of the cells is suitable as an oral drug delivery system.

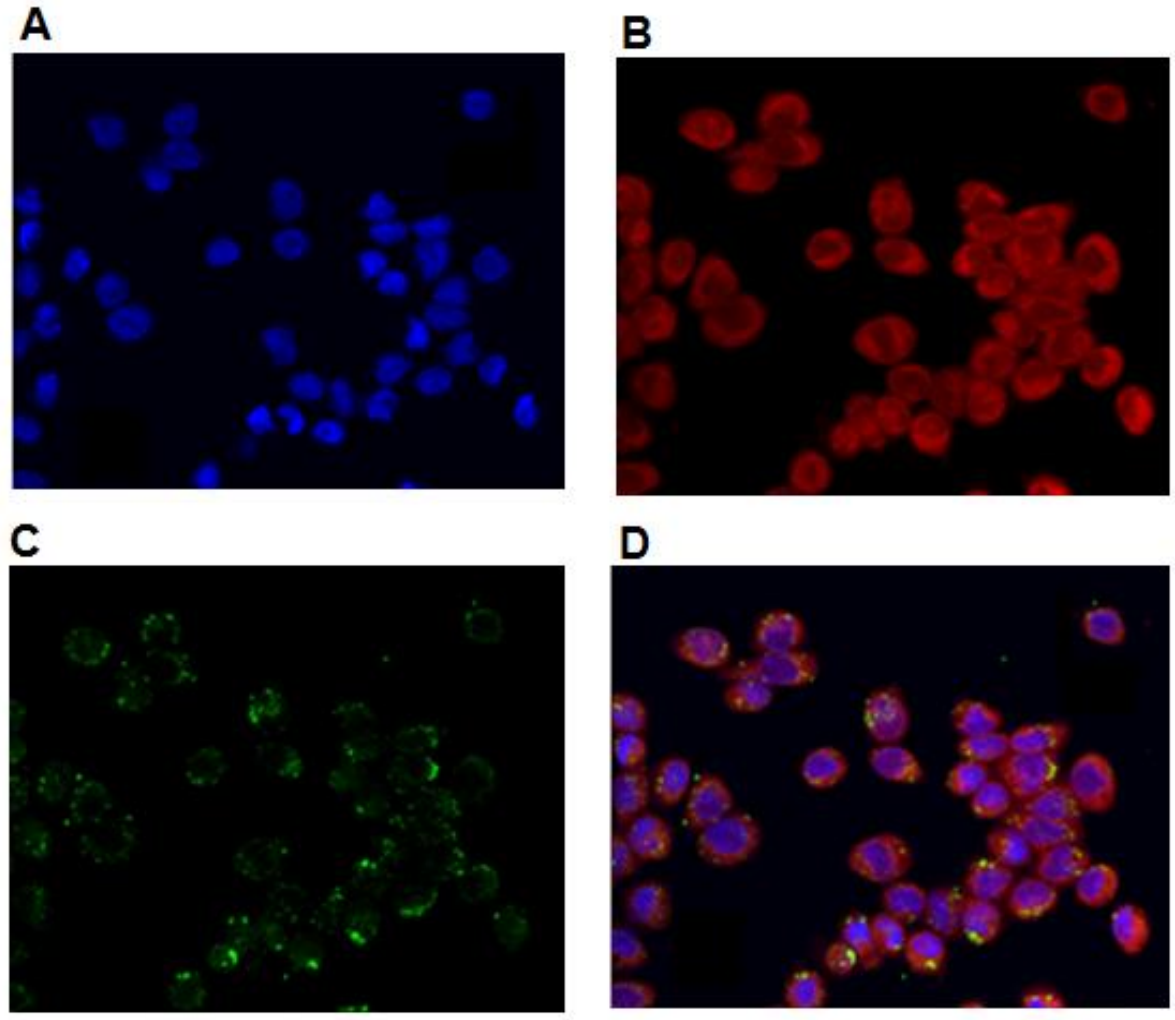

Figure 5-6. Confocal laser scanning microscopy image Z-stack images of co-cultured cells after 2 hr incubation with FITC-TMC/PLGA-TPGS NPs at 37ºC showing a perinuclear accumulation of particles. Merged image of nuclei: blue (A), cytoplasm: red (B) FITC labelled NPs: green (C), and colour overlay images (D) confirming uptake of intact NPs. (Magnification: 600 ×).

In summary of cellular uptake study on different time, temperature and drug concentration, we conclude the uptake process is time -, temperature- and concentration dependant. The gemcitabine loaded TMC-CSK NPs shows a relatively greater cellular uptake capability compared to plain drug solution, and drug loaded TMC modified PLGA-TPGS NPs.

From the temperature dependant uptake results, we can deduce the uptake process associates with endocytosis pathway. In addition, the rate and extent of uptake of NPs via endocytosis pathway is dependent on the availability of receptors/carriers. Saturation of these carriers would result in a decrease in particle internalization. This theory coordinates to the results from Figure 5-3, a saturation limit of the receptors leads to reduction of the drug uptake at the later stage. Moreover, the decrease of drug uptake at the later stage is also related to the drug exocytosis process govern by P-gp efflux pump, which transports drug and drug loaded NPs out of cells (Cartiera, Johnson et al. 2009).

Furthermore, the effect of particle size on the uptake of NPs by Caco-2/HT29-MTX-E12 cells is rather significant. Norris and Sinko studied that, the uptake of NPs by Caco-2 cells is in a size-dependent manner. An increase in particle size leads to a decrease in particle permeability. According to the Stokes-Einstein equation: $D = \frac{kT}{6\eta\pi r}$ or $P = \frac{kT}{6\eta\pi h}$, the diffusion of particles through mucin is restricted by the particle size (Norris and Sinko 1997).

This phenomenon was resulted from an increase surface area following a decrease of the particle size, thereby increasing the attachment/binding of particles to cell membrane and led to an increase in the internalization of particles into cells. In addition, the effect of particle size on the uptake efficiency may also due to different transport mechanisms. The particle size being investigated ranged from 173 to 500 nm. In general, pinocytosis occurs when particles are less than 100 nm, receptor-mediated endocytosis mostly occurs when particles size is about 100-200 nm, while larger particles are taken up by phagocytosis (Couvreur and Puisieux 1993). Particles with a size of larger than 500 nm are adsorbed by membranous (M) cells concentrated in follicle-associated epithelial tissue called Peyer's patches (Jepson, Clark et al. 1996). M cells play a major role in the endocytosis of microparticles. However, the exact uptake mechanism remains unclear. Therefore in the following studies, the further mechanisms of the NPs uptake were investigated.

5.5.5 Mechanisms of cellular uptake of drug loaded NPs

The mechanisms of the cellular uptake for the two optimal nanoparticulate delivery systems were investigated under different conditions. For drug loaded TMC modified PLGA-TPGS NPs, as shown in Figure 5-7, the cellular uptake of the drug loaded NPs at 37ºC for 2 hrs was set as control.

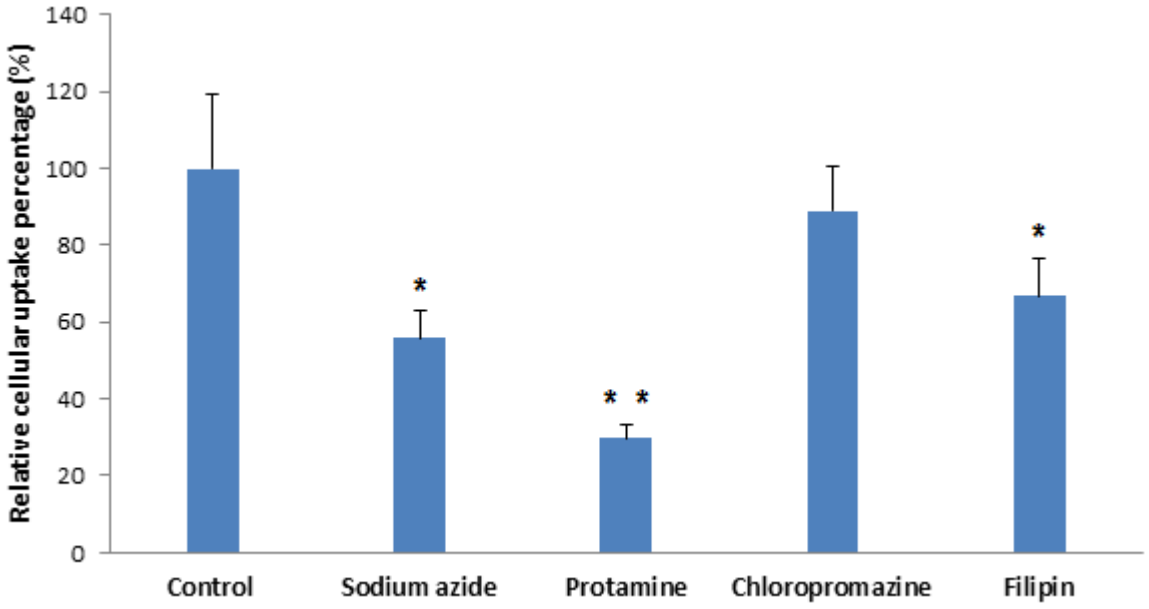

Figure 5-7. Uptake of drug loaded TMC modified PLGA-TPGS NPs by Caco-2/HT29-MTX-E12 cells at different conditions (mean ± SD, n = 3; Significant difference from control. *: $p < 0.05$, **: $p < 0.01$).

With the addition of sodium azide, which could block the active transport processes (Behrens, Pena et al. 2002), the uptake of drug loaded NPs was significantly decreased ($P < 0.05$), which indicates the uptake process is energy dependant active transport process. Previously we found the cellular uptake of the NPs reduced at lower temperature of 4ºC compared to 37ºC, indicating it is an energy dependant uptake process. Here by adding sodium azide, it confirms it undergoes active transport pathway.

With addition of protamine, which is an adsorptive-mediated endocytosis inhibitor, led to the strongest decreased internalization to 29.66 ± 3.72% for the drug loaded TMC modified PLGA-TPGS NPs ($P < 0.01$). This might be due to the competition of adsorptive

endocytosis (Sai, Kajita et al. 1998). These results demonstrated that the active transport processes, involving adsorptive endocytosis, might play an important role on the uptake of TMC modified PLGA-TPGS NPs.

Chlorpromazine and filipin are the two compounds that have been reported to block the clathrin and caveolae mediated endocytosis pathways, respectively. Chlorpromazine at a concentration of 6–10 μg/ml could disrupt the assembly and disassembly of clathrin and filipin at a concentration of 1 μg/ml is known to disrupt caveolae structure by binding to cholesterol and disorganizing the caveolin (Huang, Ma et al. 2002). With the additions of chlorpromazine and filipin, they were found to inhibit the uptake of TMC modified PLGA-TPGS NPs to 89.04 ± 11.32% and 66.66 ± 10.04% in the cells and the addition of filipin significantly inhibits the cellular uptake of the NPs ($p < 0.05$).

Hence, these results implied that the increased internalization of drugs from TMC modified PLGA-TPGS NPs, it undergoes active transport pathway and mainly associated with adsorptive mediated endocytosis as well as caveolae mediated endocytosis.

Bestpfe.com

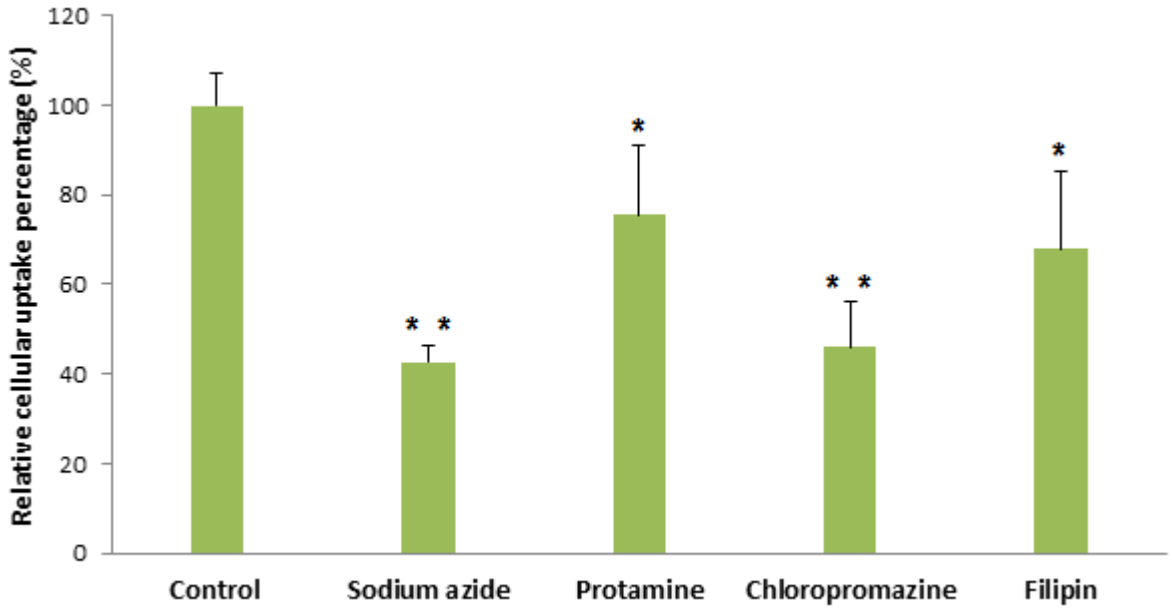

Figure 5-8. Uptake of drug loaded TMC-CSK NPs by Caco-2/HT29-MTX-E12 cells at different conditions (mean ± SD, n=3; Significant difference from control. *: $p<0.05$, **: $p<0.01$).

The mechanism studies for the drug loaded TMC-CSK NPs was shown in Figure 5-8. First, the cellular uptake of the drug loaded TMC-CSK NPs at 37ºC for 2 hrs was shown as control. With the addition of sodium azide, the uptake of drug loaded NPs was significantly decreased to 42.62 ± 3.72% ($P < 0.01$), which demonstrated the cellular uptake of TMC-CSK NPs is also an energy dependant active transport process. With addition of protamine, resulted in a decreased internalization to 75.61 ± 10.32% for the drug loaded TMC-CSK NPs ($P < 0.05$). With the additions of chlorpromazine and filipin, they were both found to significantly inhibit the uptake of TMC-CSK NPs to 46.12 ± 10.04% and 68.03 ± 17.11% in the cells ($p < 0.05$), and the addition of chlorpromazine more significantly inhibits the cellular uptake of the NPs ($p < 0.01$).

From all the results, it could be concluded that the CSK peptide receptor may exist on HT29-MTX-E12 cells, thus facilitate the cellular uptake of the CSK modified TMC NPs. The mechanism investigations revealed that beside of the active transport processes and adsorptive mediated uptake of the TMC-CSK NPs, the enhanced internalization of CSK peptide modified NPs also involved in both clathrin and caveolae mediated endocytosis.

5.6 Drug transport studies

5.6.1 Gemcitabine transport studies in the absence or presence of optimal NPs

The absorption of gemcitabine into systemic circulation means that gemcitabine transports across intestinal epithelial membrane into the blood stream. In other words, the permeated gemcitabine from the apical side, either through the transcellular way or the paracellular way, should be released and delivered to the basolateral side of cell membranes. Hence, the accumulated gemcitabine permeation across the intestinal epithelial membrane via the optimal nanoparticulate delivery systems was investigated, as well as to further investigate the transport mechanisms of the optimal NPs across the cell membrane. In our study, the co-cultured cell model consisting of both absorptive enterocyte-like Caco-2 cells and the mucus-producing HT29-MTX-E12 cells were applied for the first time to evaluate the transport of TMC modified PLGA-TPGS NPs and TMC-CSK NPs. It is a suitable *in vitro* model to evaluate the transport of oral delivered vehicles as well as the influence of mucus. The apparent permeability coefficient (P_{app}) of atenolol and propranolol for the co-cultured cell model were 2.46×10^{-6} and 1.10×10^{-5} cm s^{-1}, respectively, which implied the integrity of the cell membrane (Artursson and Karlsson 1991, Hilgendorf, Spahn‐Langguth et al. 2000). Meanwhile, only the cell membranes with TEER values within the range of 300 – 450 Ω cm^2 were used in this study.

BESTPFE.COM
List of research project topics and materials

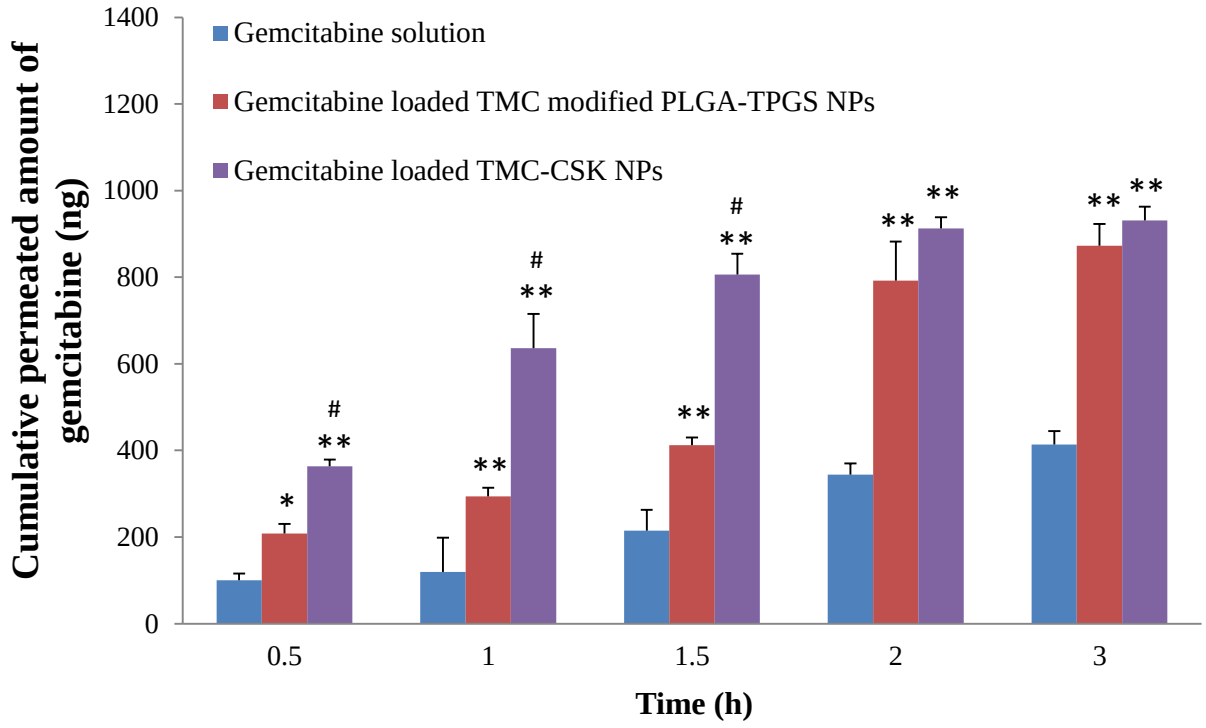

Figure 5-9. Transport studies of drug solution and drug loaded NPs across the co-cultured cells over 3 hr at 37ºC (mean ± SD, n = 3; *: $p < 0.05$ *vs* control; **: $p < 0.01$ *vs* control; #: $p < 0.05$ *vs* TMC modified PLGA-TPGS NPs).

The cumulative transported drug amount from gemcitabine solution (control), gemcitabine loaded TMC modified PLGA-TPGS NPs, and gemcitabine loaded TMC-CSK NPs over 3 hr at 37ºC were shown in Figure 5-9. The transport exhibited time-dependent dependent properties for all the groups. The gemcitabine loaded TMC-CSK NPs showed greatest drug transport over the cell membrane, of 931.5 ng gemcitabine permeated through the cell membrane over 3 hr. Which was 2.25-fold greater in drug amount transported compared to drug solution ($p < 0.01$), and a 1.07-fold greater in drug amount transported compared to gemcitabine loaded TMC modified PLGA-TPGS NPs.

Figure 5-9 also showed a relatively faster transport of gemcitabine loaded TMC-CSK NPs from 0.5 to 2 hr period compared to drug solution and drug loaded TMC modified PLGA-TPGS NPs. In contrast, the drug solution showed a steadily transport over the cell membrane, however much less of drug amount being transported compared to the drug loaded NPs. The drug loaded TMC modified PLGA-TPGS NPs showed a more rapid transport over the cell membrane from 1.5 hr to 2 hr.

Overall, the drug loaded TMC-CSK NPs showed an overall greater cellular uptake and drug transport. These results revealed the absorption enhancing ability of CSK peptide modified NPs across the epithelial membrane and it has exhibited significant cellular targeting effect.

5.6.2 Drug transport mechanisms

The mechanisms of the optimal drug loaded NPs transport over the epithelial membrane were investigated under different conditions.

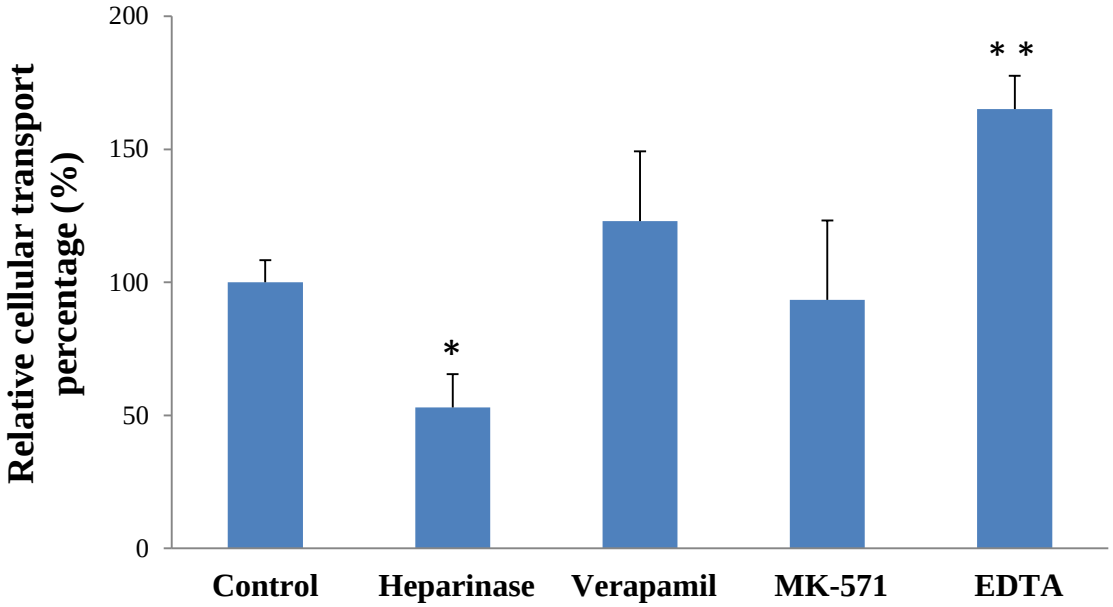

Figure 5-10. Transport of gemcitabine loaded TMC modified PLGA-TPGS NPs by co-cultured cells with addition of heparinise, verapamil, MK-571, and EDTA (mean ± SD, n = 3; Significant difference from control. *: $p < 0.05$, **: $p < 0.01$).

The transport of drug loaded TMC modified PLGA-TPGS NPs over 5 hr at 37ºC was set as control. Drug loaded TMC modified PLGA-TPGS NPs with addition of various chemicals to interact with cellular transport paths, compared with the control group. Results were shown in Figure 5-10. With an addition of heparinase (50 μM), it showed a significant decrease of drug transport ($p < 0.05$), demonstrating the positive charge of the TMC modification plays an important role in the transport process. Due to the elimination of the negative charged property on cell surface by adding heparinase, the positive charged TMC coating has no longer attributing its electrostatic interaction with the cell surface, thus lowering the uptake of

the NPs. In another word, this result demonstrated that the electrostatic interactions are responsible for an effective cell and NP interaction by improving NP attachment to the negatively charged cell surface.

With addition of P-gp inhibitor (100 μM verapamil) caused an increase in relative cellular transport percentage compared to the control group, indicating the P-gp efflux pump affects the transport process to some extent. In another word, by blocking the P-gp efflux pump, more drug loaded NPs are being transported through the cell membrane, which means the P-gp pumps are actually transporting the intracellular drug back to the intestinal lumen, and is considered another barrier for oral drug delivery of gemcitabine. However, there was no significant increase when MRP2 inhibitor (100 μM MK-571) was present, suggesting P-gp might play a major role in the efflux transport of gemcitabine on the Caco-2/HT29-MTX-E12 cell membrane.

Ten mM EDTA was used as a penetration enhancer. The relative cellular transport percentage was significantly elevated compared to the control group ($p < 0.05$). As previously mentioned, EDTA may affect the tight junction opening process, thus allowing the gemcitabine loaded NPs to be transported via paracellular pathway directly, therefore significantly facilitated the transport of gemcitabine (Erlij and Martínez-Palomo 1972).

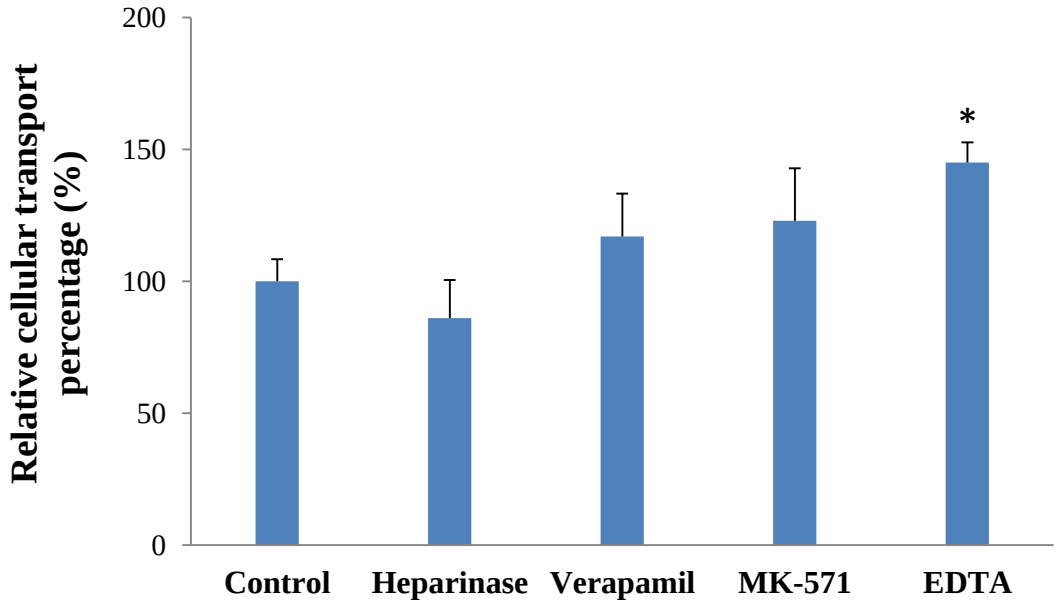

Figure 5-11. Transport of gemcitabine loaded TMC-CSK NPs by co-cultured cells with addition of heparinise, verapamil, MK-571, and EDTA (mean ± SD, n = 3; Significant difference from control. *: $p < 0.05$).

From Figure 5-11, the control group is the transport of gemcitabine loaded TMC-CSK NPs over 5 hr at 37ºC. The involving transport mechanisms of the delivery system were investigated.

The addition of 50 μM heparinase led to a decrease of drug transport, indicating the positive charged TMC component has influences in facilitating the TMC-CSK NPs transport across the cell membrane, due to the electrostatic interaction of TMC and the mucosal cell surface. The addition of heparinase Due to the elimination of the negative charged property on cell surface by adding heparinise, the positive charged TMC coating has no longer attributing its electrostatic interaction with the cell surface, thus lowering the uptake of the NPs.

With addition of P-gp inhibitor (100 μM verapamil) and MRP2 inhibitor (100 μM MK-571), they both caused increase in relative cellular transport percentage of TMC-CSK NPs compared to the control group, indicating the P-gp and MRP2 efflux pump affects the transport process of the TMC-CSK NPs. These results demonstrations the P-gp pumps and MRP2 are two barriers for oral delivery of TMC-CSK NPs, since they both efflux the drug loaded NPs back to the intestinal lumen. However, although both drug efflux pumps are limiting the cellular transport of TMC-CSK NPs, this drug delivery system still presented a

greater drug transport capability across the Caco-2/HT29-MTX-E12 cell membrane compared to drug solution and drug loaded TMC modified PLGA-TPGS NPs, demonstrating the CSK peptide has attributed great influence in intestinal mucosal cell targeting and facilitating the overall cellular transport process.

Furthermore, the addition of EDTA (10 μM), the relative cellular transport percentage was significantly increased compared to the control group ($p < 0.05$). Indicating EDTA promoted the transport of the drug loaded TMC-CSK NPs via paracellular pathway.

5.7 Conclusion

The cytotoxicity of gemcitabine solution, gemcitabine loaded TMC modified PLGA-TPGS NPs, and gemcitabine loaded TMC-CSK NPs to Caco-2/HT29-MTX-E12 cells was examined using MTT assay. They all showed dose dependant and with IC_{50s} of 529.4 ± 67.2 $\mu g.mL^{-1}$, 1881.4 ± 51.5 $\mu g.mL^{-1}$ and 1682.4 ± 27.9 $\mu g.mL^{-1}$, respectively. Indicating the two optimal NPs are less toxic toward the intestinal epithelial cells compared to drug solution.

The cellular uptake of gemcitabine loaded TMC modified PLGA-TPGS NPs, and gemcitabine loaded TMC-CSK NPs by Caco-2/HT29-MTX-E12 cells showed time-, temperature-, and concentration- dependant manner. Gemcitabine loaded TMC-CSK NPs showed a relatively greater cellular uptake capability compared to the other groups. In addition, the mechanism of the cellular uptake was subsequently investigating, showing the gemcitabine loaded TMC modified PLGA-TPGS NPs undergo active transport involving adsorptive mediated endocytosis and caveloae mediated endocytosis, while the gemcitabine loaded TMC-CSK NPs undergo active transport associate with adsorptive mediated uptake of the TMC-CSK NPs, the enhanced internalization of CSK peptide modified NPs also involved in both clathrin and caveolae mediated endocytosis.

The enhanced uptake is a consequence of better particles-cells interaction resulting in higher endocytotic uptake and/or higher retention time of NPs in cells, thus greater drug transport across the cell membrane. Therefore in the drug transport studies, drug loaded TMC-CSK NPs also showed a relatively greater drug transport compared to the other two groups of drug solution, and drug loaded TMC modified PLGA-TPGS NPs. All the three groups showed time dependant in drug transport process. For the further transport mechanism studies, both NP formulations showed electrostatic interaction with the intestinal epithelial cells, P-gp efflux are affect the cellular transport for both NPs, while MRP2 only affect TMC-CSK NPs to some extent. Moreover, EDTA absorption enhancer has significant effect in facilitating the both NPs cellular transport. It was interesting to find that although both cellular efflux pumps were affecting the TMC-CSK NPs transport over the cell membrane, the TMC-CSK NPs still presented a greater cellular uptake and transport process, this revealed the absorption enhancing ability of CSK peptide modified NPs across the epithelium assigned by their targeting effect is significant.

Therefore, we conclude that in drug uptake and transport studies, the drug loaded TMC-CSK NPs showed a predominately promising drug delivery system with low toxicity, greater cellular uptake and transport via Caco-2/HT29-MTX-E12 cell membrane. This is a very encouraging result for the development of gemcitabine incorporated TMC-CSK NPs to improve the gemcitabine oral bioavailability, and leads to great therapeutic anticancer effect.

Chapter 6

In Vivo Pharmacokinetic and Pharmacodynamics Studies

Bestpfe.com

Chapter 6. *In vivo* pharmacokinetic and pharmacodynamics studies

6.1 Introduction

From previous *in-vitro* and *ex-vivo* studies, the gemcitabine loaded TMC modified PLGA-TPGS NPs and the gemcitabine loaded TMC-CSK NPs both showed great physicochemical properties in characterization and promising results in cellular uptake and transport studies on Caco-2/HT29-MTX-E12 cell membrane. However, in order to further study their potential to be the novel oral delivery systems for gemcitabine to treat breast cancer, *in-vivo* pharmacokinetic and pharmacodynamics studies were carried out. As the ultimate aim of the research is to see whether these developed nanoparticulate delivery systems are able to improve the oral bioavailability of gemcitabine and the level of improvement. Furthermore, the therapeutic anticancer effect of these gemcitabine loaded NPs on breast cancer were also investigated in this chapter.

6.2 Breast cancer 4T1 cells

6.2.1 Cell culture

The breast cancer cell line 4T1, is derived from a BALB/c mammary tumour. The 4T1 breast cancer cell line was purchased from American Type Culture Collection (ATCC; Rockville, MD). It was cultured in Roswell Park Memorial Institute (RPMI) medium 1640 basic (Gibco, Grand Island, USA) containing 10% fetal calf serum (Hyclone, Logan, UT, USA), 1% penicillin-streptomycin-glutamine (Life Technology, NY, USA) and 1% nonessential amino acids (Life Technology, NY, USA) at 37 °C, 98% humidity and 5% CO_2. Culture medium was changed every 2 days until cells grew to 90% confluence. For subculturing, the cells were dissociated with 0.25% trypsin-EDTA, split in a ratio of 1:3.

6.2.2 Cytotoxicity studies

The cytotoxicity study was evaluated using a MTT assay with 4T1 cancer cells. Drug solution and drug-loaded NPs were evaluated and their IC_{50s} were determined. Briefly, 5 × 10^3 4T1 cells per well in 96 well microtiter plates (in triplicate) were incubated in 5% CO_2 for 24 hr. (Serial dilutions of drug solution and drug loaded NPs were prepared, and a 100 µL of the diluted samples were added to the growth medium and further incubated for 72 hr for drug solution and drug loaded NPs under the same conditions. To evaluate cell survival, 20 µL of MTT solution (5 mg/mL in PBS) was added to each well and incubated for 4 hr, then the medium containing MTT was gently replaced with 200 µL of DMSO and placed on a shaking plate for 15 min, to dissolve formazan crystals. Thus, the MTT assay assessed cell viability by measuring the enzymatic reduction of yellow tetrazolium MTT to a purple formazan at 540 nm using a SepctraMax Plus 384 (Molecular Devices, Sunnyvale, USA). The absorbance of test (treated cells) and control (untreated cells) were used for the determination of the percentage cell viability, using the same method mentioned in section 5.4.2 in previous chapter, the percentage of cell activity was calculated as: Cell activity = $(Ab_{exp} - Ab_{neg}) / (Ab_{con} - Ab_{neg}) \times 100$ %, where Ab_{exp} is the value of experiment group absorbance at 540 nm; Ab_{neg} is the value of blank group absorbance at 690 nm; Ab_{con} is the value of control group absorbance at 540 nm. Finally, the IC_{50s} for gemcitabine solution and drug loaded NPs were also calculated (Fotakis and Timbrell 2006).

6.3 *In vivo* animal studies

6.3.1 Animal housing and care

6.3.1.1 Male Sprague-Dawley (SD) rats for pharmacokinetic study

Pharmacokinetic studies were conducted using a male Sprague-Dawley (SD) rat model (Figure 6-1A). The male SD rats weighing 200 ± 20 g were purchased from BK Lab Animal Ltd (Shanghai, China) and housed at 25 ± 1 °C on a scheduled 12 hr light/dark cycle, and humidity of 50 ± 10% with free access to food and water. The animal studies were carried out in accordance with guidelines evaluated and approved by the ethics committee of Fudan University (Shanghai, China), approval number 2015-04-YJ-LWY-01.

BESTPEE.COM
List of research project topics and materials

6.3.1.2 BALB/c nude mice for pharmacodynamics studies

Pharmacodynamic studies were conducted using a male albino, laboratory-bred strain (BALB/c) nude mice model (Figure 6-1B). The BALB/c nude mice (6 - 8 weeks) weighing 23 ± 2 g were purchased from BK Lab Animal Ltd (Shanghai, China) and housed in the same conditions as the SD rats. Experiments were conducted under ethics approval 2015-04-YJ-LWY-01.

6.3.2 *In vivo* acute toxicity studies

BALB/c nude mice were used for *in-vivo* pharmacodynamics studies. However, there was no suitable oral dose data for gemcitabine was reported in the literature. Therefore, in order to inform a maximum tolerated oral dose of gemcitabine for this animal model. Thus, *in vivo* acute toxicity studies were conducted prior to the pharmacodynamics study using BALB/c nude mice.

To conduct the *in-vivo* toxicity studies. Briefly, ten healthy male BALB/c mice (6 - 8 weeks) weight 23 ± 2 g per group were administered gemcitabine solution through oral gavage. Five different dosages of 60, 120, 240, 480, and 960 mg/kg were given to each group of mice (n=10). Subsequently, mice survival and variation in body weight, moving behaviours, and physical reaction were observed over a period of seven days. Finally, according to the mice survival results, the lethal dose (LD_{50}) of gemcitabine was calculated. LD_{50} is the amount of an ingested substance that kills 50 percent of the tested animals. It is expressed in mg/kg, or milligrams of substance per kilogram of body weight (Randhawa 2009). Therefore from the LD_{50} results, the maximum tolerated oral dose of gemcitabine for BALB/c nude mice was determined. Generally, 1/6 of the LD_{50} is considered as an effective as well as a maximum tolerated dose of drug to the specific animal model (Gupta 2011, Hauschild and King 2011).

6.3.3 *In vivo* Pharmacokinetic studies

Male SD rats weighing 200 ± 20 g were used for *in vivo* pharmacokinetic studies. Twenty four animals were divided evenly between 4 groups (n = 6). The first group was administered gemcitabine solution by oral gavage (Figure 6-1A) while the second and third groups

received either drug loaded TMC modified PLGA-TPGS NPs or drug loaded TMC-CSK NPs orally. The final group were intravenously injected with gemcitabine solution. All groups received a gemcitabine dose of 80 mg/kg, 1/6 of the reported LD_{50} of SD rats (Hussain, Sasidharan et al. 2009). Each dose was orally administrated to the rats through 16G curved gavage needles (Cadence, Staunton, USA). Blood samples were collected at predetermined intervals, centrifuged at 42018 g for 5 min and the plasma was stored at -70 $^{\circ}$C until analysis. Gemcitabine in the plasma was extracted following the addition of 1 mL of acetonitrile, vortexed for 1 min and centrifuged at 101890 g for 15 min. The supernatant was filtered and determined by HPLC.

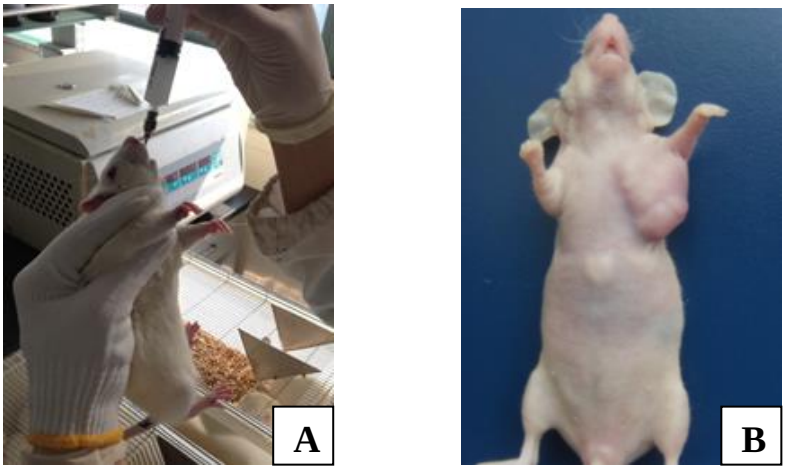

Figure 6-1. A photograph of male SD rat was administered drug solution by oral gavage (A); a photograph of a solid 4T1 breast tumour bearing BALB/c nude mouse (B).

6.3.4 *In vivo* pharmacodynamics studies

4T1 breast cancer cells were cultured, collected and injected subcutaneously to the prep axillary (*armpit*) *area* of mice (n = 6). Mice were maintained until solid tumours developed (Figure 6-1B). Gemcitabine solution, gemcitabine loaded TMC modified PLGA-TPGS NPs or the gemcitabine loaded TMC-CSK NPs were administrated at 30 mg/kg on days 0, 2 and 4. Tumor size and body weight were measured every 2 days. A Vernier caliper (0-150 mm × 0.02, Mitutoyo, Japan) was used to measure the tumor size. The experiment was terminated after 12 days, the mice were euthanized and the tumors were harvested from different groups.

6.3.5 Histological studies

After the pharmacodynamic study which lasted 12 days, one mouse from each group was euthanized and heart, liver, spleen, lung and kidney were excised with necropsies and determined by hematoxylin and eosin (H&E) staining pathological examination, to determine any incidental toxicity from administration of drug solution, and drug load NPs.

6.3.6 Statistical analysis

IC_{50} in the cytotoxicity studies was calculated from nonlinear regression analysis using GraphPad Prism Version 5.02 (Graphpad Software Inc, San Diego, USA). The serum pharmacokinetic parameters were calculated using non-compartmental model of Phoenix WinNonlin software program 5.2.1 (Certara, Princeton, USA). Required pharmacokinetics parameters such as time to reach the maximum serum concentration (T_{max}) (hr), peak serum concentration (C_{max}) (ng/mL), total area under the serum concentration-time the curve from 0 to 24 hr (AUC_{0-24}) (ng.hr/mL), and mean residence time (MRT) (hr) were determined. Absolute bioavailability between each formulation and free drug was calculated using the equation: Absolute bioavailability = AUC_{test} formulation/$AUC_{free\ drug}$ × 100 %.

Statistical data analyses were performed using Microsoft Excel 2010 software (Redmond, WA). Data comparisons were conducted using regression analysis, ANOVA tests and two-tailed t-tests. A p-value of ≤ 0.05 was pre-defined as the minimum level of significance. All data were expressed as mean ± SD.

6.4 Results and discussion

6.4.1 Cytotoxicity studies

The cytotoxicity of the TMC, TMC-CSK, PLGA and PLGA-TPGS polymers alongside gemcitabine loaded NPs were determined in 4T1 breast cancer cells. The TMC, TMC-CSK, PLGA and PLGA-TPGS polymers showed no significant cytotoxicity after 3 hrs of incubation indicating the biocompatibility of these polymers with 4T1 breast cancer cells. From Figure 6-2, gemcitabine solution, gemcitabine loaded TMC modified PLGA-TPGS NPs and gemcitabine loaded TMC-CSK NPs all demonstrated some dose dependent cytotoxicity over 72 hrs with IC_{50}s, of 7548.64 ± 31.2 $ng.mL^{-1}$, 5712.63 ± 46.3 $ng.mL^{-1}$ and 10485.51 ± 47.4 $ng.mL^{-1}$, respectively. Both drug loaded NP formulations had higher IC_{50s} than gemcitabine solution which can be attributed to the drug being encapsulated in the NPs. According to the definitely of IC_{50}, the lower the IC_{50} indicating less equivalent drug amount is required to trigger half number of the cell deaths. The drug loaded TMC-CSK NPs showed lower IC_{50} than that of drug loaded TMC modified PLGA-TPGS NPs, demonstrating drug loaded TMC-CSK NPs may have great anticancer effect on 4T1 tumour cells.

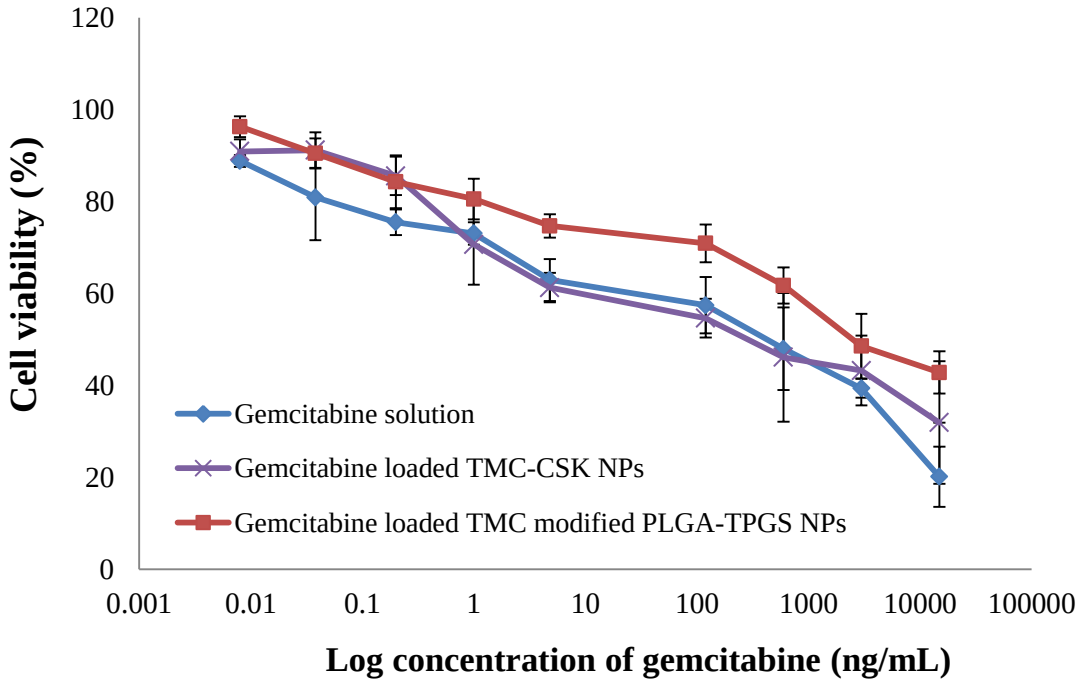

Figure 6-2. Cytotoxicity of gemcitabine solution and drug loaded TMC-CSK NPs and drug loaded TMC modified PLGA-TPGS NPs on 4T1 breast cancer cells at the tested concentrations over 72 hr (mean ± SD, n=3).

6.4.2 *In-vivo* acute toxicity studies

Since the effective and well tolerated drug dosage of gemcitabine for BALB/c nude mice was not reported in the literature. Therefore the *in-vivo* acute toxicity study was required to inform a suitable oral dosage of gemcitabine prior to *in-vivo* studies with BALB/c nude mice. Figure 6-3 displays body weight changes of mice orally administered one of five different dosages over 10 days. At doses above 60 mg/kg, gemcitabine caused a decline in body weight. The higher the dosage, the larger the decrease in weight. At the highest dosage of 960 mg/kg, all the mice died after 4 days, while 3, 6, 9, and 10 mice survived through to 10 days at 480 mg/kg, 240 mg/kg, 120 mg/kg and 60 mg/kg dosing respectively. Furthermore, over the 10 days' observation, the groups at doses above 60 mg/kg suffered from diarrhoea, with slow reactions and decreased movement during the study. Symptoms were more severe in groups administrated higher doses of gemcitabine. From Figure 6-4, the number of deaths was plotted against log concentration to determine the dosage required to kill 50% of the mice giving an LD_{50} of 204.17 mg/kg.

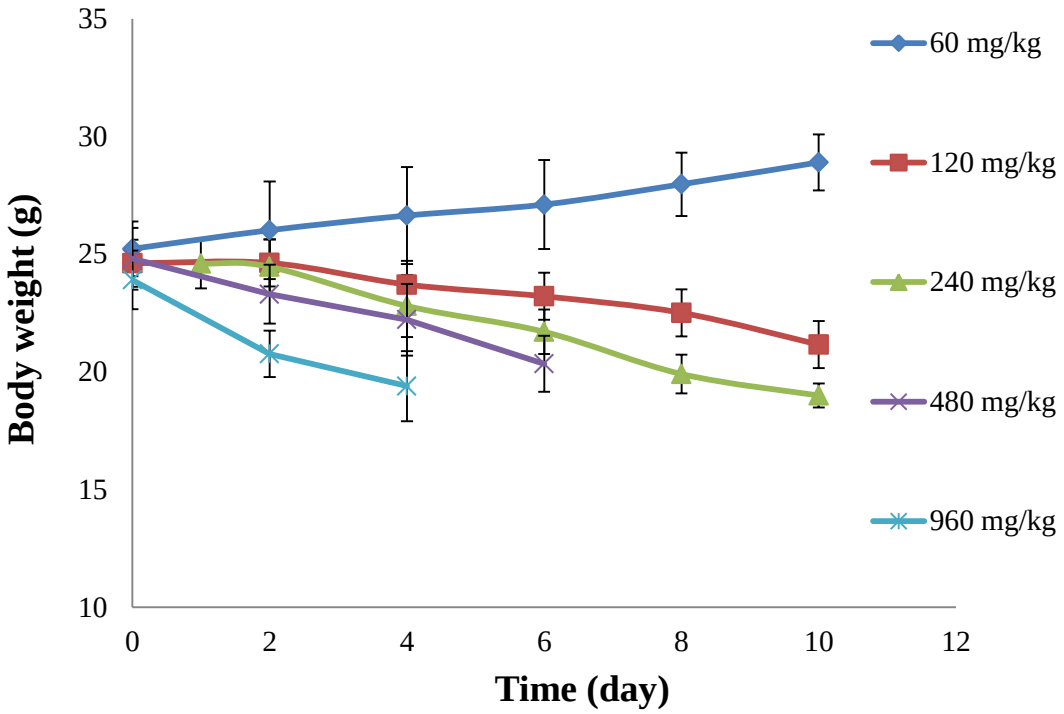

Figure 6-3. Body weight change of BALB/c nude mice after oral administration of various dosage over 10 days (mean ± SD, n = 10).

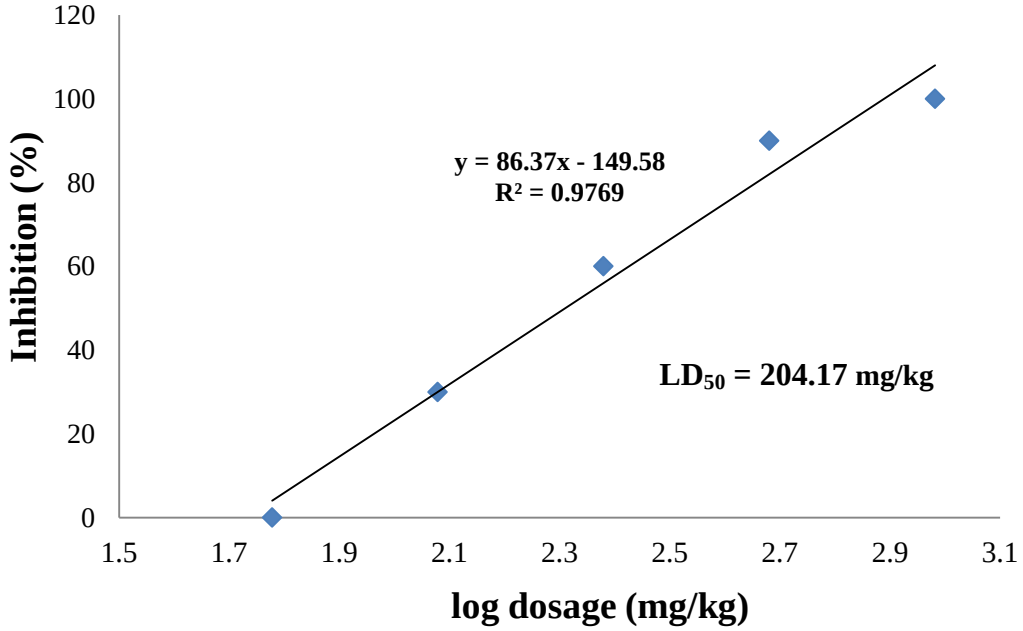

Figure 6-4. Percentage inhibition versus logarithm of dosages to determine LD_{50} of gemcitabine in BALB/c nude mice.

6.4.3 *In vivo* Pharmacokinetic studies

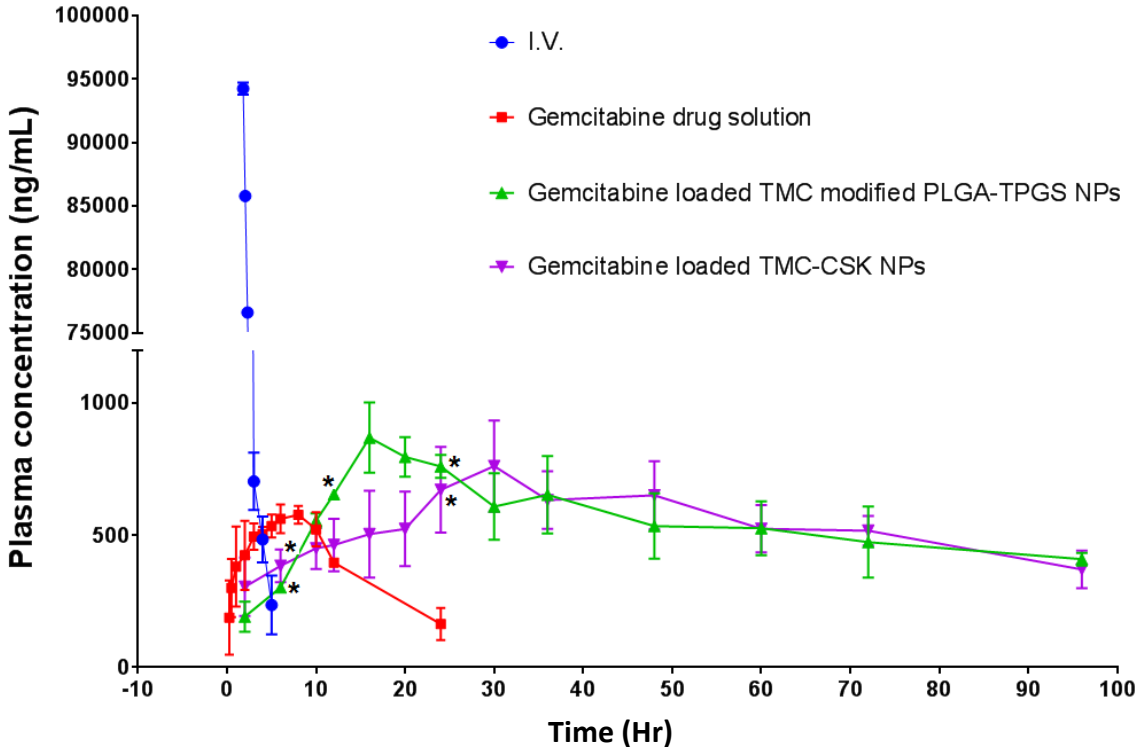

Figure 6-5. Plasma concentration of gemcitabine in SD rats following oral administration of gemcitabine solution, drug loaded TMC modified PLGA-TPGS NPs, drug loaded TMC-CSK NPs and i.v. injection of gemcitabine solution (mean ± SD, n = 6). Oral administration group results had significant difference from i.v. administration of gemcitabine. (**p < 0.001), Significant difference from oral administration of gemcitabine solution: (*p < 0.05).

Pharmacokinetic study was carried out to determined the oral bioavailability and all other pharmacokinetic parameters of plain drug solution, drug loaded NPs. The plasma drug concentration versus time profile for oral administration of drug solution, drug loaded TMC modified PLGA-TPGS NPs and drug loaded TMC-CSK NPs, and following intravenous (i.v.) administration of drug solution in SD rats (n = 6) are shown in Figure 6-5. Table 6-1 has shown all the resulting pharmacokinetic parameters which were analysed by GraphPad Prism Software 6.0 version. Veltkamp *et al.* (2008) found that the oral bioavailability of pure gemcitabine solution was very low due to extensive first pass effect but it is well tolerable at lower doses (Veltkamp, Pluim et al. 2008). Following oral administration, gemcitabine loaded TMC modified PLGA-TPGS NPs and gemcitabine loaded TMC-CSK NPs were able

to increase gemcitabine oral bioavailability by 5 and 5.5 fold compared with gemcitabine solution, respectively. The maximum drug concentration of gemcitabine loaded TMC-CSK NPs was of 868.8 ± 88.6 ng/mL attained 16 hr after oral administration, which was higher than that of gemcitabine loaded TMC modified PLGA-TPGS NPs which was of 761.0 ± 214.3 ng/mL at 30 hr. A higher C_{max} demonstrated majority of drug loaded NPs was capable of bypassing hepatic first pass metabolism and reached the systemic circulation. Delayed T_{max} indicated the fact that, after intestinal transit, majority of drug was released while they were presenting in the systemic circulation (Joshi, Kumar et al. 2014). Additionally, the area under curve (AUC) value of gemcitabine loaded TMC-CSK NPs was 51363 ± 705 ng.h/mL, which was 1.1-fold higher than gemcitabine loaded TMC modified PLGA-TPGS NPs that of 46457 ± 2124 ng.h/mL. The higher AUC indicating the drug loaded NPs sustained release the drug candidate from NPs, which would protect the drug from metabolism. Hao *et al*. (2003) has reported a self-microemulsifying drug delivery system for oral delivery of gemcitabine, their developed carrier system has enhanced the C_{max} significantly but half-life ($t_{1/2}$) has not been improved (Hao, Wang et al. 2013). In this study, the $t_{1/2}$ of gemcitabine loaded TMC-CSK NPs and gemcitabine loaded TMC modified PLGA-TPGS NPs were 77.16 ± 24.20 hr and 69.98 ± 20.50 hr respectively, which was improved significantly compared with gemcitabine solution that of 9.40 ± 2.13 hr. Finally, the absolute oral bioavailability of gemcitabine loaded TMC-CSK NPs (55.97%), was 1.1-fold and 5.7-fold higher than that of gemcitabine loaded TMC modified PLGA-TPGS NPs (50.63%) and gemcitabine solution (9.86%), respectively.

Bestpfe.com

Table 6-1. Pharmacokinetic parameters of gemcitabine in SD rats following oral administration of gemcitabine solution, gemcitabine loaded TMC NPs, gemcitabine loaded TMC-CSK NPs and i.v. injection of gemcitabine solution (mean ± SD, n = 6).

PK parameters	**Gemcitabine (i.v.)**	**Gemcitabine solution (oral)**	**Drug loaded TMC-CSK NPs (oral)**	**Drug loaded TMC modified PLGA-TPGS NPs (oral)**
C_{max} (ng/mL)	94152 ± 3435	577.1 ± 98.2	868.8 ± 88.6	761.0 ± 214.3
T_{max} (h)	0.25	8	30	16
$AUC_{0\text{-}inf}$ (ng.h/mL)	93050 ± 1459	9176 ± 785	51363 ± 705	46457 ± 2124
$T_{1/2}$ (h)	1.18 ± 0.85	9.40 ± 2.13	77.16 ± 24.20	69.98 ± 20.50
Absolute Oral bioavailability	100%	9.86%	55.97%	50.63%

C_{max}: maximum plasma concentration; T_{max}: time at which C_{max} is reached; $T_{1/2}$: half-life.

6.4.4 *In vivo* pharmacodynamics studies

In Figure 6-6, the size of 4T1 breast tumours increased markedly over the study period in the untreated control group, while the tumour had a significantly reduced growth rate ($p < 0.01$) in both of the gemcitabine loaded NPs groups. Among all these groups, the gemcitabine loaded TMC-CSK NPs group had the greatest inhibition against tumour growth, with 3.12-fold and 1.78-fold reduction compared to saline control group and gemcitabine solution group, respectively. This result corresponds to the *in-vivo* pharmacokinetic studies with greater oral bioavailability and longer plasma half-life of gemcitabine loaded TMC-CSK NPs group compared to all other groups. Figure 6-7 has shown a photograph of the solid tumours, with saline control group, 3 doses of 30 mg/kg drug solution and equivalent drug loaded NPs groups, given on days 0, 2, 4 harvested on day 12. The results confirmed the significant reduction of tumour growth size in the drug loaded NPs groups compared to the saline and drug solution group.

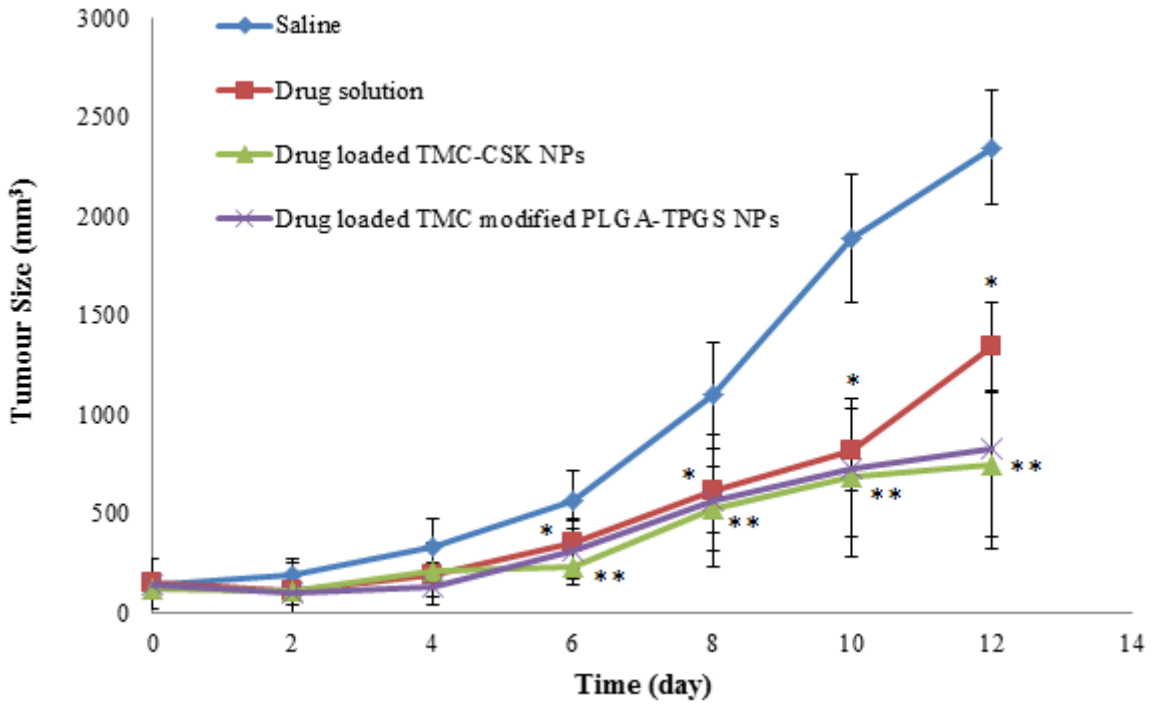

Figure 6-6. Following administration of saline or the time course of tumour size in BALB/c nude mice recorded during the period of treatment of drug solution, drug loaded TMC-CSK NP, drug loaded TMC modified PLGA-TPGS NPs and without treatment (saline group) over 12 days (mean ± SD, n = 6, significant difference from saline control. *: $p < 0.05$).

BEST PFE.COM
List of research project topics and materials

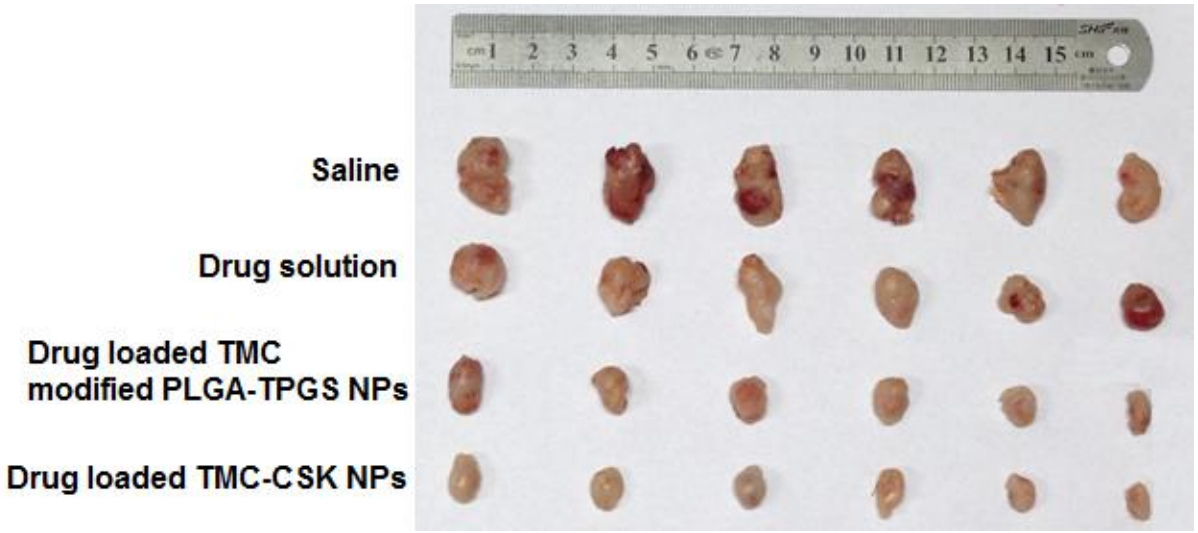

Figure 6-7. A photograph of the solid tumours, with saline, 3 doses of 30 mg/kg drug solution and equivalent drug loaded TMC modified PLGA-TPGS NPs and drug loaded TMC-CSK NPs, given on days 0, 2, 4 harvested on day 12.

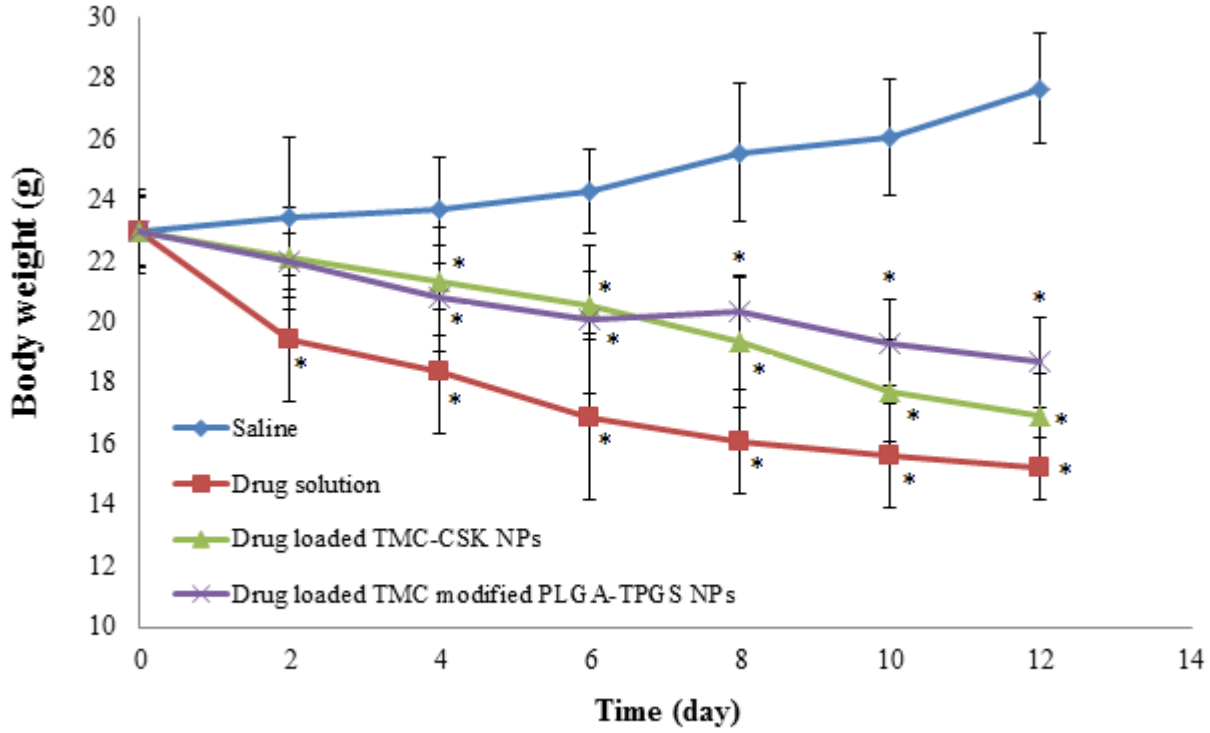

Figure 6-8. The profile of body weight change of BALB/c nude mice during the period of treatment over 12 days (mean ± SD, n = 6, significant difference from control. *: $p < 0.05$).

From Figure 6-8, a large drop in body weight of the nude mice for the gemcitabine solution group and drug loaded NPs groups was observed. The greatest decrease in body weight was in the gemcitabine solution group, and may reflect the highest systemic toxicity (von der Maase, Hansen et al. 2000). However, compared to the control group, the must less weight lost was observed in both NPs groups, which it indicates that the both NPs are absorbed intact in the systemic circulation and release gradually and caused fewer side effects perhaps. However, the safety profile remains a limiting factor which will need to be addressed in the future.

6.4.5 Histological studies

Representative photomicrographs of the heart, liver, spleen, lung and kidney are displayed in Figure 6-9 following 12 days of treatment with gemcitabine solution and gemcitabine NPs. No major evidence of toxicities was discernible in these organs for both NPs groups. (Therefore only the gemcitabine loaded TMC-CSK NPs group shown here as the representative images of the healthy organs). However, a low degree of inflammation was found in the liver samples of drug solution group (arrow labelled in Figure 6-9), indicating the early stage of chronic inflammation, which is likely due to the direct hepatic toxicity from gemcitabine solution (Robinson, Lambiase et al. 2003). Saif *et al* found that four case reports regarding severe hepatic toxicity of gemcitabine leading to rapid deterioration in patients' health status and death (Saif, Shahrokni et al. 2007). The results suggest the toxicity of the unformulated gemcitabine was higher than the gemcitabine encapsulated within the NPs. No gross residue of the NPs was seen in the tested organs, which demonstrated the consistency with the biodegradability of the two nanoparticulate delivery systems. No major signs of toxicity were found in these organs for the both NPs groups, which may be due to the fact that gemcitabine were not accumulating in these targeted tissues, or it can be due to insufficient time for the drug to harm these tissue thus no obvious observation was occurred.

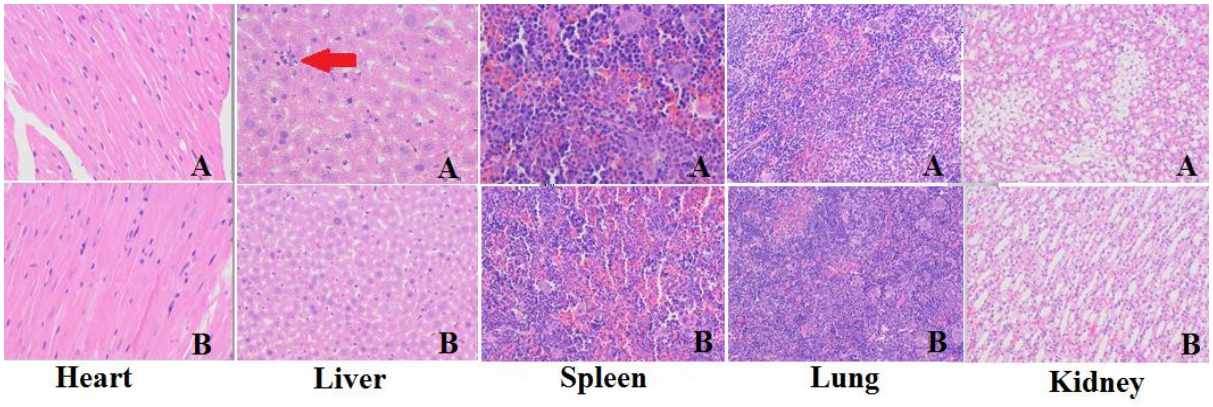

Figure 6-9. A) Representative photomicrography of heart, liver, spleen, lung and kidney with H&E staining. Gemcitabine solution, B) gemcitabine loaded TMC-CSK NPs. No significant toxicities were discernible in the tested organs.

6.5 Conclusion

From the *in vivo* pharmacokinetic and pharmacodynamics studies, the developed nanoparticulated delivery systems of TMC-CSK NPs and TMC modified PLGA-TPGS NPs have shown promising results compared to drug solution (i.e NPs groups have shown lower toxicity profiles and a relative higher value of IC_{50} against 4T1 breast cancer cells). The plasma half-life and oral bioavailability of gemcitabine were significantly increase up to 4 or 5 folds by TMC-CSK and TMC modified PLGA-TPGS NPs groups specially slightly better results was achieved in TMC-CSK NPs group.

In-vivo pharmacodynamics studies demonstrated the promising ability of gemcitabine loaded TMC-CSK and TMC modified PLGA-TPGS NPs groups to inhibit the growth of tumour cells, suggesting that both of the developed nanoparticulate delivery systems are a suitable for the oral delivery of gemcitabine. However, the safety profiles for the novel delivery systems still remain a major challenge, which can be focused on in the future studies.

Chapter 7

General Discussion and Future Perspectives

Chapter 7 . General discussion and future perspectives

7.1 General discussion

In New Zealand, breast cancer affects one in nine women over their lifetime, with over 70% of women are diagnosed of breast cancer at the age of 50 years or older, and over 600 deaths every year, which makes it the highest rate of incidence cancer in women (Ferlay, Soerjomataram et al. 2015, Torre, Bray et al. 2015). Breast cancer is caused by genetic abnormalities which trigger breast cells to grow in an uncontrollable manner, this uncontrollable cell growth would eventually lead to form a tumour (Bansil and Turner 2006, Al-Qadi, Grenha et al. 2012).

The most common chemotherapy for breast cancer treatment is through parenteral administration of anticancer drugs. However, this often leads to high peak of drug above the MTC in systemic circulation, followed by a fast elimination of drug from the plasma, resulting in a limited AUC of gemcitabine (Silverstein and Rodgers 2004, Mei, Zhang et al. 2013).

Oral chemotherapy is preferred since it is has better patient adherence, good therapeutic efficacy, and low cost. However, the biological and physical barriers in GIT offer various obstacles to oral delivery of drugs. These obstacles include the exposure of the drug candidates to the harsh acidic environment and various digestive enzymes in the GIT which may degrade the oral administered drugs. In addition, the difficulty of the drug compounds to permeate across the intestinal mucosal epithelial membrane is another major obstacle for oral drug delivery.

Gemcitabine is an antineoplastic drug and it is effective in treating a variety of malignancies, including breast, pancreatic, lung, and bladder cancers (von der Maase, Hansen et al. 2000, Blackstein, Vogel et al. 2002, Oettle, Post et al. 2007, Conroy, Desseigne et al. 2011). However, due to its highly hydrophilic property, results in low permeability over the intestinal epithelial cell membrane, thus lower the oral bioavailability. In addition, gemcitabine has a low plasma half-life of approximate 8 - 17 min (Brusa, Immordino et al. 2007), indicating a fast metabolism of the drug candidate, which is another drawback that

leads to the low oral bioavailability of gemcitabine. Therefore, there is a need to develop a suitable novel drug delivery system for oral delivery of gemcitabine to enhance its oral bioavailability, and thus improve the therapeutic efficacy.

Nanoparticulate drug delivery systems have been researched to improve therapeutic efficacy while reducing side effects. The application of nanoparticulate delivery systems in a wide range of therapy is already confirmed. However, only a few papers have been published on using NPs for oral delivery of gemcitabine to the treatment of cancers. Polymeric particles encapsulated drugs from the external medium in the GIT thereby protecting the drugs from chemical or enzymatic degradation as well as to enhance the permeation across the intestinal epithelial membrane, thus improving the oral bioavailability.

TMC is a derivative of chitosan but has more advantages over chitosan. Most importantly, TMC has shown great mucoadhesion property and has been widely used to fabricate NPs for oral delivery of various drug candidates. CSK peptide has been reported to have intestinal epithelial goblet cells targeting property. Thus with CSK modification on TMC NPs would facilitate the drug loaded NPs to permeate through the intestinal epithelial membrane. Therefore, in this study a drug loaded TMC-CSK NPs was developed. PLGA is also a widely used to fabricate NPs due to its biodegradable and biocompatible properties, and well protection of encapsulated drug as well as great stability. TPGS is a derivative of natural vitamin E with the nature of nontoxic. TPGS was reported to enhance the drug entrapment efficiency, loading capacity, stability and preventing the efflux by inhibition of P-gp efflux pump (Ma, Zheng et al. 2010). Bearing all these benefits of the polymers in mind, a second novel delivery system of TMC modified PLGA-TPGS NP was developed for oral delivery of gemcitabine.

The two novel oral delivery systems have shown great potential as oral drug carrier systems to deliver gemcitabine either in cellular uptake and transport studies or *in vivo* pharmacokinetic and pharmacodynamc studies. The two developed NP systems have shown significant improvement of oral bioavailability of gemcitabine compared to that of drug solution ($p < 0.05$), thus reached the ultimate aim of this research project.

In Chapter 2, an isocratic RP-HPLC method for the quantification of gemcitabine was developed and validated showing good linearity and sensitivity with acceptable accuracy and precision. Therefore, the developed analytical method is suitable for its intended purpose. The robustness test and all other parameters have confirmed the analytical method has complied with the requirement of ICH guideline for the development of HPLC analytical method. However, the extra care should be taken during preparation of the mobile phase as the method is very sensitive to change in the ratio of ACN and buffer. The change of pH in mobile phase also significantly affects the elution time and the peak shape of gemcitabine in HPLC.

Following forced degradation, all the gemcitabine peaks were adequately resolved from the degradation products, which ensured the acceptability of this analytical method. The results from forced degradation studies also demonstrated gemcitabine is stable in acid, base environments as well as when exposes to light and under heat-stressed conditions. It only shows a relatively degradation was in oxidative-stress condition. The degradation products were not identified in this part of studies, however most of the degradation products can be identified referring to the literatures. Such as the major degradation product formed under oxidative stress, 4-amino-1-(2-deoxy-2,2-difluro-a-D-erythro-pentofuranosyl) pyrimidin-2(1H)-one which had been reported by Naga M *et al* (Naga Malleswararao, Suryanaryana et al. 2012).

This analytical method was used to analyse gemcitabine in all other experiments such as *in-vitro* drug release studies and enzymatic degradation studies. The enzymatic degradation studies demonstrated that gemcitabine can be degraded by the digestive enzyme to some extent, and the results also demonstrated that gemcitabine, following encapsulation in PLGA NPs, was protected from degradation. These two studies have ensured the application of the developed HPLC analytical method is promising.

In Chapter 3, PLGA and TPGS polymers were conjugated to form PLGA-TPGS random copolymers. FTIR was used to reveal the conjugation of the PLGA and TPGS polymers. Subsequently, using the synthesized polymers to fabricate TMC modified PLGA-TPGS NPs by using a modified solvent evaporation method.

Formulation optimization has been defined as the implementation of systematic approaches to achieve the best combination of product and process characteristics under a given set of conditions (Anteneh 2015). Drug formulation usually involves several variables which influence the formulation characteristics. The traditional approach to develop a formulation is to alter one variable at a time while keeping all the other factors at constant level (Nazzal and Khan 2002). However, this may not the best method to develop an optimized formulation, as the method does not reveal much on the interactions between the variables. Hence of late, factorial designs have become a regular practice globally in the formulation optimization by generating mathematical equations and graphic outcomes, thus depicting a complete picture of variation of the responses as a function of the factors. For easy screening, we concentrated on a 2 levels design at which 'low' and 'high' (-1, +1), respectively, with a centre point for moderate ('0'). In our study, the effects of 3 different factors of concentration of PLGA-TPGS and TPGS stabilizer as well as the 2^{nd} ultrasonication time, on the two responses of particle size and drug entrapment efficiency were evaluated. This design allows estimating all main and interaction effects between these 3 considered factors simultaneously. These interactions are the key to achieving the optimal conditions. But if it is supposed that the effects between the low and moderate factor level (−1, 0) differ from those between moderate and high factor level (0, +1) (non-linear behaviour of response as function of factor levels), therefore two levels with the moderate centre point is important (−1, 0, +1), in order to obtained the curvature of the 3D response surface and better way to evaluate the interaction effects between the factors. Through adding the central points (0) at the intermediate level we were able to estimate the errors of the factorial design and to evaluate the quality of the system repeatability (Vander Heyden, Khots et al. 1993, Radaic, Paula et al. 2015). In our studies, the effects of formulation parameters on the particles physicochemical properties were investigated using CCD with two levels and a centre point design. It was found that concentrations of PLGA-TPGS and TPGS stabilizer as well as the 2^{nd} ultrasonication time had significant effects on the particle size. The particle size increased as the concentration of PLGA-TPGS increased, whereas, the particle size was decreased by an increase of TPGS stabilizer concentration and the 2^{nd} ultrasonication time. Among all the variables, different 2^{nd} ultrasonication time has the most significant influence on particle size of NPs. The effect of these three variables on the particle size can be arranged in the sequence 2^{nd} ultrasonication time > PLGA-TPGS concentration > TPGS concentration.

Morphological examination showed that all particles had a spherical shape with smooth surface. The mean particle size of the prepared NPs varied from 201 to 315 nm, thus, a control of particle size can be achieved by combining the three formulation parameters. As the 2nd ultrasonication time had a greatest effect on the particle size. Therefore, when preparing the TMC modified PLGA-TPGS NPs using solvent evaporation technique, the ultrasonication time must be controlled within a proper range. High intensity of ultrasonication may produce smaller particle size, but it might also results in particle breakage or forming larger pores on the particles surface which lead to drug loss. Moreover, particle size is important in delivering chemotherapeutic agents because of its implications for permeation and retention (Chow and Ho 2013). According to He *et al.*, NPs smaller than 300 nm in diameter are able to penetrate the mucus layer more efficiency, and enhanced intestinal absorption via M cells and enterocytes (He, Yin et al. 2012). These NPs must be larger than 8 nm, however, as NPs smaller than this will permeate inter-endothelial junctions in healthy tissues leading to increased side effects (He, Yin et al. 2012). Interestingly, cancer cells have larger inter-endothelial junctions (between 40 and 1000 nm) (He, Yin et al. 2012), which facilitate greater permeation for our optimal NPs which are approximately between 150 nm to 250 nm. This, along with poor lymphatic drainage in tumours encourages NPs retention and reduces potential side effects, and should be considered for cancer targeting. Win, Feng and colleagues demonstrated that polymeric NPs sized 100-200 nm were optimal for uptake in Caco-2 cell lines, and the NPs may be internalised by receptor-mediated endocytosis (Win and Feng 2005). These findings suggest that our optimal NPs with a size range of 150 nm to 250 nm may have an absorptive advantage over the intestinal epithelial membrane, as well as more drug uptake by cancer cells due to EPR effect.

The entrapment efficiency was found between 69 and 81%. The three tested factors were all positively affecting the drug entrapment efficiency. The drug entrapment efficiency of the NPs is increased when the PLGA-TPGS and TPGS concentration are elevated, while the 2nd ultrasonication time is reduced. The effect of formulation parameters on the drug entrapment efficiency according to the level of impact was 2nd ultrasonication time > TPGS concentration > PLGA-TPGS concentration.

Using Central Composite Design, an optimal formulation condition was found. The optimum formulation with drug entrapment efficiency of 77.82% at size of 216.97 nm was achieved by

BESTPDF.COM
List of research project topics and materials

using 1% w/v PLGA-TPGS, 0.6% w/v TPGS and 150 sec 2nd ultrasonication time. Under the same formulation conditions, TMC coated NPs were prepared subsequently. The final optimal TMC modified PLGA-TPGS NPs show a particle size of 243.21 ± 21.72 nm, zeta potential of +14.70 ± 1.31 mV, entrapment efficiency of 76.43 ± 0.21%, and loading capacity of 5.32 ± 0.12%.

In vitro release profiles showed that TMC modified PLGA-TPGS NPs exhibited an initial burst release followed by slow release over time. Surface adsorption of gemcitabine, rather than entrapping the gemcitabine in the polymer matrix, resulted in substantially faster burst release. After the initial burst, it was expected that the release of the gemcitabine incorporated within the matrix would be influenced by the degradation rate of the copolymer and by the diffusion of the drug through the channels generated during the NPs erosion process. (The drug release mechanism was found following Korsmeyer-Peppas model indicates the drug release is governed by diffusion through the matrix as well as matrix erosion). In addition, the drug release depends on the degradation behaviour of the polymer employed. Release rates can be modified by varying the PLGA and TPGS ratio in the copolymer, the copolymer molecular weight, and the porosity of the polymer matrix. Therefore, controlled release of gemcitabine from TMC modified PLGA-TPGS NPs can be achieved by changing the polymers compositions and modifying formulation parameters.

The *ex-vivo* permeation studies on porcine intestinal epithelial membrane showed that the drug loaded TMC modified PLGA-TPGS NPs had a higher permeation rate compared to drug solution. TMC has been reported to increase drug permeability due to a combination of increased mucoadhesion, promoting residency time, as well as the ability to open tight junctions (Schipper, Olsson et al. 1997). Therefore, TMC coating NPs allows promoting the permeation of the NPs to across the intestinal epithelial membrane. In addition, the positive charge of TMC has effect on the negative charged mucin, due to the electrostatic effect, the TMC coated NPs can well bind to the epithelial membrane, thus enhance the drug loaded NPs permeation.

Moreover, the drug loaded TMC modified PLGA-TPGS NPs demonstrated good stability over three months at 4°C. Drug content was reduced and NPs were aggregated when they were kept at high temperature and moisture. This was caused by polymer degradation at such conditions. Therefore, humid environment should be avoided for the NPs storage.

In Chapter 4, a novel nanoparticulate delivery system of drug loaded TMC-CSK NP was developed and optimized. TMC was successfully synthesised from chitosan via methylation, following a period of pre-formulation optimisation. Chitosan of > 90% deacetylation resulted in greater TMC yield, and was used thereafter. Beyond degree of chitosan deacetylation, other factors must also be considered when attempting to optimise the synthesis of TMC-based NPs. For chitosan, it is known that degree of chitosan deacetylation also impacts the degree of crystallinity, NP degradation time, cellular adhesion (and therefore uptake), drug release, inflammatory response, osteogenesis response, absorption and toxicity (Hidaka, Ito et al. 1999, Freier, Koh et al. 2005, Bowman and Leong 2006, Yuan, Chesnutt et al. 2011). Though not explored in the present study, these characteristics offer opportunities for formulation enhancement in the future. Research is needed to determine the ideal degree of chitosan deacetylation when considering NP design.

The two-step synthesis in turn resulted in a higher TMC yield, and involved several innovations during the synthetic process, including increased stirring times and larger quantities of CH_3I for methylation. Other ideal conditions for favourable TMC synthesis were found to be constant stirring at 450 rpm, temperature of 60°C, a light-free environment, and purification via dialysis membrane. CSK conjugation was achieved under strict environmental conditions to ensure high yield and minimal peptide degradation. NP formulation was trialled within predetermined parameter boundaries, and the optimal conditions found to be stirring at 450 rpm for an hr at room temperature with 0.07 mL of Tween 80 added to prevent aggregation. Under these conditions, we produced gemcitabine-loaded TMC-CSK NPs with the most favourable properties overall.

The applications of this formulation are potentially very useful and industrially simple, though must first overcome several pragmatic limitations. From our research, TMC-CSK has demonstrated favourable particle size and zeta potential to potentiate drug absorption, promising drug entrapment efficiency, sustained drug release profile and great drug permeation over porcine epithelial membrane, as well as good long term stability.

Statistical analysis identified a relationship between formulation parameters and particle size. Through ANOVA tests, TMC concentration was shown to have a significant effect on particle size ($p < 0.05$). When the concentration of TPP was independently altered (i.e. the

ratio between TMC and TPP), there were observed effects on particle size. A TMC : TPP ratio of 3 : 1 yielded the smallest particle size and a TMC:TPP ratio of 1 : 1 the largest. Through t-tests however, only the difference between 3 : 1 and 1 : 1 was shown to be significant ($p < 0.05$). Therefore further investigation is warranted to fully characterise the relationship between TMC : TPP ratio and particle size. Comparing polymers, TMC NPs displayed a smaller mean size than chitosan NPs ($p < 0.05$), and is consistent with previous works (Boonyo, Junginger et al. 2008, Dehousse, Garbacki et al. 2010, Yien, Zin et al. 2012). According to Dehoussea *et al.*, the higher charge density on TMC compared to chitosan results in formation of compact NPs. A theory supported by Ing *et al*. who claimed that TMC NPs had smaller sizes due to the strong electrostatic interactions with polyanionic TPP (Dehousse, Garbacki et al. 2010, Yien, Zin et al. 2012). The effect of CSK on reducing particle size is also observed in the present study. This contradicts work by Jin *et al,* who found that insulin-loaded TMC-CSK NPs exhibited greater size (Jin, Song et al. 2012). According to the authors, this may have been due to the introduction of CSK which bears a molecular weight of 1018 Da and negative charge character. It is important to note that both insulin and CSK bear an overall negative charge, and electrostatic repulsion may have played a role in increasing particle size compared to our formulation. Gemcitabine, by comparison, is of known neutral physiological charge (Konerding, James et al. 2002), and may not have interfered in the electrostatic interactions of TMC and CSK to the same degree. This would have resulted in more compact NPs compared to insulin loaded TMC-CSK NPs.

The present study yielded an average EE of 73.3% across all TMC formulations with no statistically significant difference between formulations (except for formulation D, which was later excluded on the basis of size). This value does not differ greatly from past studies involving chitosan, which have reported encapsulation efficiencies of 78.2% and 80% using bovine serum albumin and insulin respectively (Gan and Wang 2007). For chitosan, incorporation of most drugs occurs via interaction with free positive amine groups (Pan, Li et al. 2002). Gemcitabine interacts through both ionic and hydrogen bonding when formulated via ionic gelation (Hosseinzadeh, Atyabi et al. 2012). Since EE is comparable for all polymers, it is speculated that the interaction still occurs via interactions with residue primary amine groups and available hydrogens, even for methylated TMC (and TMC-CSK). Increased TMC concentration may cause greater hindrance to drug entrapment (Vandenberg, Drolet et al. 2001). Research has shown a lower polymer : TPP mass ratio promotes entrapment. A proposed explanation for this is that a higher TPP mass may cause a rise in

solution pH, leading to an increased overall negative surface charge of a given drug and subsequently enhanced ionic interaction between polymer and drug. For these reasons, formulation parameters were controlled within predefined ranges based on previous works by Gan and Wang (Gan and Wang 2007). Moreover, TMC-CSK NPs displayed a lower EE value relative to TMC and chitosan nanoparticles ($p \leq 0.05$). TMC and CSK are large molecules and conjugation creates stearic hindrance when a third molecule, such as gemcitabine, attempts to incorporate itself (Wang and Huang 2003).

Morphological studies were conducted using SEM. The SEM photographs of individual TMC and TMC-CSK NPs revealed slightly rough surfaces when prepared via ionic gelation, with a polyhedron shape inconsistent with most other findings (Bala, Hariharan et al. 2004, Khursheed 2011). Other research has demonstrated typically spherical polymeric nanoparticles when optimally prepared via ionic gelation because spheres are the most energetically favourable conformation in solution (Bala, Hariharan et al. 2004). One theory which may explain our observation has been posed by Gan *et al*, who postulated that polyhedral shapes are possible where gelation acts to form a nucleus from which polymeric crystallisation occurs, thereby resulting in polyhedral NPs (Gan and Wang 2007). It is also known that freeze dried NPs are susceptible to expansion and fragmentation, and may elicit more rough surfaces than if otherwise measured as a fresh formulation (Choi, Briancon et al. 2004). Hence the true size of the NPs may be smaller and more symmetrical than depicted. A potential complication of unpredictable NP morphology is, in turn, unpredictable drug release (Champion, Katare et al. 2007). An inconsistency with our results has been the observation for TMC NPs, which are typical in shape and surface and may indicate less break-down via freeze drying (Mu and Feng 2003). Aggregation is minimal across preparations indicating relative NP stability, which is concordant with our relatively high surface charges determined via electro-kinetic studies analysing zeta potential.

Sustained but total drug release is a desirable parameter of a NP delivery formulation because it prolongs the effective dose of a given drug (Natarajan, Nugraha et al. 2014). Non-formulated gemcitabine demonstrates rapid release *in vitro* which has problematic implications, including increased risk of side effects, potentially causing local cytotoxic damage and meaning increased frequency of dose administration to sustain a target therapeutic concentration (Zhang, Gu et al. 2008). The drug loaded NPs have demonstrated more sustain release profiles compared to drug solution across measured time points. The

sustained release of the NPs can prolong the effective drug dosage retain in systemic circulation, thus to avoid the frequent drug administration. Additionally, sustain drug release is able to prolong the drug candidate remain within the therapeutic window, improve the AUC and avoid the high peak of drug above the MTC in systemic circulation (Uhrich, Cannizzaro et al. 1999).

CSK modified TMC NPs showed superior permeability over TMC NPs has been reported to be due to a combination of both increased mucoadhesion, as well as a goblet cell targeting CSK peptide which has a transient tight junction opening capability (Jin, Song et al. 2012). There are contrasting opinions regarding the effect of mucous on TMC NP permeation. Behrens *et al*. reported increased permeation with increased mucous presence (Behrens, Pena et al. 2002), directly contrasting other observations that the mucous layer hindered TMC NP permeation (Kerec, Bogataj et al. 2005). Bowman and Leong had investigated the inconsistent relationship between permeation and the mucous layer and suggested reasons for both phenomena (Bowman and Leong 2006). The observed increased permeation is attributed to ionic attraction between TMC and mucous. This attraction increases drug concentration in the extracellular environment and produces a gradient which according to Fick's Law, is favourable for drug permeation (Sherwood 2008). TMC-CSK in turn demonstrates superior permeation to TMC, consistent with the literature reported (Jin, Song et al. 2012). A possible explanation may be CSKs innate ability to actively target goblet cells and promote endocytosis (Jin, Song et al. 2012).

Apparent permeability coefficient (P_{app}) is the rate at which a drug will cross the intestinal epithelial membrane and enter the portal circulation (Youdim, Avdeef et al. 2003). Results showed the TMC-CSK NPs had a higher P_{app} than TMC NPs due to the ability of CSK to target goblet cells to some extent for the TMC-CSK NPs to be up-taken and transported across the epithelial membrane via paraceullar route (Jin, Song et al. 2012). High P_{app} corresponds with high oral absorption, which is important for future applications as modulation may offer opportunities to increase oral bioavailability.

This foundation work has served to formulate and optimise a TMC-CSK nanoparticulate delivery system for gemcitabine, with potential for oral delivery. From this, we are confident of the promise that this formulation bears for the future beyond its infancy, though it will require ongoing investigation and optimisation hereafter.

Chapter 5 have primarily investigated the cellular uptake and transport of the two optimal drug loaded nanoparticulate delivery systems on the co-cultured Caco-2/HT29-MTX-E12 cell membrane, aiming at providing basic information for rational design of optimal drug carriers. The co-culture of Caco-2 and HT29-MTX-E12 cells simulate an entire intestinal epithelial membrane, as it exhibits morphological characteristics similar to the intestinal enterocytes, they have effective tight junctions and contain a number of active transporters, metabolic enzymes as well as the P-gp and MRPs efflux pumps etc. (Hu 1993, Saito and Inui 1993, Delie and Rubas 1997).

Cytotoxicity studies showed both drug loaded NPs were considered non-toxic up to 300 µg/ml (with less than 10% cell death). Indicating the NPs have greater protection of the entrapped gemcitabine from exposing to the intestinal epithelium, thus lower the toxicity of gemcitabine towards to the co-culture of Caco-2 and HT29-MTX-E12 cells. Between the two formulations, drug loaded TMC modified PLGA-TGPS NPs showed a higher IC_{50} compared to drug loaded TMC-CSK NPs, demonstration an overall less toxicity of the TMC modified PLGA-TPGS NPs toward intestinal epithelial cells.

From the *in vitro* cells uptake studies it may be concluded that drug concentration, temperature, uptake time, and the particle size of the NPs all showed significant influence in the drug uptake amount. The rank order of drug uptake is the group of drug loaded TMC-CSK NPs > drug loaded TMC modified PLGA-TPGS NPs > drug solution, under 2 hr incubation at 37 °C. The results also showed the drug loaded NPs had much higher cellular uptake at 37°C than that at 4°C, indicating the cellular uptake is an energy dependent process. In addition, the longer incubation time of drug loaded NPs with cell membrane, the higher amount of the drug uptake, indicating the process is time-dependant and also the uptake was found concentration dependent as well. However, both the drug loaded NPs reached a plateau after certain time demonstrating there was a saturation limit in exposure time, resulted in fewer NPs being internalized into the cells. Moreover, an enhanced cellular uptake could be achieved by decreasing particles size, therefore, the smaller particle size of the nanocarrier is preferred in the characterization studies. Furthermore, the CLSM images showed the distribution of green FITC labelled NPs within the cells after 2 hr incubation, indicating the NPs were distributed throughout the cytoplasm and perinuclear region, thus confirmed the drug loaded NPs had been truly internalized into the cells and were not just adsorbed onto the

cell membranes. The cellular uptake mechanisms were subsequently investigated, demonstrating the process undergoes active transport pathway and mainly associated with adsorptive mediated endocytosis as well as caveolae mediated endocytosis which is consistent to the literature report by Jin *et al* (Jin et al. 2012).

The transport exhibited time-dependent properties for drug solution and the drug loaded NPs. The drug loaded TMC-CSK NPs showed greatest drug transport over the cell membrane compared to the drug solution and drug loaded TMC modified PLGA-TPGS NPs, this result revealed the absorption enhancing ability of CSK peptide modified NPs across the epithelial membranes assigned by their targeting effect is significant. Nevertheless, the transport of the optimal NPs could be significantly increased by efflux pumps inhibitor or absorption enhancers, and decreased by ATP inhibitors, which is in agreement with Suzuki and Lonnerdal, who had studied the entire drug transport process over intestinal epithelial membranes (endocytosis, intracellular trafficking, exocytosis, and transcytosis) of NPs in intestinal epithelial cells (Suzuki and Lönnerdal 2002).

Cell membrane is negatively charged due to the presence of heparin sulfate proteoglycans and glycosaminoglycan. Heparinase is an inhibitor of glycosaminoglycan sulfatation and could hydrolyse proteoglycans (Culley, Fadlon et al. 2003). Therefore with addition of heparinase, it can neutralize the negative charge of the cell surface, thus the positive charge TMC component has no effect in the electrostatic interaction with the cell surface, which lowering the uptake of the NPs. P-gp and MRP_2 are transporters primarily expressed on the apical membranes of the epithelia. They played crucial roles in resisting drug absorption of intestinal mucosa by efflux of drug from the gut epithelial cell back into the intestinal lumen and preventing their absorption into blood (Collett, Higgs et al. 1999). Therefore, deactivation of efflux pump may enhance the transport of drugs into the cells. Inhibition of P-gp mediated gemcitabine elimination showed a main mechanism leading to elevated gemcitabine concentration in our study. These findings, along with studies by others identity that P-gp plays the dominant role in restricting various anticancer drug plasma concentrations (Tsuji 1998, Krishna and Mayer 2000, Mazel, Clair et al. 2001, Vauthier, Dubernet et al. 2003, Aller, Yu et al. 2009). However, for the TMC modified PLGA-TPGS NPs group, the addition of the MRP_2 inhibitor to Caco-2/HT29-MTX-E12 cell membrane resulted in a reduction in the efflux of gemcitabine from AP side to BL side. The data suggested that the role of MRP_2 in the efflux of gemcitabine loaded TMC modified PLGA-TPGS NPs may have

been neglected. The cumulative permeated drug amount from AP to BL of all groups across the cell membrane was significantly increased in the presence of EDTA. Such effect generally supposed to act on tight junctions between adjacent epithelial cells by manipulating paracellular permeability. However, charged molecules or drugs above 400 - 600 Da cannot pass tight junctions because the intercellular space only has a size of up to 7 nm, depending on the cell type (Watson, Rowland et al. 2001, Van Itallie, Holmes et al. 2008). In particular, the permeability of gemcitabine was more restricted by tight junctions. Hence, many studies focused on the investigation of absorption enhancers with compounds acting *via* one or more mechanisms besides opening of the tight junctions (Haffejee, Du Plessis et al. 2001, Yu, Wang et al. 2013). The mechanism of action to enhance the absorption of NPs could be possible explained by addition of an absorption enhancer EDTA. EDTA is able to activate the cellular protein kinase C (PKC) by depletion of extracellular calcium via chelation, resulting in tight junction opening, thus lead to expansion of paracellular route and facilitate the transport of the components through paracellular pathway. Or enhancing the mucoadhesiveness of the NPs (presence of TMC), leading to enhance endocytosis pathway (Bowman and Leong 2006, Kesarwani and Gupta 2013, Velmurugan and Dodla 2013).

According to the literature, many research used the TEER values to predict the tight junction opening phenomenon between adjacent cells. When the tight junctions open, the expansion of paracellular region leads to enhance the overall hydrophilic characteristic between apical and basolateral side of the cell membrane. Therefore a decrease of TEER is expected. In another word, a decrease of TEER would have reflected an increase of the paracellular permeability (Ranaldi, Marigliano et al. 2002, Kesarwani and Gupta 2013). During the cellular transport experiment, the TEER was determined every 30 min. However, there was not any change in TEER values observed. Therefore we assume the tight junction opening process did not performed. Interestingly, TMC based NPs had reported to enhance mucoadhesion toward the mucosal cells surface and trigger the tight junction opening, and facilitate the cellular transport. Our results did not compliant with the literatures, thus in the future studies, whether the optimal NPs can trigger tight junction opening shall be further investigated. A major protein associates with tight junction is known as claudin-4. Therefore after the cells were treated with the drug loaded NPs, the culture medium is removed, and Western blotting for claudin-4 can be evaluated with immunofluorescence staining. If the caludin-4
at cell-cell contact site became segmented and discontinuous, and the red fluorescence signal became much weaker compared to the control group (without any treatment), it indicates the

loss of tight junction function, meaning with the treatment of drug loaded NPs leads to tight junction opening (Yeh, Hsu et al. 2011, Zhang, Zhu et al. 2014). Furthermore, after treatment of drug loaded NPs, the gene level expression of claudin-4 protein that induced by the NP treatments can be evaluated by real time polymerase chain reaction (PCR) technique. By evaluating the claudin-4 protein expression and its mRNA level, it can deduce the tight junction opening performance (Yeh, Hsu et al. 2011, Zhang, Zhu et al. 2014).

For the cellular uptake and transport studies, the co-cultured Caco-2 and HT29-MTX-E12 cells model was set and studied. As Caco-2 cells might not reflect the complete physiology of the intestine, which may result in inappropriate *in vitro/in vivo* correlations (Shi, Cao et al. 2015). Therefore, the co-cultured of the Caco-2 and HT29-MTX-E12 represents an advanced intestinal *in vitro* triple culture permeability model which includes enterocytes, and mucus secreting HT29-MTX cells. In addition, M cells possess a high transcytotic capacity and transport a wide variety of materials, including different types of NPs (Frey and Neutra 1997, Shi, Cao et al. 2015). A study carried out by Harde Das *et al.* reported that ~ 77.9% of absorbed solid lipid NPs were transported into systematic circulation *via* lymph through M cell uptake, which is the major transport pathway (Harde, Das et al. 2011). Therefore, in the future cellular studies, the addition of cell line representing M cells can be considered. It is expected the higher uptake and transport drug amounts of drug loaded NPs will be detected in presence of M cells, which may play a major role in NPs entry of the intestinal epithelium (Antunes, Andrade et al. 2013). From the cellular uptake and transport studies, compared with the free drug and the drug loaded NPs formulations significantly enhanced drug uptake and permeability over intestinal epithelial membranes.

In chapter 6, the *in vivo* pharmacokinetic and pharmacodynamics studies have shown the two optimal NPs have enhanced the oral bioavailability in SD rats and great antitumour effect in BALB/c nude mice.

The cytotoxicity study on 4T1 breast cancer cells, it indicated the safety profile of the synthesized TMC, TMC-CSK, PLGA and PLGA-TPGS polymers, and the drug loaded TMC-CSK NPs showed lower IC_{50} then that of drug loaded TMC modified PLGA-TPGS NPs, demonstrating drug loaded TMC-CSK NPs may have great anticancer effect on 4T1 tumour cells. Since lower the IC_{50} indicating less equivalent drug amount is required to

trigger half number of the cell deaths. However, both of the drug loaded NPs show less toxic to the 4T1 tumour cells compare to the plain drug solution, this may be attributed to the encapsulated drug were not burst released to immediate kill the tumour cells. Since the drug solution is impossible to expose to the tumour cell directly via oral administration, and considering all the physicochemical barriers for oral drug delivery, therefore the application of the drug carrier system is still very necessary.

An effective maximum tolerate drug dose was predicted based on the LD_{50} results obtaining from the *in-vivo* toxicity studies. The predicted dosage showed a great antitumor effect in BALB/c nude mice in pharmacodynamics studies. However, the dosage showed rather toxic to the mice according to the weight loss profile over treatment period. A good standard *in-vivo* acute toxicity studies is normally carried out on 10 male nude mice and 10 female nude mice, with a total number of 20 mice for one dosage group (Rezkalla, Kloner et al. 1988, Parra, Yhebra et al. 2001). In our studies, due to the budget, only 10 male nude mice were assigned to an individual dosage group, therefore, this might reduce the accuracy for the drug dosage prediction.

The plasma half-life and oral bioavailability were significantly improved by loading the drug into the optimal nanoparticulate delivery systems. The drug loaded NPs gemcitabine loaded TMC-CSK NPs showed greatest elevation in oral bioavailability and plasma half-life compared with other groups, which indicating the significant contribution of CSK peptide in promoting drug absorption *in vivo*. The T_{max} of TMC modified PLGA-TPGS NPs showed greater than that of TMC-CSK NPs, this may be attributed to the relatively slower degradation of PLGA-TPGS copolymer compared with the TMC polymer of the TMC based NPs.

The *in-vivo* pharmacodynamics studies demonstrated the promising ability of gemcitabine loaded TMC-CSK NPs and gemcitabine loaded TMC modified PLGA-TPGS NPs to inhibit the growth of tumour cells, suggesting that both of the developed nanoparticulate delivery systems are suitable to deliver gemcitabine orally. Between these two formulations, drug loaded TMC-CSK NPs showed slightly greater inhibition on tumour growth compared with drug loaded TMC modified PLGA-TPGS NPs. This result corresponds to the *in-vivo* pharmacokinetic studies, that the drug loaded TMC-CSK NPs had shown a greater oral bioavailability and longer plasma half-life compared to all other groups. However, the weight

BEST PPT.COM
List of research project topics and materials

loss of the treated nude mice was significant, indicating the safety profile of the gemcitabine loaded delivery system remains a major challenge. The high toxic effect of the drug loaded NPs might be due to the nonselective delivery of drugs to tumour sites that leads to severe side effects, since they can also affect other normal non-targeted organs and tissues. Secondly, the predicted dose from *in-vivo* acute toxicity study might still be too high as previously discussed. Very interestingly, there is no visible toxicity was found from histological studies towards the organs (heart, liver, spleen, lung and kidney) through all formulation groups whereas the drug solution group showed minor toxicity to the liver.

7.2 Limitation and future perspectives

This study was carried out to investigate the feasibility and potential of the two developed polymeric NPs for use in oral delivery of gemcitabine. The two developed formulations were able to achieve the objectives. However, the formulations could be further improved. During the project, the following limitations were encountered, and future directions that could be taken from this research are listed.

- In drug release studies, the initial burst release of the gemcitabine loaded NPs was attributed to the release of the gemcitabine on the surface of NPs or underneath the surface of NPs. The burst effect of the NPs attracted much attention because it may result in the severe adverse action to the GIT (Le Corre, Rytting et al. 1997, Matsumoto, Matsukawa et al. 1997).

  After PLGA-TPGS NPs were formed, the NPs were washed with sucrose solution to remove the residues adsorb on particle surface residues include un-entrapped drugs. Therefore, repeat the washing step is necessary to ensure the un-entrapped gemcitabine is fully eliminated. In addition, formulation parameters also significantly affect the drug release profile, thus the formulation parameters can be further optimised to reduce the burst release.

- According to the literature, the great mucoadhesive property of TMC polymer would lead to tight junction opening for greater drug loaded TMC NPs transport. However, in this project, the TEER between apical and basolateral side of the cell membrane

during drug transport process was determined, and no changes were observed indicating tight junction opening did not perform in this case. Further investigation on tight junction opening performance is necessary. As mentioned earlier, the tight junction associated protein, claudin-4 can be focussed. The claudin-4 protein expression and gene expression can be determined by Western blotting and PCR methods, to evaluate the tight junction opening performance.

- CSK peptide was known as a goblet cells targeting peptide. However, there is not experiment data as strong evidence to support this theory. In this study, CSK modified NPs have shown great permeability over the intestinal epithelial membrane. But the fact that it is particularly target to goblet cells remains uncertain. Moreover, the literature reported that CSK peptide tends to bind to the goblet cells and trigger tight junction to open for the TMC modified NPs to permeate through paracellular pathway. However, our drug transport studies showed tight junction did not open by the TMC-CSK NPs group. Therefore the 'mysterious' CSK peptide should be further investigated, and the concept should be confirmed in the future studies.

- In acute toxicity studies, the predicted effective maximum tolerated dosage from LD_{50} showed very effective in tumour growth inhibition. However, based on the overall safety profile, the mice showed significant weight loss, demonstrating the dose might be over the suitable tolerated level for BALB/c nude mice.

  In the future, in order to predict a more accurate drug dosage with promising anticancer effect and maximum tolerated level for BALB/c nude mice. A greater number of mice should be assigned to each individual dosage when conducting the *in-vivo* acute toxicity studies.

- From the weight loss profiles of the drug loaded NPs treated mice, in histology studies, toxicity signs in the tested organs were expected for the drug loaded NPs groups. However, no major signs of toxicity were found in the tested organs for the both NPs groups. These might be due to the fact that the histological photomicrographs were taken by only one dimensional section of the tested organs, and the particular region did not show any toxicity signs. Therefore in the future, various dimensional sections of the tested organs should be evaluated when taking the

histological photomicrographs. Moreover, another better way to evaluate the toxicity causes to the healthy organs, is by determination of *in vivo* drug distribution. The amount of drug distributed to different organs was extracted and measured. This could directly determine the amount of drug expose to the particular organs.

- The high toxic effect of the drug loaded NPs might be due to the nonselective delivery of drugs to tumour sites that leads to severe side effects, since they can also affect other normal non-targeted organs and tissues. Therefore breast cancer cell targeting ligands such as epidermal growth factor (EGF) (Agus, Akita et al. 2002), or RGD-4C peptide (Arap, Pasqualini et al. 1998) could be conjugated onto the NPs to improve the targeting to cancer cells, as well as avoiding exposure to the healthy organs

7.3 Conclusive remarks

From all the studies performed, this research fulfilled the objective for the development and optimization of nanoparticulate systems (TMC modified PLGA-TPGS NPs, and TMC-CSK NPs) for oral delivery of gemcitabine, and enhanced the gemcitabine oral bioavailability and anticancer therapeutic efficacy. Specially, these studies showed that:

i. A stability-indicating HPLC analytical method was developed and validated. This method has been used for quantifying gemcitabine as well as gemcitabine in the formulation matrix.

ii. Two nanoparticulate delivery systems were developed, and gemcitabine was successfully encapsulated into both delivery systems. In addition, the TMC modified PLGA-TPGS NP was optimized using a specific factorial design, CCD.

iii. The two optimized drug loaded NPs were characterized in terms of particle size, drug distribution, zeta potential, entrapment efficiency, particle morphology, *in vitro* drug release, *ex vivo* drug permeation and long term stability.

iv. A co-cultured Caco-2 and HT29-MTX-E12 cell model was successfully set up. The rate and extent of Caco-2/HT29-MTX-E12 cell uptake and transport of the two optimal drug loaded NPs were determined. The associated cellular uptake and transport mechanisms were subsequently investigated.

v. The *in vivo* pharmacokinetic and pharmacodynamics studies were conducted using SD rat model and BALB/c nude mouse model, respectively. All the pharmacokinetic parameters including gemcitabine half-life and absolute oral bioavailability were determined. The extent of tumour growth rate inhibition was investigated. In addition, the overall safety profiles of nude mice by taking the drug solution and drug loaded NPs were evaluated.

This project has demonstrated that TMC modified PLGA-TPGS NPs and TMC-CSK NPs can be utilised as controlled release drug delivery systems for oral delivery of gemcitabine. They have fulfilled the project aim of improving the oral bioavailability of gemcitabine, and elevating its therapeutic efficacy. All the results confirmed the developed NPs have great potential to become effective oral chemotherapy products for gemcitabine to treat breast cancer.

References

Abbruzzese, J. L., et al. (1991). "A phase I clinical, plasma, and cellular pharmacology study of gemcitabine." Journal of Clinical oncology **9**(3): 491-498.

Abo-Riziq, A., et al. (2011). "Conformational structure of tyrosine, tyrosyl-glycine, and tyrosyl-glycyl-glycine by double resonance spectroscopy." The Journal of Physical Chemistry A **115**(23): 6077-6087.

Agnihotri, S. A., et al. (2006). "Controlled release of cephalexin through gellan gum beads: Effect of formulation parameters on entrapment efficiency, size, and drug release." European Journal of Pharmaceutics and Biopharmaceutics **63**(3): 249-261.

Agnihotri, S. A., et al. (2004). "Recent advances on chitosan-based micro- and nanoparticles in drug delivery." Journal of Controlled Release **100**(1): 5-28.

Agullo, G., et al. (1994). "Quercetin exerts a preferential cytotoxic effect on active dividing colon carcinoma HT29 and Caco-2 cells." Cancer letters **87**(1): 55-63.

Agus, D. B., et al. (2002). "Targeting ligand-activated ErbB2 signaling inhibits breast and prostate tumor growth." Cancer cell **2**(2): 127-137.

Aktaş, Y., et al. (2005). "Development and brain delivery of Chitosan−PEG nanoparticles functionalized with the monoclonal antibody OX26." Bioconjugate Chemistry **16**(6): 1503-1511.

Al-Qadi, S., et al. (2012). "Microencapsulated chitosan nanoparticles for pulmonary protein delivery: in vivo evaluation of insulin-loaded formulations." Journal of controlled release **157**(3): 383-390.

Alcon, V., et al. (2005). "Mucosal delivery of bacterial antigens and CpG oligonucleotides formulated in biphasic lipid vesicles in pigs." The AAPS Journal **7**(3): E566-E571.

Ali, I., et al. (2013). "Analyses of anticancer drugs by capillary electrophoresis: a review." Biomedical Chromatography **27**(10): 1296-1311.

Allen, T. M. and J. M. Everest (1983). "Effect of liposome size and drug release properties on pharmacokinetics of encapsulated drug in rats." Journal of Pharmacology and Experimental Therapeutics **226**(2): 539-544.

Aller, S. G., et al. (2009). "Structure of P-glycoprotein reveals a molecular basis for poly-specific drug binding." Science **323**(5922): 1718-1722.

Amidon, G. L., et al. (1995). "A theoretical basis for a biopharmaceutic drug classification: the correlation of in vitro drug product dissolution and in vivo bioavailability." Pharmaceutical research **12**(3): 413-420.

Anderson, J. M. and M. S. Shive (1997). "Biodegradation and biocompatibility of PLA and PLGA microspheres." Advanced Drug Delivery Reviews **28**(1): 5-24.

Ansari, D., et al. (2013). "Pancreatic cancer–cost for overtreatment with gemcitabine." Acta Oncologica **52**(6): 1146-1151.

Anteneh, A. (2015). PHYSICOCHEMICAL CHARACTERIZATION OF PLECTRANTHUS EDULIS (ETHIOPIAN POTATO) STARCH AND ITS EVALUATION AS A DISINTEGRANT IN PARACETAMOL TABLET FORMULATIONS, AAU.

Anton, N., et al. (2010). "Reverse micelle-loaded lipid nano-emulsions: new technology for nano-encapsulation of hydrophilic materials." International journal of pharmaceutics **398**(1): 204-209.

Antunes, F., et al. (2013). "Establishment of a triple co-culture in vitro cell models to study intestinal absorption of peptide drugs." European Journal of Pharmaceutics and Biopharmaceutics **83**(3): 427-435.

Arap, W., et al. (1998). "Cancer treatment by targeted drug delivery to tumor vasculature in a mouse model." Science **279**(5349): 377-380.

Armbruster, D. A., et al. (1994). "Limit of detection (LQD)/limit of quantitation (LOQ): comparison of the empirical and the statistical methods exemplified with GC-MS assays of abused drugs." Clinical chemistry **40**(7): 1233-1238.

Artursson, P. and J. Karlsson (1991). "Correlation between oral drug absorption in humans and apparent drug permeability coefficients in human intestinal epithelial (Caco-2) cells." Biochemical and biophysical research communications **175**(3): 880-885.

Artursson, P. and C. Magnusson (1990). "Epithelial transport of drugs in cell culture. II: Effect of extracellular calcium concentration on the paracellular transport of drugs of different lipophilicities across monolayers of intestinal epithelial (Caco-2) cells." Journal of Pharmaceutical Sciences **79**(7): 595-600.

Artursson, P., et al. (1996). "Caco-2 monolayers in experimental and theoretical predictions of drug transport." Advanced drug delivery reviews **22**(1): 67-84.

Artursson, P., et al. (2001). "Caco-2 monolayers in experimental and theoretical predictions of drug transport." Advanced Drug Delivery Reviews **46**(1–3): 27-43.

Arya, G., et al. (2011). "Enhanced antiproliferative activity of Herceptin (HER2)-conjugated gemcitabine-loaded chitosan nanoparticle in pancreatic cancer therapy." Nanomedicine: Nanotechnology, Biology and Medicine **7**(6): 859-870.

Astete, C. E. and C. M. Sabliov (2006). "Synthesis and characterization of PLGA nanoparticles." Journal of Biomaterials Science, Polymer Edition **17**(3): 247-289.

Avasthi, P. S. and V. Koshy (1988). "The anionic matrix at the rat glomerular endothelial surface." The Anatomical Record **220**(3): 258-266.

Azzi, G., et al. (1990). "Permeability of the normal rat brain, spinal cord and dorsal root ganglia microcirculations to immunoglobulins G." Biology of the Cell **68**(1-3): 31-36.

Badawy, S. S., et al. (1996). "Potentiometric determination of L-dopa, carbidopa, methyldopa and aspartame using a new trinitrobenzenesulfonate selective electrode." Electroanalysis **8**(11): 1060-1064.

Bakshi, M. and S. Singh (2002). "Development of validated stability-indicating assay methods--critical review." Journal of Pharmaceutical and Biomedical Analysis **28**(6): 1011-1040.

Bala, I., et al. (2004). "PLGA nanoparticles in drug delivery: the state of the art." Critical Reviews™ in Therapeutic Drug Carrier Systems **21**(5).

Baldeschwieler, J. D. (1983). "Tumor-imaging potential of liposomes loaded with In-111-NTA: biodistribution in mice." J Nucl Med **24**: 45-51.

Bansil, R. and B. S. Turner (2006). "Mucin structure, aggregation, physiological functions and biomedical applications." Current Opinion in Colloid & Interface Science **11**(2): 164-170.

Barzegar-Jalali, M., et al. (2008). "Kinetic analysis of drug release from nanoparticles." Journal of Pharmacy and Pharmaceutical Sciences **11**(1): 167-177.

Beaucage, G., et al. (2004). "Particle size distributions from small-angle scattering using global scattering functions." Journal of applied crystallography **37**(4): 523-535.

Beaumier, P. L. and K. J. Hwang (1983). "Effects of liposome size on the degradation of bovine brain sphingomyelin/cholesterol liposomes in the mouse liver." Biochimica et Biophysica Acta (BBA)-Biomembranes **731**(1): 23-30.

Behrens, I., et al. (2002). "Comparative uptake studies of bioadhesive and non-bioadhesive nanoparticles in human intestinal cell lines and rats: the effect of mucus on particle adsorption and transport." Pharmaceutical research **19**(8): 1185-1193.

Behrens, I., et al. (2001). "Transport of lipophilic drug molecules in a new mucus-secreting cell culture model based on HT29-MTX cells." Pharmaceutical research **18**(8): 1138-1145.

Berchane, N. S., et al. (2007). "Effect of mean diameter and polydispersity of PLG microspheres on drug release: Experiment and theory." International journal of pharmaceutics **337**(1): 118-126.

Berezkin, V. G. (2001). "M.S. Tswett's intellectual heritage and modern chromatography." Journal of Analytical Chemistry **56**(6): 587-592.

Bergamini, M. F., et al. (2005). "A disposable electrochemical sensor for the rapid determination of levodopa." Journal of Pharmaceutical and Biomedical Analysis **39**(1-2): 54-59.

Bestpfe.com

Berkland, C., et al. (2002). "Precise control of PLG microsphere size provides enhanced control of drug release rate." Journal of controlled release **82**(1): 137-147.

Biggs, S., et al. (2008). New frontiers in colloid science: a celebration of the career of Brian Vincent, Royal Society of Chemistry.

Blackstein, M., et al. (2002). "Gemcitabine as first-line therapy in patients with metastatic breast cancer: a phase II trial." Oncology **62**(1): 2-8.

Blanco, M. D. and M. J. Alonso (1997). "Development and characterization of protein-loaded poly(lactide-co-glycolide) nanospheres." European Journal of Pharmaceutics and Biopharmaceutics **43**(3): 287-294.

Blaschko, H. and T. L. Chruściel (1960). "The decarboxylation of amino acids related to tyrosine and their awakening action in reserpine-treated mice." The Journal of Physiology **151**(2): 272-284.

Blessy, M., et al. (2014). "Development of forced degradation and stability indicating studies of drugs—A review." Journal of Pharmaceutical Analysis **4**(3): 159-165.

Boonyo, W., et al. (2008). "Preparation and characterization of particles from chitosan with different molecular weights and their trimethyl chitosan derivatives for nasal immunization." Journal of Metals, Materials and Minerals **18**(2): 59-56.

Borisagar, S., et al. (2012). "A validated stability-indicating HPTLC method for the estimation of gemcitabine HCl in its dosage form." JPC-Journal of Planar Chromatography-Modern TLC **25**(1): 77-80.

Bowman, K. and K. W. Leong (2006). "Chitosan nanoparticles for oral drug and gene delivery." International journal of nanomedicine **1**(2): 117.

Box, G. E. P., et al. (1978). Statistics for experimenters: An introduction to design, data analysis and model building. New York, John Wiley and Sons.

Box, G. E. P. and K. B. Wilson (1951). "On the experimental attainment of optimum conditions." Journal of the Royal Statistical Society. Series B (Methodological) **13**(1): 1-45.

Brahma N, S. and K. Kwon H (2007). Drug delivery - oral route. Encyclopedia of pharmaceutical technology. J. Swarbrick. New York, Informa Healthcare. **2**.

Brandau, T. (2002). "Preparation of monodisperse controlled release microcapsules." International Journal of Pharmaceutics **242**(1–2): 179-184.

Brechue, W. F. and T. H. Maren (1993). "pH and drug ionization affects ocular pressure lowering of topical carbonic anhydrase inhibitors." Investigative ophthalmology & visual science **34**(8): 2581-2587.

Brusa, P., et al. (2007). "Antitumor activity and pharmacokinetics of liposomes containing lipophilic gemcitabine prodrugs." Anticancer research **27**(1A): 195-199.

Budhian, A., et al. (2007). "Haloperidol-loaded PLGA nanoparticles: systematic study of particle size and drug content." International journal of pharmaceutics **336**(2): 367-375.

Cafaggi, S., et al. (2007). "Preparation and evaluation of nanoparticles made of chitosan or N-trimethyl chitosan and a cisplatin–alginate complex." Journal of controlled release **121**(1): 110-123.

Calvo, P., et al. (1997). "Development of positively charged colloidal drug carriers: chitosan-coated polyester nanocapsules and submicron-emulsions." Colloid and Polymer Science **275**(1): 46-53.

Campbell, N. R. C. and B. Hasinoff (1989). "Ferrous sulfate reduces levodopa bioavailability: Chelation as a possible mechanism." Clinical Pharmacology and Therapeutics **45**(3): 220-225.

Cannazza, G., et al. (2005). "Detection of levodopa, dopamine and its metabolites in rat striatum dialysates following peripheral administration of l-DOPA prodrugs by mean of HPLC-EC." Journal of Pharmaceutical and Biomedical Analysis **36**(5): 1079-1084.

Carafa, M., et al. (2002). "Lidocaine-loaded non-ionic surfactant vesicles: characterization and in vitro permeation studies." International Journal of Pharmaceutics **231**(1): 21-32.

Cartiera, M. S., et al. (2009). "The uptake and intracellular fate of PLGA nanoparticles in epithelial cells." Biomaterials **30**(14): 2790-2798.

BESTPFE.COM
List of research project topics and materials

Carvalho, F. C., et al. (2010). "Mucoadhesive drug delivery systems." Brazilian Journal of Pharmaceutical Sciences **46**(1): 1-17.

Champion, J. A., et al. (2007). "Particle shape: a new design parameter for micro-and nanoscale drug delivery carriers." Journal of controlled release **121**(1): 3-9.

Chattopadhyay, P., et al. (2006). "Drug encapsulation using supercritical fluid extraction of emulsions." Journal of pharmaceutical sciences **95**(3): 667-679.

Chen, G., et al. (2015). "Mucoadhesive polymers-based film as a carrier system for sublingual delivery of glutathione." Journal of Pharmacy and Pharmacology **67**(1): 26-34.

Chen, G., et al. (2014). "Deformable liposomes by reverse-phase evaporation method for an enhanced skin delivery of (+)-catechin." Drug development and industrial pharmacy **40**(2): 260-265.

Chen, G., et al. (2015). "Development and validation of a stability indicating isocratic HPLC method for gemcitabine with application to drug release from poly lactic-co-glycolic acid nanoparticles and enzymatic degradation studies." Journal of Pharmacy and Pharmacology.

Chen, G., et al. (2015). "Development and validation of a stability indicating isocratic HPLC method for gemcitabine with application to drug release from poly lactic-co-glycolic acid nanoparticles and enzymatic degradation studies." Journal of Pharmacy and Pharmacology **67**(11): 1528-1536.

Chen, L.-T. (1978). "Microcirculation of the spleen: and open or closed circulation?" Science **201**(4351): 157-159.

Chen, X., et al. (2005). "Determination of levodopa by capillary zone electrophoresis using an acidic phosphate buffer and its application in the analysis of beans." Food Chemistry **92**(2): 381-386.

Chiou, W. L. (1978). "Critical evaluation of the potential error in pharmacokinetic studies of using the linear trapezoidal rule method for the calculation of the area under the plasma level-time curve." Journal of pharmacokinetics and biopharmaceutics **6**(6): 539-546.

Choi, M. J., et al. (2004). "Effect of freeze-drying process conditions on the stability of nanoparticles." Drying technology **22**(1-2): 335-346.

Chow, E. K.-H. and D. Ho (2013). "Cancer nanomedicine: from drug delivery to imaging." Science translational medicine **5**(216): 216rv214-216rv214.

Clark, M. A., et al. (2000). "Lectin-mediated mucosal delivery of drugs and microparticles." Advanced drug delivery reviews **43**(2): 207-223.

Clough, G. and L. H. Smaje (1984). "Exchange area and surface properties of the microvasculature of the rabbit submandibular gland following duct ligation." The Journal of physiology **354**(1): 445-456.

Coates, A., et al. (1992). "Prognostic value of quality-of-life scores during chemotherapy for advanced breast cancer. Australian New Zealand Breast Cancer Trials Group." Journal of Clinical oncology **10**(12): 1833-1838.

Cochran, W. G. and G. M. Cox (1957). Experimental designs. New York, John Wiley and Sons.

Coello, J., et al. (2000). "Simultaneous kinetic-spectrophotometric determination of levodopa and benserazide by bi- and three-way partial least squares calibration." Talanta **53**(3): 627-637.

Cohen, S., et al. (1994). "Novel approaches to controlled-release antigen delivery." International Journal of Technology Assessment in Health Care **10**(01): 121-130.

Collett, A., et al. (1999). "Modulation of the Permeability of H2 Receptor Antagonists Cimetidine and Ranitidine by P-Glycoprotein in Rat Intestine and the Human Colonic Cell Line Caco-21." The Journal of pharmacology and experimental therapeutics **288**(1): 178-178.

Collett, A., et al. (1996). "Comparison of HT29-18-C1 and Caco-2 cell lines as models for studying intestinal paracellular drug absorption." Pharmaceutical research **13**(2): 216-221.

Conroy, T., et al. (2011). "FOLFIRINOX versus gemcitabine for metastatic pancreatic cancer." New England Journal of Medicine **364**(19): 1817-1825.

Constantinou, C., et al. (2008). "Vitamin E and cancer: an insight into the anticancer activities of vitamin E isomers and analogs." International journal of cancer **123**(4): 739-752.

Costa, P. and J. M. Sousa Lobo (2001). "Modeling and comparison of dissolution profiles." European Journal of Pharmaceutical Sciences **13**(2): 123-133.

Costantino, L., et al. (2009). Colloidal systems for CNS drug delivery. Progress in Brain Research. S. Hari Shanker, Elsevier. **180:** 35-69.

Couvreur, P., et al. (1997). "Multiple emulsion technology for the design of microspheres containing peptides and oligopeptides." Advanced Drug Delivery Reviews **28**(1): 85-96.

Couvreur, P. and F. Puisieux (1993). "Nano- and microparticles for the delivery of polypeptides and proteins." Advanced Drug Delivery Reviews **10**(2–3): 141-162.

Culley, F. J., et al. (2003). "Proteoglycans are potent modulators of the biological responses of eosinophils to chemokines." European journal of immunology **33**(5): 1302-1310.

Daldrup-Link, H. E., et al. (2000). "Assessing permeability alterations of the blood-bone marrow barrier due to total body irradiation: in vivo quantification with contrast enhanced magnetic resonance imaging." Bone marrow transplantation **25**(1): 71-78.

Dash, S., et al. (2010). "Kinetic modeling on drug release from controlled drug delivery systems." Acta Pol Pharm **67**(3): 217-223.

Davda, J. and V. Labhasetwar (2002). "Characterization of nanoparticle uptake by endothelial cells." International Journal of Pharmaceutics **233**(1-2): 51-59.

Davis, J. L., et al. (2006). "Mucosal permeability of water-soluble drugs in the equine jejunum: a preliminary investigation." Journal of veterinary pharmacology and therapeutics **29**(5): 379-385.

Davis, S. S. (1997). "Biomédical applications of nanotechnology — implications for drug targeting and gene therapy." Trends in Biotechnology **15**(6): 217-224.

de Britto, D., et al. (2012). "N, N, N-trimethyl chitosan nanoparticles as a vitamin carrier system." Food Hydrocolloids **27**(2): 487-493.

Deen, W. M., et al. (1976). "Permeability of renal peritubular capillaries to neutral dextrans dextrans and endogenous albumin." American Journal of Physiology--Legacy Content **231**(2): 283-291.

Deftereos, N. T., et al. (1993). "Flow injection chemiluminometric determination of epinephrine, norepinephrine, dopamine and L-dopa." Analyst **118**(6): 627-632.

Dehousse, V., et al. (2010). "Comparison of chitosan/siRNA and trimethylchitosan/siRNA complexes behaviour in vitro." International journal of biological macromolecules **46**(3): 342-349.

Delie, F. and W. Rubas (1997). "A human colonic cell Line sharing similarities with enterocytes as a model to examine oral absorption: Advantages and limitations of the Caco-2 model." Critical Reviews in Therapeutic Drug Carrier Systems **14**(3): 66.

Derakhshandeh, K. and S. Fathi (2012). "Role of chitosan nanoparticles in the oral absorption of Gemcitabine." International journal of pharmaceutics **437**(1): 172-177.

Desai, M. P., et al. (1996). "Gastrointestinal uptake of biodegradable microparticles: effect of particle size." Pharmaceutical research **13**(12): 1838-1845.

Desai, M. P., et al. (1997). "The mechanism of uptake of biodegradable microparticles in Caco-2 cells is size dependent." Pharmaceutical Research **14**(11): 1568-1573.

Devine, P. L. and I. F. C. McKenzie (1992). "Mucins: structure, function, and associations with malignancy." Bioessays **14**(9): 619-625.

Dintaman, J. M. and J. A. Silverman (1999). "Inhibition of P-glycoprotein by D-α-tocopheryl polyethylene glycol 1000 succinate (TPGS)." Pharmaceutical research **16**(10): 1550-1556.

Dongre, V. G., et al. (2008). "Simultaneous determination of metoprolol succinate and amlodipine besylate in pharmaceutical dosage form by HPLC." Journal of pharmaceutical and biomedical analysis **46**(3): 583-586.

Doshi, P. S. and D. J. Edwards (1981). "Effects of l-dopa on dopamine and norepinephrine concentrations in rat brain assessed by gas chromatography." Journal of Chromatography A **210**(3): 505-511.

Dufes, C., et al. (2004). "Glucose-targeted niosomes deliver vasoactive intestinal peptide (VIP) to the brain." International Journal of Pharmaceutics **285**(1–2): 77-85.

Dunne, M., et al. (2000). "Influence of particle size and dissolution conditions on the degradation properties of polylactide-co-glycolide particles." Biomaterials **21**(16): 1659-1668.

El-Dien, F. A. N., et al. (2005). "Two spectrophotometric assays for dopamine derivatives in pharmaceutical products and in biological samples of schizophrenic patients using copper tetramine complex and triodide reagent." Journal of Biomedicine and Biotechnology **1**: 1-9.

El-Shabouri, M. H. (2002). "Positively charged nanoparticles for improving the oral bioavailability of cyclosporin-A." International journal of pharmaceutics **249**(1): 101-108.

Erlij, D. and A. Martínez-Palomo (1972). "Opening of tight junctions in frog skin by hypertonic urea solutions." The Journal of membrane biology **9**(1): 229-240.

Faisant, N., et al. (2002). "PLGA-based microparticles: elucidation of mechanisms and a new, simple mathematical model quantifying drug release." European journal of pharmaceutical sciences **15**(4): 355-366.

Fan, T., et al. (2014). "Design and evaluation of solid lipid nanoparticles modified with peptide ligand for oral delivery of protein drugs." European Journal of Pharmaceutics and Biopharmaceutics **88**(2): 518-528.

Fanali, S., et al. (2000). "Quality control of benserazide-levodopa and carbidopa-levodopa tablets by capillary zone electrophoresis." ELECTROPHORESIS **21**(12): 2432-2437.

Feng, S.-S., et al. (2009). "Poly(lactide)–vitamin E derivative/montmorillonite nanoparticle formulations for the oral delivery of Docetaxel." Biomaterials **30**(19): 3297-3306.

Feng, S.-S., et al. (2004). "Nanoparticles of biodegradable polymers for clinical administration of paclitaxel." Current Medicinal Chemistry **11**: 413-424.

Feng, S. S. (2004). "Nanoparticles of biodegradable polymers for new-concept chemotherapy." Expert Review of Medical Devices **1**(1): 115-125.

Feng, S. S. (2011). "Chemotherapeutic engineering: Concept, feasibility, safety and prospect-a tribute to shu chien's 80th birthday." Cellular and Molecular Bioengineering **4**(4): 708-716.

Ferlay, J., et al. (2015). "Cancer incidence and mortality worldwide: sources, methods and major patterns in GLOBOCAN 2012." International journal of cancer **136**(5): E359-E386.

Filella, M., et al. (1997). "Analytical applications of photon correlation spectroscopy for size distribution measurements of natural colloidal suspensions: capabilities and limitations." Colloids and Surfaces A: Physicochemical and Engineering Aspects **120**(1): 27-46.

Fogh, J., et al. (1977). "One hundred and twenty-seven cultured human tumor cell lines producing tumors in nude mice." Journal of the National Cancer Institute **59**: 221-226.

Fonseca, C., et al. (2002). "Paclitaxel-loaded PLGA nanoparticles: preparation, physicochemical characterization and *in vitro* anti-tumoral activity." Journal of Controlled Release **83**(2): 273-286.

Foster, K. A., et al. (2001). "Microparticulate uptake mechanisms of *in-vitro* cell culture models of the respiratory epithelium." Journal of Pharmacy and Pharmacology **53**(1): 57-66.

Fotakis, G. and J. A. Timbrell (2006). "In vitro cytotoxicity assays: comparison of LDH, neutral red, MTT and protein assay in hepatoma cell lines following exposure to cadmium chloride." Toxicology Letters **160**(2): 171-177.

Fredenberg, S., et al. (2011). "The mechanisms of drug release in poly (lactic-co-glycolic acid)-based drug delivery systems—a review." International journal of pharmaceutics **415**(1): 34-52.

Freier, T., et al. (2005). "Controlling cell adhesion and degradation of chitosan films by N-acetylation." Biomaterials **26**(29): 5872-5878.

Frey, A. and M. R. Neutra (1997). "Targeting of mucosal vaccines to Peyer's patch M cells." Behring Institute Mitteilungen(98): 376-389.

Fu, X., et al. (2005). "Effects of formulation factors on encapsulation efficiency and release behaviour *in vitro* of huperzine A-PLGA microspheres." Journal of Microencapsulation **22**(7): 705-714.

Gad, S. (2008). Pharmaceutical manufacturing handbook: production and processes. New Jersey, Wiley-Interscience.

Gali-Muhtasib, H., et al. (2006). "Thymoquinone: a promising anti-cancer drug from natural sources." The international journal of biochemistry & cell biology **38**(8): 1249-1253.

Gan, L.-S. L. and D. R. Thakker (1997). "Applications of the Caco-2 model in the design and development of orally active drugs: elucidation of biochemical and physical barriers posed by the intestinal epithelium." Advanced Drug Delivery Reviews **23**(1–3): 77-98.

Gan, Q. and T. Wang (2007). "Chitosan nanoparticle as protein delivery carrier—systematic examination of fabrication conditions for efficient loading and release." Colloids and Surfaces B: Biointerfaces **59**(1): 24-34.

Gasco, M. R. (1993). Method for producing solid lipid microspheres having a narrow size distribution, Google Patents.

Geys, J., et al. (2006). "*In vitro* study of the pulmonary translocation of nanoparticles: A preliminary study." Toxicology Letters **160**(3): 218-226.

Giannasca, P. J., et al. (1999). "Human intestinal M cells display the sialyl Lewis A antigen." Infection and immunity **67**(2): 946-953.

González, A. G. (1993). "Optimization of pharmaceutical formulations based on response-surface experimental designs." International Journal of Pharmaceutics **97**(1-3): 149-159.

Govender, T., et al. (1999). "PLGA nanoparticles prepared by nanoprecipitation: drug loading and release studies of a water soluble drug." Journal of controlled release **57**(2): 171-185.

Grès, M.-C., et al. (1998). "Correlation between oral drug absorption in humans, and apparent drug permeability in TC-7 cells, a human epithelial intestinal cell line: comparison with the parental Caco-2 cell line." Pharmaceutical research **15**(5): 726-733.

Grit, M. and D. J. A. Crommelin (1993). "Chemical stability of liposomes: implications for their physical stability." Chemistry and physics of lipids **64**(1-3): 3-18.

Grit, M., et al. (1993). "Hydrolysis of saturated soybean phosphatidylcholine in aqueous liposome dispersions." Journal of pharmaceutical sciences **82**(4): 362-366.

Grob, R. L. and E. F. Barry (2004). Modern practice of gas chromatography, John Wiley & Sons.

Guetens, G., et al. (2002). "Hyphenated techniques in anticancer drug monitoring: I. Capillary gas chromatography–mass spectrometry." Journal of Chromatography A **976**(1): 229-238.

Guideline, I. C. H. H. T. (2005). "Validation of analytical procedures: text and methodology." Q2 (r1) **1**.

Guo, L., et al. (2009). "A novel spectrophotometric method for the determination of levodopa with the detection system of potassium ferricyanide-Fe(III)." Journal of the Chinese Chemistry Society **56**: 568-574.

Gupta, R. C. (2011). Toxicology of organophosphate & carbamate compounds, Academic Press.

Habgood, M. D., et al. (2000). "Determinants of passive drug Entry into the central nervous system." Cellular and Molecular Neurobiology **20**(2): 231-253.

Haffejee, N., et al. (2001). "Intranasal toxicity of selected absorption enhancers." Die Pharmazie **56**(11): 882-888.

Hamilton, R. J. and S. P. A. (1982). Introduction to high performance liquid chromatography. London, Chapman and Hall.

Han, C. and B. Wang (2005). "Factors that impact the developability of drug candidates." Drug Delivery: Principles and Applications, Second Edition: 1-18.

Bestpte.com

Hansen, D. W., et al. (1992). "Systemic analgesic activity and .delta.-opioid selectivity in [2,6-dimethyl-Tyr1, D-Pen2, D-Pen5]enkephalin." Journal of Medicinal Chemistry **35**(4): 684-687.

Hao, W.-H., et al. (2013). "In vitro and in vivo studies of pharmacokinetics and antitumor efficacy of D07001-F4, an oral gemcitabine formulation." Cancer chemotherapy and pharmacology **71**(2): 379-388.

Harde, H., et al. (2011). "Solid lipid nanoparticles: an oral bioavailability enhancer vehicle." Expert opinion on drug delivery **8**(11): 1407-1424.

Harfouche, R., et al. (2009). "Nanoparticle-mediated targeting of phosphatidylinositol-3-kinase signaling inhibits angiogenesis." Angiogenesis **12**(4): 325-338.

Harush-Frenkel, O., et al. (2007). "Targeting of nanoparticles to the clathrin-mediated endocytic pathway." Biochemical and biophysical research communications **353**(1): 26-32.

Hauschild, V. and J. King (2011). "as Chemical Warfare Agents: Community Preparedness Guidelines." Toxicology of Organophosphate & Carbamate Compounds: 47.

Hayakawa, T., et al. (1980). "A simple and specific determination of trypsin in human duodenal juice." Gastroenterologia Japonica **15**(2): 135-139.

He, C., et al. (2010). "Effects of particle size and surface charge on cellular uptake and biodistribution of polymeric nanoparticles." Biomaterials **31**(13): 3657-3666.

He, C., et al. (2012). "Size-dependent absorption mechanism of polymeric nanoparticles for oral delivery of protein drugs." Biomaterials **33**(33): 8569-8578.

Hermanson, G. T. (2008). Chapter 2 - The Chemistry of Reactive Groups. Bioconjugate Techniques (Second Edition). New York, Academic Press**:** 176-178.

Heslinga, M. J., et al. (2009). "Fabrication of biodegradable spheroidal microparticles for drug delivery applications." Journal of Controlled Release **138**(3): 235-242.

Hidaka, Y., et al. (1999). "Histopathological and immunohistochemical studies of membranes of deacetylated chitin derivatives implanted over rat calvaria." Journal of biomedical materials research **46**(3): 418-423.

Higuchi, T. (1963). "Mechanism of sustained-action medication. Theoretical analysis of rate of release of solid drugs dispersed in solid matrices." Journal of Pharmaceutical Sciences **52**(12): 1145-1149.

Hilgendorf, C., et al. (2000). "Caco-2 versus caco-2/HT29-MTX co-cultured cell lines: permeabilities via diffusion, inside-and outside-directed carrier-mediated transport." Journal of pharmaceutical sciences **89**(1): 63-75.

Hilgers, A. R., et al. (1990). "Caco-2 cell monolayers as a model for drug transport across the intestinal mucosa." Pharmaceutical research **7**(9): 902-910.

Ho, G., et al. (1997). "Role of heparan sulfate proteoglycans in the uptake and degradation of tissue factor pathway inhibitor-coagulation factor Xa complexes." Journal of Biological Chemistry **272**(27): 16838-16844.

Hong, C.-Y., et al. (2011). "In vitro cytotoxicity and intracellular bioimaging of dendritic platinum nanoparticles by differential interference contrast (DIC)." Chemistry Letters **40**(4): 408-409.

Hosseinzadeh, H., et al. (2012). "Chitosan–Pluronic nanoparticles as oral delivery of anticancer gemcitabine: preparation and in vitro study." International journal of nanomedicine **7**: 1851.

Houchin, M. L. and E. M. Topp (2008). "Chemical degradation of peptides and proteins in PLGA: a review of reactions and mechanisms." Journal of pharmaceutical sciences **97**(7): 2395-2404.

Hu, M. (1993). "Comparison of uptake characteristics of thymidine and zidovudine in a human intestinal epithelial model system." Journal of Pharmaceutical Sciences **82**(8): 829-833.

Hu, Y. F., et al. (2006). "Effects of genetic polymorphisms of CYP3A4, CYP3A5 and MDR1 on cyclosporine pharmacokinetics after renal transplantation." Clinical and experimental pharmacology and physiology **33**(11): 1093-1098.

BEST PPE.COM
List of research project topics and materials

Huang, M., et al. (2002). "Uptake of FITC-chitosan nanoparticles by A549 cells." Pharmaceutical research **19**(10): 1488-1494.

Hubatsch, I., et al. (2007). "Determination of drug permeability and prediction of drug absorption in Caco-2 monolayers." Nature protocols **2**(9): 2111-2119.

Huet, C., et al. (1987). "Absorptive and mucus-secreting subclones isolated from a multipotent intestinal cell line (HT-29) provide new models for cell polarity and terminal differentiation." The Journal of Cell Biology **105**(1): 345-357.

Hung, L.-H., et al. (2010). "PLGA micro/nanosphere synthesis by droplet microfluidic solvent evaporation and extraction approaches." Lab on a Chip **10**(14): 1820-1825.

Hunter, R. J. (2013). Zeta potential in colloid science: principles and applications, Academic press.

Hussain, A., et al. (2004). "Absorption enhancers in pulmonary protein delivery." Journal of controlled release **94**(1): 15-24.

Hussain, A., et al. (2009). "Clove (Syzygium aromaticum) extract potentiates gemcitabine cytotoxic effect on human cervical cancer cell line." Int J Cancer Res **5**: 95-104.

ICH (2005). "Guideline Q2 (R1): Validation of Analytical Procedures: Text and Methodology

".

Illum, L., et al. (1986). "Evaluation of carrier capacity and release characteristics for poly(butyl 2-cyanoacrylate) nanoparticles." International Journal of Pharmaceutics **30**(1): 17-28.

Ingebrigtsen, L. and M. Brand (2002). "Determination of the size distribution of liposomes by SEC fractionation, and PCS analysis and enzymatic assay of lipid content." AAPS PharmSciTech **3**(2): 9-15.

Ingebrigtsen, L. and M. Brandl (2002). "Determination of the size distribution of liposomes by SEC fractionation, and PCS analysis and enzymatic assay of lipid content." AAPS PharmSciTech **3**(2): 9-15.

Ivić, M. L. A., et al. (2016). Contribution to the Recent Advances in Electrochemical Analysis of Pharmaceuticals. Biomedical and Pharmaceutical Applications of Electrochemistry, Springer**:** 89-195.

Jacobs, C. and R. H. Müller (2002). "Production and characterization of a budesonide nanosuspension for pulmonary administration." Pharmaceutical research **19**(2): 189-194.

Jain, R. A. (2000). "The manufacturing techniques of various drug loaded biodegradable poly(lactide-co-glycolide) (PLGA) devices." Biomaterials **21**(23): 2475-2490.

Jalil, R. and J. R. Nixon (1990). "Biodegradable poly(lactic acid) and poly(lactide-co-glycolide) microcapsules: problems associated with preparative techniques and release properties." Journal of Microencapsulation **7**(3): 297-325.

Jani, P., et al. (1990). "Nanoparticle uptake by the rat gastrointestinal mucosa: quantitation and particle size dependency." Journal of Pharmacy and Pharmacology **42**(12): 821-826.

Janoria, K. G. and A. K. Mitra (2007). "Effect of lactide/glycolide ratio on the in vitro release of ganciclovir and its lipophilic prodrug (GCV-monobutyrate) from PLGA microspheres." International journal of pharmaceutics **338**(1): 133-141.

Jansen, P. J., et al. (2000). "The degradation of the antitumor agent gemcitabine hydrochloride in an acidic aqueous solution at pH 3.2 and identification of degradation products." Journal of pharmaceutical sciences **89**(7): 885-891.

Jepson, M. A., et al. (1996). "Targeting to intestinal M Cells." Journal of Anatomy **189**: 507-516.

Jiang, M., et al. (2012). "Cationic core–shell liponanoparticles for ocular gene delivery." Biomaterials **33**(30): 7621-7630.

Jin, Y., et al. (2012). "Goblet cell-targeting nanoparticles for oral insulin delivery and the influence of mucus on insulin transport." Biomaterials **33**(5): 1573-1582.

Johnson, J. C., et al. (1973). "An improved method for the assay of dopa." Analytical Biochemistry **54**(1): 129-136.

Joshi, G., et al. (2014). "Enhanced bioavailability and intestinal uptake of Gemcitabine HCl loaded PLGA nanoparticles after oral delivery." European Journal of Pharmaceutical Sciences **60**: 80-89.

Jung, T., et al. (2000). "Biodegradable nanoparticles for oral delivery of peptides: is there a role for polymers to affect mucosal uptake?" European Journal of Pharmaceutics and Biopharmaceutics **50**(1): 147-160.

Kafil, J. B. and B. S. Dhingra (1994). "Stability-indicating method for the determination of levodopa, levodopa--carbidopa and related impurities." Journal of Chromatography A **667**(1-2): 175-181.

Kafka, A. P., et al. (2010). "Rapid and specific high-performance liquid chromatography for the in vitro quantification of d-Lys 6-GnRH in a microemulsion-type formulation in the presence of peptide oxidation products." Biomedical Chromatography **24**(2): 132.

Kang, S. K., et al. (2008). "Identification of a peptide sequence that improves transport of macromolecules across the intestinal mucosal barrier targeting goblet cells." Journal of biotechnology **135**(2): 210-216.

Katas, H. and H. O. Alpar (2006). "Development and characterisation of chitosan nanoparticles for siRNA delivery." Journal of controlled release **115**(2): 216-225.

Kerec, M., et al. (2005). "Permeability of pig urinary bladder wall: the effect of chitosan and the role of calcium." European journal of pharmaceutical sciences **25**(1): 113-121.

Kesarwani, K. and R. Gupta (2013). "Bioavailability enhancers of herbal origin: An overview." Asian pacific journal of tropical biomedicine **3**(4): 253-266.

Kesisoglou, F., et al. (2007). "Nanosizing — Oral formulation development and biopharmaceutical evaluation." Advanced Drug Delivery Reviews **59**(7): 631-644.

Khursheed, A. (2011). Scanning electron microscope optics and spectrometers, World Scientific.

Kim, S. H., et al. (2005). "Target-specific cellular uptake of PLGA nanoparticles coated with poly(l-lysine)−poly(ethylene glycol)−folate conjugate." Langmuir **21**(19): 8852-8857.

King, G. L. and S. M. Johnson (1985). "Receptor-mediated transport of insulin across endothelial cells." Science **227**(4694): 1583-1586.

Kirkland, J. J., et al. (1977). "Sampling and extra-column effects in high-performance liquid chromatography; influence of peak skew on plate count calculations." Journal of chromatographic science **15**(8): 303-316.

Kirstein, M. N., et al. (2006). "High-performance liquid chromatographic method for the determination of gemcitabine and 2′, 2′-difluorodeoxyuridine in plasma and tissue culture media." Journal of Chromatography B **835**(1): 136-142.

Konan, Y. N., et al. (2002). "Preparation and characterization of sterile and freeze-dried sub-200 nm nanoparticles." International Journal of Pharmaceutics **233**(1–2): 239-252.

Konerding, D., et al. (2002). "NMR structure of a gemcitabine-substituted model Okazaki fragment." Biochemistry **41**(3): 839-846.

Konstantinos, A. (2004). "Pegylated poly(lactide) and poly(lactide-co-glycolide) nanoparticles: Preparation, properties and possible applications in drug delivery." Current Drug Delivery **1**: 321-333.

Korsmeyer, R. W., et al. (1983). "Mechanisms of solute release from porous hydrophilic polymers." International Journal of Pharmaceutics **15**(1): 25-35.

Kraft, J. C., et al. (2014). "Emerging research and clinical development trends of liposome and lipid nanoparticle drug delivery systems." Journal of pharmaceutical sciences **103**(1): 29-52.

Krishna, R. and L. D. Mayer (2000). "Multidrug resistance (MDR) in cancer: mechanisms, reversal using modulators of MDR and the role of MDR modulators in influencing the

pharmacokinetics of anticancer drugs." European journal of pharmaceutical sciences **11**(4): 265-283.

Kubicka, S., et al. (2000). "Phase II study of systemic gemcitabine chemotherapy for advanced unresectable hepatobiliary carcinomas." Hepato-gastroenterology **48**(39): 783-789.

Kulkarni, S. A. and S.-S. Feng (2013). "Effects of particle size and surface modification on cellular uptake and biodistribution of polymeric nanoparticles for drug delivery." Pharmaceutical research **30**(10): 2512-2522.

Kumar, K., et al. (2014). "Bioadhesive polymers: Novel tool for drug delivery." Artificial cells, nanomedicine, and biotechnology **42**(4): 274-283.

Kumar, M. N. V. R., et al. (2004). "Preparation and characterization of cationic PLGA nanospheres as DNA carriers." Biomaterials **25**(10): 1771-1777.

Lao, L. L., et al. (2008). "Modeling of drug release from biodegradable polymer blends." European Journal of Pharmaceutics and Biopharmaceutics **70**(3): 796-803.

Larson, R. G. (1999). Foams, emulsions, and blends, The structure and rheology of complex fluids. New Yord, Oxiford University.

Le Corre, P., et al. (1997). "*In vitro* controlled release kinetics of local anaesthetics from poly(D, L-lactide) and poly(lactide-co-glycolide) microspheres." Journal of Microencapsulation **14**(2): 243-255.

Lee, C. C., et al. (2005). "Designing dendrimers for biological applications." Nature biotechnology **23**(12): 1517-1526.

Lesuffleur, T., et al. (1990). "Growth adaptation to methotrexate of HT-29 human colon carcinoma cells is associated with their ability to differentiate into columnar absorptive and mucus-secreting cells." Cancer Research **50**(19): 6334-6343.

Lewis, G. A., et al. (1999). Pharmaceutical experimental design. New York, Markel Dekker.

Li, D., et al. (2012). "Development of an isocratic HPLC method for catechin quantification and its application to formulation studies." Fitoterapia **83**(7): 1267-1274.

Li, H., et al. (2009). "Enhancement of gastrointestinal absorption of quercetin by solid lipid nanoparticles." Journal of controlled release **133**(3): 238-244.

Li, S. (1999). "Hydrolytic degradation characteristics of aliphatic polyesters derived from lactic and glycolic acids." Journal of Biomedical Materials Research **48**(3): 342-353.

Lian, T. and R. J. Y. Ho (2001). "Trends and developments in liposome drug delivery systems." Journal of Pharmaceutical Sciences **90**(6): 667-680.

Liang, X.-L., et al. (2012). "Transport properties of puerarin and effect of Radix Angelicae Dahuricae extract on the transport of puerarin in Caco-2 cell model." Journal of ethnopharmacology **144**(3): 677-682.

Liao, L. F., et al. (2002). "FTIR study of adsorption and photochemistry of amide on powdered TiO 2: Comparison of benzamide with acetamide." Physical Chemistry Chemical Physics **4**(18): 4584-4589.

Lin, N.-M., et al. (2004). "Determination of gemcitabine and its metabolite in human plasma using high-pressure liquid chromatography coupled with a diode array detector." Acta Pharmacologica Sinica **25**: 1584-1589.

Lipinski, C. A. (2000). "Drug-like properties and the causes of poor solubility and poor permeability." Journal of pharmacological and toxicological methods **44**(1): 235-249.

Liu, J., et al. (2012). "Preparation and characterization of cationic curcumin nanoparticles for improvement of cellular uptake." Carbohydrate polymers **90**(1): 16-22.

Liu, K. and E. Kiran (2008). "High-pressure solution blending of poly (ε-caprolactone) with poly (methyl methacrylate) in acetone+ carbon dioxide." Polymer **49**(6): 1555-1561.

Liu, Y., et al. (2003). "Fluorometric determination of 3,4-dihydroxyphenylalanine with 2-cyanoacetamide." Journal of Fluorescence **13**(2): 123-128.

Lockman, P. R., et al. (2004). "Nanoparticle surface charges alter blood–brain barrier integrity and permeability." Journal of Drug Targeting **12**(9-10): 635-641.

Lockman, P. R., et al. (2002). "Nanoparticle technology for drug delivery across the blood-brain barrier." Drug Development and Industrial Pharmacy **28**(1): 1-13.

Loo, S. C. J., et al. (2010). "Drug release from irradiated PLGA and PLLA multi-layered films." Journal of pharmaceutical sciences **99**(7): 3060-3071.

Lopedota, A., et al. (2007). "Effect of cyclodextrins on physico-chemical and release properties of Eudragit RS 100 microparticles containing glutathione." Journal of Inclusion Phenomena and Macrocyclic Chemistry **57**(1-4): 425-432.

Losa, R., et al. (2006). "Simultaneous determination of gemcitabine di-and triphosphate in human blood mononuclear and cancer cells by RP-HPLC and UV detection." Journal of Chromatography B **840**(1): 44-49.

Losa, R., et al. (2005). "Development and validation of an ion pair HPLC method for gemcitabine and 2′, 2′-difluoro-2′-deoxyuridine determination." Analytica chimica acta **528**(2): 255-260.

Lough, W. J. and I. W. Wainer (1995). High performance liquid chromatography: fundamental principles and practice. London, Blackie Academic & Professional.

Lu, R. H., et al. (1999). "Degradation and aggregation of human calcitonin in vitro." Pharmaceutical research **16**(3): 359-367.

Luan, X. and R. Bodmeier (2006). "Modification of the tri-phasic drug release pattern of leuprolide acetate-loaded poly (lactide-co-glycolide) microparticles." European Journal of Pharmaceutics and Biopharmaceutics **63**(2): 205-214.

Lutty, G. A., et al. (2010). "Development of the human choriocapillaris." Eye **24**(3): 408-415.

Ma, Y., et al. (2010). "Nanoparticles of poly (lactide-co-glycolide)-da-tocopheryl polyethylene glycol 1000 succinate random copolymer for cancer treatment." Nanoscale research letters **5**(7): 1161-1169.

Maa, Y.-F. and S. J. Prestrelski (2000). "Biopharmaceutical powders particle formation and formulation considerations." Current pharmaceutical biotechnology **1**(3): 283-302.

Magenheim, B., et al. (1993). "A new in vitro technique for the evaluation of drug release profile from colloidal carriers-ultrafiltration technique at low pressure." International journal of pharmaceutics **94**(1): 115-123.

Mahler, G. J., et al. (2009). "Characterization of Caco-2 and HT29-MTX cocultures in an in vitro digestion/cell culture model used to predict iron bioavailability." The Journal of nutritional biochemistry **20**(7): 494-502.

Makadia, H. K. and S. J. Siegel (2011). "Poly lactic-co-glycolic acid (PLGA) as biodegradable controlled drug delivery carrier." Polymers **3**(3): 1377-1397.

Makhlof, A., et al. (2011). "A mucoadhesive nanoparticulate system for the simultaneous delivery of macromolecules and permeation enhancers to the intestinal mucosa." Journal of controlled release **149**(1): 81-88.

Manjunath, K. and V. Venkateswarlu (2005). "Pharmacokinetics, tissue distribution and bioavailability of clozapine solid lipid nanoparticles after intravenous and intraduodenal administration." Journal of controlled release **107**(2): 215-228.

Manuela Garrido, E., et al. (1997). "Flow injection amperometric determination of l-dopa, epinephrine or dopamine in pharmaceutical preparations." Journal of Pharmaceutical and Biomedical Analysis **15**(6): 845-849.

Marcolino-Júnior, L. H., et al. (2001). "Flow injection determination of levodopa in tablets using a solid-phase reactor containing lead(IV) dioxide immobilized." Journal of Pharmaceutical and Biomedical Analysis **25**(3-4): 393-398.

Marks, D. C., et al. (1992). "The MTT cell viability assay for cytotoxicity testing in multidrug-resistant human leukemic cells." Leukemia research **16**(12): 1165-1173.

Marschütz, M. K. and A. Bernkop-Schnürch (2000). "Oral peptide drug delivery: polymer–inhibitor conjugates protecting insulin from enzymatic degradation in vitro." Biomaterials **21**(14): 1499-1507.

Mathialagan, N. and T. R. Hansen (1996). "Pepsin-inhibitory activity of the uterine serpins." Proceedings of the National Academy of Sciences **93**(24): 13653-13658.

Bestpfe.com

Matsson, P., et al. (2009). "Identification of novel specific and general inhibitors of the three major human ATP-binding cassette transporters P-gp, BCRP and MRP2 among registered drugs." Pharmaceutical research **26**(8): 1816-1831.

Matsumoto, A., et al. (1997). "The polymer-alloys method as a new preparation method of biodegradable microspheres: principle and application to cisplatin-loaded microspheres." Journal of Controlled Release **48**(1): 19-27.

Mazel, M., et al. (2001). "Doxorubicin-peptide conjugates overcome multidrug resistance." Anti-cancer drugs **12**(2): 107-116.

Mei, L., et al. (2013). "Pharmaceutical nanotechnology for oral delivery of anticancer drugs." Advanced drug delivery reviews **65**(6): 880-890.

Merck (2001). The Merck Index. NJ, Merck & Co., INC.

Mislick, K. A. and J. D. Baldeschwieler (1996). "Evidence for the role of proteoglycans in cation-mediated gene transfer." Proceedings of the National Academy of Sciences **93**(22): 12349-12354.

Mittal, G., et al. (2007). "Estradiol loaded PLGA nanoparticles for oral administration: Effect of polymer molecular weight and copolymer composition on release behavior in vitro and in vivo." Journal of Controlled Release **119**(1): 77-85.

Möckel, J. E. and B. C. Lippold (1993). "Zero-order drug release from hydrocolloid matrices." Pharmaceutical research **10**(7): 1066-1070.

Moghimi, S. M., et al. (2001). "Long-circulating and target-specific nanoparticles: Theory to practice." Pharmacological Reviews **53**(2): 283-318.

Mondal, N., et al. (2010). "Preparation, characterization, and biodistribution of letrozole loaded PLGA nanoparticles in Ehrlich Ascites tumor bearing mice." International journal of pharmaceutics **397**(1): 194-200.

Montgomery, D. C. (1999). Design and analysis of experiments New York, John Wiley and Sons.

Mourya, V. K. and N. N. Inamdar (2009). "Trimethyl chitosan and its applications in drug delivery." Journal of Materials Science: Materials in Medicine **20**(5): 1057-1079.

Mu, L. and S. S. Feng (2003). "A novel controlled release formulation for the anticancer drug paclitaxel (Taxol®): PLGA nanoparticles containing vitamin E TPGS." Journal of controlled release **86**(1): 33-48.

Mu, L. and P. H. Seow (2006). "Application of TPGS in polymeric nanoparticulate drug delivery system." Colloids and Surfaces B: Biointerfaces **47**(1): 90-97.

Murakami, H., et al. (1997). "Influence of the degrees of hydrolyzation and polymerization of poly (vinylalcohol) on the preparation and properties of poly (DL-lactide-co-glycolide) nanoparticle." International journal of pharmaceutics **149**(1): 43-49.

Musumeci, T., et al. (2006). "PLA/PLGA nanoparticles for sustained release of docetaxel." International journal of pharmaceutics **325**(1): 172-179.

Myers, D. (1999). Surfaces, interfaces, and colloids: principles and applications. New York, Wiley-VCH.

Myers, R. H., et al. (2009). Response surface methodology : process and product optimization using designed experiments New York, Wiley.

Naga Malleswararao, C. S., et al. (2012). "STABILITY INDICATING UPLC METHOD FOR THE RAPID SEPARATION OF RELATED COMPONENTS OF GEMCITIBINE HYDROCHLORIDE." Journal of Liquid Chromatography & Related Technologies **35**(18): 2511-2523.

Nagaraja, P., et al. (1998). "Spectrophotometric methods for the determination of certain catecholamine derivatives in pharmaceutical preparations." Talanta **46**(1): 39-44.

Nagaraja, P., et al. (2001). "A new sensitive and selective spectrophotometric method for the determination of catechol derivatives and its pharmaceutical preparations." Journal of Pharmaceutical and Biomedical Analysis **25**(3-4): 417-424.

Natarajan, J. V., et al. (2014). "Sustained-release from nanocarriers: a review." Journal of controlled release **193**: 122-138.

BESTPFE.COM
List of research project topics and materials

Nazzal, S. and M. A. Khan (2002). "Response surface methodology for the optimization of ubiquinone self-nanoemulsified drug delivery system." AAPS PharmSciTech **3**(1): 23-31.

Neuzil, J., et al. (2007). "Vitamin E analogs, a novel group of “mitocans,” as anticancer agents: the importance of being redox-silent." Molecular pharmacology **71**(5): 1185-1199.

Norris, D. A., et al. (1998). "The effect of physical barriers and properties on the oral absorption of particulates." Advanced drug delivery reviews **34**(2): 135-154.

Norris, D. A. and P. J. Sinko (1997). "Effect of size, surface charge, and hydrophobicity on the translocation of polystyrene microspheres through gastrointestinal mucin." Journal of Applied Polymer Science **63**(11): 1481-1492.

Oettle, H., et al. (2007). "Adjuvant chemotherapy with gemcitabine vs observation in patients undergoing curative-intent resection of pancreatic cancer: a randomized controlled trial." Jama **297**(3): 267-277.

Olsson, Y. and T. S. Reese (1971). "Permeability of vasa nervorum and perineurium in mouse sciatic nerve studied by fluorescence and electron microscopy." Journal of Neuropathology & Experimental Neurology **30**(1): 105-119.

Pahwa, R. and W. C. Koller (1998). "Advances in the treatment of Parkinson's disease." Drugs of Today **34**(2): 95-105.

Pan, Y., et al. (2002). "Bioadhesive polysaccharide in protein delivery system: chitosan nanoparticles improve the intestinal absorption of insulin in vivo." International journal of pharmaceutics **249**(1): 139-147.

Pandey, R., et al. (2005). "Oral solid lipid nanoparticle-based antitubercular chemotherapy." Tuberculosis **85**(5): 415-420.

Panyam, J. and V. Labhasetwar (2003). "Biodegradable nanoparticles for drug and gene delivery to cells and tissue." Advanced Drug Delivery Reviews **55**(3): 329-347.

Panyam, J., et al. (2004). "Solid-state solubility influences encapsulation and release of hydrophobic drugs from PLGA/PLA nanoparticles." Journal of pharmaceutical sciences **93**(7): 1804-1814.

Pappenheimer, J. R. (1987). "Physiological regulation of transepithelial impedance in the intestinal mucosa of rats and hamsters." The Journal of membrane biology **100**(1): 137-148.

Pardridge, W. M. and L. Mietus, J (1979). "Transport of steroid hormones through the rat blood-brain barrier: primary role of albumin-bound hormone." The Journal of Clinical Investigation **64**(145-154).

Parra, A. L., et al. (2001). "Comparative study of the assay of Artemia salina L. and the estimate of the medium lethal dose (LD50 value) in mice, to determine oral acute toxicity of plant extracts." Phytomedicine **8**(5): 395-400.

Parsons, P. G. (1985). "Modification of dopa toxicity in human tumour cells." Biochemical Pharmacology **34**(10): 1801-1807.

Patil, S., et al. (2007). "Protein adsorption and cellular uptake of cerium oxide nanoparticles as a function of zeta potential." Biomaterials **28**(31): 4600-4607.

Pavia, D. L. (2006). Introduction to organic laboratory techniques: Chemistry 36, Stanford University, Thomson/Wadsworth.

Pecora, R. (2013). Dynamic light scattering: applications of photon correlation spectroscopy, Springer Science & Business Media.

Peltonen, L. and J. Hirvonen (2008). "Physicochemical characterization of nano-and microparticles." Current Nanoscience **4**(1): 101-107.

Pérez-Ruiz, T., et al. (2007). "Flow injection fluorimetric determination of L-dopa and dopamine based on a photochemical inhibition process." Microchimica Acta **158**(3): 299-305.

Peterson, M. D. and M. S. Mooseker (1993). "An *in vitro* model for the analysis of intestinal brush border assembly. I. Ultrastructural analysis of cell contact-induced brush border assembly in Caco-2BBe cells." Journal of Cell Science **105**(2): 445-460.

Petros, R. A. and J. M. DeSimone (2010). "Strategies in the design of nanoparticles for therapeutic applications." Nature reviews Drug discovery **9**(8): 615-627.

Phenrat, T., et al. (2009). "Particle size distribution, concentration, and magnetic attraction affect transport of polymer-modified Fe0 nanoparticles in sand columns." Environmental science & technology **43**(13): 5079-5085.

Pillai, O. and R. Panchagnula (2001). "Polymers in drug delivery." Current Opinion in Chemical Biology **5**(4): 447-451.

Pistonesi, M., et al. (2004). "Simultaneous determination of levodopa and benserazide by stopped-flow injection analysis and three-way multivariate calibration of kinetic-spectrophotometric data." Journal of Pharmaceutical and Biomedical Analysis **36**(3): 541-547.

Plank, C., et al. (1996). "Activation of the complement system by synthetic DNA complexes: a potential barrier for intravenous gene delivery." Human gene therapy **7**(12): 1437-1446.

Porter, C. J. H. and W. N. Charman (1997). "Uptake of drugs into the intestinal lymphatics after oral administration." Advanced drug delivery reviews **25**(1): 71-89.

Prausnitz, M. R. and J. S. Noonan (1998). "Permeability of cornea, sclera, and conjunctiva: a literature analysis for drug delivery to the eye." Journal of pharmaceutical sciences **87**(12): 1479-1488.

Qi, L., et al. (2005). "Cytotoxic activities of chitosan nanoparticles and copper-loaded nanoparticles." Bioorganic & medicinal chemistry letters **15**(5): 1397-1399.

Qiao, M., et al. (2005). "Injectable biodegradable temperature-responsive PLGA–PEG–PLGA copolymers: synthesis and effect of copolymer composition on the drug release from the copolymer-based hydrogels." International journal of pharmaceutics **294**(1): 103-112.

Radaic, A., et al. (2015). "Factorial Design and Development of Solid Lipid Nanoparticles (SLN) for Gene Delivery." Journal of nanoscience and nanotechnology **15**(2): 1793-1800.

Ranaldi, G., et al. (2002). "The effect of chitosan and other polycations on tight junction permeability in the human intestinal Caco-2 cell line." The Journal of nutritional biochemistry **13**(3): 157-167.

Randhawa, M. A. (2009). "Calculation of LD50 values from the method of Miller and Tainter, 1944." J Ayub Med Coll Abbottabad **21**(3): 184-185.

Rejman, J., et al. (2005). "Role of clathrin-and caveolae-mediated endocytosis in gene transfer mediated by lipo-and polyplexes." Molecular Therapy **12**(3): 468-474.

Reynolds, D. W., et al. (2002). "Available guidance and best practices for conducting forced degradation studies." Pharmaceutical Technology **26**(2): 48.

Rezkalla, S., et al. (1988). "Effect of metoprolol in acute coxsackievirus B3 murine myocarditis." Journal of the American College of Cardiology **12**(2): 412-414.

Robinson, J. R. (1978). Sustained and controlled release drug delivery systems, M. Dekker.

Robinson, K., et al. (2003). "CASE REPORT: Fatal Cholestatic Liver Failure Associated with Gemcitabine Therapy." Digestive diseases and sciences **48**(9): 1804-1808.

Romieu, I., et al. (1990). "Oral contraceptives and breast cancer review and meta-analysis." Cancer **66**(11): 2253-2263.

Rouxel, D., et al. (2011). "Effect of ultrasonication and dispersion stability on the cluster size of alumina nanoscale particles in aqueous solutions." Ultrasonics sonochemistry **18**(1): 382-388.

Rubas, W., et al. (1996). "Flux measurements across Caco-2 monolayers may predict transport in human large intestinal tissue." Journal of pharmaceutical sciences **85**(2): 165-169.

S Bansal, S., et al. (2013). "Validated RP-HPLC method for the simultaneous analysis of gemcitabine and LY-364947 in liposomal formulations." Current drug targets **14**(9): 1061-1069.

Saab, M. M., et al. "INTERNATIONAL JOURNAL OF DRUG FORMULATION AND RESEARCH DESIGN AND EVALUATION OF MUCOADHESIVE BUCCAL PATCHES FOR LOCAL DELIVERY OF CHLORHEXIDINE DIGLUCONATE."

Saberi, A. H., et al. (2013). "Fabrication of vitamin E-enriched nanoemulsions: factors affecting particle size using spontaneous emulsification." Journal of colloid and interface science **391**: 95-102.

Sacchi, A., et al. (2006). "Synergistic antitumor activity of cisplatin, paclitaxel, and gemcitabine with tumor vasculature-targeted tumor necrosis factor-α." Clinical Cancer Research **12**(1): 175-182.

Sahni, J. K., et al. (2008). "Potential prospects of chitosan derivative trimethyl chitosan chloride (TMC) as a polymeric absorption enhancer: synthesis, characterization and applications." Journal of Pharmacy and Pharmacology **60**(9): 1111-1119.

Sai, Y., et al. (1998). "Adsorptive-mediated endocytosis of a basic peptide in enterocyte-like Caco-2 cells." American Journal of Physiology-Gastrointestinal and Liver Physiology **275**(3): G514-G520.

Saif, M. W., et al. (2007). "Gemcitabine-induced liver fibrosis in a patient with pancreatic cancer." Jop **8**(4): 460-467.

Saito, H. and K. Inui (1993). "Dipeptide transporters in apical and basolateral membranes of the human intestinal cell line Caco-2." American Journal of Physiology - Gastrointestinal and Liver Physiology **265**(2): G289-G294.

Salmaso, S. "DEVELOPMENT OF pH RESPONSIVE, MULIMODAL TARGETED LIPOSOMES FOR DRUG AND PROTEIN DELIVERY TO CANCER TISSUES." nizing committee: 12.

Sambuy, Y., et al. (2005). "The Caco-2 cell line as a model of the intestinal barrier: influence of cell and culture-related factors on Caco-2 cell functional characteristics." Cell Biology and Toxicology **21**(1): 1-26.

Sanders, E. and C. T. Ashworth (1961). "A study of particulate intestinal absorption and hepatocellular uptake: Use of polystyrene latex particles." Experimental Cell Research **22**(0): 137-145.

Sandri, G., et al. (2010). "Insulin-loaded nanoparticles based on N-trimethyl chitosan: in vitro (Caco-2 model) and ex vivo (excised rat jejunum, duodenum, and ileum) evaluation of penetration enhancement properties." AAPS PharmSciTech **11**(1): 362-371.

Sansdrap, P. and A.-J. Moës (1997). "In vitro evaluation of the hydrolytic degradation of dispersed and aggregated poly (DL-lactide-co-glycolide) microspheres." Journal of controlled release **43**(1): 47-58.

Schieffer, G. W. (1979). "Reversed-phase high-performance liquid chromatographic investigation of levodopa preparations II: Levodopa determination." Journal of Pharmaceutical Sciences **68**(10): 1299-1301.

Schipper, N. G. M., et al. (1997). "Chitosans as absorption enhancers for poorly absorbable drugs 2: mechanism of absorption enhancement." Pharmaceutical research **14**(7): 923-929.

Schipper, N. G. M., et al. (1999). "Chitosans as absorption enhancers of poorly absorbable drugs: 3: Influence of mucus on absorption enhancement." European Journal of Pharmaceutical Sciences **8**(4): 335-343.

Schneeberger, E. E. (1974). "THE PERMEABILITY OF THE ALVEOLAR-CAPILLARY MEMBRANE TO ULTRASTRUCTURAL PROTEIN TRACERS." Annals of the New York Academy of Sciences **221**(1): 238-243.

Schoevaart, R., et al. (2004). "Preparation, optimization, and structures of cross-linked enzyme aggregates (CLEAs)." Biotechnology and Bioengineering **87**(6): 754-762.

Scott, R. P. W. (1994). Liquid chromatography for the analyst. New York, Marcel Dekker, INC.

Sherwood, L. (2008). "Cengage Learning (Firm)." Human physiology: from cells to systems. 7th ed. Australia.

Sherwood, L. (2015). Human physiology: from cells to systems, Cengage learning.

Shi, L.-L., et al. (2015). "Optimization of process variables of zanamivir-loaded solid lipid nanoparticles and the prediction of their cellular transport in Caco-2 cell model." International journal of pharmaceutics **478**(1): 60-69.

Shi, N., et al. (2001). "Brain-specific expression of an exogenous gene after i.v. administration." Proceedings of the National Academy of Sciences **98**(22): 12754-12759.

Shire, S. J., et al. (2004). "Challenges in the development of high protein concentration formulations." Journal of pharmaceutical sciences **93**(6): 1390-1402.

Shrivastava, A. and V. B. Gupta (2011). "Methods for the determination of limit of detection and limit of quantitation of the analytical methods." Chronicles of Young Scientists **2**(1): 21.

Siddhuraju, P. and K. Becker (2001). "Rapid reversed-phase high performance liquid chromatographic method for the quantification of L-Dopa (L-3,4-dihydroxyphenylalanine), non-methylated and methylated tetrahydroisoquinoline compounds from Mucuna beans." Food Chemistry **72**(3): 389-394.

Sieval, A. B., et al. (1998). "Preparation and NMR characterization of highly substitutedN-trimethyl chitosan chloride." Carbohydrate polymers **36**(2): 157-165.

Silverstein, S. B. and G. M. Rodgers (2004). "Parenteral iron therapy options." American journal of hematology **76**(1): 74-78.

Sinko, P. J. (2006). Martin's physical pharmacy and pharmaceutical sciences. Philadelphia, Lippincott Williams & Wilkins.

Sistla, R., et al. (2005). "Development and validation of a reversed-phase HPLC method for the determination of ezetimibe in pharmaceutical dosage forms." Journal of pharmaceutical and biomedical analysis **39**(3): 517-522.

Smart, J. D. (2005). "The basics and underlying mechanisms of mucoadhesion." Advanced drug delivery reviews **57**(11): 1556-1568.

Snehalatha, M., et al. (2008). "Etoposide-loaded PLGA and PCL nanoparticles I: preparation and effect of formulation variables." Drug Delivery **15**(5): 267-275.

Snoeys, J., et al. (2007). "Species differences in transgene DNA uptake in hepatocytes after adenoviral transfer correlate with the size of endothelial fenestrae." Gene therapy **14**(7): 604-612.

Snyder, L. R. and J. J. Kirkland (1979). Liquid-solid chromatography. Introduction to modern liquid chramotography. New York, John Wiley and Sons Inc.

Snyman, D., et al. (2003). "Evaluation of the mucoadhesive properties of N-trimethyl chitosan chloride." Drug development and industrial pharmacy **29**(1): 61-69.

Södergård, A. and M. Stolt (2002). "Properties of lactic acid based polymers and their correlation with composition." Progress in Polymer Science **27**(6): 1123-1163.

Sonavane, G., et al. (2008). "In vitro permeation of gold nanoparticles through rat skin and rat intestine: effect of particle size." Colloids and Surfaces B: Biointerfaces **65**(1): 1-10.

Sondhi, D., et al. (1998). "Peptide and protein phosphorylation by protein tyrosine kinase Csk: insights into specificity and mechanism." Biochemistry **37**(1): 165-172.

Song, X., et al. (2008). "Dual agents loaded PLGA nanoparticles: systematic study of particle size and drug entrapment efficiency." European Journal of Pharmaceutics and Biopharmaceutics **69**(2): 445-453.

Song, X., et al. (2008). "PLGA nanoparticles simultaneously loaded with vincristine sulfate and verapamil hydrochloride: systematic study of particle size and drug entrapment efficiency." International journal of pharmaceutics **350**(1): 320-329.

Sonia, T. A. and C. P. Sharma (2012). "An overview of natural polymers for oral insulin delivery." Drug discovery today **17**(13): 784-792.

Sottani, C., et al. (2007). "Simultaneous determination of gemcitabine, taxol, cyclophosphamide and ifosfamide in wipe samples by high-performance liquid chromatography/tandem mass spectrometry: protocol of validation and uncertainty of measurement." Rapid communications in mass spectrometry **21**(7): 1289-1296.

Sottani, C., et al. (2004). "Validated procedure for simultaneous trace level determination of the anti-cancer agent gemcitabine and its metabolite in human urine by high-performance liquid chromatography with tandem mass spectrometry." Rapid communications in mass spectrometry **18**(10): 1017-1023.

Stetsko, G. (1986). "Statistical experimental design and its application to pharmaceutical development problems." Drug Development and Industrial Pharmacy **12**(8-9): 1109-1123.

Bestpfe.com

Summers, M. A., et al. (2004). "Use of verapamil as a potential P-glycoprotein inhibitor in a patient with refractory epilepsy." Annals of Pharmacotherapy **38**(10): 1631-1634.

Suzuki, Y. A. and B. Lönnerdal (2002). "Characterization of mammalian receptors for lactoferrin." Biochemistry and Cell Biology **80**(1): 75-80.

Takahashi, H. and T. B. Fitzpatrick (1964). "Quantitative determination of Dopa; Its application to measurement of Dopa in urine and in the assay of tyrosinase in serum1." The Journal of Investigative Dermatology **42**(1): 161-165.

Takahashi, S., et al. (1994). "Long-term changes in the haversian systems following high-dose irradiation. An ultrastructural and quantitative histomorphological study." J Bone Joint Surg Am **76**(5): 722-738.

Teradal, N. L., et al. (2012). "Electrochemical investigations of an anticancer drug in the presence of sodium dodecyl sulfate as an enhancing agent at carbon paste electrode." Journal of Applied Electrochemistry **42**(11): 917-923.

Thanoo, B. C., et al. (1993). "Oral Sustained-release Drug Delivery Systems using Polycarbonate Microspheres Capable of Floating on the Gastric Fluid." Journal of Pharmacy and Pharmacology **45**(1): 21-24.

Thanou, M., et al. (2001). "Chitosan and its derivatives as intestinal absorption enhancers." Advanced drug delivery reviews **50**: S91-S101.

Tiyaboonchai, W. (2003). "Chitosan nanoparticles: a promising system for drug delivery." Naresuan University Journal **11**(3): 51-66.

Todokoro, H. and M. Ezumi (1999). Scanning electron microscope, Google Patents.

Tomita, M., et al. (1996). "Absorption-enhancing mechanism of EDTA, caprate, and decanoylcarnitine in Caco-2 cells." Journal of pharmaceutical sciences **85**(6): 608-611.

Tomita, M., et al. (1988). "Enhancement of colonic drug absorption by the transcellular permeation route." Pharmaceutical research **5**(12): 786-789.

Torre, L. A., et al. (2015). "Global cancer statistics, 2012." CA: a cancer journal for clinicians **65**(2): 87-108.

Tsuji, A. (1998). "P-glycoprotein-mediated efflux transport of anticancer drugs at the blood-brain barrier." Therapeutic drug monitoring **20**(5): 588-590.

Uchiyama, T., et al. (1999). "Enhanced Permeability of Insulin across the Rat Intestinal Membrane by Various Absorption Enhancers: Their Intestinal Mucosal Toxicity and Absorption-enhancing Mechanism of n-Lauryl-β-D-maltopyranoside." Journal of Pharmacy and Pharmacology **51**(11): 1241-1250.

Uhrich, K. E., et al. (1999). "Polymeric systems for controlled drug release." Chemical reviews **99**(11): 3181-3198.

Unger, F., et al. (2007). "Branched polyesters based on poly [vinyl-3-(dialkylamino) alkylcarbamate-co-vinyl acetate-co-vinyl alcohol]-graft-poly (d, l-lactide-co-glycolide): effects of polymer structure on cytotoxicity." Biomaterials **28**(9): 1610-1619.

Van Eerdenbrugh, B., et al. (2009). "A screening study of surface stabilization during the production of drug nanocrystals." Journal of pharmaceutical sciences **98**(6): 2091-2103.

Van Itallie, C. M., et al. (2008). "The density of small tight junction pores varies among cell types and is increased by expression of claudin-2." Journal of cell science **121**(3): 298-305.

Vandenberg, G. W., et al. (2001). "Factors affecting protein release from alginate–chitosan coacervate microcapsules during production and gastric/intestinal simulation." Journal of controlled release **77**(3): 297-307.

Vander Heyden, Y., et al. (1993). "Three-level screening designs for the optimisation or the ruggedness testing of analytical procedures." Analytica chimica acta **276**(1): 189-195.

Vauthier, C., et al. (2003). "Drug delivery to resistant tumors: the potential of poly (alkyl cyanoacrylate) nanoparticles." Journal of controlled release **93**(2): 151-160.

Velmurugan, S., et al. (2014). "Microparticulate drug carriers: A promising approach for the delivery of anti HIV drugs." Int J Pharm Pharm Sci **6**(2): 31-39.

BEST PFE.COM
List of research project topics and materials

Velmurugan, S. and S. Dodla (2013). "Buccal penetration enhancers-an overview." Asian Journal of Pharmaceutical and Clinical Research **6**(3): 39-47.

Veltkamp, S. A., et al. (2008). "Oral administration of gemcitabine in patients with refractory tumors: a clinical and pharmacologic study." Clinical Cancer Research **14**(11): 3477-3486.

Veltkamp, S. A., et al. (2008). "Extensive metabolism and hepatic accumulation of gemcitabine after multiple oral and intravenous administration in mice." Drug Metabolism and Disposition **36**(8): 1606-1615.

Venturoli, D. and B. Rippe (2005). "Ficoll and dextran vs. globular proteins as probes for testing glomerular permselectivity: effects of molecular size, shape, charge, and deformability." American Journal of Physiology-Renal Physiology **288**(4): F605-F613.

Vihola, H., et al. (2002). "Binding and release of drugs into and from thermosensitive poly (N-vinyl caprolactam) nanoparticles." European journal of pharmaceutical sciences **16**(1): 69-74.

von der Maase, H., et al. (2000). "Gemcitabine and cisplatin versus methotrexate, vinblastine, doxorubicin, and cisplatin in advanced or metastatic bladder cancer: results of a large, randomized, multinational, multicenter, phase III study." Journal of Clinical oncology **18**(17): 3068-3077.

Vorbrodt, A. W. (1987). "Demonstration of anionic sites on the luminal and abluminal fronts of endothelial cells with poly-L-lysine-gold complex." Journal of Histochemistry and Cytochemistry **35**(11): 1261-1266.

Wainer, I. W. (1985). Liquid chromatography in pharmaceutical development: An introduction. USA, Aster Publishing Corporation.

Walgren, R. A., et al. (2000). "Cellular uptake of dietary flavonoid quercetin 4′-β-glucoside by sodium-dependent glucose transporter SGLT1." Journal of Pharmacology and Experimental Therapeutics **294**(3): 837-843.

Walter, E., et al. (1996). "HT29-MTX/Caco-2 cocultures as an in vitro model for the intestinal epithelium: In vitro–in vivo correlation with permeability data from rats and humans." Journal of pharmaceutical sciences **85**(10): 1070-1076.

Wang, C. H. and Y. Y. Huang (2003). "Encapsulating Protein into Preformed Liposomes by Ethanol-Destabilized Method." Artificial cells, blood substitutes, and biotechnology **31**(3): 303-312.

Wang, F., et al. (2011). "Synergistic effect of folate-mediated targeting and verapamil-mediated P-gp inhibition with paclitaxel-polymer micelles to overcome multi-drug resistance." Biomaterials **32**(35): 9444-9456.

Wang, J., et al. (2011). "More effective nanomedicines through particle design." Small **7**(14): 1919-1931.

Wang, J., et al. (2002). "Characterization of the initial burst release of a model peptide from poly (D, L-lactide-co-glycolide) microspheres." Journal of controlled release **82**(2): 289-307.

Warren, R. A., et al. (1997). "Saturation of the endocytic pathway for the transferrin receptor does not affect the endocytosis of the epidermal growth factor receptor." Journal of Biological Chemistry **272**(4): 2116-2121.

Watson, C. J., et al. (2001). "Functional modeling of tight junctions in intestinal cell monolayers using polyethylene glycol oligomers." American Journal of Physiology-Cell Physiology **281**(2): C388-C397.

Weiss, J., et al. (2008). "Solid lipid nanoparticles as delivery systems for bioactive food components." Food Biophysics **3**(2): 146-154.

Weissenboeck, A., et al. (2004). "Binding and uptake of wheat germ agglutinin-grafted PLGA-nanospheres by Caco-2 monolayers." Pharmaceutical Research **21**(10): 1917-1923.

Whitney, C. M. (2007). "Medications for Parkinson's disease." Neurologist **13**(6): 387-388.

Wikman-Larhed, A. and P. Artursson (1995). "Co-cultures of human intestinal goblet (HT29-H) and absorptive (Caco-2) cells for studies of drug and peptide absorption." European journal of pharmaceutical sciences **3**(3): 171-183.

Wikman, A., et al. (1993). "A drug absorption model based on the mucus layer producing human intestinal goblet cell line HT29-H." Pharmaceutical research **10**(6): 843-852.

Williams, A. C. and B. W. Barry (2012). "Penetration enhancers." Advanced drug delivery reviews **64**: 128-137.

Wilson, G., et al. (1990). "Transport and permeability properties of human Caco-2 cells: an in vitro model of the intestinal epithelial cell barrier." Journal of controlled release **11**(1-3): 25-40.

Win, K. Y. and S.-S. Feng (2005). "Effects of particle size and surface coating on cellular uptake of polymeric nanoparticles for oral delivery of anticancer drugs." Biomaterials **26**(15): 2713-2722.

Wisse, E., et al. (2008). "The size of endothelial fenestrae in human liver sinusoids: implications for hepatocyte-directed gene transfer." Gene therapy **15**(17): 1193-1199.

Witt, K. and T. Davis (2006). "CNS drug delivery: Opioid peptides and the blood-brain barrier." The AAPS Journal **8**(1): E76-E88.

Witt, K. A., et al. (2001). "Peptide drug modifications to enhance bioavailability and blood-brain barrier permeability." Peptides **22**(12): 2329-2343.

Wu, G. (2000). "The determination of levodopa in plasma by HPLC: A cautionary note." Chromatographia **52**(5): 371-372.

Wu, X. S. (1995). Synthesis and propertis of biodegradable lactic/glycolic acid polymers. Encyclopedic Handbook of Biomaterials and Bioengineering. Wise. New York, Marcel Dekker**:** 1015-1054.

Wulff-Pérez, M., et al. (2014). "In vitro duodenal lipolysis of lipid-based drug delivery systems studied by HPLC–UV and HPLC–MS." International journal of pharmaceutics **465**(1): 396-404.

Wyatt, P. J. and D. N. Villalpando (1997). "High-precision measurement of submicrometer particle size distributions." Langmuir **13**(15): 3913-3914.

Xu, F., et al. (2009). "Brain delivery and systemic effect of cationic albumin conjugated PLGA nanoparticles." Journal of Drug Targeting **17**(6): 423-434.

Yamaguchi, Y., et al. (2002). "Insulin-loaded biodegradable PLGA microcapsules: initial burst release controlled by hydrophilic additives." Journal of controlled release **81**(3): 235-249.

Yang, J., et al. (1993). "Rare earth as fluorescence probe to determine 3,4-dihydroxydroxyphenylalanine." Analytical Letters **26**(10): 2291-2306.

Yang, L., et al. (2009). "Enhancement the oral bioavailability of praziquantel by incorporation into solid lipid nanoparticles." Die Pharmazie-An International Journal of Pharmaceutical Sciences **64**(2): 86-89.

Yang, S. C., et al. (1999). "Body distribution in mice of intravenously injected camptothecin solid lipid nanoparticles and targeting effect on brain." Journal of controlled release **59**(3): 299-307.

Yeh, T.-H., et al. (2011). "Mechanism and consequence of chitosan-mediated reversible epithelial tight junction opening." Biomaterials **32**(26): 6164-6173.

Yien, L., et al. (2012). "Antifungal activity of chitosan nanoparticles and correlation with their physical properties." International journal of biomaterials **2012**.

Yılmaz, B. and Y. Y. Kadıoğlu (2004). "Comparison of zero-and second-order derivative spectrophotometric and HPLC methods for the determination of gemcitabine in human plasma." Il Farmaco **59**(5): 425-429.

Yoshioka, S. and S. Valentino J (2004). Stability of drugs and dosage forms. New York, Kluwer Academic/Plenum Publishers.

Youdim, K. A., et al. (2003). "In vitro trans-monolayer permeability calculations: often forgotten assumptions." Drug discovery today **8**(21): 997-1003.

Youk, H.-J., et al. (2005). "Enhanced anticancer efficacy of α-tocopheryl succinate by conjugation with polyethylene glycol." Journal of controlled release **107**(1): 43-52.

Yoza, N., et al. (1980). "Optimization of high-performance liquid chromatography of inorganic polyphosphates for routine analyses." Journal of Chromatography A **196**(3): 471-480.

Yu, L., et al. (1999). "Vitamin E-TPGS increases absorption flux of an HIV protease inhibitor by enhancing its solubility and permeability1." Pharmaceutical research **16**(12): 1812-1817.

Yu, Q., et al. (2013). "The effect of various absorption enhancers on tight junction in the human intestinal Caco-2 cell line." Drug development and industrial pharmacy **39**(4): 587-592.

Yu, X., et al. (2011). "Biodegradable polymer microcapsules fabrication through a template-free approach." Langmuir **27**(16): 10265-10273.

Yuan, H., et al. (2007). "Studies on oral absorption of stearic acid SLN by a novel fluorometric method." Colloids and Surfaces B: Biointerfaces **58**(2): 157-164.

Yuan, Y., et al. (2011). "Deacetylation of chitosan: Material characterization and in vitro evaluation via albumin adsorption and pre-osteoblastic cell cultures." Materials **4**(8): 1399-1416.

Yücel, Ç., et al. (2013). "Nanoparticle and liposome formulations of doxycycline: transport properties through Caco-2 cell line and effects on matrix metalloproteinase secretion." Biomedicine & Pharmacotherapy **67**(6): 459-467.

Zarifpour, M., et al. (2013). "Preparation and Characterization of Trimethyl Chitosan Nanospheres Encapsulated with Tetanus Toxoid for Nasal Immunization Studies." transport **1**: 4.

Zaro, J. L. and W.-C. Shen (2003). "Quantitative comparison of membrane transduction and endocytosis of oligopeptides." Biochemical and Biophysical Research Communications **307**(2): 241-247.

Zhang, D., et al. (2006). "Preparation of oridonin-loaded solid lipid nanoparticles and studies on them in vitro and in vivo." Nanotechnology **17**(23): 5821.

Zhang, J., et al. (2014). "Mechanism study of cellular uptake and tight junction opening mediated by goblet cell-specific trimethyl chitosan nanoparticles." Molecular pharmaceutics **11**(5): 1520-1532.

Zhang, L., et al. (2008). "Nanoparticles in medicine: therapeutic applications and developments." Clinical pharmacology and therapeutics **83**(5): 761-769.

Zhang, S., et al. (2009). "Size-Dependent Endocytosis of Nanoparticles." Advanced Materials **21**(4): 419-424.

Zhang, Y. and L. Z. Benet (2001). "The gut as a barrier to drug absorption." Clinical pharmacokinetics **40**(3): 159-168.

Zidan, A. S., et al. (2013). "Formulation and transport properties of tenofovir loaded liposomes through Caco-2 cell model." Journal of liposome research **23**(4): 318-326.

Zorc, B., et al. (1993). "Macromolecular prodrugs. II. Esters of l-dopa and [alpha]-methyldopa." International Journal of Pharmaceutics **99**(2-3): 135-143.